




1-1-2013

# Defining the Role of Mechanical Signals During Nerve Root Compression in the Development of Sustained Pain and Neurophysiological Correlates that Develop in the Injured Tissue and Spinal Cord

Kristen Nicholson

University of Pennsylvania, [nkristen@seas.upenn.edu](mailto:nkristen@seas.upenn.edu)

Follow this and additional works at: <http://repository.upenn.edu/edissertations>

 Part of the [Biomechanics Commons](#), [Biomedical Commons](#), and the [Neuroscience and Neurobiology Commons](#)

---

## Recommended Citation

Nicholson, Kristen, "Defining the Role of Mechanical Signals During Nerve Root Compression in the Development of Sustained Pain and Neurophysiological Correlates that Develop in the Injured Tissue and Spinal Cord" (2013). *Publicly Accessible Penn Dissertations*. 785.

<http://repository.upenn.edu/edissertations/785>

---

# Defining the Role of Mechanical Signals During Nerve Root Compression in the Development of Sustained Pain and Neurophysiological Correlates that Develop in the Injured Tissue and Spinal Cord

## **Abstract**

Cervical nerve root injury commonly leads to pain. The duration of an applied compression has been shown to contribute to both the onset of persistent pain and also the degree of spinal cellular and molecular responses related to nociception that are produced. This thesis uses a rat model of a transient cervical nerve root compression to study how the duration of an applied compression modulates both peripherally-evoked activity in spinal cord neurons during a root compression and the resulting neuronal and glutamatergic responses in the nerve root and spinal cord. Studies define the compression duration threshold that inhibits peripherally-evoked action potentials in the spinal cord during a root compression to be at  $6.6 \pm 3.0$  minutes and this is similar to the threshold for eliciting persistent mechanical allodynia after a cervical root compression that lies between 3 and 10 minutes. Furthermore, neurotransmission remains inhibited for at least 10 minutes after a painful nerve root compression and this may contribute to the subsequent development of neuropathology in the root, spinal neuronal hyperexcitability, downregulation of spinal GLT-1 and upregulation of spinal GLAST at day 7. Additional studies examine the role of the spinal glutamatergic system in mediating radicular pain by administering Riluzole to inhibit glutamate release at day 1 or ceftriaxone daily to upregulate spinal GLT-1, separately. Both treatments abolished behavioral sensitivity and the associated neuronal hyperexcitability that is normally observed in the deep laminae of the dorsal horn. Additionally, Riluzole mitigated the axonal neuropathology in the root that normally develops by day 7 while ceftriaxone restored the spinal expression of GLAST. Together these studies identify how one aspect of nerve root biomechanics, compression duration, modulates neuronal and glutamatergic responses in the nerve root and spinal cord that are associated with cervical radicular pain. Day 1 was identified as a critical time-point when inhibiting glutamate signaling in the central nervous system can prevent persistent nerve root-mediated pain that is likely maintained by downregulation of spinal GLT-1. Finally, these studies suggest that primary afferent regulation of spinal GLT-1 may have a critical role in transducing the biomechanics of a nerve root compression into radicular pain.

## **Degree Type**

Dissertation

## **Degree Name**

Doctor of Philosophy (PhD)

## **Graduate Group**

Bioengineering

## **First Advisor**

Beth A. Winkelstein

---

**Keywords**

electrophysiology, glutamate, glutamate transporter, injury, nerve root

**Subject Categories**

Biomechanics | Biomedical | Neuroscience and Neurobiology

DEFINING THE ROLE OF MECHANICAL SIGNALS DURING NERVE ROOT  
COMPRESSION IN THE DEVELOPMENT OF SUSTAINED PAIN AND  
NEUROPHYSIOLOGICAL CORRELATES THAT DEVELOP IN THE  
INJURED TISSUE AND SPINAL CORD

Kristen J. Nicholson

A DISSERTATION  
in  
Bioengineering

Presented to the Faculties of the University of Pennsylvania in

Partial Fulfillment of the Requirements for the

Degree of Doctor of Philosophy

2013

Supervisor of Dissertation

---

Beth A. Winkelstein  
Professor of Bioengineering

Graduate Group Chairperson

---

Jason A. Burdick  
Professor of Bioengineering

Dissertation Committee:

Kristy Arbogast, Research Associate Professor of Pediatrics  
Kelly L. Jordan-Sciutto, Associate Professor of Pathology  
Brian Litt, Professor of Neurology and Bioengineering

## ACKNOWLEDGMENTS

I would first like to thank Dr. Kristy Arbogast, Dr. Kelly Jordan-Sciutto and Dr. Brian Litt for taking the time to sit on my thesis committee. I am particularly grateful for my advisor, Dr. Beth Winkelstein, for her commitment and time devoted to my training. Thank you to all the members of the Spine Pain Research Lab for the years of advice, support and friendship. Thank you especially to Christine, Jenn and Ling for always being there to discuss anything and everything. I would like to specifically acknowledge Taylor for her assistance in many aspects of the research presented in this thesis. I am also thankful for the support of Ben, Julia and Sijia who were instrumental in the completion of many studies presented here.

I would like to thank my family and friends for their encouragement and unconditional love. Thank you to my mom for always being there to listen to me and for always trusting in me and to Dave for taking such good care of Paco. Thank you to my dad for his constant belief in me and to Cindy for her encouraging words when I need them. I am especially thankful for Keri, Kyle, Alexis and Melena for being such amazing role models for me. I would like to thank Ben, Heather, Jason, Steve and Wei for their support and friendship over the years. Finally, I would like to thank my dog, Paco, for being the most loving and happy dog I could ask for.

## ABSTRACT

### DEFINING THE ROLE OF MECHANICAL SIGNALS DURING NERVE ROOT COMPRESSION IN THE DEVELOPMENT OF SUSTAINED PAIN AND NEUROPHYSIOLOGICAL CORRELATES THAT DEVELOP IN THE INJURED TISSUE AND SPINAL CORD

Kristen J. Nicholson

Beth A. Winkelstein

Cervical nerve root injury commonly leads to pain. The duration of an applied compression has been shown to contribute to both the onset of persistent pain and also the degree of spinal cellular and molecular responses related to nociception that are produced. This thesis uses a rat model of a transient cervical nerve root compression to study how the duration of an applied compression modulates both peripherally-evoked activity in spinal cord neurons *during* a root compression and the resulting neuronal and glutamatergic responses in the nerve root and spinal cord. Studies define the compression duration threshold that inhibits peripherally-evoked action potentials in the spinal cord *during* a root compression to be at  $6.6 \pm 3.0$  minutes and this is similar to the threshold for eliciting persistent mechanical allodynia after a cervical root compression that lies between 3 and 10 minutes. Furthermore, neurotransmission remains inhibited for at least 10 minutes after a painful nerve root compression and this may contribute to the subsequent development of neuropathology in the root, spinal neuronal hyperexcitability, downregulation of spinal GLT-1 and upregulation of spinal GLAST at day 7. Additional

studies examine the role of the spinal glutamatergic system in mediating radicular pain by administering Riluzole to inhibit glutamate release at day 1 or ceftriaxone daily to upregulate spinal GLT-1, separately. Both treatments abolished behavioral sensitivity and the associated neuronal hyperexcitability that is normally observed in the deep laminae of the dorsal horn. Additionally, Riluzole mitigated the axonal neuropathology in the root that normally develops by day 7 while ceftriaxone restored the spinal expression of GLAST. Together these studies identify how one aspect of nerve root biomechanics, compression duration, modulates neuronal and glutamatergic responses in the nerve root and spinal cord that are associated with cervical radicular pain. Day 1 was identified as a critical time-point when inhibiting glutamate signaling in the central nervous system can prevent persistent nerve root-mediated pain that is likely maintained by downregulation of spinal GLT-1. Finally, these studies suggest that primary afferent regulation of spinal GLT-1 may have a critical role in transducing the biomechanics of a nerve root compression into radicular pain.

## TABLE OF CONTENTS

	Page
Acknowledgments . . . . .	ii
Abstract . . . . .	iii
Table of Contents . . . . .	v
List of Tables . . . . .	x
List of Figures . . . . .	xii
<b>CHAPTER 1. Introduction and Background. . . . .</b>	<b>1</b>
1.1 Introduction . . . . .	1
1.2 Background . . . . .	5
1.2.1 Cervical Spine & Nerve Root Anatomy. . . . .	5
1.2.2 Cervical Radiculopathy. . . . .	9
1.2.3 Nerve Root Biomechanics . . . . .	12
1.2.4 In vivo Models of Mechanical Injury to the Nerve Root.. . . .	16
1.2.5 Nociception in the Nerve Root & the Spinal Cord . . . . .	21
1.2.6 Glutamatergic System in the Spinal Cord. . . . .	25
<b>CHAPTER 2. Rationale, Context and Hypotheses . . . . .</b>	<b>28</b>
2.1 Rationale & Context . . . . .	28
2.2 Overall Hypothesis & Specific Aims . . . . .	30
<b>CHAPTER 3. Defining a Duration Threshold to Modulate Evoked Neuronal Firing     Rates in the Spinal Cord &amp; the Development of Axonal Pathology. . . . .</b>	<b>35</b>



3.1 Overview . . . . .	35
3.2 Relevant Background . . . . .	37
3.3 Afferent Discharge Rates During & After Root Compression. . . . .	43
3.3.1 Methods . . . . .	43
3.3.2 Results . . . . .	55
3.4 Axonal Morphology in the Root After 3 or 15 Minute Compressions. . . . .	59
3.4.1 Methods . . . . .	59
3.4.2 Results . . . . .	62
3.5 Discussion . . . . .	64
3.6 Integration & Conclusions. . . . .	74

**CHAPTER 4. Behavioral Sensitivity is Mediated by the Duration of a Transient**

<b>Dorsal Root Compression . . . . .</b>	<b>78</b>
4.1 Overview . . . . .	78
4.2 Relevant Background . . . . .	80
4.3 Mechanical Allodynia Depends on the Duration of Compression . . . . .	84
4.3.1 Methods . . . . .	84
4.3.2 Results . . . . .	85
4.4 Thermal Hyperalgesia After Transient Root Compressions . . . . .	88
4.4.1 Methods . . . . .	88
4.4.2 Results . . . . .	90
4.5 Discussion . . . . .	92
4.6 Integration & Conclusions . . . . .	97

**CHAPTER 5. Glutamate Transporters & Excitatory Signaling in the Spinal Cord**

**following Painful Nerve Root Compression . . . . . 99**

5.1 Overview . . . . . 99

5.2 Relevant Background . . . . . 101

5.3 Temporal Response of Spinal Glutamate Transporters . . . . . 105

    5.3.1 Methods . . . . . 105

    5.3.2 Results . . . . . 107

5.4 Evoked Afferent Signaling in the Spinal Cord . . . . . 110

    5.4.1 Methods . . . . . 110

    5.4.2 Results . . . . . 114

5.5 Discussion . . . . . 118

5.6 Integration & Conclusions. . . . . 125

**CHAPTER 6. Upregulation of GLT-1 by Ceftriaxone Treatment Alleviates Nerve**

**Root-Mediated Pain . . . . . 129**

6.1 Overview . . . . . 129

6.2 Relevant Background . . . . . 132

6.3 Methods. . . . . 135

    6.3.1 Surgical Procedures & Ceftriaxone Administration . . . . . 135

    6.3.2 Behavioral Assessments & Immunohistochemistry . . . . . 136

    6.3.3 Electrophysiological Recordings . . . . . 137

6.4 Results . . . . . 140

    6.4.1 Spinal GLT-1 Upregulation by Ceftriaxone . . . . . 140

    6.4.2 Behavioral Sensitivity After Ceftriaxone Treatment . . . . . 141

6.4.3 Effect of Ceftriaxone on Spinal GLAST & GFAP Expression . . .	146
6.4.4 Evoked Action Potentials in the Spinal Cord After Ceftriaxone Treatment . . . . .	148
6.5 Discussion . . . . .	152
6.6 Integration & Conclusions. . . . .	160
<b>CHAPTER 7. Riluzole Treatment of Nerve Root-Mediated Pain . . . . .</b>	<b>164</b>
7.1 Overview . . . . .	164
7.2 Relevant Background . . . . .	167
7.3 Methods. . . . .	169
7.3.1 Surgical Procedures & Riluzole Administration . . . . .	169
7.3.2 Behavioral Assessments . . . . .	170
7.3.3 Immunohistochemistry . . . . .	172
7.3.4 Electrophysiology . . . . .	174
7.4 Results . . . . .	177
7.5 Discussion . . . . .	187
7.6 Integration & Conclusions. . . . .	193
<b>CHAPTER 8. Summary, Synthesis &amp; Future Work. . . . .</b>	<b>196</b>
8.1 Introduction . . . . .	196
8.2 Summary . . . . .	197
8.3 Synthesis. . . . .	209
8.4 Future Work . . . . .	218

<b>APPENDIX A. Protocol to Count Electrically-Evoked Action Potentials . . .</b>	<b>225</b>
<b>APPENDIX B. Electrically-Evoked Action Potential Counts During a Nerve Root     Compression . . . . .</b>	<b>230</b>
<b>APPENDIX C. Mechanical Allodynia &amp; Thermal Hyperalgesia . . . . .</b>	<b>233</b>
<b>APPENDIX D. Quantification of Spinal Protein Using Immunohistochemistry .</b>	<b>249</b>
<b>APPENDIX E. Quantification of Evoked Action Potentials in the Dorsal Horn .</b>	<b>301</b>
<b>APPENDIX F. Matlab Code for Quantifying Immunohistochemistry of Spinal     Cord Sections . . . . .</b>	<b>319</b>
<b>REFERENCES . . . . .</b>	<b>322</b>

## LIST OF TABLES

		Page
<b>Table 3.1</b>	Summary of NF200 and IB4 ratings . . . . .	63
<b>Table 7.1</b>	Summary of the NF200, CGRP, and IB4 ratings . . . . .	182
<b>Table 7.2</b>	Distribution of WDR and LTM neurons . . . . .	186
<b>Table B.1</b>	Number of action potentials for the 15 minute study in Chapter 3 . . . . .	231
<b>Table B.2</b>	Number of action potentials for the 3 minute study in Chapter 3 . . . . .	232
<b>Table C.1</b>	Mechanical allodynia following 3 and 10 minute compressions for 7 days for Chapter 4 . . . . .	235
<b>Table C.2</b>	Mechanical allodynia following 15 minute compression for 7 days for Chapter 4 . . . . .	235
<b>Table C.3</b>	Thermal hyperalgesia following 3 and 15 minute compressions for 7 days for Chapters 4 and 5 . . . . .	236
<b>Table C.4</b>	Mechanical allodynia following 3 and 15 minute compressions for 7 days for Chapter 4 and 5 . . . . .	237
<b>Table C.5</b>	Mechanical allodynia following 3 and 15 minute compressions for 7 days for Chapter 5. . . . .	238
<b>Table C.6</b>	Mechanical allodynia for 7 days for the ceftriaxone treatment in Chapter 6 . . . . .	239
<b>Table C.7</b>	Thermal hyperalgesia for 7 days for the ceftriaxone treatment in Chapter 6 . . . . .	241
<b>Table C.8</b>	Mechanical allodynia for 7 days for the electrophysiologic studies after ceftriaxone treatment in Chapter 6 . . . . .	242
<b>Table C.9</b>	Mechanical allodynia for 7 days for the Riluzole treatment studies in Chapter 7 . . . . .	244
<b>Table C.10</b>	Thermal hyperalgesia for 7 days for the Riluzole treatment studies in Chapter 7 . . . . .	246

<b>Table C.11</b>	Mechanical allodynia for 7 days for the electrophysiologic studies after Riluzole treatment in Chapter 7 . . . . .	247
<b>Table D.1</b>	Quantification of spinal GLT-1 after 3 and 15 minute compressions at days 1 and 7 for Chapter 5 . . . . .	251
<b>Table D.2</b>	Quantification of spinal GLAST after 3 and 15 minute compressions at days 1 and 7 for Chapter 5 . . . . .	259
<b>Table D.3</b>	Quantification of spinal EAAC1 after 3 and 15 minute compressions at days 1 and 7 for Chapter 5 . . . . .	268
<b>Table D.4</b>	Quantification of spinal GLT-1 after ceftriaxone treatment at day 7 for Chapter 6 . . . . .	277
<b>Table D.5</b>	Quantification of spinal GFAP after ceftriaxone treatment at day 7 for Chapter 6 . . . . .	282
<b>Table D.6</b>	Quantification of spinal GLAST after ceftriaxone treatment at day 7 for Chapter 6 . . . . .	288
<b>Table D.7</b>	Quantification of CGRP in the superficial laminae after Riluzole treatment at day 7 for Chapter 7 . . . . .	291
<b>Table D.8</b>	Quantification of CGRP in the deep laminae after Riluzole treatment at day 7 for Chapter 7 . . . . .	297
<b>Table E.1</b>	Spinal neuronal firing in the superficial laminae at day 7 after 15 minute compression for Chapter 5 . . . . .	303
<b>Table E.2</b>	Spinal neuronal firing in the deep laminae at day 7 after 3 & 15 minute compressions for Chapter 5 . . . . .	306
<b>Table E.3</b>	Spinal neuronal firing in the deep laminae at day 7 after ceftriaxone treatment for Chapter 6 . . . . .	308
<b>Table E.4</b>	Spinal neuronal firing in the deep laminae at day 7 after Riluzole treatment for Chapter 7 . . . . .	314

## LIST OF FIGURES

	Page
<b>Figure 1.1</b> Overview of nerve root and spinal sensory pathways in pain . . . . .	5
<b>Figure 1.2</b> Spinal cord and nerve root anatomy . . . . .	6
<b>Figure 1.3</b> Axial section of the spinal cord and nerve roots . . . . .	8
<b>Figure 1.4</b> Mechanical response of the rat nerve root under compression . . . . .	14
<b>Figure 1.5</b> Laminar distribution of primary afferents in dorsal horn and response characteristics of spinal neurons . . . . .	23
<b>Figure 1.6</b> Glutamatergic synapse in the spinal cord. . . . .	26
<b>Figure 3.1</b> Experimental test set-up for recording electrically-evoked action potentials in the spinal cord . . . . .	44
<b>Figure 3.2</b> Study design to measure evoked action potentials during a nerve root compression . . . . .	45
<b>Figure 3.3</b> Surgical exposure for recording extracellular potentials . . . . .	46
<b>Figure 3.4</b> Flow chart for identifying and selecting neurons in the spinal cord . . . . .	48
<b>Figure 3.5</b> Representative extracellular recordings in the spinal cord during mechanical stimulation to the forepaw . . . . .	51
<b>Figure 3.6</b> Representative extracellular recordings in the spinal cord after an electrical stimulus to the forepaw . . . . .	52
<b>Figure 3.7</b> Evoked spikes during and after a 3 or a 15 minute root compression . . . . .	56
<b>Figure 3.8</b> Average change in evoked spikes six to ten minutes after a root compression applied for 3 or 15 minutes . . . . .	58
<b>Figure 3.9</b> Surgical exposure to apply a 10gf clip to the C7 nerve root . . . . .	60
<b>Figure 3.10</b> Representative images of the nerve root labeled for NF200 and IB4 after a 3 or a 15 minute compression . . . . .	63

<b>Figure 3.11</b>	Schematic representation of the “response-space” between injury parameters and the degree of root injury that develops . . . . .	71
<b>Figure 4.1</b>	Mechanical allodynia after a compression applied for 3 or 10 minutes . . . . .	86
<b>Figure 4.2</b>	Mechanical allodynia following a 15 minute root compression. . . . .	87
<b>Figure 4.3</b>	Device for measuring thermal hyperalgesia in the rat. . . . .	89
<b>Figure 4.5</b>	Thermal hyperalgesia after a 3 or a 15 minute nerve root compression . . . . .	91
<b>Figure 4.5</b>	Mechanical allodynia after a 3 or a 15 minute nerve root compression . . . . .	92
<b>Figure 5.1</b>	GLT-1 expression in the superficial laminae at days 1 and 7 after a root compression applied for 3 or 15 minutes . . . . .	108
<b>Figure 5.2</b>	GLAST expression in the superficial laminae at days 1 and 7 after a root compression applied for 3 or 15 minutes . . . . .	109
<b>Figure 5.3</b>	EAAC1 expression in the superficial laminae at days 1 and 7 after a root compression applied for 3 or 15 minutes . . . . .	110
<b>Figure 5.4</b>	Mechanical allodynia at day 7 after 3 or 15 minute root compressions . . . . .	115
<b>Figure 5.5</b>	Total number of evoked spikes in the superficial laminae at day 7 after a 15 minute compression . . . . .	116
<b>Figure 5.6</b>	Total number of evoked spikes in the deep laminae at day 7 after a 15 minute compression . . . . .	116
<b>Figure 5.7</b>	Neuronal phenotype distribution in the superficial laminae at day 7 . . . . .	117
<b>Figure 5.8</b>	Neuronal phenotype distribution in the deep laminae at day 7 . . . . .	117
<b>Figure 6.1</b>	Spinal GLT-1 expression at day 7 after ceftriaxone treatment. . . . .	141
<b>Figure 6.2</b>	Mechanical allodynia in the ipsilateral forepaw for 7 days for daily ceftriaxone treatments . . . . .	142
<b>Figure 6.3</b>	Mechanical allodynia in the contralateral forepaw for 7 days for daily ceftriaxone treatments . . . . .	144
<b>Figure 6.4</b>	Thermal hyperalgesia for 7 days for daily ceftriaxone treatments . . . . .	145



<b>Figure 6.5</b>	Spinal GFAP expression at day 7 after daily ceftriaxone treatments . . .	146
<b>Figure 6.6</b>	Spinal GLAST expression at day 7 after daily ceftriaxone treatments . . .	147
<b>Figure 6.7</b>	Mechanical allodynia at day 7 after daily ceftriaxone treatments . . .	149
<b>Figure 6.8</b>	Spinal neuronal excitability at day 7 after daily ceftriaxone treatments . . .	150
<b>Figure 6.9</b>	Phenotype distribution of spinal neurons at day 7 after daily ceftriaxone treatments . . . . .	151
<b>Figure 7.1</b>	Mechanical allodynia for 7 days after Riluzole treatment at day 1 . . .	179
<b>Figure 7.2</b>	Thermal hyperalgesia for 7 days after Riluzole treatment at day 1 . . .	180
<b>Figure 7.3</b>	Representative images of the nerve root labeled for NF200, CGRP and IB4 after a nerve root compression treated with Riluzole . . . . .	181
<b>Figure 7.4</b>	Spinal CGRP at day 7 after a day 1 Riluzole treatment . . . . .	183
<b>Figure 7.5</b>	Mechanical allodynia at day 7 after a day 1 Riluzole treatment . . . . .	184
<b>Figure 7.6</b>	Neuronal excitability at day 7 after a day 1 Riluzole treatment . . . . .	185
<b>Figure 7.7</b>	Firing rate of WDR and LTM neurons in response to light brushing and a noxious pinch . . . . .	187
<b>Figure 8.1</b>	Schematic of the temporal behavioral, neuronal, and glutamatergic responses in the forepaw, nerve root and spinal cord . . . . .	198
<b>Figure 8.2</b>	Effects of ceftriaxone and Riluzole on radicular pain and associated neuronal and glutamatergic responses in the root and spinal cord . . . . .	203
<b>Figure 8.3</b>	Proposed schema of the neuronal and glutamatergic responses in the nerve root and spinal cord after a painful 15 minute compression . . . . .	217
<b>Figure A.1</b>	Example post-stimulus histogram generated by Spike2 . . . . .	226
<b>Figure A.2</b>	Dialogue box specifying settings for a post-stimulus histogram . . . . .	227
<b>Figure A.3</b>	Screen shot showing a stimulus train applied to the forepaw and extracellular potentials recorded in the spinal cord . . . . .	228
<b>Figure A.4</b>	Dialogue box to generate a post-stimulus histogram in Spike2 . . . . .	229

---

# CHAPTER 1

## Introduction & Background

---

### 1.1 Introduction

Studies in Europe and North America estimate the annual incidence of neck pain to range from 10-21% (Côté et al. 2004, Hoy et al. 2010) and that up to two-thirds of individuals will experience neck pain in their lives (Côté et al. 1998). As many as 35-66% of those cases persist for at least one year (Hoy et al. 2010), and are defined as “chronic.” In the United States, health care costs for individuals with spine-related pain are as high as 70% greater for than those without; in 2005, total annual health care expenditures for individuals with spine-related pain in the United States was estimated to be \$85 billion (Martin et al. 2008). Although neck pain can be attributed to a variety of spinal tissues, including the facet joints, ligaments, and surrounding musculature, the cervical nerve roots are particularly vulnerable to mechanical injury due to foraminal impingement, disc herniation, direct spinal trauma, and/or foraminal stenosis (Cornefjord et al. 1997, Krivickas & Wilbourn 2000, Nuckley et al. 2002, Olmarker et al. 1989a, Panjabi et al. 2006, Wainner & Gill 2000).

Pain, as defined by the International Association for the Study of Pain (IASP) is “an unpleasant sensory and emotional experience associated with actual or potential tissue damage, or described in terms of such damage” (Merskey & Bogduk 1994).

According to the IASP, *pain* is a psychological state and, as such, the pain field defines specific types of hypersensitivities that often accompany the sensation of pain, such as allodynia and hyperalgesia, to provide both clinicians and researchers with objective methods to assess the presence pain (DeLeo & Winkelstein 2002, Merskey & Bogduk 1994, Mogil 2009, Sandkuhler 2009). *Allodynia*, defined by the IASP is “pain due to a stimulus that does not normally provoke pain,” while *hyperalgesia* is “increased pain from a stimulus that normally provokes pain” (Merskey & Bogduk 1994). In rodent models, allodynia is commonly reported as an increase in the number of painful responses (i.e. paw withdrawals) that are evoked by a normally innocuous stimulus. Hyperalgesia, on the other hand, is often reported as a lowered threshold for eliciting a response to a noxious stimulus. Mechanical and thermal hypersensitivity are the two most commonly utilized behavioral tests in animal models of chronic pain (Mogil 2009). Although thermal hyperalgesia can describe a lowered threshold to a cold or hot stimulus, the studies in this thesis refer to thermal hyperalgesia as a lowered threshold to heat. It is important to distinguish that noxious stimuli are those that can cause tissue damage and “nociception” is the neural process and associated cellular mechanisms of encoding noxious stimuli by nociceptive neurons (Merskey & Bogduk 1994, Sandkuhler 2009). Pain that is caused by a lesion or a disease of the central or peripheral nervous system is broadly defined as neuropathic pain (Merskey & Bogduk 1994, Sandkuhler 2009). Radicular pain describes a specific subtype of neuropathic pain that is associated with nerve root lesions (Merskey & Bogduk 1994, Wainner & Gill 2000).

The clinical syndrome of cervical radiculopathy encompasses a pathology of the cervical nerve roots with symptoms of pain and numbness that radiate from the spine to

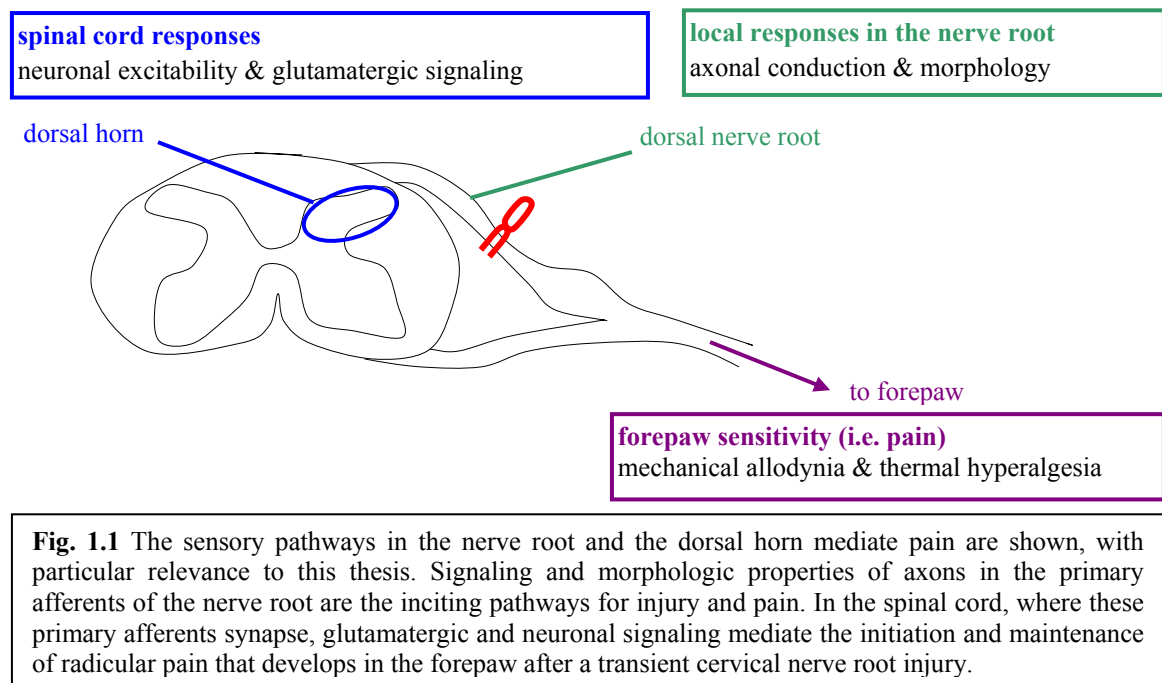
the shoulders, arms, and hands (Abbed & Coumans 2007, Wall & Melzack 1994). Disc herniation and cervical spondylosis are common sources of sustained loading to the nerve root (Abbed & Coumans 2007). Yet, nerve roots are also susceptible to transient loading via trauma from sports and automotive injuries (Krivickas & Wilbourn 2000, Panjabi et al. 2006, Stuber 2005, Tominaga et al. 2006). Although each of these loading scenarios can result in pain (Bergfield & Aulicio 1988, Swanik et al. 1996), only a subset of them actually develops into *chronic* pain (Mogil 2009). Identifying critical loading conditions, such as the duration of the applied insult, that induce chronic pain after transient nerve root compression will help understand and design for the prevention and diagnosis of painful radiculopathy. Studies to investigate nociceptive-related responses within the nerve root and spinal cord, including neuron activity and chemical signaling, will provide insight into treating painful radiculopathy by identifying the critical neurochemical pathways that contribute to chronic radicular pain.

The studies detailed in this thesis use a rat model of cervical radiculopathy to define the mechanical and neuronal mechanisms of nerve root-mediated pain. The relationship between the duration of a nerve root compression and afferent signaling through the nerve root is first established by identifying the critical duration of compression that reduces the frequency of peripherally-evoked action potentials through the nerve root *during* its compression. For compression durations that are above or below that critical duration, additional studies evaluate the firing rate of action potentials through the root immediately after compression was removed and the subsequent development of axonal pathology in the root, spinal neuronal hyperexcitability and behavioral sensitivity. Together, those studies describe the relationship between

compression duration, behavioral sensitivity and associated neuronal pathologies in both the nerve root and the spinal cord. To characterize the contribution of the glutamatergic system to nerve root-mediated pain, the temporal expression of spinal glutamate transporters is quantified after both painful and nonpainful nerve root compressions; different drugs are used to (1) modulate the spinal expression of the glutamate transporter, GLT-1 and (2) inhibit pre-synaptic glutamate release, separately. Ceftriaxone was administered by daily lumbar punctures in order to increase the expression of GLT-1 and, therefore, reduce extracellular glutamate concentrations in the central nervous system (Rasmussen et al. 2011). In a separate study, the sodium channel blocker, Riluzole, was administered by a single intraperitoneal injection in order to inhibit glutamate release by pre-synaptic neurons (Wu et al. 2013). Behavioral sensitivity and neuronal hyperexcitability were quantified following both treatments to determine relative pain symptoms when glutamate uptake is increased or when glutamate release is inhibited. Despite the multi-dimensional aspects of pain, mechanical allodynia is the only behavioral assessment that has been characterized for transient cervical nerve root compressions to date. Therefore, the studies in this thesis also assess the development and maintenance of both mechanical allodynia and thermal hyperalgesia following compression durations above and below the critical duration described earlier, and for each of the pharmacological interventions.

The three aims and associated hypotheses of this thesis are summarized in the next chapter (Chapter 2), which also outlines the organization of the remaining chapters. Specific background is presented separately in each chapter, as appropriate to those topics, hypotheses and specific experiments. The general background material presented

in this chapter is intended to provide relevant information on the topics of nerve root anatomy, cervical radiculopathy and nerve root biomechanics. That foundation in the anatomy and biomechanics of the nerve roots provides the context for the discussions of animal models of radiculopathy and the sensory circuits involved in pain that follow. A brief overview is included describing neuronal circuits in the nerve root and dorsal horn of the spinal cord (Fig. 1.1) and also a general description of synaptic glutamatergic signaling in the central nervous system. Axonal conduction and morphology are the focus here, as related to the primary afferents in the nerve root; the role of spinal glutamate and spinal neuronal signaling in mediating neuropathic pain is also described (Fig. 1.1).



## 1.2 Background

### 1.2.1 Cervical Spine & Nerve Root Anatomy

The vertebral column of the spine consists of 33 vertebrae, divided into five separate anatomic regions: cervical, thoracic, lumbar, thoracic, sacral, and coccygeal.

There are seven vertebrae in the cervical region (Martini et al. 2003). The spinal canal is formed by the vertebral foramen of each bony vertebra that encloses and surrounds the spinal cord (Fig. 1.2A). The bilateral pedicles lie along the posterolateral border of each vertebral foramen and the opposing pedicles from the adjacent vertebrae collectively form the intervertebral foramen that encloses the afferent (dorsal) and efferent (ventral) nerve roots as they extend from the spinal cord to the periphery at each spinal level (Fig. 1.2A) (Haller et al. 1971, Martini et al. 2003, Olmarker 1991, de Peretti et al. 1989). A pair of afferent and efferent nerve roots fuses together at each spinal level to form a nerve as the dorsal and ventral roots pass through the foramen (Haller et al. 1971, Martini et al. 2003).

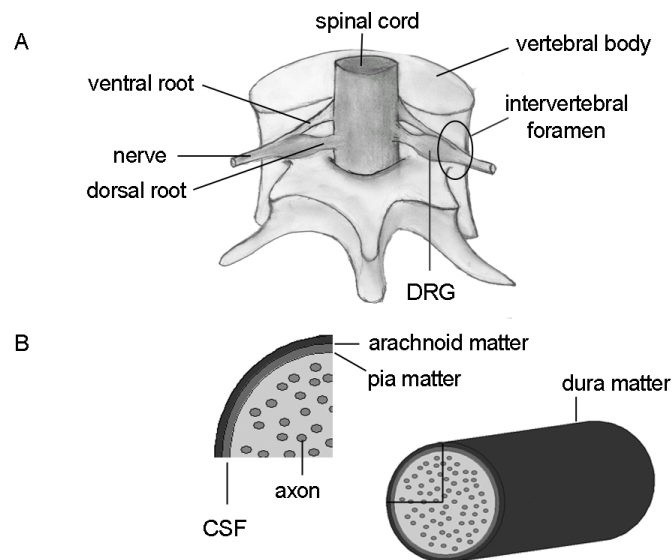


**Fig. 1.2** Relevant spinal and nerve root anatomy. **(A)** Dorsal view of the ventral and dorsal roots exiting the spinal cord and forming a nerve as they pass through the intervertebral foramen formed by the adjacent vertebrae. The dorsal root ganglion (DRG) is at the distal end of the dorsal nerve root and contains the cell bodies of afferent axons. **(B)** Schematic showing a generic nerve root, its structures and the organization of its axons. The nerve root is enclosed by three layers of meninges (pia matter, arachnoid matter, dura matter); cerebrospinal fluid (CSF) lies between the arachnoid and pia matter. For clarity, the outlined region in the oblique view is enlarged.

Once the nerve enters the periphery, it branches out as the individual axons within it continue towards their specific sites of innervation. By convention, in the cervical region, each nerve root is named for the spinal level of the vertebra inferior to (i.e. below) it; although, in the remaining regions of the spine the nerve roots are named for their superior vertebra. Despite there being only seven cervical vertebrae, the nerve root between the lowest cervical vertebra (C7) and the next first thoracic vertebra (T1) is named as the C8 nerve root (Martini et al. 2003).

At each spinal level, the ventral and dorsal nerve roots exit the spinal cord anteriorly and posteriorly, respectively (Figs. 1.2 & 1.3) (Martini et al. 2003). The efferent neurons that relay information from the spinal cord to the periphery compose the ventral nerve root. The afferents, which relay information from the periphery to the central nervous system, are contained in the dorsal nerve root. As the ventral and dorsal nerve roots pass through the intervertebral foramen, they join together to form a spinal nerve. At the distal, more-peripheral, end of the dorsal nerve root there is a visible enlargement called the dorsal root ganglion (DRG) that contains the cell bodies of the afferent neurons (Figs. 1.2 & 1.3). The cell bodies of the efferent neurons in the ventral nerve root lie within the spinal cord (Figs. 1.2 & 1.3). Due to the separation of afferents and efferents, an injury to a single dorsal or ventral nerve root has either sensory or motor consequences.



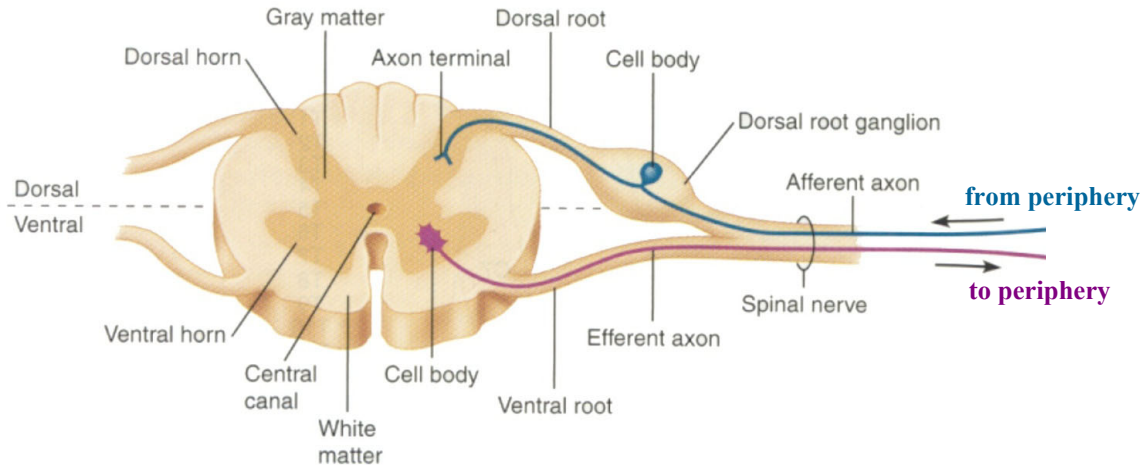


**Fig 1.3** Axial section of the spinal cord and the nerve roots that exit towards the periphery. The primary afferent axons transmit sensory information from the periphery to the primary synapse at the axon terminal in the dorsal horn of the spinal cord. (adapted from Germann & Stanfield 2002)

The nerve root is a collection of axons enclosed together by three layers of meninges (Fig. 1.2) that form synapses with second order neurons in the dorsal horn of the spinal cord (Fig. 1.3) (Haller et al. 1971, Martini et al. 2003). The meninges are organized, from deep to superficial: the pia mater, the arachnoid mater, and the dura mater. Cerebrospinal fluid (CSF) flows within the subarachnoid space, between the arachnoid mater and pia mater, and transports nutrients and chemical messengers to the neural tissues (Martini et al. 2003). The dura mater of the nerve roots is continuous with the epineurium of the nerve, as well as with the dura mater of the spinal cord.

Anatomically, the nerve roots are protected by the meninges, the CSF and the bony elements that surround them. The dura is thought to provide much of the tensile support for the nerve roots (Beel et al. 1986, Maikos et al. 2008). Tensile testing of the dura mater of rat cranial and spinal dura mater has shown it to be 2-1,000 times stiffer than the neural tissue it surrounds, suggesting a similar role for the dura of the nerve roots (Maikos et al. 2008). Just as the meninges protect the afferent axons in tension, the CSF

and vertebrae protect the nerve root from compressive forces. The CSF protects the neural tissue it encloses, including the brain and spinal cord, by damping any blunt forces to these structures (Ommaya 1968). However, it has also been hypothesized that the pressure gradients that can be established within the CSF surrounding the spinal cord and nerve roots during rapid motions of the spine, such as can occur during trauma, can be sufficiently high to cause injury to the axons within the nerve root (Boström et al. 1996, Svensson et al. 1993). The intervertebral foramen, through which the nerve roots pass, normally protects them from direct blunt trauma. However, rapid and/or nonphysiological motions of the neck that is associated with trauma can narrow the intervertebral space, and compress the nerve root (Nuckley et al. 2002, Panjabi et al. 2006, Tanaka et al. 2000). Osteoarthritis of the intervertebral foramen, known as spondylosis, can also narrow the foramen and impinge on the nerve roots that pass through it (Wainner & Gill 2000). Therefore, although the CSF and the adjacent vertebrae provide mechanical protection to the nerve roots under normal conditions, these fluid and bony structures may themselves compress the nerve roots when trauma and/or degenerative disease is present.

### **1.2.2 Cervical Radiculopathy**

Nerve roots are susceptible to injuries from a variety of trauma-related causes in the neck, as well as additional local changes in the surrounding environment that result from progression of other diseases and/or disorders (Abbed & Coumans 2007). For example, nerve roots can be injured from a slow-onset foraminal narrowing due to aging

or from a disc herniation that can impart both mechanical and inflammatory influences on the nerve root (Abbed & Coumans 2007, Jenis & An 2000). In addition, traumatic loading events of the cervical spine can compress the nerve root by altering the geometry of the intervertebral foramen or by putting the nerve root in traction when stretching of the spinal cord generates tension along the nerve roots (Sairyo et al. 2010, Sunderland 1974). Brachial plexopathies, commonly referred to as *burners* or *stingers*, is a collection of trauma-related nerve root injuries that are hypothesized to be caused by traction or compression to the nerve roots in the cervical region of the spine (Clancy et al. 1977, Stuber 2005). Compression-related burners can occur when there is compression of the nerve root by the intervertebral foramen as a result of cervical spine extension that is combined with rotation, lateral flexion, and/or compression of the spine (Stuber 2005). Traumatic nerve root injuries occur over rapid time frames with high-magnitude loads applied to the tissue. In contrast, nerve root injuries associated with local pathologies often have a slower-onset of loading than those associated with trauma and can be more chronic in nature.

Both trauma- and pathology-induced nerve root injuries can produce symptoms of varying severity and persistence. Clinically, nerve root injuries can manifest as radicular pain and numbness, and/or deficits in motor and reflex functions (Abbed & Coumans 2007, Wainner & Gill 2000). The severity of the symptoms can be classified as *acute*, *subacute*, or *chronic* (Abbed & Coumans 2007). Acute radiculopathy typically results from a traumatic event and presents with the most severe pain, often described as “sharp” or “burning” pain that can be persistent. The symptoms of subacute radiculopathy, on the other hand, are typically short-lived, but may be reoccurring. Subacute radiculopathy is

most-often associated with a pre-existing condition of the spine such as spondylosis. Both acute and subacute radiculopathy can develop into chronic radiculopathy when the symptoms do not respond to treatment (Abbed & Coumans 2007, Thoomes et al. 2013). The specific location of the presenting symptoms after a nerve root injury depends on which nerve root is injured. In general, areas of skin are innervated by a single nerve root; the term *dermatome* is used to describe such an area of skin. Injuries to the C7 nerve root, for example, result in sensitivity and numbness in the associated dermatome, which includes the arm, forearm, and middle finger (Abbed & Coumans 2007). Injuries to the C4 nerve root affect the neurons that innervate the back of the neck and shoulder regions (Abbed & Coumans 2007). Clinical studies cite the C7 nerve root as the most commonly affected cervical root in patients diagnosed with cervical radiculopathy, with a reported incidence rate of 46-69% (Carette & Fehlings 2005, Kuijper et al. 2009, Wainner & Gill 2000).

Treatment for radiculopathy can be broadly categorized into operative and non-operative interventions (Carette & Fehlings 2005, Thoomes et al. 2013, Wainner & Gill 2000). When surgery is appropriate, the most common procedure is an anterior cervical decompression and fusion (ACDF) to relieve the nerve root of impingement by the local vertebrae and/or the intervertebral disc (Wainner & Gill 2000). A posterior surgical approach involving a laminectomy or laminoplasty is often used when multiple levels of decompression are required (Carette & Fehlings 2005). Surgical complications are not common (<5% incident rate), but can be severe, including spinal cord injury, nerve palsy, perforation of the esophagus and/or mechanical failure of implanted instruments (Carette

& Fehlings 2005). For these reasons, non-operative treatments are preferred as the first course of therapy for radicular pain.

In most cases, cervical radiculopathy is initially treated conservatively with analgesics, physiotherapy or immobilization (Thoomes et al. 2013). The current analgesic agents for radiculopathy fall into two categories: opioids and nonsteroidal anti-inflammatory drugs (NSAIDs) (Carette & Fehlings 2005, Thoomes et al. 2013). However, there is limited clinical data regarding the effectiveness of each type of drug and there are significant risks associated with each, including addiction (opioids) and renal failure (NSAIDs) (Carette & Fehlings, Kuijper et al. 2009, Thoomes et al. 2013). Epidural nerve root injections, also known as *nerve root blocks*, are another common treatment for cervical radiculopathy and can provide long-term relief for up to 60% of patients (Carette & Fehlings 2005). Like surgery, complications to nerve root blocks are rare, but can be severe, and include spinal cord or brainstem infarctions that can cause severe neurological damage (Carette & Fehlings 2005). When taken as prescribed, analgesics carry the least risk. However, due to a lack of clinical evidence that opioids and NSAIDs are effective in resolving radicular pain (Carette & Fehlings 2005, Kiuipper et al. 2009), a 2011 report commissioned by the National Institute of Health (NIH), cites a critical need for new pharmacological approaches to treat chronic pain (Institute of Medicine 2011).

### **1.2.3 Nerve Root Biomechanics**

As with other soft tissues in the body, the response of neural tissue to mechanical loading depends on the size, shape, organization, and composition of that tissue (Beel et

al., 1986, Maikos et al. 2008, Ommaya 1968, de Peretti et al. 1989). Additionally, the mechanical properties depend on the specific conditions related to loading, such as the rate and duration of an applied load or deformation (Bedford & Liechti 2000, Fung 1967, Gefen & Margulies 2004). The simplest description of a material's response to mechanical loading relates the amount of stress in the material to the amount of strain. Stress and strain are scaled measures of the force and deformation within a material that are normalized with respect to the geometry of the specimen. As such, they inherently account for shape effects as they contribute to mechanical responses. *Stress* ( $\sigma$ ) is defined as the amount of force over a given cross-sectional area. Accordingly, it can vary with direction and at different points in a structure. *Strain* ( $\epsilon$ ) represents the amount of deformation a material undergoes with respect to its original shape. For a linear elastic material, the amount of stress is linearly related to the amount of strain it experiences, and the slope of the line relating the two is the *modulus of elasticity* ( $E$ ) of the material. Similarly, the relationship between the applied force and the resulting deformation of a structure is described by the *stiffness* of that structure.

Many tissues, including neural tissue, exhibit complicated biomechanical responses that are not easily described by simple linear relationships (Fung 1967, Gefen & Margulies 2004, Hubbard et al. 2008b). *Elastic* materials deform instantaneously with an applied force and, likewise, instantaneously return to their original shape after the applied force is removed. For this type of material, the amount of stress is only a function of strain. *Viscous* fluids demonstrate a time-dependent deformation to an applied load, and the stress that develops in response to that deformation depends on the rate of strain.

In general, neural tissue responds to loading partly as if it were an elastic material, but also by undergoing viscous fluid flow. This type of mechanical behavior is *viscoelastic* and describes many biologic tissues (Fig. 1.4) (Bedford & Liechti 2000, Fung 1967, Navajas et al. 1995, Provenzano et al. 2001).

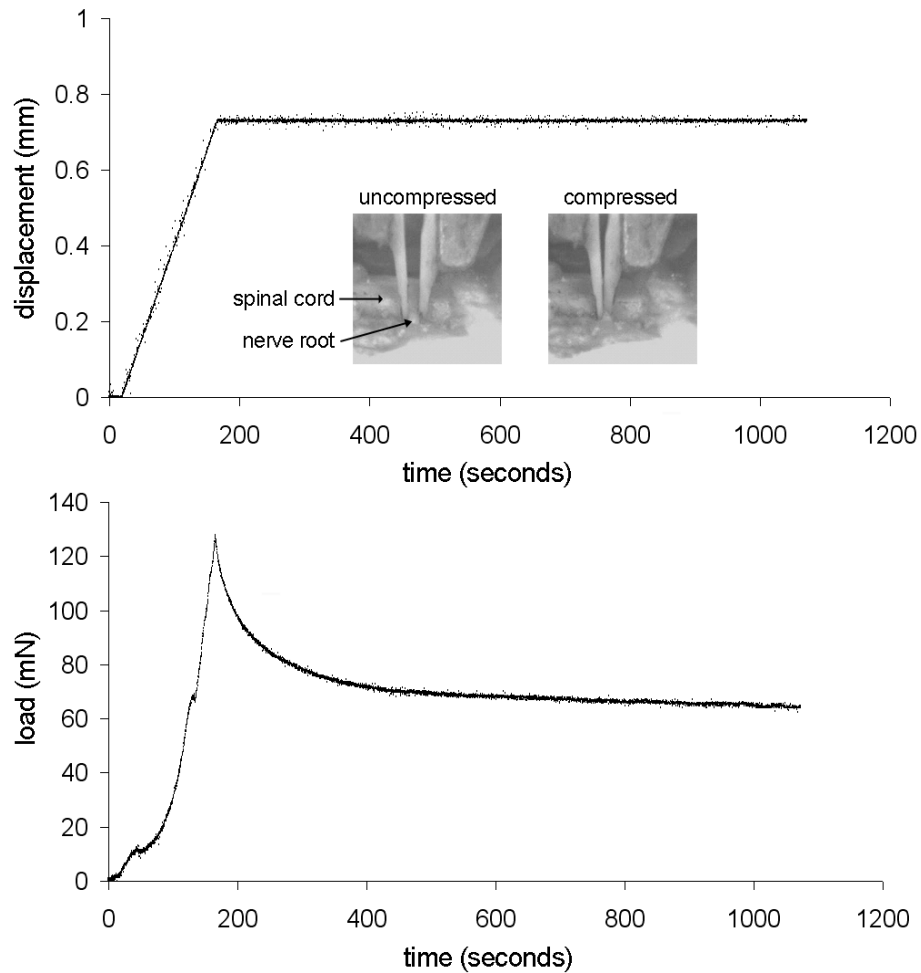


**Fig 1.4** Representative response of the rat nerve root under a compressive displacement of 0.73mm. Images of the nerve root prior to compression (uncompressed) and under compression are shown. After reaching a peak load (127mN), the root undergoes a rapid relaxation in load until the tissue approaches a steady-state equilibrium response. This load-relaxation response is typical of viscoelastic materials.

Nerve roots exhibit viscoelastic responses when loaded (Fig. 1.4). This is due to the mechanical behavior of the materials they contain as well as the interaction between those materials (Haller et al. 1971, Stodieck et al. 1986). Viscoelastic materials exhibit

several time-dependent responses to load; most basically, the stress-strain relationship varies with the rate of loading and with the length of time that a tissue is held under deformation (Fig. 1.4) (Hubbard et al. 2008b). For such tissues, the modulus of elasticity varies with the rate at which the tissue is strained. Additionally, when the tissue is held under constant deformation, the amount of applied stress experienced in the tissue actually decreases with time (Fig. 1.4). Conversely, the tissue will also continue to deform over time when it is held under a constant stress. These two behaviors of the material are referred to as *stress-relaxation* and *creep*, respectively. The specific loading conditions applied to nerves and nerve roots are, therefore, important to consider when describing the mechanical response of these tissues.

The mechanical behavior of neural tissues in compression or tension is typically characterized by reporting the load-deformation or stress-strain behavior as described above, but for specific rates of loading. The typical stress-strain curve describing the elastic response has three distinct regions; a toe region, a linear region, and a yield or failure region (Beel et al. 1986, Haftek 1970, Kwan et al. 1992, Singh et al. 2006). In the toe region, the tissue can undergo substantial deformation with the generation of only minimal force. For example, the isolated tibial nerve of the rabbit can sustain tensile strains as large as 15% before any appreciable stress develops in that tissue (Kwan et al. 1992). As neural tissue undergoes further tensile deformation beyond the initial toe region, more force is required to produce the deformation, and the slope of the load-deformation curves becomes approximately linear. Finally, as deformation continues and the nerve or nerve root is stretched beyond its linear elastic region, the tissue will begin to yield, marked by a reduction in slope of the stress-strain slope. As with other materials,



yield indicates the initiation of sub-structural failures and is followed by a complete rupture of the tissue that occurs when deformation continues beyond its ability to support any additional force (Martin et al. 1998). Both the stiffness and the yield of the nerve root are important in characterizing thresholds for its injury. A quasi-linear viscoelastic model for *in vivo* compression has been developed for the lumbar nerve roots in the rat (Hubbard et al. 2008b). Using that model, it was determined that deformation thresholds for axonal injury in the nerve root depend on the rate of loading. Specifically, the displacement required to reach the magnitude threshold for inducing axonal injury is 23% less when the root is dynamic loaded (2mm/sec) compared to quasistatic loading (0.004mm/sec) (Hubbard et al. 2008b). Magnitude and duration thresholds for nerve root injuries are likely similarly modulated by the loading rate. To date, that study by Hubbard et al. (2008) is the only reported experimental work defining the compressive stress-strain properties of the nerve root, owing largely to experimental challenges that exist with making such measurements to these small and very soft materials. Although the mechanical properties of nerve roots in compression is limited, many studies have reported that the *physiologic* consequences of compression do depend on the magnitude, duration, and rate of loading; these are discussed in more detail in the next section (Section 1.2.4).

#### **1.2.4 *In Vivo* Models of Mechanical Injury to the Nerve Root**

Although complete rupture or separation of the nerve root is certainly an injury, less severe damage to nerve root tissue also produces serious physiological consequences, including tears to the meninges and/or the axon membrane, cytoskeletal fragmentation

within the axons, and impaired blood flow in the nerve root tissues (Clark et al. 1992, Dyck et al. 1990, Garfin et al. 1990, Singh et al. 2009). For that reason, injuries to the nerve root must also be understood in the context of the physiological responses that are induced, as well as the associated mechanical response of the axons, meninges and CSF that make up the nerve root. Specific clinical symptoms of nerve root injury include weakness, paralysis, pain and sensitivity (Abbed & Coumans 2007, Jensen & Baron 2003, Woolf & Mannion 1999). However, the severity of these symptoms is not always easily quantifiable, making it difficult for clinicians to diagnose and treat the condition. Pain, in particular, is difficult to evaluate objectively because the sensation and verbal description of pain can vary from one individual to another (Backonja & Stacey 2004). Although pain is subjective and is not typically quantified, increased sensitivity to stimuli can be evaluated in humans and in animal models. Allodynia is one measure of behavioral sensitivity that provides a quantitative assessment of increased sensitivity to a nonpainful stimulus and can be measured by counting the frequency of responses that is evoked for a given stimulus. Other methods for measuring pain in animal models include observing changes in gait, posture or the frequency of directed behaviors such as guarding or licking (Mogil 2010).

Nerve roots are subject to many loading conditions that modulate their physiology. It has been demonstrated in animal models that compression to the nerve root can produce a host of biologic responses, including behavioral hypersensitivity, decreased axonal conduction velocity and blood flow, as well as edema and swelling (Garfin et al. 1990, Hubbard & Winkelstein 2005, Igarashi et al. 2005, Olmarker et al. 1989a,b). Moreover, many of these physiologic responses depend on the magnitude,

duration and rate of applied tissue compression (Kobayashi et al. 1993, 2005a,b, Olmarker et al. 1989a,b, Pedowitz et al. 1992). In a study of compression to the cauda equina in pigs, blood flow in the capillaries of the nerve roots was stopped for compression pressures above 40mmHg (Olmarker et al. 1989b). In a similar model, compression of 100mmHg resulted in a decrease in the amplitude of axonal conduction after 30 minutes of applied compression, while 200mmHg produced an immediate decrease in axonal conduction amplitude with complete blockage of axonal conduction if applied for 100 minutes (Garfin et al. 1990). Similarly, the rate of compression has also been shown to affect neuronal function. Olmarker et al. (1990) demonstrated a more-pronounced decrease in conduction velocities if the porcine nerve root is compressed rapidly when compared to slower compression rates. These findings indicate a multidimensional response of the nerve root physiology to compressive loading that is sensitive to magnitude, duration, and rate.

Studies of nerve root injury in the rat show that functional and sensory behavioral changes are modulated by the *degree* of tissue deformation, the *magnitude* of compression load, and the *duration* of the applied compression (Hubbard et al. 2008a, Rothman et al. 2010, Winkelstein et al. 2002). For example, a compression load of only 26mN to the rat C7 nerve root for 15 minutes elicits behavioral sensitivity in the forepaw within 24 hours, but a compression load of 38mN is required to induce behavioral mechanical sensitivity that is sustained for 1 week (Hubbard et al. 2008a). Using that same rat model, for similar magnitudes of load, allodynia is significantly elevated after 15 minutes of compression compared to that produced for a compression applied for only 30 seconds (Rothman et al. 2010). In that study, the loads applied to the nerve root were

above the threshold previously identified for inducing sustained allodynia (Hubbard et al. 2008a). The magnitude threshold for producing changes in behavioral sensitivity at this shorter duration of compression (30 seconds) was hypothesized to be higher than that needed for a longer duration of compression (Rothman et al. 2010). The amount of strain applied to the nerve root in compression also modulates allodynia. Both 19% and 42% of strain to the L5 nerve root of rats elicits increased sensitivity in the hind paw, with more sensitivity for higher tissue strains (Winkelstein et al. 2002). Identifying the mechanical basis by which transient and chronic nerve root injuries are produced is an important step in understanding the mechanisms by which clinical symptoms vary with respect to the magnitude and duration of a nerve root compression.

In order to study pain responses and relationships to tissue loading, a rat model of transient C7 nerve root compression was developed (Hubbard & Winkelstein 2005, Hubbard et al. 2008a) (Fig. 1.4). The dermatome associated with the C7 nerve root in the rat includes the forepaw and studies establish that transient compressions to this root elicit persistent forepaw sensitivity (Hubbard & Winkelstein 2005, Takahashi & Nakajima 1996). Increased sensitivity in that model of cervical radiculopathy develops within one day of the injury and can persist for nearly four weeks (Rothman et al. 2007). Due to the different rates of development and aging between rats and humans, that study suggests that a transient nerve root compression could produce pain for at least 14 months in humans (Andreollo et al. 2012, Rothman et al. 2007). That same model of a transient cervical nerve root compression also shows that the development of behavioral sensitivity is modulated by both the magnitude and duration of compression (Hubbard et al. 2008a, Rothman et al. 2010).

Painful transient nerve root compression produces an early inflammatory response in the nerve root tissues, spinal inflammation, and axonal damage in the compressed root (Hubbard & Winkelstein 2005, Hubbard & Winkelstein 2008, Hubbard et al. 2008a,b, Rothman et al. 2009a,b, Rothman et al. 2010). In the context of that model, a transient injury to the nerve root is one that is not sustained, but can last for up to 15 minutes. Although this duration can be longer than those associated with most traumatic events, it is considerably shorter than a sustained compression that can last for one day to several weeks (Colburn et al. 1999, Hashizume et al. 2000, Kobayashi et al. 2004). Within one hour of a compression of the C7 nerve root that is sufficient to produce persistent behavioral sensitivity, mRNA levels of the inflammatory cytokines, IL-6 and TNF- $\alpha$ , are elevated in the ipsilateral DRG spinal cord (Rothman et al. 2009b). This almost immediate increase in pro-inflammatory cytokine mRNA levels provides evidence that the early response of afferents to a transient compression may play a role in establishing the persistent pain that develops following nerve root trauma.

As early as one day after that same painful nerve root injury, hallmarks of spinal inflammation, including activation and proliferation of microglia, also develop (Rothman et al. 2009a). Further, by seven days after a transient painful injury, the axons of the injured nerve root show signs of degeneration and the spinal inflammation becomes even more pronounced, with both activated astrocytes and microglia (Hubbard & Winkelstein 2005, Hubbard & Winkelstein 2008). Together with a decrease in neuropeptide expression in the spinal cord at this same time point (Hubbard et al. 2008a), the pathology of the nerve root axons suggests that neuronal signaling through the nerve root to the spinal cord may be altered following a painful injury. Although these prior studies

collectively demonstrate that transient cervical nerve root compression produces a host of nociceptive responses, they do not address *how* the neural tissue responds during the applied compression or whether the neuropathologies that develop in the root are associated with dysfunctional signaling in the central nervous system.

### **1.2.5 Nociception in the Nerve Root & Spinal Cord**

Axons in the nerve root are categorized with respect to their degree of myelination and physiologic properties (Basbaum et al. 2009, Wall & Melzack 1994). Myelinated, A fibers include the A $\beta$  fibers that respond to nonnoxious mechanical stimulation, and the A $\delta$  nociceptors that transmit acute, “fast” pain (Basbaum et al. 2009, Todd 2010). The smaller, unmyelinated, C fibers transmit diffuse, “slow” pain (Basbaum et al. 2009, Todd 2010). The C fibers are further classified into two subpopulations according to their biochemical properties: (1) peptidergic and (2) non-peptidergic fibers. Peptidergic fibers release neuropeptides, such as substance P, while non-peptidergic fibers express the c-Ret neurotrophic receptor and bind isolectin-IB4 (Basbaum et al. 2009). Dorsal nerve root crush can produce degeneration of both myelinated and unmyelinated axons in the nerve root (Di Maio et al. 2011, Ramer et al. 2000). Treatments that selectively restore only the population of myelinated nerve root fibers after the crush injury do not restore sensation by day 20 (Ramer et al. 2000). Only when treated with the neurotrophic factor, glial cell line-derived neurotrophic factor (GDNF), that promotes neuronal survival, do both fiber populations regenerate and does sensation return to the forepaw (Ramer et al. 2000),

suggesting that normal function and sensation requires preservation of *both* myelinated and unmyelinated fibers.

Mechanical trauma to neural tissue, including the nerve root, damages the cytoskeleton of the neurons and impairs action potential conduction through them (Chen et al. 1992, Jancalek & Dubovy 2007, LaPlaca & Prado 2010, Serbest et al. 2007). Neurofilaments are one of the major components of the neuron cytoskeleton; they give axons their mechanical strength and stability and are involved in axonal transport (Serbest et al. 2007). Blunt force trauma to, or stretching of, neurons disrupts their neurofilament structure, resulting in a loss of axonal transport and an accumulation of neurofilament proteins within the axon (Chen et al. 1992, Serbest et al. 2007). Mechanical trauma to axons also damages the plasma membranes and myelin sheath, preventing the propagation of action potentials, which is required for neuronal signaling (Chen et al. 1992, Mosconi & Kruger 1996, Serbest et al. 2007, Staal & Vickers 2011). For the axons in the nerve root, the magnitude of an applied compression has been shown to determine whether Wallerian degeneration develops and axonal transport is reduced; each of these pathologies are only evident if the magnitude of compression is sufficiently large (Hubbard & Winkelstein 2008, Kobayashi et al. 2005). Furthermore, the magnitude threshold for reducing the expression of neurofilament proteins in the nerve root is similar to the magnitude threshold for eliciting persistent mechanical allodynia in the rat after a nerve root compression (Hubbard & Winkelstein 2008, Hubbard et al. 2008a). This close relationship between axonal pathology in the root and behavioral sensitivity strongly suggests that morphological changes in the nerve root may be an indicator, if not a contributor, to nerve root-mediated pain (Hubbard & Winkelstein 2008).

In the dorsal horn of the spinal cord, sensory neurons are categorized by their response to different types of stimuli, which is dictated by the type(s) of primary afferents that synapse with them (Basbaum et al. 2009, Todd 2010, Urch & Dickenson 2003, Woolf & Fitzgerald 1983). In general, the nociceptive C fibers terminate in the superficial laminae (I-II) of the dorsal horn and the mechanoreceptors terminate in the deep laminae (III-V) (Fig. 1.5A) (Basbaum et al. 2009, Todd 2010). Second order neurons that selectively respond to innocuous stimuli are low-threshold mechanoreceptors (LTMs), while nociceptive specific (NS) neurons are only activated by noxious stimuli (Fig. 1.5B) (Hains et al. 2003, Saito et al. 2008). Wide dynamic range (WDR) neurons receive both nonnoxious and noxious stimuli and there is a positive correlation between the frequency of firing by these neurons and the strength of the input stimulus (Fig. 1.5B) (Hains et al. 2003, Urch & Dickenson 2003).

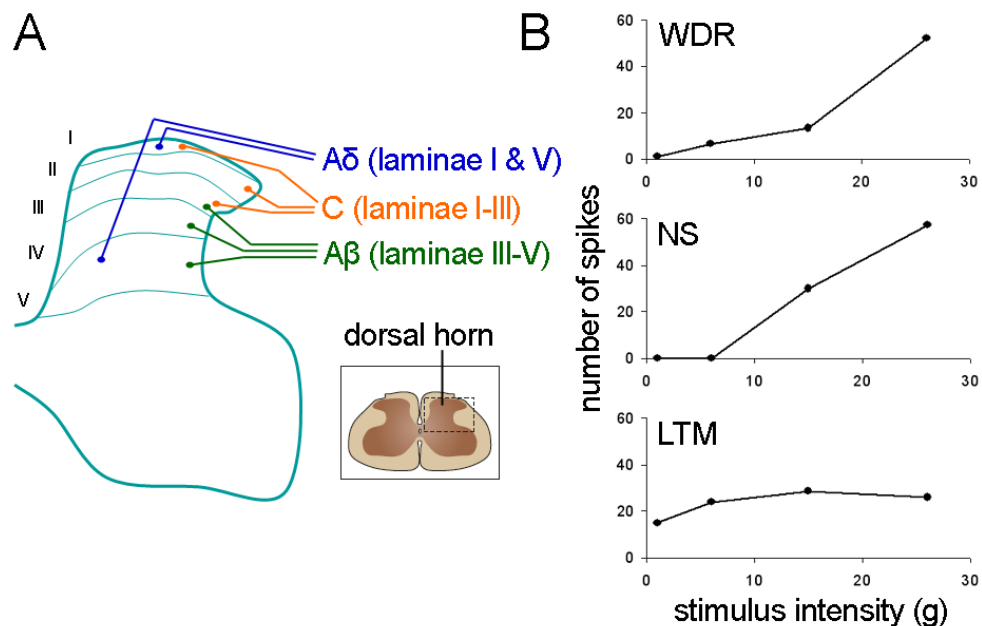


**Fig. 1.5 (A)** The A and C fibers synapse in distinct regions of laminae I-V of the dorsal horn. **(B)** Characteristic responses of wide dynamic range (WDR) and nociceptive specific (NS) neurons, and low threshold mechanoreceptors (LTMs) in the spinal cord when mechanical stimuli of graded magnitudes (1-26g) are applied to the peripheral tissues. (parts of this figure are adapted from Todd 2010)



Electrophysiological recordings in the spinal cord of rats demonstrate that mechanical deformation to neural tissues changes the frequency of evoked action potentials through the deformed region (Cata et al. 2006, Hains et al. 2003, Terashima et al. 2011, Urch & Dickenson 2003). Electrically-evoked compound action potentials, which sum the amplitude of action potentials from a group of neurons, decrease in amplitude in the nerve roots of the porcine cauda equina during an applied compression (Garfin et al. 1990, Pedowitz et al. 1992). Although those studies demonstrate that compression of the nerve root can reduce the number of action potentials transmitted by the axons within it, behavioral sensitivity was not evaluated in that context. Therefore, it is not clear whether there is a relationship between the radicular pain and neuronal dysfunction that develops while compression is applied to the nerve root (Garfin et al. 1990, Pedowitz et al. 1992).

After pain is established in rodent models of injury to the peripheral nerve and spinal cord, dorsal horn neurons increase their frequency of firing in response to stimulation by peripheral stimuli (Hains et al. 2003, Hao et al. 1992, Liu et al. 2011, Shim et al. 2005). Although the firing rate of *spontaneous* neurons is known to increase after a painful sustained lumbar nerve root ligation (Terashima et al. 2011), it is not known whether the firing rate of spinal neurons also increases when *evoked* in the periphery by stimuli known to elicit withdrawal responses in rats after a painful nerve root compression (Hubbard & Winkelstein 2005, Rothman et al. 2010). An increase in the firing rate of spinal cord neurons is associated with an increase in the proportion of WDR neurons after a spinal cord hemisection or a constriction of the sciatic nerve (Hains et al.

2003, Keller et al. 2007). However, whether a nerve root compression similarly changes the phenotype distribution of spinal cord neurons is unknown.

### **1.2.6 The Glutamatergic System in the Spinal Cord**

Glutamate is the primary excitatory neurotransmitter in the CNS (Basbaum et al. 2009, Danbolt 2001, Inquimbert et al. 2012). It is released by pre-synaptic neurons, which package the cytoplasmic glutamate of axon terminals in vesicular glutamate transporters (VGluts) (Featherstone 2009, Takamori et al. 2000). When the intracellular calcium concentration of the axon terminal increases in response to an action potential, the VGluts fuse with the plasma membrane allowing the contents (glutamate) to enter the synaptic cleft (Fig. 1.6). Action potentials are generated by voltage-gated sodium channels, which have an activation gate and an inactivation gate (Armstrong 2006). At rest, sodium channels are in their deactivated state, with the activation gate closed and the inactivation gate open. When the transmembrane potential depolarizes, the activated gate opens and there is a fast sodium current as sodium ions rapidly flow into the neuron, further depolarizing the transmembrane potential. The action potential ceases when the inactivation gate of the sodium channel closes. However, a small percentage of sodium channels fail to inactivate and remain activated (open), causing a persistent sodium current that outlasts the fast sodium current during the initial action potential event (Lee et al. 2000, Stafstrom 2007).

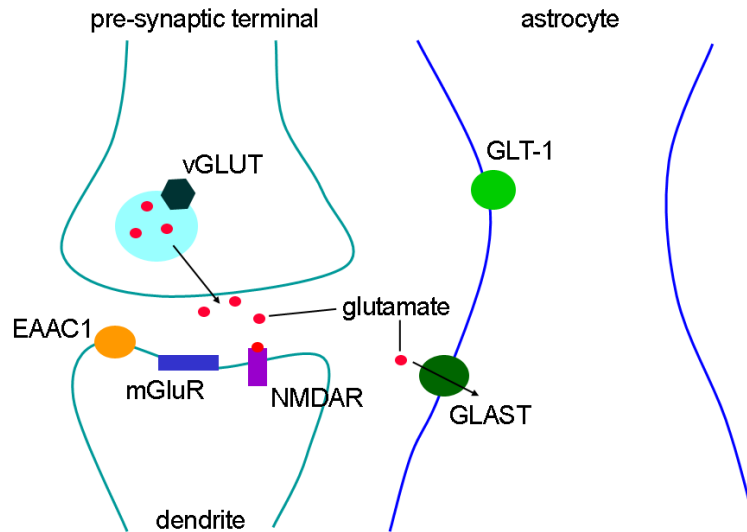


**Fig. 1.6** Synaptic glutamatergic signaling in the central nervous system. Glutamate is released by the terminal of the pre-synaptic axon and activates glutamate receptors (NMDA, mGluR) on the dendritic spine of the post-synaptic neuron. Glutamate transporters on neurons (EAAC1) and astrocytes (GLT-1, GLAST) take up excess extracellular glutamate from the synaptic cleft.

Selective inhibition of the persistent sodium current reduces *repetitive* firing (action potentials) after a single stimulus, decreasing the amount of glutamate released at the pre-synaptic terminal (Bellingham 2010, Lee et al. 2000, Wang et al. 2004). Although there are several sodium channel blockers that preferentially inhibit the persistent sodium current, including Phenytoin, Lamotrigine and Riluzole (Coderre et al. 2007, Stafstrom 2007), Riluzole has been shown to be particularly effective for reducing glutamate concentrations in the CNS (Coderre et al. 2007, Lamanaukas 2008). In fact, spinal glutamate concentrations are reduced by more than 50% within 30 minutes of a systemic injection of Riluzole (Coderre et al. 2007). Although glutamate is required for normal afferent signaling, excess glutamate following traumatic brain and spinal cord injuries can induce excitotoxicity due to overstimulation of glutamate receptors (Basbaum et al. 2009, Ren & Dubner 2008, Tao et al. 2005). Therefore, sodium channel blockers that

have traditionally been used as anesthetics and anticonvulsants, are now being explored for their potential clinical use as a neuroprotective agent after neural tissue injuries.

Once released into the synaptic space, glutamate can either act on a glutamate receptor or be taken up by a glutamate transporter (Fig. 1.6). Under normal conditions the glutamate receptors are responsible for regulating neuronal excitability, but may also contribute to neuro-excitotoxicity when excessively stimulated by glutamate (Basbaum et al. 2009, Ren & Dubner 2008, Tao et al. 2005). The activation of glutamate receptors is regulated by glutamate transporters. However, findings from rodent models of neuropathy indicate that down-regulation of these transporters in the spinal cord may contribute to persistent behavioral sensitivity (Hu et al. 2010, Sung et al. 2003, Xin et al. 2009). Three excitatory amino acid transporters (EAATs) have been identified in the human spinal cord (Queen et al. 2007): EAAT1 and EAAT2 are expressed on glial cells and their rodent homologues are GLT-1 and GLAST, respectively. EAAT3, with the rodent homologue EAAC1, is primarily found on neurons (Queen et al. 2007). After a painful nerve injury, each of these transporters is downregulated in the dorsal horn by day 7 (Hu et al. 2010, Sung et al. 2003, Xin et al. 2009, Yang et al. 2009). It has been reported that both astrocytes and microglia are activated in the dorsal horn for painful nerve root compressions by day 7 (Hubbard & Winkelstein 2005, Rothman et al. 2010), suggesting that the glial-specific transporters (GLT-1, GLAST) may also be modulated by a painful nerve root compression as well. The spinal expression of these transporters, however, has not been evaluated in any model of radiculopathy to date.

---

## CHAPTER 2

### Rationale, Context, Hypotheses & Aims

---

#### 2.1 Rationale & Context

Cervical radiculopathy is a common, painful condition involving injury to the cervical nerve root (Abbed & Coumans 2007, Hogg-Johnson et al. 2008). The development of behavioral sensitivity from a cervical nerve root compression has been shown to be determined by the compression mechanics, including both the magnitude and duration of the applied load (Hubbard et al. 2008a, Rothman et al. 2010). Clinically, cervical nerve roots are prone to both sustained and transient compressions associated with disc herniations and trauma induced rapid neck motions, respectively (Carette et al. 2005, Thoomes et al. 2012, Wainner & Gill 2000). These different modes of loading can mediate the course of clinical symptoms that develops (Abbed & Coumans 2007). Symptoms associated with radiculopathy, including pain and weakness, may resolve within minutes, but most often persist for as long as five months (Krivickas & Wilbourn 2000, Wainner & Gill 2000). Animal models of nerve root injury also demonstrate that the severity of symptoms and tissue injury are both mediated by the type of insult (Colburn et al. 1999, Hubbard et al. 2008a, Kobayashi et a. 2005a); yet, the relationship between the duration of a nerve root compression and the subsequent development of pain as well as the underlying pathophysiology still remains unclear.

Studies demonstrate that nerve root compressions that occur for longer durations lead to the development of more pronounced deficits in conduction of afferent signals across the nerve root of the cauda equina in the pig (Pedowitz et al. 1992, Rydevik et al. 1991). It is unclear, however, whether impaired signaling during compression is an indicator for the development of subsequent behavioral sensitivity or of other neuronal pathophysiologies that develop after a nerve root injury, including axonal degeneration in the root and enlargement of axon terminals in the dorsal horn of the spinal cord (Hubbard & Winkelstein 2008, Kobayashi et al. 2008). Furthermore, the signaling properties of afferents are undefined at time-points when behavioral sensitivity persists after a painful nerve root compression, despite evidence of spinal inflammation and altered neurotransmitter levels that would suggest disruption of the normal neurotransmission in the spinal cord after a nerve root compression (Kobayashi et al. 2005, Rothman & Winkelstein 2007).

Enhanced excitatory signaling by the neurotransmitter, glutamate, is a hallmark of pain after neural tissue trauma (Laird & Bennett 1993, Nguyen et al. 2009, Shim et al. 2005). In addition to its role as an excitatory neurotransmitter, glutamate can also modify the excitability of neurons by modulating the strength of excitatory synapses (Diamond 2001, Jordain et al. 2007). Thus, regulation of extracellular glutamate is vital for normal neuronal function. Glutamate transporters regulate synaptic glutamate by removing glutamate from the extracellular space (Danbolt 2001, Kim et al. 2011, Rothstein et al. 1996, Tao et al. 2005, Zhang et al. 2012) and an imbalance in these transporters is associated with neuronal hyperexcitability in the spinal cord of rats (Cata et al. 2006, Somers & Clemente 2002, Sung et al. 2003). In many animal models of neural tissue

trauma, including spinal cord and peripheral nerve injury, the normal expression of spinal glutamate transporters is downregulated in the presence of behavioral sensitivity (Sung et al. 2003, Wang et al. 2008b, Xin et al. 2009), suggesting that an imbalance in glutamate uptake by these transporters contributes to neuropathic pain. It is unclear, however, whether spinal glutamate transporter expression is mediated by a painful nerve root compression or whether the spinal glutamatergic system contributes to the development of nerve root-mediated pain.

## **2.2 Overall Hypothesis & Specific Aims**

The objective of this work is to use a rodent model of cervical radiculopathy to determine the role of the duration of a transient nerve root compression for producing sustained behavioral sensitivity and associated changes in spinal neuronal activity and glutamate transporter expression. The **overall hypothesis** is that there is a duration threshold, longer than which, compression of the nerve root disrupts the normal activity of its afferents that also is associated with the subsequent development of persistent pain and axonal degeneration within the nerve root. Further, painful nerve root compression is associated with an imbalance in the spinal glutamatergic system which contributes to hyperexcitability of the spinal neurons. This hypothesis is tested through the following specific hypotheses and specific aims:

**Hypothesis 1.** Neuronal conductance across the C7 nerve root held under an applied compression continuously decreases until a critical duration is reached. When a nerve

root compression is held for a period beyond that critical duration, signaling across the axons of the nerve root remains depressed even after the applied compression is removed from the root. Furthermore, the axons of the nerve root will have a morphology that exhibits characteristics of injury as late as 7 days after the root compression and behavioral sensitivity will develop in the forepaw of the rat. Conversely, when an applied compression to the nerve root is removed before the critical duration is reached, neuronal signaling in the root will return to pre-compression levels soon after the nerve root is relieved of compression and there will be no evidence of axonal damage or behavioral sensitivity 7 days after the applied compression.

**Aim 1:** Measure evoked neuronal activity in the spinal cord during an applied compression to the nerve root and evaluate the extent of axonal degeneration induced in the nerve root and the temporal behavioral sensitivity response.

- 1a.** Record evoked neuronal responses in the superficial dorsal horn of the spinal cord using electrical stimulation of the forepaw during compression of the C7 dorsal nerve root. Quantify the number of evoked action potentials as a function of the compression duration to define a duration that significantly decreases evoked activity relative to baseline in the context of behavioral sensitivity.
- 1b.** Validate the nerve root compression duration identified in Aim 1a for producing painful and nonpainful responses, by measuring mechanical allodynia and thermal hyperalgesia in the affected forepaws for up to 7 days following injury.
- 1c.** Quantify and compare the degree of axonal degeneration in the nerve root that develops at day 7 following nerve root compressions for both the painful and



nonpainful groups, separately, using immunohistochemistry and fluorescence microscopy. Myelinated fibers will be identified using NF200, and peptidergic and non-peptidergic unmyelinated fibers will be identified using CGRP and IB4, respectively.

**Hypothesis 2.** Neuronal hyperexcitability due to insufficient glutamate uptake underlies the persistent behavioral sensitivity that develops after a transient nerve root injury.

**Aim 2.** Define and compare the response of spinal glutamate transporters and evoked neuronal activity in the spinal cord induced by a painful and a nonpainful nerve root compression, separately.

**2a.** Quantify and compare the glial and neuronal expression of glutamate transporters (GLT1, GLAST, EAAC1) in the dorsal horn following painful and nonpainful root compressions, using immunofluorescence at days 1 and 7.

**2b.** Record and compare the neuronal activity in the superficial spinal cord that is evoked by mechanical stimulation to the forepaw at day 7, following painful and nonpainful nerve root compressions, separately.

**Hypothesis 3.** Regulating glutamate signaling after a painful nerve root compression will alleviate behavioral sensitivity as well as the spinal neuronal hyperexcitability that develops. In addition, inhibiting sodium channel-dependent glutamate release will prevent the development of injury in the nerve root axons.

**Aim 3.** Pharmacologically block spinal glutamate release and promote spinal glutamate clearance, separately, to evaluate the role of glutamatergic signaling in persistent behavioral sensitivity and neuronal hyperexcitability following a painful nerve root compression.

**3a.** Deliver ceftriaxone via daily intrathecal injection following a painful nerve root compression; evaluate forepaw sensitivity for up to 7 days and quantify spinal GLT-1 expression at day 7 using immunofluorescence.

**3b.** Deliver Riluzole via an intraperitoneal injection following a painful nerve root compression; evaluate forepaw sensitivity for up to 7 days and quantify axonal degeneration in the nerve root at day 7 using immunofluorescence.

**3c.** Measure the mechanically-evoked neuronal activity in the superficial spinal cord at day 7 after painful nerve root compressions treated with ceftriaxone and Riluzole, in separate studies.

In completing these aims, spinal electrophysiological recordings were made *in vivo* using a model of a painful nerve root compression developed in our lab (Hubbard & Winkelstein 2005). By measuring the number of action potentials in the spinal cord that were evoked by a peripheral, electrical stimulus, a critical duration of applied compression ( $6.6 \pm 3.0$  minutes) to inhibit neuronal signaling across the root was identified in Aim 1a. Using that duration threshold, studies in Aims 1a, 1c and 2b compared neuronal properties *immediately* after the applied compression and at day 7 between nerve root compression durations that were above (15 minutes) and below (3 minutes) that critical duration. Specifically, after removing the applied compression, afferent

conductance across the root was measured for 10 minutes and, in separate studies, the subsequent development of axon pathology in the root (Aim 1c) and hyperexcitability of dorsal horn neurons (Aim 2b) were evaluated at day 7. To contextualize that duration threshold in terms of the development of pain, behavioral sensitivity was evaluated for 7 days in Aim 1b following compressions above and below (3, 10, 15 minutes) the 6.6 minute threshold. Together, these studies establish the conditions used throughout the rest of the thesis that identify the role of spinal excitatory signaling in the initiation or persistence of pain resulting from mechanical nerve root trauma.

An imbalance in the glutamatergic system is associated with the development of behavioral sensitivity in rodent models of peripheral inflammation, sciatic nerve ligation and spinal cord contusion (Inquimbert et al. 2012, Kim et al. 2008, Liaw et al. 2008). Studies in Aim 2a investigated the temporal expression of glutamate transporters in the spinal cord, which regulate extracellular glutamate. The glial glutamate transporter, GLT-1, is thought take up as much as 80% of the glutamate in the central nervous system (Danbolt 2001). Therefore, studies in Aims 3a and 3c evaluated neuronal excitability of dorsal horn neurons and behavioral sensitivity after pharmacologically upregulating GLT-1 with ceftriaxone following a painful nerve root compression. To also evaluate the role of pre-synaptic glutamate signaling in nerve root-mediated pain, studies in Aims 3b and 3c pharmacologically inhibited pre-synaptic glutamate with Riluzole; axonal degeneration in the root and neuronal excitability in the spinal cord were assessed using the methods established in Aims 1c and 2b.

---

## CHAPTER 3

# Defining a Duration Threshold to Modulate Evoked Neuronal Firing Rates in the Spinal Cord & the Development of Axonal Pathology

---

*This chapter has been adapted from a published manuscript:*

Nicholson KJ, Quindlen JC, Winkelstein BA. “Development of a Duration Threshold for Modulating Evoked Neuronal Responses After Nerve Root Compression Injury.” *Stapp Car Crash Journal*, 55:1-24, 2011.

### 3.1 Overview

Cervical radiculopathy is a painful neurologic condition that is often attributed to an impingement of the cervical nerve root (Carette et al. 2005, Wainner & Gill 2000). Pain that radiates down the shoulder and arm can persist even if there is no evidence of sustained compression to the root (Krivickas & Wilbourn 2000, Kuijper et al. 2011). In the rat, a transient compression to the cervical nerve root produces persistent behavioral sensitivity in the forepaw (Hubbard et al. 2008a, Rothman & Winkelstein 2007). The development of behavioral sensitivity has been shown to be mediated by the duration of the compression (Rothman et al. 2010). Specifically, when the magnitude of an applied load to the nerve root is held constant, pain only develops if the compression is applied for a sufficiently long duration (Rothman et al. 2010); however, the duration threshold for eliciting behavioral sensitivity has not been defined. Like behavioral sensitivity, the

compression duration also mediates the development of pathophysiological responses in the tissues of the nerve root that develop during the applied compression (Rydevik et al. 1991, Pedowitz et al. 1992). For example, when the cauda equina is held under compression, afferent conduction, blood flow and nutrient flow all continuously decrease in the compressed roots with increasing time of compression (Garfin et al. 1990, Olmarker et al. 1989b, Rydevik et al. 1991, Pedowitz et al. 1992). Despite the critical role that afferents have in transmitting nociceptive signals, no study has established whether transmission through the afferents of the root is impaired by a *painful* nerve root compression or whether impaired signaling through the root *during* the compression period is associated with the subsequent pathology of the nerve root axons that only develops after a painful nerve root compression (Hubbard & Winkelstein 2008).

Work presented in this chapter focuses on the studies outlined in Aims 1a and 1c. These studies define the functional and morphological response of the afferents in the C7 nerve root both during and after a transient nerve root compression. The frequency of electrically-evoked afferent firing through the C7 nerve root of the rat was quantified during a compression known to elicit persistent behavioral sensitivity (Section 3.3). In that study, a duration threshold of  $6.6 \pm 3.0$  minutes was defined as the critical duration for inhibiting axonal conduction through the root. Using that threshold, recovery of afferent signaling through the C7 nerve root was compared between separate groups of rats that underwent a C7 nerve root compression for longer (15 minutes) or shorter (3 minutes) times than the critical duration by measuring the frequency of afferent discharge rates for the first 10 minutes after compression was removed. In a second study (Section 3.4), the development of axonal pathology in the root at day 7 after compression was compared

between groups of rats that underwent the same 3 or 15 minute root compressions as in the first study.

The studies presented here establish the role of compression duration in mediating both electrophysiologic and morphological responses of the axons in the nerve root in a painful model of nerve root trauma. In order to contextualize these neuron-specific outcomes to the development of persistent behavioral sensitivity, the studies in Chapter 4 quantify mechanical allodynia and thermal hyperalgesia in groups of rats that underwent a nerve root compression below or above the critical duration of  $6.6 \pm 3.0$  minutes identified in this study. Studies presented in Chapter 5 complement the current studies by measuring the frequency of evoked action potentials in the spinal cord at day 7 in order to characterize neuronal signaling at a time-point when behavioral sensitivity is maintained.

### **3.2 Relevant Background**

Although neck pain can originate from a variety of spinal tissues, the cervical nerve roots are vulnerable to injury from foraminal impingement, disc herniation, direct spinal trauma, and/or foraminal stenosis (Cornefjord et al. 1997, Krivickas & Wilbourn 2000, Nuckley et al. 2002, Olmarker et al. 1989a, Panjabi et al. 2006, Wainner & Gill 2000). The effect of compression duration is of particular relevance to nerve root injury because the nerve root can be susceptible to both sustained *and* transient mechanical loading (Abbed & Coumans 2007, Panjabi et al. 2006, Svensson et al. 1993). Sustained nerve root loading occurs from a disc herniation and spondylosis (Abbed & Coumans 2007, Wainner & Gill 2000), while transient loading to the root can result from sports

and automotive traumas (Krivickas & Wilbourn 2000, Panjabi et al. 2006, Stuber 2005, Tominaga et al. 2006).

The clinical course of symptoms and rate of recovery have been reported to differ from different modes of loading to the nerve root (Abbed & Coumans 2007). Pain and weakness associated with a transient insult to the nerve root exhibit varied responses which can resolve within minutes or persist for as long as five months (Krivickas & Wilbourn 2000, Wainner & Gill 2000). Although nerve root injuries may result from a variety of loading scenarios and the severity of the symptoms may differ considerably, the relationships between the duration of the nerve root compression, pathophysiology and symptoms are poorly defined.

Compression to the nerve root produces immediate changes in the evoked signal conduction along the fibers of the compressed root, both clinically and in animal models (Fumihiko et al. 1996, Morishita et al. 2006, Pedowitz et al. 1992, Rydevik et al. 1991, Takahashi et al. 2003, Takamori et al. 2010). Intraoperative studies in patients with symptomatic lumbar radiculopathy from root impingement associated with disc herniation and spinal stenosis demonstrate decreases in the amplitude of compound muscle action potentials that are evoked by an electrical stimulation to the affected nerve root (Morishita et al. 2006, Takamori et al. 2010). Furthermore, the severity of the amplitude decrease is mediated by the magnitude of the pressure in the intervertebral foramen (Morishita et al. 2006). This finding suggests that neuronal signaling across the root may be mediated by the local mechanical loading profile of the root. In support of this hypothesis, Takamori et al. (2010) demonstrated that the duration of the root compression also mediates the response of electrically-evoked neuronal activity. In that

study, pre-operative patients were placed in a prone position with their leg slowly raised until the onset of pain and/or numbness. When that position was reproduced during surgery, the amplitude of the action potentials evoked at the S1 root and measured in the gastrocnemius muscle decreased by 41% as early as within one minute, and by 63% after three minutes of impingement (Takamori et al. 2010). This change in evoked action potentials that continued to develop throughout the period of nerve root impingement demonstrates that there is a time-dependent response of the nerve root's electrophysiologic properties to deformation and suggests that changes in neuronal signaling through the root during compression may contribute to radiculopathy symptoms. Further, it is likely that specific loading parameters, such as magnitude and duration, may play a role in modulating these electrophysiologic responses. Finally, although clinical electrophysiologic studies, such as nerve conduction tests and needle electromyography, are sensitive and specific diagnostic tools for nerve root compression (Abbed & Coumans 2007, Wainner & Gill 2000), a clear understanding of the functional changes that neurons undergo during compressions and that result in pain is still limited, which also impairs injury prevention efforts.

Many animal models of evoked neuronal signaling through the nerve roots in the cauda equina demonstrate that this signaling is modulated during and after compression (Fumihiko et al. 1996, Garfin et al. 1990, Rydevik et al. 1991, Pedowitz et al. 1992). In studies compressing the cauda equina of pigs, both 75mmHg and 100mmHg of pressure applied for 120 minutes each decreased the amplitude of electrically-evoked compound nerve action potentials by 41% and 74%, respectively (Rydevik et al. 1991). After compression was removed from the cauda equina, the amplitude of the action potentials



returned to pre-compression levels in the pigs that received 75mmHg of compression, but not in those receiving 100mmHg of compression (Rydevik et al. 1991). When 100mmHg of compression was applied to the cauda equina for 240 minutes, the decrease in action potential amplitude during compression was even greater and remained more-pronounced even after compression was removed relative to the shorter (120 minute) compression period (Pedowitz et al. 1992). Although these electrophysiological studies suggest that neuronal function is related to nerve root loading and that it is mediated by the compression duration, the outcomes in those studies reflect the collective response of all of the nerve roots in the cauda equina and do not recapitulate the mechanical scenario applied to an individual nerve root. Further, those studies only investigated the acute responses and did not define the relationship between the onset, or extent, of longer-lasting damage in the nerve root.

The immediate changes in the electrophysiological properties of compressed axons in the nerve root may likely be related to the longer-term pathophysiology that develops in the nerve root, such as edema, inflammation, and thickening of the intraradicular connective tissue (Beck et al. 2010, Jancalek & Dubovy 2007, Kobayashi et al. 2004, Mosconi & Kruger 1996). Neuronal dysfunction, in particular, may be more indicative of developing pain symptoms due to its central role in pain transmission. Injured axons following mechanical trauma and compression exhibit axonal swelling, loss of cytoskeleton proteins, separation and disorganization of the myelin sheath, loss of axonal transport, Wallerian degeneration, and a decrease in axon packing density (Guertin et al. 2005, Jancalek & Dubovy 2007, Kobayashi et al. 2004, Kobayashi et al. 2005a, Mosconi & Kruger 1996, Myers et al. 2003, Serbest et al. 2007). Like the

functional changes in neurons during compression, the degenerative changes in axons that develop at later times after a transient compression are also mediated by compression magnitude (Hubbard & Winkelstein 2008, Kobayashi et al. 2005a), suggesting that there may be an association between the neuronal responses during nerve root compression and those neuronal responses that develop after compression. Yet, no study has established whether these acute neuronal outcomes are related to the persistent neuronal injury and/or dysfunction that develop.

Mechanical loading to the nerve root initiates a cascade of neuronal, inflammatory, and degenerative responses by producing an acute insult to the axonal, connective, and vascular tissues of the nerve root (Kobayashi et al. 2004, Rydevik et al. 1984, Winkelstein et al. 2002). For example, severe axonal injury can induce degeneration of the axonal process distal to the cell body via Wallerian degeneration (Park et al. 2004, Stoll & Müller 1999). For the central axons of primary afferents, which make up the dorsal nerve root, this degeneration can occur proximal to the site of injury, nearer to the spinal cord (Hubbard & Winkelstein 2008, Kobayashi et al. 2008). Axonal degeneration, marked by neurofilament degradation and loss of axonal integrity, is evident as early as 15 minutes after spinal cord injury, but may also be present as late as three weeks after injury to the peripheral nerves (Kobayashi et al. 2008, Park et al. 2004, Ramer et al. 2000, Schumacher et al. 1999). The degree of degeneration is modulated by the local tissue mechanics and is also associated with persistent pain after a transient compression to the cervical nerve root (Dyck et al. 1990, Kobayashi et al. 2005a, Hubbard & Winkelstein 2008). Disruption to the axonal structure at both early and late time points has been found to be more pronounced for greater loads and for longer

durations of applied loads (Dyck et al. 1990, Hubbard & Winkelstein 2008, Kobayashi et al. 2005a, Kobayashi et al. 2008). Previous studies also have demonstrated that the presence of axonal degeneration of the myelinated axons in the nerve root is associated with sustained behavioral sensitivity after compression, making axonal integrity an important tissue-injury marker for nerve-root mediated pain and suggesting that neuronal dysfunction and pathology may be related to pain (Hubbard & Winkelstein 2008, Hubbard et al. 2008a). Despite the fact that both myelinated and unmyelinated axons are important for normal sensation and also for detecting the location and intensity of a noxious stimulus (Ramer et al. 2000, Wall & Melzack 1994), no study has evaluated the response of unmyelinated nerve root fibers to a transient nerve root compression. Furthermore, although there is an association between degeneration of the axons and the magnitude of the load that is applied to the root (Hubbard & Winkelstein 2008), it is not known how compression duration affects axonal injury or whether axonal degeneration is associated with the duration-mediated neuronal responses initiated during compression. Defining the role of compression duration in altering the morphology of unmyelinated and myelinated axons in the nerve root at a time-point relevant to pain provides added insight into how neuronal dysfunction and/or injury following mechanical root loading relates to symptoms of radiculopathy.

The studies in this chapter test the hypothesis that when nerve roots undergo compression, there is an associated change in the number of electrically-evoked action potentials through the compressed nerve root. It is further hypothesized that there is a period of compression longer than which that applied compression can produce prolonged changes in the function of the affected axons; those modifications can manifest

as sustained changes in the electrophysiologic properties and structural breakdown of the axons after the initial insult. As such, the goal of the studies in this chapter was to identify if there is a critical duration of applied compression to the nerve root that alters the electrically-evoked discharge rate of the neurons from that root during and after compression, and also to evaluate if that neuronal activity relates to the sustained changes in function and the extent of neuronal damage in the root that develop after such compression.

### **3.3 Afferent Discharge Rates During & After Root Compression**

#### **3.3.1 Methods**

All procedures were approved by the Institutional Animal Care and Use Committee at the University of Pennsylvania. Rats were housed under USDA- and AAALAC-compliant conditions with a 12-12 hour light-dark cycle and free access to food and water. Studies were performed using only male Holtzman rats (Harlan Sprague-Dawley; Indianapolis, IN), weighing 300-480g at the start of the study.

In order to evaluate the electrophysiologic response of the afferents in the compressed nerve root, extracellular recordings were made in the superficial laminae of the dorsal horn during and after compression was applied to the C7 nerve root for 15 minutes, a period previously determined to produce immediate and sustained pain (Hubbard et al. 2008a). Spinal extracellular recordings were made while afferents were evoked using an electrical stimulus applied to the area of the forepaw that corresponds to the dermatome innervated by the C7 root (Fig. 3.1). Neuronal activity was quantified by

measuring the number of electrically-evoked action potentials (spikes) during the painful compression in order to define the time at which the conduction of peripherally-evoked spikes is significantly reduced (Fig. 3.2). Based on that critical compression duration, a separate electrophysiological study was also performed in which the nerve root compression was applied for a period of time that was shorter than that identified compression duration. The goal of that study was to define the neuronal activation patterns for a subcritical duration of compression and to compare the prolonged, post-compression response in those patterns to the response for the longer duration, painful compression (Fig. 3.2).

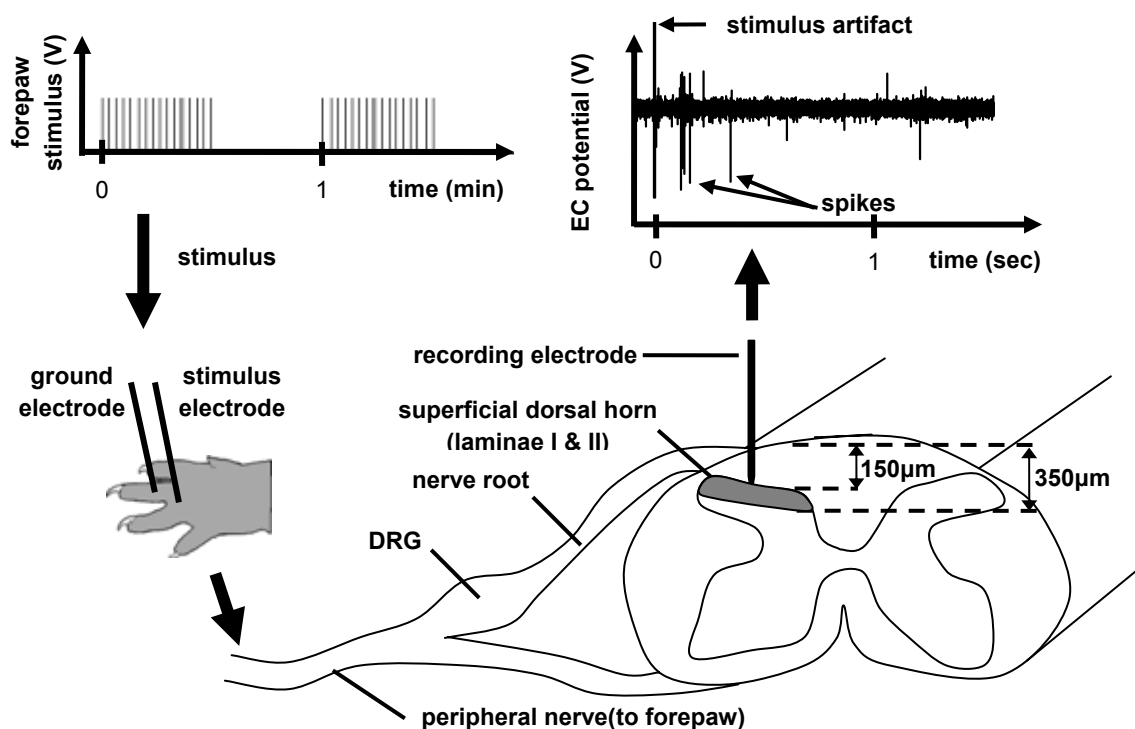
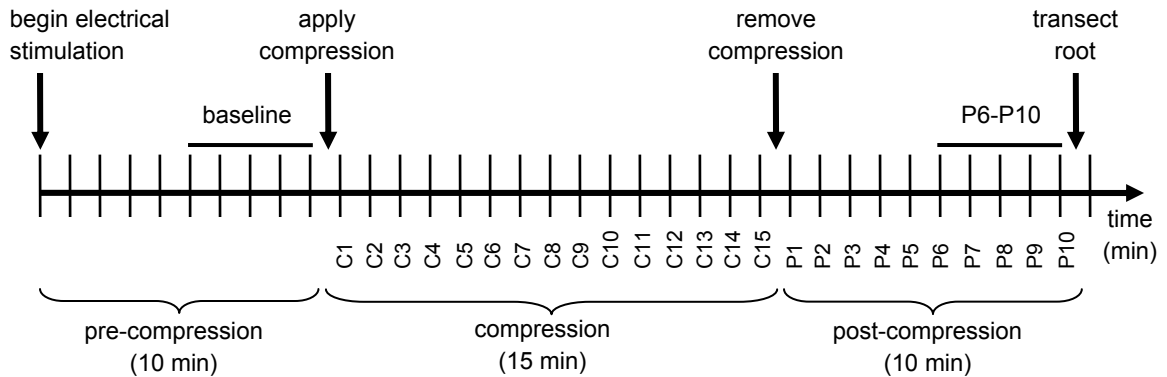


**Fig. 3.1** Schematic showing experimental test set-up for recording peripherally-evoked spikes in the superficial dorsal horn of the spinal cord. An electrical stimulus (16-train pulse) is applied to the forepaw at 1-minute intervals using a pair of stainless steel electrodes to stimulate neurons in the forepaw. Extracellular (EC) recordings of the evoked action potentials are made in the superficial dorsal horn by initially inserting the tungsten recording probe at a depth of 150µm below the pial surface and searching through the depth of 350µm. The number of action potentials evoked by each stimulus train is quantified during and after a transient compression to the C7 nerve root.

**timeline for 15 minute compression group**



**timeline for 3 minute compression group**

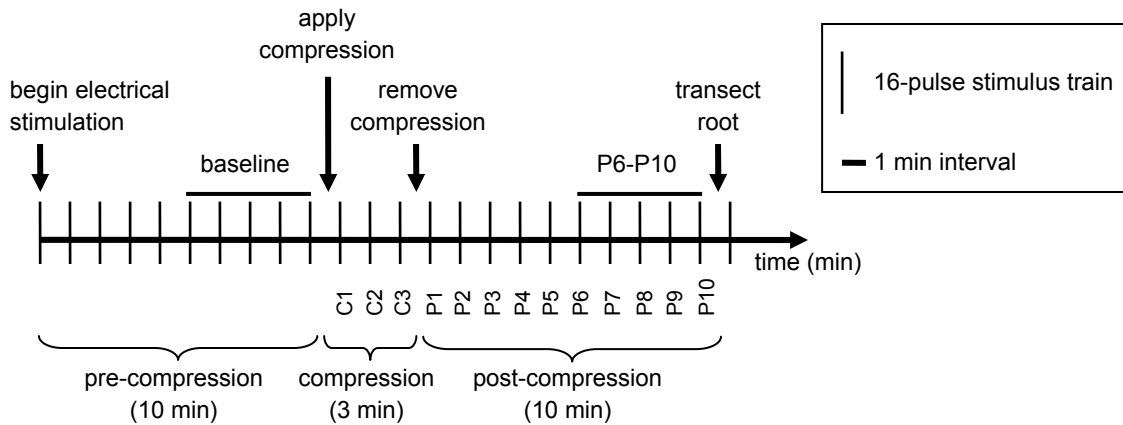


**Fig. 3.2** Study design to measure the number of spikes evoked by electrical stimulation (a 16-pulse stimulus) to the forepaw at 1-minute intervals prior to, during and after a 3 minute and a 15 minute compression to the nerve root. Prior to compression, evoked activity is measured for a period of 10 minutes, followed by a single compression to the C7 nerve root of either 15 or three minutes. Post-compression spikes are recorded for a period of 10 minutes. After each study, the nerve root is transected. Each neuron's response is measured as a percent change from its average response measured during the last five minutes before compression (in the baseline period). The post-compression response of neurons in each group is compared using the number of spikes at the 10th minute of the post-compression period (P10) and during the last five minutes of the post-compression period (P6-P10).

Anesthesia was induced via intraperitoneal injection of sodium pentobarbital (50mg/kg). To maintain proper levels of anesthesia, supplementary doses of sodium pentobarbital were given as needed throughout the procedures. With the rat placed in a prone position, a dorsal incision was made along the back of the neck at the midline from the base of the skull to the spinous process of T2. The C5-T1 vertebrae were exposed by

removing the paraspinal muscle and soft tissue. The cervical spinal cord from C6-C8 and the C7 nerve root on the right side were exposed using a bilateral dorsal laminectomy and partial facetectomy. The overlying dura was also removed and warm mineral oil (Fisher Scientific; Pittsburgh, PA) was used to cover the exposed spinal cord to prevent the cord from dehydrating. Following the surgical exposure, the rat was immobilized on a stereotaxic frame (Kopf Instruments; Tujunga, CA) using bilateral ear bars and a vertebral clamp at the T2 vertebra (Fig. 3.3). The core temperature of the rat was maintained between 36–37° during all procedures using a heating plate with a temperature controller and isolated rectal probe (Physitemp Instruments, Inc.; Clifton, NJ).

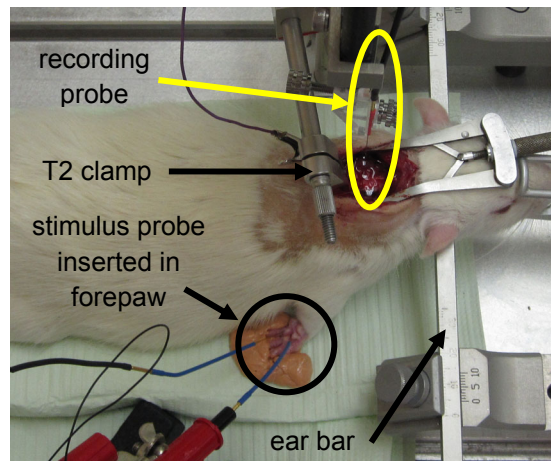


**Fig. 3.3** Surgical exposure and experimental test set-up for recording extracellular potentials in the dorsal horn while applying an electrical stimulus to the forepaw.

For each rat, extracellular voltage potentials were continuously recorded using a 127 $\mu$ m diameter tungsten electrode (A-M Systems; Sequim, WA) that was inserted into the superficial dorsal horn medial to where the C7 right dorsal root enters the spinal cord (Figures 3.1 & 3.3). The recording probe was inserted to depths of between 150–350 $\mu$ m

below the pial surface in order to measure extracellular potentials in the superficial dorsal horn, where the primary afferent neurons of the dorsal root synapse with the spinal neurons (Wall & Melzack 1994). The extracellular signal from the recording electrode was amplified with a gain of 1000 (World Precision Instruments; Sarasota, FL), processed with a 60Hz noise eliminator (Quest Scientific; North Vancouver, BC), and then digitized and stored at 25kHz (CED; Cambridge, UK), using methods previously reported (Pezet et al. 2008, Quinn et al. 2010).

To identify the afferent neurons that are associated with the C7 dermatome, sensory fields in the right forepaw were located at the start of each study using a light brush stroke applied to the plantar surface of the forepaw with a cotton swab followed by a series of 10 stimuli using a noxious (10gf) von Frey filament (Hubbard & Winkelstein 2005) (Fig. 3.4). A load cell (5N capacity; SMT S-Type Model; Interface, Inc., Scottsdale, AZ) was attached to the von Frey filament and used to synchronize the application of the mechanical stimulus with the extracellular recordings that were made in the spinal cord (Fig. 3.4). Each von Frey stimulus was applied for one second at a time. A stainless steel electrode (A-M Systems; Sequim, WA) was then inserted into the forepaw in the location of the sensory field and a train of 16, 2msec-wide pulses was delivered at 0.5Hz with an amplitude of 1V at 1-minute intervals (Lapirot et al. 2009, Pezet et al. 2008, Yu et al. 2009) (Figs. 3.1 & 3.2). A ground electrode (A-M Systems; Sequim, WA) similar to the stimulus probe was also inserted into the forepaw, near the stimulus electrode (Figs. 3.1 & 3.3). The electrical stimulation protocol was repeated throughout the duration of each experiment (Fig. 3.2). The stimulus strength of 1V was



selected such that the stimulus itself did not produce any muscle contractions or twitches, but was sufficiently strong to evoke afferent action potentials.

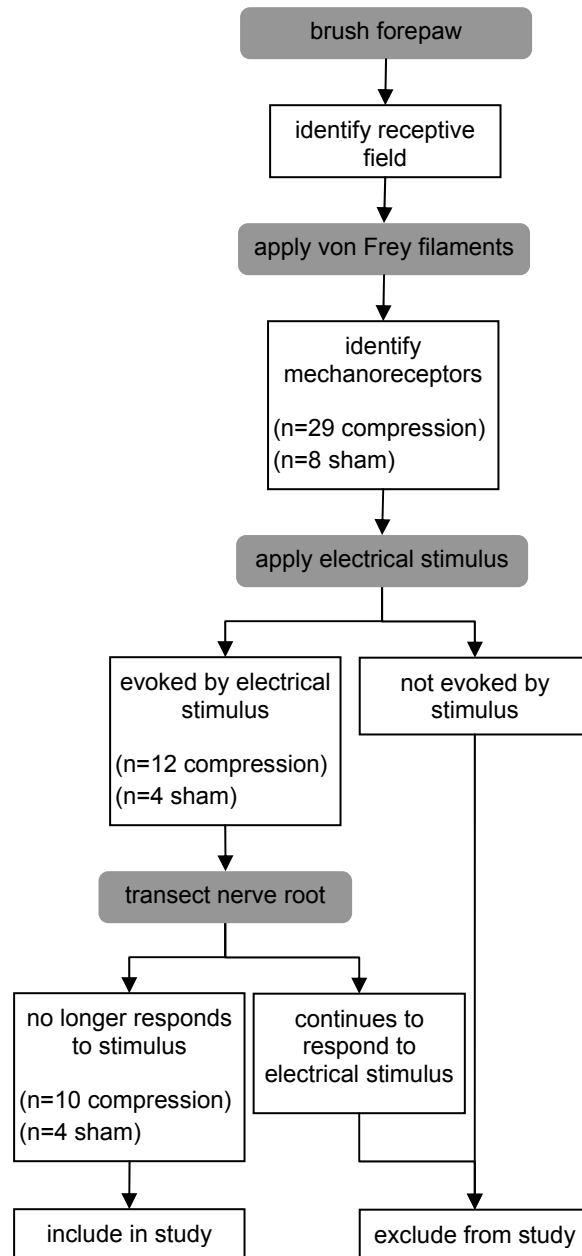


**Fig. 3.4** Flow chart illustrating the experimental procedures for identifying (shaded ovals) and selecting neurons (white boxes) for inclusion in the electrophysiologic studies. The number of neurons that was selected at each procedure in the 15 minute compression and sham groups is also shown.

Electrically-evoked action potentials were recorded in the spinal cord before, during, and after the applied compression for all rats. The baseline response of each rat to the electrical stimulation of the right forepaw was first established by delivering the stimulation train once every minute for a period of 10 minutes, prior to any additional stimulation or manipulation (Fig. 3.2) (Fumihiko et al. 1996, DeLaTorre et al. 2009, Martindale et al. 2001, Rydevik et al. 1991). After the baseline period, compression was applied to the nerve root using a calibrated 10gf microvascular clip (World Precision Instruments; Sarasota, FL) to apply a compressive strain of  $81.7 \pm 4.7\%$  over an area of  $4.0\text{mm}^2$  (Hubbard et al. 2004), and the 16-pulse stimulation train was applied at 1-minute intervals during the compression period (Fig. 3.2). In the first series of rats ( $n=3$  rats; 10 neurons), nerve root compression was applied for 15 minutes. Each rat received only one, single compression to the right C7 nerve root. After that time, the clip was removed from the nerve root and the electrical stimulation to the right forepaw continued at 1-minute intervals for a post-compression period of 10 minutes (Fig. 3.2). To account for the effects of the surgical exposure and the repeated stimulations, a separate rat (4 neurons) underwent sham procedures that included the same experimental and stimulation protocols without application of nerve root compression. Regardless of the surgical procedure, at the end of the 10 minute post-compression recording period, the C7 nerve root was fully transected and an additional electrical stimulus train was delivered in order to determine whether the spikes that were evoked by the electrical stimulus and recorded previously during the protocol were associated with an axon in the C7 root (Fig. 3.2). Any neurons that were detected to continue to respond to forepaw stimulation after the root had been transected were removed from subsequent analysis and not included in this

study (Fig. 3.4). In this way, neurons not associated with the C7 root that was being compressed were not erroneously included in the action potential counts.

All extracellular voltage recordings measured during the stimulation protocol were spike-sorted using Spike2 software (CED; Cambridge, UK) to separate the action potentials associated with individual neurons. In order to focus on the inputs of the sensory neurons in the forepaw, only those neurons that were identified to respond to the von Frey filament stimulus were analyzed in Spike2 (Figs. 3.4 & 3.5). On average, for every three mechanoreceptors that were identified during the von Frey filament stimuli, only one neuron would also be evoked by the electrical stimulus (Fig. 3.4). Thus, only that one neuron that was evoked by both the mechanical and electrical stimuli would be included in the analysis for that rat. For each sensory neuron included in the study, the baseline firing rate was determined by counting the number of spikes that occurred during one second prior to the first application of the von Frey filament (Quinn et al. 2010) (Fig. 3.5). A sensory neuron was defined as any neuron whose firing rate increased over its baseline firing rate during at least one of the 10 1-second von Frey stimulations. Neurons that did not respond to any of the applied von Frey stimuli before the start of the electrical stimulation were removed from subsequent data analysis. Activity that was evoked by electrical stimulation of the forepaw was quantified at each 1-minute interval throughout the protocol. Specifically, this was done by summing the number of spikes for each neuron that were elicited within the 10-40msec window immediately after each of the 16 stimulation pulses in order to exclude stimulus artifact and spontaneous activity (DeLaTorre et al. 2009; Ramer et al. 2000; Yu et al. 2009) (Fig. 3.6). Specific details of

the protocol to determine the latency of action potentials after the electrical stimulus are described in Appendix A.

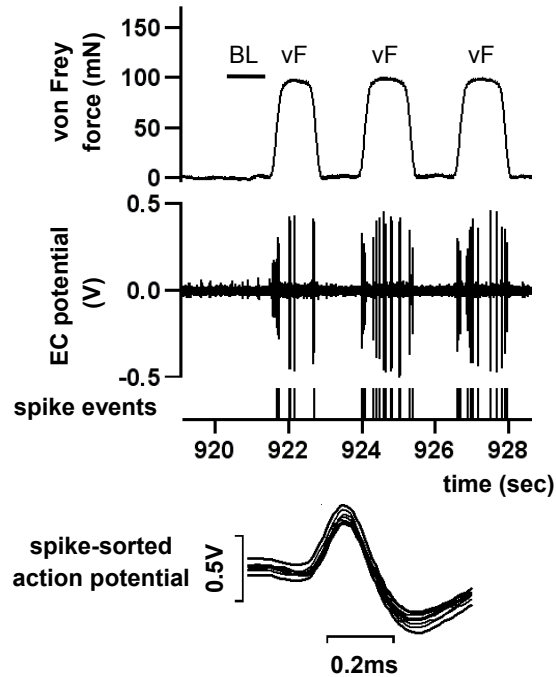


**Fig. 3.5** A representative extracellular (EC) recording during the application of a von Frey (vF) filament. The extracellular data are spike-sorted to identify neurons evoked by the mechanical stimulus to the forepaw. Neurons are determined to be evoked by the stimulus if the number of spike events during any application with the vF filament is greater than the number of spike events recorded during baseline (BL), corresponding to 1-second prior to the first stimulus.

In order to account for each neuron's individual discharge rate, the number of spikes measured at each 1-minute interval of the compression and post-compression periods was each normalized against the average number of spikes that occurred during the last five stimulations of the baseline period (Fig. 3.2). The normalized number of spikes was then averaged across neurons in the compression group and also across neurons recorded in the sham group. The number of action potentials recorded at each time period was represented as the percentage change from baseline $\pm$ SEM for that group.

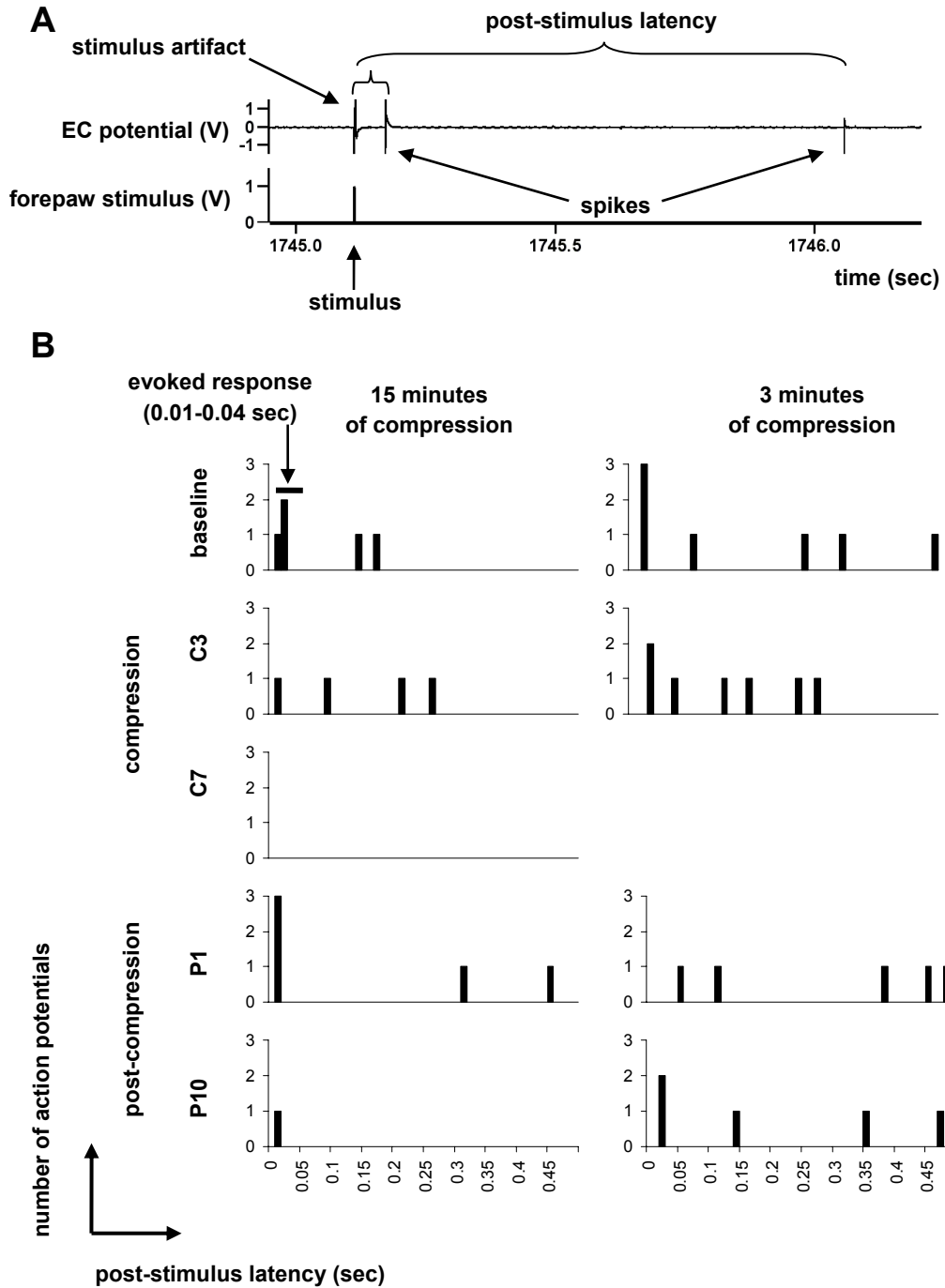


**Fig. 3.6** (A) A representative extracellular (EC) recording made in the spinal cord after a single electrical stimulus to the forepaw during compression. For each spike, the length of time (0.01-0.04sec) that occurred between application of the stimulus and the evoked spike was quantified as the post-stimulus latency. (B) Representative post-stimulus histograms (bin-width of 10ms) quantifying the number of action potentials evoked from a neuron in the 15 minute compression group and a neuron in the 3 minute compression group before compression (baseline), during compression (C3, C7), and post-compression (P1, P10).

For each of the neurons from which recordings were made in the 15 minute compression group, post hoc analysis was performed to determine the time during the compression at which the evoked neuronal activity was substantially modulated. This critical duration was defined as the average time during compression when changes in the evoked activity relative to baseline reached a maximum, using all of the neurons (10 neurons total from 3 rats) that were recorded from during the 15 minute compressions.

Differences in the number of evoked spikes between the compression and sham groups during the applied root compression were detected using a two-way, repeated measures analysis of variance (ANOVA) for injury group (sham, compression) and time (baseline through C15). All statistical analyses were performed using the raw data (i.e. the number of spikes). Action potentials counts for each neuron in the sham and compressions groups are provided in Appendix B. The percent change from baseline is reported in order to show trends in discharge rates that would otherwise be unclear due to the variation in baseline discharge rates between individual neurons.

Based on the duration threshold identified for modulating evoked neuronal activity during the 15 minute compression, a second group of rats underwent a nerve root compression that was applied for a subthreshold period of three minutes (n=6 rats; 9 neurons) (Fig. 3.2). The duration period of three minutes was selected because it is more than one standard deviation shorter than the threshold duration that was identified to modify peripherally-evoked action potentials in the spinal cord (see Section 3.3.2 for specific details). All other surgical and electrophysiological procedures were the same as described for the 15 minute compressions. Similarly, for the subthreshold compression studies, the evoked spikes were recorded during an initial 10 minute baseline period and

during the entire period of applied compression to the nerve root (i.e. three minutes) (Fig. 3.2). Recordings were also made for 10 minutes after the compression was removed from the root, analogous to the protocol for the 15 minute compression studies (Fig. 3.2). In order to account for changes in the extracellular recordings due to the surgical exposure and repeated electrical stimulus, one additional rat (3 neurons) also underwent sham procedures with the electrical stimulus protocol matching that used for the 3 minute compression group.

Comparisons during the first three minutes of compression between the 15 minute compression group and the 3 minute compression group were made using a two-way, repeated measures ANOVA for group (3 minutes, 15 minutes) and time (baseline through C3). The post-compression data for each of the two duration groups were separately compared using a two-way, repeated measures ANOVA for group (compression, sham) and time (baseline, P1-P10). In addition, to specifically evaluate the effect of compression duration on discharge rates at the end of the 10 minute recovery period (Pedowitz et al. 1992), a separate two-way, repeated measures ANOVA for group (compression, sham) and time (baseline, P10) was performed for each compression duration study. To make a more direct comparison between the pre-compression discharge rate (baseline), and the post-compression discharge rates, comparisons were also made between baseline and the average number of spikes measured over the last five minutes post-compression (P6-P10), using a two-way ANOVA for group (compression, sham) and time (baseline, average of P6-P10) for each duration group, separately. Post-hoc, pairwise comparisons with Bonferroni correction tested for differences in the main effects, where applicable. Significance for all comparisons was defined at  $\alpha=0.05$ .

### 3.3.2 Results

A total of 10 neurons that responded to the von Frey and electrical stimuli were recorded at a mean depth of  $221 \pm 63 \mu\text{m}$  in the dorsal horn of the spinal cord in the studies with 15 minutes of applied compression. In the corresponding sham group, recordings were made from a total of 4 neurons at a depth of  $150 \mu\text{m}$ . Compression of the C7 nerve root significantly decreased the discharge rate over the entire compression and post-compression period (C1-P10) compared to sham procedures ( $p=0.035$ , two-way interaction group X time). Similarly, during the compression period alone (C1-C15), there was also a significant decrease in the discharge rate during the C7 nerve root compression compared to sham ( $p=0.012$ , two-way interaction group X time; Fig. 3.7). As early as two minutes after the start of the applied compression, evoked spikes were reduced by  $37 \pm 24\%$  relative to baseline. The number of action potentials that was evoked by the electrical stimulus continued to decrease over time during the compression and was  $76 \pm 13\%$  lower than baseline at 7 minutes into the compression (Fig. 3.7A), while the discharge rate during sham procedures was only  $9 \pm 9\%$  less than baseline (Fig. 3.7A). After seven minutes of compression, neuronal discharge rates remained 50-80% lower than the comparable baseline activity for the remaining period of the compression and the entire post-compression period (Fig. 3.7A). On average, the maximum decrease in neuronal activity occurred at  $6.6 \pm 3.0$  minutes into the compression period. As such, this time was taken as the duration-threshold for modulating evoked neuronal activity during a 98mN compression to the nerve root. Moreover, for the subsequent electrophysiologic and immunohistochemistry studies, a subthreshold duration of 3 minutes of compression was applied because it was a time less than the average minus one standard deviation (i.e.



3.6 minutes); experimentally, it was not feasible to both apply a compression for 3.6 minutes and to synchronize the electrical stimulation and measurement protocols across studies (Fig. 3.2). Appendix B summarizes the action potential count for each of the neurons that was recorded in the 15 minute compression study and the subsequent 3 minute compression study, as well as each of the corresponding sham groups.

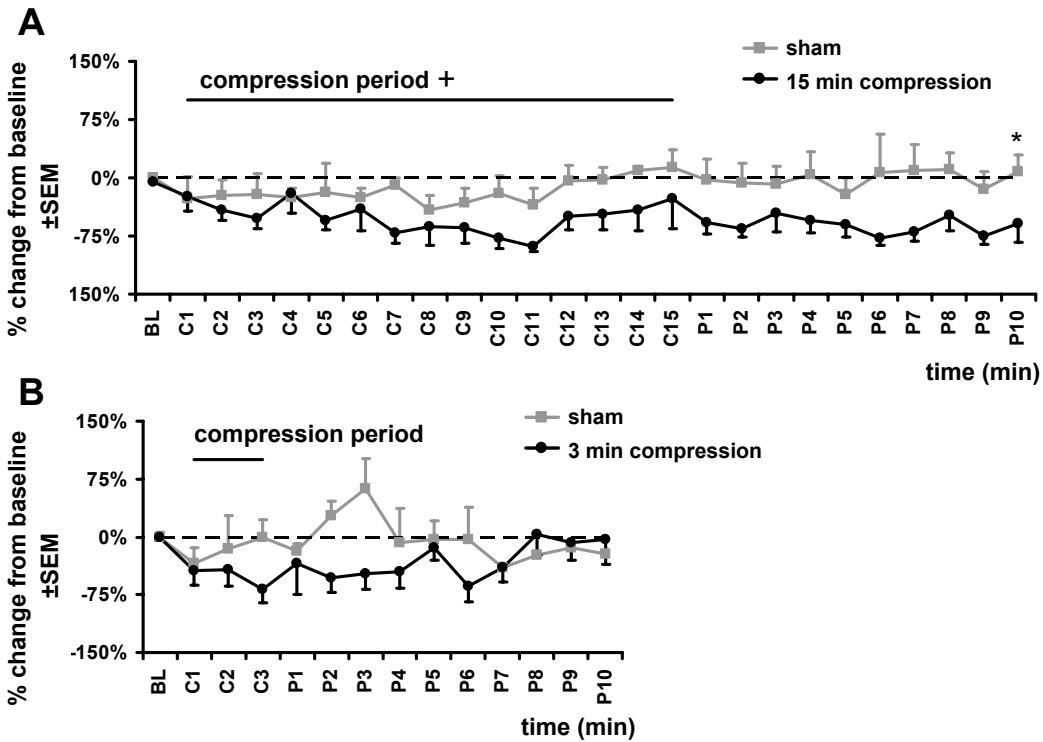


**Fig. 3.7** Evoked spikes during and after compression applied to the C7 nerve root and corresponding sham procedures applied for a period of 15 minutes (**A**) or for a period of 3 minutes (**B**), expressed as a percent change from baseline (BL). The number of spikes is counted at 1-minute intervals during a nerve root compression held for 15 minutes (C1-C15) or three minutes (C1-C3). After compression is removed from the nerve root, evoked action potentials are counted at 1-minute intervals for a post-compression period of 10 minutes (P1-P10). The number of evoked spikes during compression in the 15 minute group (C1-C15) is significantly decreased over time relative to sham procedures ( $+p=0.012$ , group X time). There is no change for the 3 minute compression. The number of evoked spikes at the end of the post-compression period (P10) is significantly less than baseline and sham ( $*p=0.018$ , group X time) after a 15 minute compression, but not after a 3 minute compression. Comparing the first three minutes of the compression period, there is no significant difference between the 3 minute and the 15 minute compression groups; however, both groups significantly decreased over time ( $p=0.032$ ).

In the subthreshold compression study, recordings were made from nine neurons at a depth of  $251 \pm 79 \mu\text{m}$  in rats that received compression for 3 minutes (Fig. 3.7B). There was no significant difference in the depth of the neurons from which recordings were made in the 15 minute and 3 minute compression groups ( $p=0.370$ ), as evaluated by a t-test. For the corresponding sham group for the 3 minute study, recordings were made from three neurons at a depth of  $160 \mu\text{m}$ . No significant differences were detected during the first three minutes of compression between the group that received 15 minutes of compression and the group that received 3 minutes of compression ( $p=0.373$ , group;  $p=0.543$ , group X time). Significance was only detected over time ( $p=0.032$ ) for the two injury groups; there was a significant difference in the discharge rates measured during compression from baseline at C2 ( $p=0.005$ ) and C3 ( $p=0.035$ ). At two minutes into the compression, the discharge rate was reduced by  $42 \pm 21\%$  relative to baseline in the three minute group (Fig. 3.7B). This decrease in evoked action potentials at two minutes of compression in the subthreshold duration group was similar to that observed in the 15 minute compression group ( $37 \pm 24\%$ ; Fig. 3.7A).

The electrically-evoked discharge rate that was measured after the compression was removed from the nerve root exhibited differences based on the duration of the applied compression (Figures 3.6-3.8). Although there was a significant difference ( $p=0.001$ ) between the post-compression discharge rates (average of baseline, P1-P10) after 15 minutes of compression compared to its sham, no significant differences were detected in post-compression discharge rates after 3 minutes of compression compared to its corresponding sham group. At the end of the post-compression period (P10), the number of evoked spikes in the 15 minute compression group remained lower than

baseline by  $58 \pm 25\%$  and was significantly different than sham and baseline ( $p=0.018$ , two-way interaction group X time) (Fig. 3.7A). Yet, in the 3 minute compression group evoked activity had returned to within  $3 \pm 33\%$  of baseline and was not significantly different from baseline or sham ( $p=0.088$ , two-way interaction group x time) (Fig. 3.7B). Similarly, 15 minutes of compression significantly reduced the average discharge rate measured during the last five minutes of the post-compression period (P6-P10) compared to baseline and sham ( $p=0.020$ , two-way interaction group X time), but not a 3 minute compression ( $p=0.125$ , two-way interaction group X time) (Fig. 3.8). On average, the number of spikes measured at P6-P10 after a 15 minute compression was  $56 \pm 14\%$  lower than baseline, while the number of spikes after a 3 minute compression was  $22 \pm 12\%$  lower than baseline during this 5-minute period (P6-P10) (Fig. 3.8).

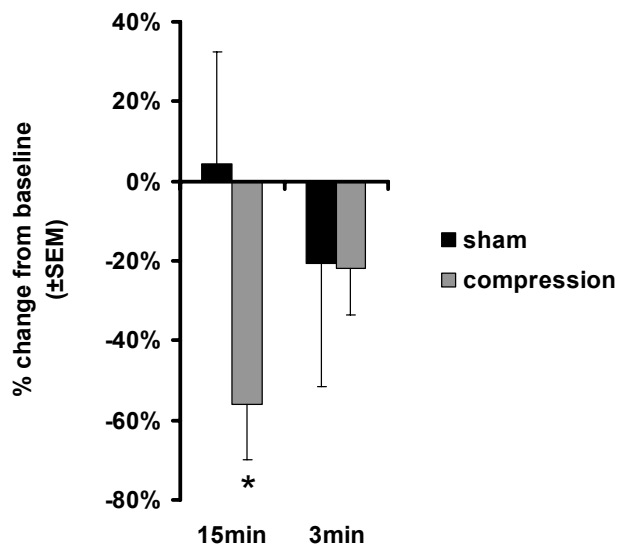


**Fig. 3.8** Average change from baseline during the last 5 minutes of the post-compression period (P6-P10) after compression applied for 3 or 15 minutes, or the corresponding sham procedures. The number of spikes after 15 minutes of compression is significantly ( $p=0.020$ ) less than sham and baseline.

### **3.4 Axonal Morphology in the Root After 3 or 15 Minute Compressions**

#### **3.4.1 Methods**

Rats used in this study were included to evaluate if the duration threshold of  $6.6 \pm 3.0$  minutes for inducing immediate changes in neuronal discharge patterns (Section 3.3) relates to the development of axonal pathology in the root 7 days after a nerve root compression that is applied to the root for either 3 or 15 minutes. In order to evaluate the extent of axonal injury in the C7 nerve root 7 days after a nerve root compression, a morphological examination of the root was performed using immunohistochemistry to fluorescently label the axons of the nerve root. On post-injury day 7 the nerve roots were harvested from rats that received a compression applied for 3 minutes (subthreshold) (n=6 rats) or 15 minutes (n=4 rats). A sham group (n=5 rats) that underwent the same nerve root exposure without compression was also included to account for the effects of anesthesia, surgical exposure and any tissue manipulation.

Surgical procedures were performed under anesthesia induced with inhalation isoflurane (4% for induction, 2% for maintenance). Previously described procedures for transiently compressing the nerve root with a calibrated microvascular clip were used to vary the duration of an applied compression, as described in Section 3.3 (Hubbard & Winkelstein 2005, Rothman et al. 2010). With the rat in a prone position, a dorsal incision was made from the base of the skull to the spinous process of T2. The overlying muscle and soft tissue were removed to expose the C6 and C7 vertebrae. The right C7 dorsal nerve root was exposed via a C6-C7 hemilaminectomy and facetectomy on the right side. A small incision was made in the dura over the C7 nerve root and the 10gf clip

was used to apply compression to the dorsal nerve root (Fig. 3.9). After surgery, the wound was closed using 3-0 polyester suture surgical staples. The rats were allowed to recover in room air with free access to food and water.

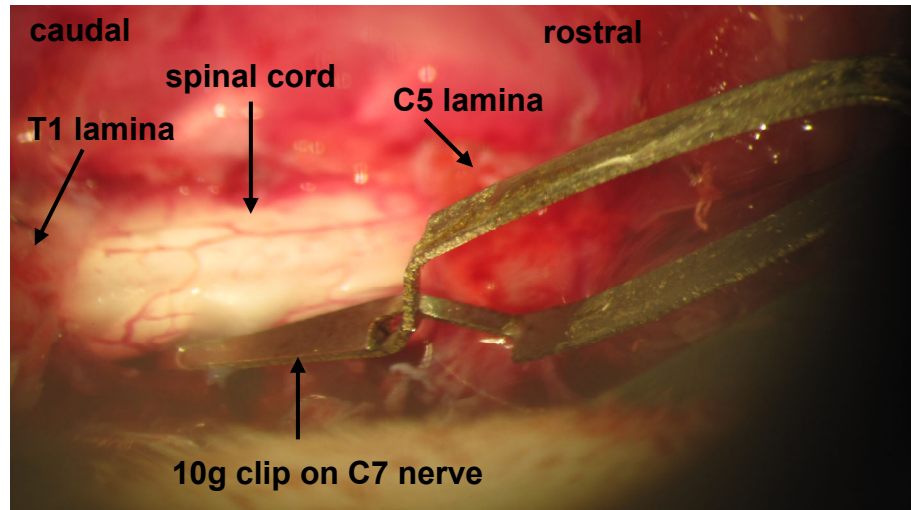


**Fig. 3.9** Image showing the surgical procedure to apply a 10gf clip to the C7 nerve root.

At day 7 after the surgical procedure, rats were given an overdose of sodium pentobarbital (65mg/kg) via intraperitoneal injection and then transcardially perfused with 200ml of Dulbecco's Phosphate-Buffered Saline (PBS; Mediatech, Inc.; Manassas, VA) followed by 300ml of 4% paraformaldehyde (Sigma; St. Louis, MO). The C7 ipsilateral nerve root was exposed via a bilateral C6-C7 laminectomy and facetectomy and harvested en bloc with the adjacent spinal cord and dorsal root ganglion attached at the proximal and distal ends of the root, respectively (Fig. 3.1). Tissues were post-fixed in 4% paraformaldehyde overnight and then transferred to 30% sucrose at 4°C for five days and embedded in OCT medium (Sakura Finetek USA, Inc.; Torrance, CA) for cryosectioning. The nerve roots were sectioned (14µm) along the long-axis, near the

centerline of the root and then thaw-mounted directly onto slides. Matched nerve roots were also harvested from normal naïve rats (n=2) and were also included in tissue processing for comparison.

Slides were immunofluorescently labeled for neurofilament-200 (NF200) and isolectin-B4 (IB4) to identify myelinated and unmyelinated fibers, respectively. Slides were blocked in 10% normal donkey serum (Millipore; Billerica, MA) with 0.3% Triton X-100 (Bio-Rad Laboratories; Hercules, CA) for two hours and incubated overnight at 4°C in mouse anti-NF200 (1:500; Sigma; St. Louis, MO) and biotinylated IB4 (5µg/ml; Sigma; St. Louis, MO). Slides were then incubated for two hours at room temperature in donkey anti-mouse Alexa Fluor 546 (1:1000; Invitrogen; Carlsbad, CA) and streptavidin conjugated with dichlorotriazinyl amino fluorescein (DTAF) (1:500; Jackson ImmunoResearch Laboratories, Inc.; West Grove, PA). Three tissue sections from each rat were analyzed for axonal damage. Digital images were taken of the nerve root proximal to the site of compression at 200X magnification. Each axonal marker was evaluated, separately, for signs of axonal swelling and loss of immunoreactivity as indicators of axonal damage (Hubbard et al. 2008b, Serbest et al. 2007, Singh et al. 2006). Tissue sections that displayed any signs of these abnormalities were assigned a positive score (+) and those sections that were not different from the normal uncompressed roots were assigned a score indicating the absence (-) of any changes. Evaluations were performed blinded to the group.

### 3.4.2 Results

Generally, axonal staining for NF200 and IB4 in the C7 right nerve root did not differ from normal tissue for either the sham or 3 minute compression groups (Table 3.1). Yet, when the nerve root was compressed for 15 minutes, both axonal markers (NF200 & IB4) demonstrated robust changes, including a loss of immunoreactivity and axonal swelling (Fig. 3.10 & Table 3.1). In all but one of the nerve roots compressed for 3 minutes (Rat #118), NF200 labeling exhibited long, myelinated axons with an even distribution in their staining (Fig. 3.10). IB4 labeled long, thin axons that also exhibited an even distribution along the nerve root for all samples except Rat #118 (Table 3.1). Neither the myelinated nor the unmyelinated populations of axons exhibited substantial signs of axonal discontinuity or axonal swellings in either the sham or the 3 minute compression groups. Of the six rats that underwent a nerve root compression for 3 minutes, only one (Rat #118) exhibited signs of decreased NF200-immunoreactivity and axonal swelling in both the unmyelinated (IB4) and myelinated (NF200) axon populations (Table 3.1). However, the remaining five rats that received compression for 3 minutes showed normal morphology. Likewise, no pathology was observed in any of the five roots that that received sham procedures (Fig. 3.10 & Table 3.1). In contrast, three of the four nerve roots that were compressed for a period of 15 minutes exhibited altered immunoreactivity for both NF200 and IB4, including both a decrease in NF200-immunoreactivity and also the presence of axonal swelling (Fig. 3.10 & Table 3.1).

**Table 3.1** Summary of NF200 and IB4 ratings.

Group	Rat ID	NF200	IB4
Sham	97	-	-
	104	-	-
	105	-	-
	117	-	-
	121	-	-
3min	98	-	-
	99	-	-
	103	-	-
	115	-	-
	118	+	+
	120	-	-
15min	82	-	-
	83	+	+
	84	+	+
	85	+	+

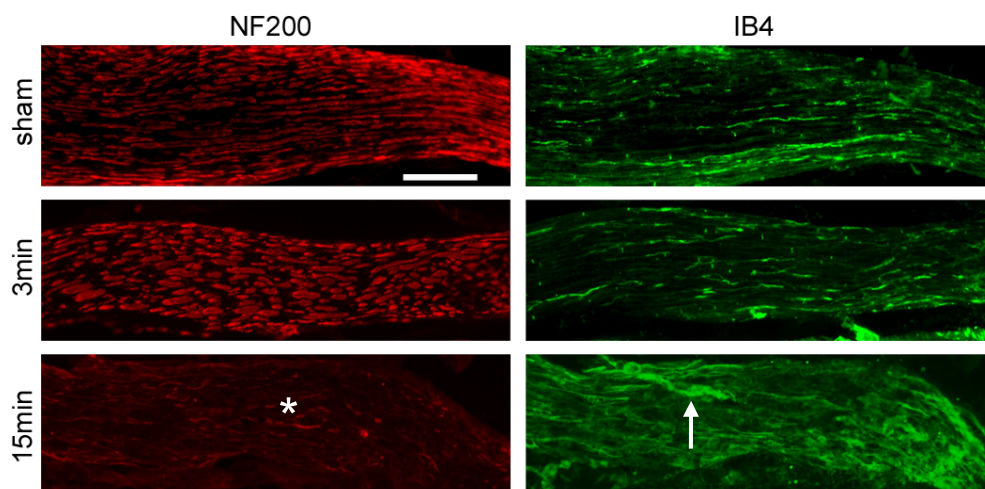


**Fig. 3.10** Representative images of C7 nerve roots labeled for myelinated axons (NF200) and unmyelinated axons (IB4) at day 7 following sham procedures or a C7 root compression. Sham operated roots show even distribution of immunolabeling for both NF200 and IB4. Both the myelinated and unmyelinated axons appear intact along the length of the root. Most of the nerve roots in the 3 minute (3min) compression group also exhibit this even distribution of NF200 and IB4. However, most of the nerve roots in the 15 minute (15min) compression group have evidence of root damage, including a loss of NF200-immunoreactivity (\*) and axonal swelling (arrow). Scale bar (50 $\mu$ m) applies to all.



### 3.5 Discussion

This study provides the first quantitative evaluation of the role of compression duration in altering the frequency of neuronal signaling across the nerve root during an applied compression to the C7 nerve root. The electrophysiological data demonstrate that 15 minutes of compression of the cervical nerve root induces immediate neuronal dysfunction that is sustained even after the compression is removed and also produces robust axonal injury in the nerve root 7 days after the injury (Figs. 3.6-3.8, 3.10 & Table 3.1). Yet, neither neuronal function nor axonal morphology are significantly affected after a nerve root compression that is applied for only 3 minutes (Figs. 3.6-3.8, 3.10 & Table 3.1). Compression to the nerve root is accompanied by an immediate and continuous decrease in the number of peripherally-evoked action potentials in the spinal cord that reaches its peak at  $6.6 \pm 3.0$  minutes (Fig. 3.7A). Compression that is held longer than that time also maintains a decrease in evoked action potentials by between 50-80%, but does not decrease further in the evoked activity during compression (Figs. 3.6-3.8). In addition, for a nerve root compression held longer than that duration threshold, evoked action potentials remain lower than baseline responses by  $56 \pm 14\%$  during the last 5-minute period after compression is removed (Figures 3.7A & 3.8). Although 3 minutes of nerve root compression reduces the number of action potentials evoked from peripheral stimulation by as much as  $68 \pm 17\%$ , neuronal activity returns to pre-compression levels within 10 minutes after the compression is removed from the nerve root (Figs. 3.6-3.8). In addition, for that same subthreshold duration of compression (3 minutes), there is no evidence of axonal injury in either of the NF200- or IB4-labeled axons at day 7 after

compression (Fig. 3.10 & Table 3.1). The lack of widespread axonal injury in that group is in contrast to the substantial decrease in NF200-immunoreactivity, axonal swelling, and myelin degeneration that is observed at that time point after a compression of the C7 nerve root for 15 minutes (Fig. 3.10 & Table 3.1) (Hubbard & Winkelstein 2008). Accordingly, the prolonged decrease in evoked action potentials after a 15 minute compression observed here is likely associated with the hallmarks of axonal injury that are observed 7 days later (Hubbard & Winkelstein 2008). Taking these data together with the literature, it can be inferred that compression of the nerve root that is sustained for a period longer than 6.6 minutes not only produces sustained neuronal dysfunction, but may be associated with the neurodegenerative cascades in the axons that are associated with nerve root pathophysiology.

The established relationship between altered afferent signaling to the spinal cord and the development of behavioral sensitivity in neuropathy (Hao et al. 1992, Khan et al. 2002, Shim et al. 2005) suggests that 15 minutes of nerve root compression not only produces a sustained decrease in peripherally-evoked action potentials (Figures 3.6-3.8), but also induces behavioral sensitivity to mechanical stimuli. In fact, several rat models of inflammatory pain have demonstrated that there is an association between pain-related behaviors and the number of action potentials evoked by a transcutaneous electrical stimulus, and that both the behavioral and electrophysiologic responses are produced as early as 10 minutes after the injection of the inflammatory agent, formalin, into the hindpaw (Asante et al. 2009, DeLaTorre et al. 2009, Martindale et al. 2001, Pezet et al. 2008, Stanfa et al. 1992). Those studies suggest that the significant reduction in the number of action potentials that is observed to persist for at least 10 minutes after a 15

minute compression (Figs. 3.6-3.8) may be a sensitive indicator of enhanced nociception following nerve root compressions of this duration. Moreover, the duration-threshold of  $6.6\pm 3.0$  minutes identified here that maximally reduces electrically-evoked neuronal signaling also falls within the range of root compression durations (3-15 minutes) that produces mechanical allodynia in this model of cervical radiculopathy that was previously reported (Rothman et al. 2010). Persistent mechanical allodynia of the forepaw developed immediately (within one day) after a 15 minute compression to the C7 nerve root; yet, when the same compression is applied for a shorter, 3 minute, period it does not induce allodynia (Rothman et al. 2010). Although the current study did not investigate afferent discharge rates beyond 10 minutes after the compression was removed, studies of compression to the cauda equina in the pig report that impaired signaling across the root can continue for at least 90 minutes after the compression is removed (Pedowitz et al. 1992, Rydevik et al. 1991). Taking all of these electrophysiologic and behavioral findings together suggests that compression of the nerve root lasting longer than  $6.6\pm 3.0$  minutes is sufficient to produce sustained neuronal dysfunction and that this change in the electrophysiologic properties of the compressed neurons may be associated with the development of mechanical allodynia and pain.

Seven days after a 15 minute compression to the nerve root, robust morphological changes were evident in the myelinated and unmyelinated axons of the injured axon, compared to uninjured axons (Fig. 3.10 & Table 3.1). In contrast, seven days after a 3 minute compression, both populations appear intact throughout the length of the nerve root, with morphology consistent with uninjured axons (Fig. 3.10 & Table 3.1). Previous studies in several animal models of radiculopathy demonstrate that chronic nerve root

compression applied over a period of 1-8 weeks produces substantial pathology in the neurons of the nerve root including axonal swelling, axonal condensation, myelin fragmentation, and loss of axonal transport (Corneffjord et al. 1997, Jancalek & Dubovy 2007, Kobayashi et al. 2004). None of those studies measured nociceptive responses, but the indicators of axonal injury that were investigated are also associated with changes in pain and functional behavioral outcomes (Chen et al. 1992, Hubbard & Winkelstein 2008).

Both the rate and magnitude of compression have been shown to contribute to the development of axonal injury (Hubbard et al. 2008b, Kobayashi et al. 2005a, Olmarker et al. 1990). The 10gf compressive load applied in this study is more than twice the magnitude-threshold of 3.5gf (34.1mN) that has been identified as requisite to produce decreased NF200-immunoreactivity at day 7 after a 15 minute compression (Hubbard et al. 2008b). Although that same 98mN compressive load was used for the 3 minute compression conducted in this study, no such decrease in NF200-immunoreactivity was evident in five of the six nerve roots that were compressed for 3 minutes (Fig. 3.10 & Table 3.1). Likewise, IB4-immunoreactivity was only altered in the nerve roots that sustained a 15 minute compression and not after a 3 minute compression (Fig. 3.10 & Table 3.1). The difference in the response of NF200-labeled and IB4-labeled axons after 3 and 15 minutes of this compression magnitude suggests that compression *duration* may play a role in mediating the development of axonal pathology in the nerve root.

Changes in the nerve root structure as a whole that develop over time during its compression, such as compaction of the axons and a decrease in the overall nerve root width, may be among the underlying factors that contribute to the ability of the

compressed axons to tolerate 3 minutes of compression (Dyck et al. 1990, Rothman et al. 2010), despite the suprathreshold pain-provoking load of 98mN. Although pathology is not apparent after a 3 minute compression to the C7 nerve root (Fig. 3.10 & Table. 3.1), our evaluation approach did not incorporate more sensitive techniques, such as higher magnification scanning electron microscopy and/or axial views of the nerve root, that can detect subtle pathology in the axons, such as changes in axonal diameter size, axonal splitting, or disorganization in the myelin sheath (Guertin et al. 2005, Jancalek & Dubovy 2007, Myers et al. 1993). However, the presence of those morphologic changes in the axons parallels the presence of decreased NF200-immunoreactivity (Hubbard & Winkelstein 2008). So, the normal expression of NF200 that is observed in the nerve root after a 3 minute compression (Fig. 3.10 & Table 3.1) is likely a true indication of normal axonal morphology. Also, the absence of axonal injury after a 3 minute compression is consistent with previous reports suggesting that the development of axonal pathology after a nerve root compression is associated with behavioral sensitivity, which is also not elicited after a 3 minute compression to the nerve root (Hubbard & Winkelstein 2008, Rothman et al. 2010). Although the findings from our study demonstrate that compression duration mediates the electrophysiologic and morphologic responses of the nerve root (Figs. 3.6-3.8 & 3.10) and provides clinically-relevant insight into its response to compression, these relationships and the specific outcomes for the durations used here are specific to the rat. Additional studies are needed to determine if there are scaling issues in these metrics and outcomes as they relate to the human. Indeed, the nerve root's apparent ability to tolerate a short period of compression (Figs. 3.6-3.8, 3.10 & Table 3.1) suggests that early intervention alleviating any root compression may be sufficient for

improved functional recovery following trauma. In fact, clinical studies have shown that early treatment of nerve root and spinal cord injuries does reduce the severity and number of complications associated with injuries to these tissues (Carlstedt et al. 2000, Fehlings & Perrin 2006). In addition, intraoperative monitoring of nerve root function using electromyography and/or electrophysiology reduces the rate of neurological complications associated with spine fusion surgeries by allowing surgeons to quickly detect and resolve unintentional compression to the root that may occur during surgical manipulation (Bose et al. 2002, Kelleher et al. 2008). Although the nerve root may be able to recover from certain mechanical injuries, the fact remains that nerve root tissues are still susceptible to sustained neuronal damage even for transient compressions (Figs. 3.6-3.8, 3.10 & Table 3.1). Additional studies investigating the tolerance of nerve root tissue to traumatic injuries will provide an improved understanding of the need to prevent these injuries, provide rapid treatment, and the expected degree of recovery following these types of injuries.

Compression in this study was applied to the nerve root transiently. Yet, even a brief, 15 minute, compression is sufficient to produce sustained neuronal dysfunction and abnormal axonal morphology (Figs. 3.6-3.8, 3.10 & Table 1). Despite being transient, this duration is substantially longer than those associated with tissue loading in the neck during real-world traumatic exposures (Panjabi et al. 2006, Svensson et al. 1993). The physiologic response of the root to compression likely depends on a combination of inputs and signaling as a result of both the duration and magnitude of the insult (Fig. 5.11) (Garfin et al. 1990, Kobayashi et al. 2005b, Olmarker et al. 1989b, Olmarker et al. 1990, Pedowitz et al. 1992). Although the compression magnitude (10gf) was held

constant here, the axonal damage observed in the 15 minute group (Fig. 3.10 & Table 3.1) is also evident even when the magnitude of compression is at, or near, the magnitude threshold of 3.9gf (38.2mN) for developing persistent behavioral sensitivity (i.e. pain) in this rat model (Hubbard & Winkelstein 2008, Hubbard et al. 2008a). Furthermore, tissue damage following a transient nerve root compression has been shown to accompany sustained neuronal dysfunction (Rydevik et al. 1992). Thus, it is likely that any 15 minute compression applied using a load above the threshold load (38.2mN) for producing pain would similarly induce sustained neuronal dysfunction and axonal damage. Conversely, because axonal damage has been reported not to develop in the root after compressions below that load threshold, even for those held as long as 15 minutes (Hubbard & Winkelstein 2008), neuronal function is likely to recover following application of less severe compressions, as was observed for the 3 minute group (Figs. 3.6-3.8). Further, it is likely that for loads below 3.9gf (38.2mN) there is a similar duration of compression that would also produce pain and/or neuronal dysfunction. Such a duration would presumably be required to be much longer, and possibly even permanent, as in the case of stenosis. Indeed, currently the relationship defining the “response-space” between load, duration, neuronal dysfunction and symptomatic outcomes is not defined (Fig. 3.11). However, the present study, together with studies in the literature, begins to establish such a multi-dimensional response.

Certainly, the magnitude and durations applied to the nerve root in the present study represent only two points along the duration-magnitude response curve of the nerve root (Fig. 3.11). At the two extremes of this spectrum are (1) transient compressive injuries that deliver a brief compression with a high magnitude of force and (2) chronic

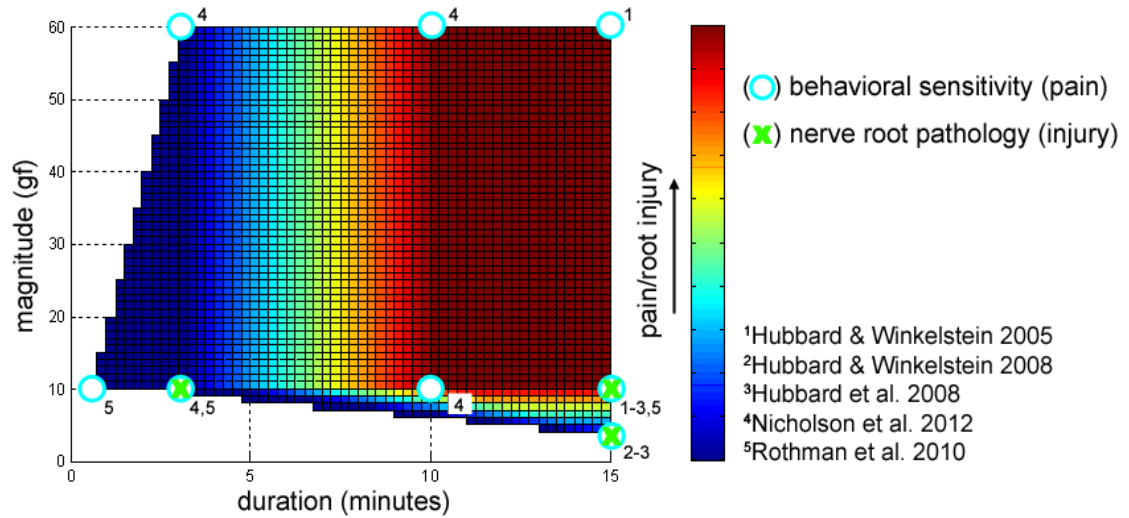


**Fig. 3.11** Schematic representation exemplifying the complex “response-space” between biomechanical injury parameters (magnitude, duration) of an applied compression and the development of behavioral sensitivity (O) or degree of associated root injury (X) after a transient C7 nerve root compression.

compressions applied at a low magnitude. In vivo studies of nerve roots crushed with a high, but undetermined, force for a very brief period (2-15 seconds), report that axonal injury and neuronal dysfunction develop in the injured nerve root, as well as pain that persists for at least seven days (Ramer et al. 2000, Sekiguchi et al. 2003). Likewise, chronic compressions also produce substantial axonal damage, the onset of which occurs earlier for higher magnitudes of compression (Kobayashi et al. 2005a). Chronic compression to the canine lumbar nerve root reduces axonal transport within one week for compressions applied with 7.5gf load and as early as one day for compressions applied with 15gf a load (Kobayashi et al. 2005a); it is not known whether pain developed for either of those compression magnitudes. Nevertheless, that study does support the notion that for chronic compressions, the rate at which pathology develops is mediated by the magnitude of the force applied to the tissue, with a greater force leading to earlier onset pathology. Based on those findings, the time-dependent decrease in discharge rates observed during compression in the present study (Figs. 3.6-3.7), also



likely varies with the magnitude of the load applied (Fig. 3.11). By extension, for any force greater or less than the 10gf applied in the current study, the duration-threshold for mediating changes in neuronal activity would be expected to develop earlier or later, respectively, than the 6.6 minutes determined during the compression period.

The current study demonstrated that nerve root compression reduces the number of peripherally-evoked action potentials in the spinal cord (Figs. 3.6-3.8). This outcome of spinal neurons was evaluated as an indicator of the electrophysiologic response of the neurons of the compressed nerve root. Inserting the recording probe in the spinal cord rather than the nerve root itself was selected because it limited the injurious exposure to the nerve root to only the compression-induced injury by the microvascular clip. Previous similar studies of nerve root crush also demonstrate that neuronal activity in the spinal cord that is evoked by a peripheral stimulus correlates with the presence of pathology in the nerve root (Ramer et al. 2000, Rydevik et al. 1991, Wang et al. 2008a). Furthermore, all extracellular recordings in the present study were made in the superficial dorsal horn, where the afferents from the nerve root synapse with second order neurons (Basbaum et al. 2009, Wall & Melzack 1994). In contrast to our findings of a sustained decrease in the discharge rate after a nerve root compression (Fig. 3.8), chronic compression of the root has been previously reported to increase the period of repetitive firing that is evoked by a mechanical stimulus applied directly to the nerve root (Howe et al. 1977). This discrepancy suggests that the changes in the electrophysiologic properties of the neurons after nerve root injury depend on the *type* and *location* of the stimulus. While no attempt was made to differentiate between primary or second order neurons in our study, transection of the nerve root at the conclusion of each recording session ensured that the

evoked responses are associated with the C7 root. It should also be noted that the electrophysiologic properties of neurons that are evoked by a peripheral electrical stimulus do not vary within the 150-350 $\mu$ m range of depths measured in the present study (Wall et al. 1981, Woolf & Fitzgerald 1983). Therefore, despite the fact that the neurons measured in the 3 minute and 15 minute sham groups were 71 $\mu$ m and 91 $\mu$ m shallower than their corresponding compression groups, respectively, it is unlikely that this experimental condition contributed to the differences in the neuronal responses measured in those groups.

Of note, the identification of the duration threshold of 6.6 minutes in this study only considered the response of action potentials that were evoked early (10-40msec) after the electrical stimulus (Fig. 3.6). The neurons associated with such action potentials are the myelinated A fibers (DeLaTorre et al. 2009, Pezet et al. 2008, Yu et al. 2009), which have a lower electrical threshold for excitation than the unmyelinated C fibers (Ramer et al. 2000). However, both fiber types have been shown to exhibit a uniform decrease in the amplitude of electrically-evoked compound action potentials in response to axonal stretch (Shi & Whitebone 2006), suggesting that the electrophysiologic results of the present study may extend to the unmyelinated C fiber population. Conversely, morphologic studies of peripheral nerve compression suggest that the myelinated fibers are more susceptible to mechanical injury (Jancalek & Dubovy 2007, Mosconi & Kruger 1997, Strain & Olson 1975). Thus, the response of myelinated fibers, rather than unmyelinated fibers, may be the more conservative estimate for nerve root compression injuries. Furthermore, several studies suggest that mechanical and thermal sensitivity are transmitted along distinct neuronal subpopulations, with A fibers transmitting mechanical

sensitivity (Cavanaugh et al. 2009, Scherrer et al. 2009). Sensitivity to a mechanical stimulus after a transient C7 nerve root compression has been well-documented (Hubbard et al. 2008a, Rothman et al. 2010). The results of the current study provide the electrophysiologic response of the compressed neurons that are associated with transmitting pain in this model of radiculopathy. As such, in addition to demonstrating a sustained decrease in normal afferent discharge rates and the development of axonal injury in the primary afferents, the present study identifies *immediate* neuronal dysfunction as a potential initiator of the mechanisms leading to persistent pain, even when the nerve root injury is only transient with no observable macroscopic signs of structural injury.

### **3.6 Integration & Conclusions**

The studies presented in this chapter are the first to demonstrate that a painful nerve root compression critically inhibits the frequency of evoked discharge rates through the nerve root *during* the compression (Fig. 3.7). Furthermore, these studies also demonstrate that when the compression duration is shorter than the duration required to critically inhibit neurotransmission through the root, the frequency of evoked discharge rates returns to pre-compression levels within 10 minutes of the removal of the compressive insult (Figs. 3.7 & 3.8) and that the morphology of the axons at day 7 in the injured root show no indications of axonal swelling or irregularities in the axonal distribution, which are normally evident after a painful nerve root compression (Fig. 3.10 & Table 3.1; Hubbard et al. 2008b). The electrophysiological impairment that develops

during the root compression (Figs. 3.7 & 3.8) and cytoskeletal damage that is evident at day 7 (Fig. 3.10 & Table 3.1) are both associated with abnormal afferent signaling (LaPlaca & Prado 2010, Serbest et al. 2007, Takamori et al. 2000). Therefore, in this model of painful nerve root trauma, radicular pain may be initiated *and* maintained by irregular neurotransmission through the root.

The duration of a nerve root compression mediates both the *immediate* functional response and the *subsequent* development of afferent pathology. Blocked axonal conduction due to a mechanical insult (Figs. 3.7 & 3.8) can be indicative of neuronal membrane mechanoporation, in which the permeability properties of the plasma membrane are changed without causing cell death (Geddes et al. 2003, LaPlaca & Prado 2010). Mechanoporation of the neuronal membrane is associated with an influx of calcium (Featherstone 2009, Takamori et al. 2000). The sustained decrease in the frequency of evoked action potentials after the 15 minute compression was removed (Fig. 3.8) further supports the hypothesis that the plasma membrane was likely unable to immediately recover after the mechanical insult and that cytosolic calcium concentrations remained elevated for a period beyond the initial compressive insult (LaPlaca & Prado 2010, LaPlaca & Thibault 1998). Persistently, high, intracellular calcium can damage mitochondria and destabilize the axon's cytoskeleton, leading to the morphological changes that are observed at day 7 (Fig. 3.10) (Serbest et al. 2007). An influx in calcium also signals the neuron to release synaptic glutamate (Featherstone 2009, Takamori et al. 2000). Therefore, even though compression to the root *decreases* the action potential propagation through the root, the associated damage to the plasma membrane of the primary afferents likely *increases* the glutamate signaling at the axon terminals in the

spinal cord (Featherstone 2009, Takamori et al. 2000). Therefore, the critical compression duration of  $6.6\pm 3.0$  minutes that impairs axonal signaling through the root (Fig. 3.7) implies that compressions to the root that last longer than 6.6 minutes likely also produce sustained damage to the neuronal membrane, leading to elevated synaptic glutamate release in the dorsal horn (Featherstone 2009, Geddes et al. 2003, LaPlaca & Prado 2010, Takamori et al. 2000). Elevated spinal glutamate also is associated with behavioral sensitivity (Cata et al. 2007, Coderre et al. 2007); therefore, that 6.6 minute critical duration may also approximate a duration threshold for the development of nerve root-mediated pain.

Studies presented in Chapter 4 test the hypothesis that the critical duration for mediating afferent discharge rates in the spinal cord *during* a C7 nerve root compression in the rat approximates the duration threshold for eliciting behavioral sensitivity. Mechanical allodynia is quantified following compressions applied to the nerve root that are more than one standard deviation shorter than (3 minutes) or longer than (10 minutes) the duration threshold ( $6.6\pm 3.0$  minute) identified in Section 3.3 (Fig. 3.7). To date, neurotrophic, neuropeptidergic and neurodegenerative responses that are relevant to persistent pain have only been characterized for compression durations of 15 minutes (Hubbard & Winkelstein 2005, Hubbard et al. 2008a, Rothman et al. 2010). Therefore, the studies in Chapter 4 also evaluate mechanical allodynia following a 15 minute compression in order to provide context for the mechanical allodynia response after the 3 and 10 minute compressions. Additionally, in order to characterize another clinically-relevant modality of radicular pain, thermal hyperalgesia is also measured following the same 3 and 15 minute nerve root compression durations (see Section 4.4).

As described above, elevated spinal glutamate due to damage sustained by the neuronal membrane during compression, may contribute to the behavioral sensitivity that develops after nerve root compressions (Featherstone 2009, Geddes et al. 2003, LaPlaca & Prado 2010, Takamori et al. 2000). Furthermore, increased concentrations of spinal glutamate and behavioral sensitivity are both associated with neuronal hyperexcitability in the spinal cord (Cata et al. 2006, Inquimbert et al. 2012, Sung et al. 2003). Under normal conditions, however, an over-accumulation of spinal glutamate is prevented by glutamate transporters that take up extracellular glutamate (Rothstein et al. 1996, Sung et al. 2003, Tao et al. 2005). Studies in Chapters 5-7 evaluate what role glutamate and its transporters have in mediating nerve root-mediated pain and neuronal excitability in the spinal cord. Specifically, the temporal expression of spinal glutamate transporters and the development of neuronal hyperexcitability are characterized for painful (15 minutes) and nonpainful (3 minutes) nerve root compressions in Chapter 5. Studies in Chapters 6 and 7 use two different pharmacological approaches to modulate separate aspects of the glutamatergic system. The effects of each pharmacological agent on persistent behavioral sensitivity and neuronal excitability in the spinal cord are evaluated following painful nerve root compression. In Chapter 6, the spinal expression of the glutamate transporter, GLT-1 is increased by daily injections of ceftriaxone, while studies in Chapter 7 inhibit pre-synaptic glutamate release using a single intraperitoneal injection of Riluzole at day 1 after root injury. By identifying the contribution of glutamate to nerve root-mediated pain in Chapters 5-7, additional insight can be garnered about how the duration-mediated neuronal dysfunction and pathology observed in the current studies (Figs. 3.7 & 3.10) drive persistent radicular pain.

---

## CHAPTER 4

# Behavioral Sensitivity is Mediated by the Duration of a Transient Dorsal Root Compression

---

*Parts of this chapter have been adapted from:*

Nicholson KJ, Guarino BB, Winkelstein BA. “Transient Nerve Root Compression Load and Duration Differentially Mediate Behavioral Sensitivity and Associated Spinal Astrocyte Activation and mGluR5 Expression.” *Neuroscience*, 209:187-95, 2012.

### 4.1 Overview

Cervical radiculopathy is characterized by pain that radiates from the neck to the shoulder and arms (Abbed & Coumans 2007). Radiculopathy can be diagnosed by physical examination, imaging studies and/or electrophysiologic tests (Kuijper et al. 2009, Wainner & Gill 2000). In the majority of cases, however, only the patient’s history and a physical examination of the sensory symptoms are used to differentiate radiculopathy from other neurological disorders (Jensen & Baron 2003, Thoomes et al. 2012, Wainner & Gill 2000). In order to improve clinical diagnosis, recent efforts have focused on characterizing the differences in presentation of hypersensitivity to thermal, vibration and pressure stimuli between patients with non-specific arm pain and those with cervical radiculopathy (Moloney et al. 2013). Because symptoms are the primary methods for diagnosing nerve root injuries, the development and utilization of animal and associated cellular models that accurately reflect the clinical sensory profile of cervical

radiculopathy can elucidate the injury mechanisms of nerve root injury, leading to improved diagnosis and treatment of these types of injuries.

The studies in this chapter focus on the experiments outlined under Aim 1b. The primary goal of work in this chapter is to evaluate the development of different types of behavioral sensitivity following nerve root compressions that are applied for varying lengths of time. In order to evaluate two of the most commonly reported types of evoked pain in clinical neuropathy (Backonja & Stacey 2004, Mogil 2009), assays focused on mechanical allodynia and thermal hyperalgesia; these are presented in Section 4.3 and Section 4.4, respectively. Based on the critical duration to mediate afferent discharge rates during compression that was identified in Chapter 3 (Nicholson et al. 2011), compression to the nerve root was applied in these studies for durations above (10, 15 minutes) and below (3 minutes) that duration in order to investigate if, and to what extent, changes in behavioral sensitivity are produced.

The findings from studies in this chapter establish the compression durations that are used in subsequent chapters to characterize the spinal glutamatergic system and excitatory signaling after painful nerve root compressions (Chapter 5) and to evaluate the effectiveness of pharmacological treatments in alleviating these types of behavioral sensitivities after a painful nerve root compression (Chapters 6 & 7). In Chapter 5, the nerve root compressions that are identified here that do and do not elicit behavioral sensitivity will be used to characterize the relationship between nerve root-mediated pain and the spinal expression of glutamate transporters and dorsal horn neuronal excitability. Chapters 6 and 7 will then use pharmacological interventions, such as ceftriaxone to reduce spinal glutamate levels by increasing glutamate uptake, and Riluzole to inhibit



glutamate release, respectively. Those studies help to more specifically characterize the role of glutamate signaling in the persistence of mechanical allodynia and thermal hyperalgesia after painful nerve root compression.

## 4.2 Relevant Background

In a rodent model of cervical nerve root injury, the development of mechanical allodynia depends on both the magnitude and duration of compression that is applied to the nerve root (Hubbard et al. 2008a, Rothman et al. 2010). In that same model, the critical duration for mediating neuronal signaling during a 10gf compression to the C7 nerve root is  $6.6 \pm 3.0$  minutes (Nicholson et al. 2011). Although that duration-threshold was defined as the critical duration to inhibit neuronal discharge rates *during* the applied compression, axonal damage and behavioral sensitivity were also found to develop *only* after a longer duration nerve root compression and to be absent in compressions applied for durations shorter than that threshold (Nicholson et al. 2011, Rothman et al. 2010). Dysfunction in afferent signaling is associated with the subsequent development of axonal injury and pain (Ramer et al. 2000, Gabay & Tal 2004), indicating that the reduced firing rate of afferents in the nerve root during compression may be an indicative marker for the behavioral sensitivity that develops within one day (Hubbard & Winkelstein 2005, Nicholson et al. 2011). Specifically, the association between dysfunction of the afferents and pain (Gabay & Tal 2004) would suggest that behavioral sensitivity only develops following compressions above the  $6.6 \pm 3.0$  minute critical duration (greater than 9.6 minutes), but not for shorter durations (less than 3.6 minutes). However, this relationship between the critical duration for modulation afferents *during*

compression and the subsequent development of behavioral sensitivity after a nerve root compression has not been defined.

Several modalities of pain are present, both clinically and in animal models, such as sensitivity to pressure, heat, cold, vibration and/or punctuate stimuli (Carette et al. 2005, Thoomes et al. 2012). Clinically, different types of neuropathic pain are characterized by the type of pain present (Moloney et al. 2013). Therefore, it is required that animal models of neuropathy, including radiculopathy, reflect the clinically relevant type(s) of pain (Mogil et al. 2010). In patients with chronic neuropathic pain, the two most reported modes of hypersensitivity are to mechanical and thermal stimuli, which are experienced by 64% and 38% of patients, respectively (Backonja et al. 2004). It should be noted that spontaneous, ongoing pain is, by far, the most common symptom and is reported in up to 96% of neuropathic pain patients (Backonja et al. 2004, Mogil et al. 2010). Evoked hypersensitivity, however, is currently considered a more reliable measure than spontaneous pain in animal models (Backonja et al. 2004, Gagliese & Melzack 2000, Mauderli et al. 2000). Nonetheless, because spontaneous pain is the best match to the human experience, researchers continue to seek to improve pain assessment in animal models. Some examples include evaluating aggression, food intake, rearing, guarding or licking (Mogil 2009). However, none of these have been shown to be reliable or sensitive measures and changes in these behaviors could be due to factors other than pain, such as stress or dehydration (Mogil 2009).

Behavioral sensitivity to different types of stimuli is mediated by specific subpopulations of afferent fibers (Braz et al. 2005, Jensen & Baron 2003). Specifically, mechanical allodynia that is evoked by a punctate stimulus, such a von Frey filament, is

mediated by sensitization of the myelinated A $\delta$  fibers (Jensen et al. 2001). Thermal hyperalgesia, on the other hand, is mediated by sensitization of unmyelinated C nociceptors (Jensen et al. 2001). Both the A and C fibers in the nerve root are susceptible to injury from root compression and axonal injury to these fibers, such as swelling and loss of myelination, has been reported to be evident as late as two weeks after a painful transient compression (Chang & Winkelstein 2011, Hubbard et al. 2008b, Kobayashi et al. 2008, Nicholson et al. 2011). Furthermore, myelin degeneration in the nerve root after a transient injury is present only after compressions that also produce mechanical allodynia (Hubbard & Winkelstein 2008), suggesting that injury to the myelinated A fibers may be an indicator and/or a requirement for the development of mechanical sensitivity in this model. Furthermore, the development of morphological damage to the A and C fibers is also mediated by the compression duration (Nicholson et al. 2011); however, to date only mechanical allodynia had been evaluated for nerve root compressions of varying durations (Nicholson et al. 2012, Rothman et al. 2010). Despite evidence that both transient and sustained compressions to the nerve root elicit thermal hyperalgesia (Hashizume et al. 2000, Huang et al. 2012), it is not known whether the development of thermal hyperalgesia after a transient nerve root compression is, like mechanical allodynia, sensitive to the compression duration.

Thermal hyperalgesia in the hind paw or forepaw of a rat can be evaluated by measuring the length of time that a rat tolerates application of a heat stimulus before removing its paw (Hargreaves et al. 1988). An automated measurement device detects a painful response (indicated by a paw withdrawal) by applying a radiant heat source that is synchronized to a timer that stops when a photoelectric cell detects a withdrawal response

(Dirig et al. 1997, Hargreaves et al. 1988). This method is sensitive enough to distinguish the severity of inflammatory-induced hyperalgesia and can track recovery over time (Jackson et al. 1995, Loyd et al. 2012, Hargreaves et al. 1988). Furthermore, this method of quantifying thermal hyperalgesia has been used to differentiate the severity of hypersensitivity following different types of nerve root injury and also to discern the development of *hypersensitivity* and *hyposensitivity* following cervical nerve root injuries (Hashizume et al. 2000, Huang et al. 2012). Its effectiveness to differentiate the severity and type of thermal sensitivity after nerve root injuries demonstrates its utility in characterizing the development of thermal hyperalgesia following nerve root compressions of varying durations.

Studies presented in this chapter test the hypothesis that the critical duration ( $6.6 \pm 3.0$  minutes) (Nicholson et al. 2011) for inhibiting afferent action potentials during an applied compression to the C7 nerve root in the rat also approximates the duration threshold for eliciting mechanical allodynia and thermal hyperalgesia in the affected forepaw. A 10gf load was applied to the C7 nerve root for compressions below (3 minutes) and above (10 & 15 minutes) that critical duration. Mechanical allodynia in the forepaw was measured for 7 days after each type of loading condition, and thermal hyperalgesia was evaluated for 7 days following the 3 and 15 minute compressions. These studies define the role of the compression duration for mediating both mechanical allodynia and thermal hyperalgesia and will also establish the loading conditions for painful and nonpainful nerve root compressions that will be used in Chapter 5.

### **4.3 Mechanical Allodynia Depends on the Duration of Compression**

The goal of this study is to evaluate the development and maintenance of mechanical allodynia following a nerve root compression applied to the root for a period that is outside one standard deviation below (3 minutes) or above (10 minutes) the  $6.6 \pm 3.0$  minute critical compression duration, above which electrically evoked action potentials transmitted through the root are critically inhibited (Nicholson et al. 2011). Previous studies established that a 15 minute compression to the nerve root elicits mechanical allodynia (Rothman et al. 2010, Hubbard & Winkelstein 2005). To provide context for the behavioral outcomes measured after the 3 minute and 10 minute compressions, mechanical allodynia was also measured in a separate group of rats following a 15 minute compression.

#### **4.3.1 Methods**

Experiments were performed using male Holtzman rats (300-400g), housed under USDA- and AAALAC-compliant conditions and given free access to food and water. All procedures were approved by the Institution Animal Care and Use Committee and adhered to the guidelines of the Committee for Research and Ethical Issues of the International Association for the Study of Pain (Zimmermann 1983). Using the same surgical methods detailed in Chapter 3, compression was applied to the C7 nerve root for either 3 minutes or 10 minutes (n=6 rats/group) using a 10gf clip (WPI, Inc., Sarasota, FL). Sham procedures (n=6 rats) with dorsal nerve root exposure but no compression were also included as controls. In a separate study to provide context, rats underwent

either a C7 nerve root compression applied for 15 minutes (n=5 rats) or the sham exposure (n=4 rats).

Behavioral hypersensitivity was evaluated by measuring bilateral forepaw mechanical allodynia prior to (baseline) and on days 1, 3, 5, and 7 following surgery (Hubbard and Winkelstein 2005, Rothman et al. 2005). For each behavioral testing session, following 20 minutes of acclimation, rats were stimulated on the plantar surface of each of the ipsilateral and contralateral forepaws using a 4.0gf von Frey filament (Stoelting Co.; Wood Dale, IL). Each testing session consisted of three rounds of 10 stimulations each, separated by 10 minutes. The total number of paw withdrawals was recorded for each forepaw of each rat and averaged across each group on each day.

Significant differences in the number of paw withdrawals were determined between groups over time using a two-way, repeated measures ANOVA. A one-way ANOVA with post-hoc Bonferroni correction tested for differences in the number of paw withdrawals between each group on each day.

### **4.3.2 Results**

Ipsilateral mechanical allodynia was only elicited by a compression applied for 10 or 15 minutes (Figs. 4.1 & 4.2). On each day that behavioral testing was performed, the number of paw withdrawals following a compression applied for 10 minutes was significantly ( $p<0.019$ ) elevated over the number of responses for both sham and the compression applied for only 3 minutes (Fig. 4.1). Furthermore, the number of paw withdrawals significantly increased over baseline ( $p<0.004$ ) only for the 10 minute compression group. There were no differences in the number of paw withdrawals

between the 3 minute compression and sham groups. Similar to the response in the 10 minute compression group, the number of paw withdrawals elicited after a 15 minute compression was significantly greater ( $p<0.011$ ) than those of sham and baseline ( $p<0.012$ ) at each post-operative time-point (Fig. 4.2).

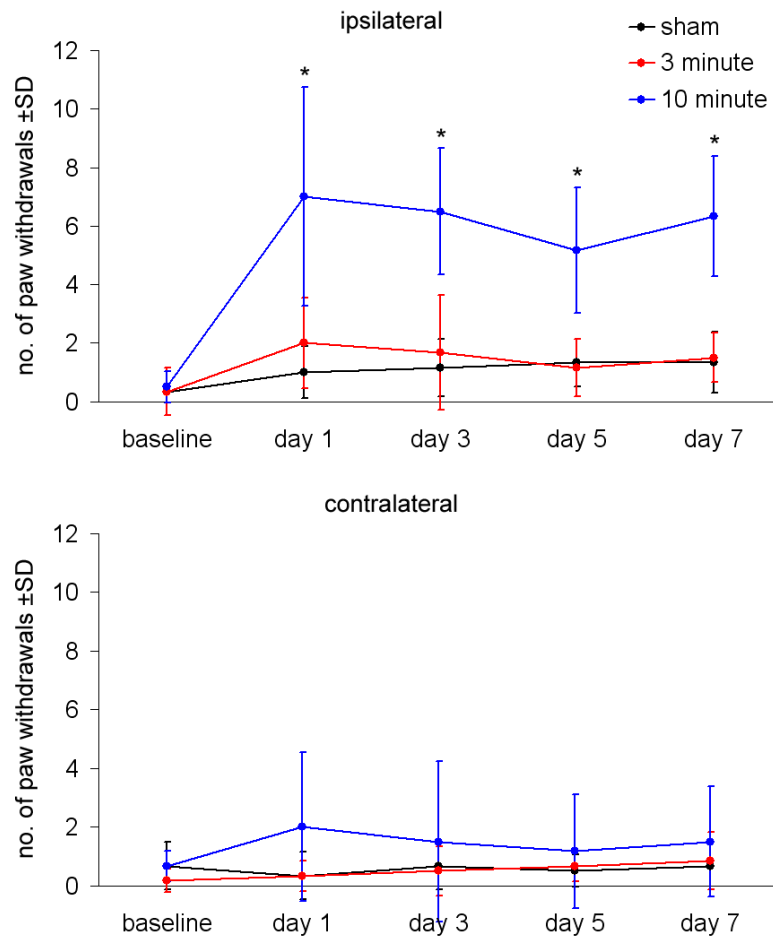


**Fig. 4.1** Average mechanical allodynia assessed in the ipsilateral and contralateral forepaws following sham, a 3 minute compression or a 10 minute compression. The number of ipsilateral paw withdrawals significantly ( $*p<0.019$ ) increased at each post-operative time-point following a 10 minute compression compared with sham and the 3 minute compression.

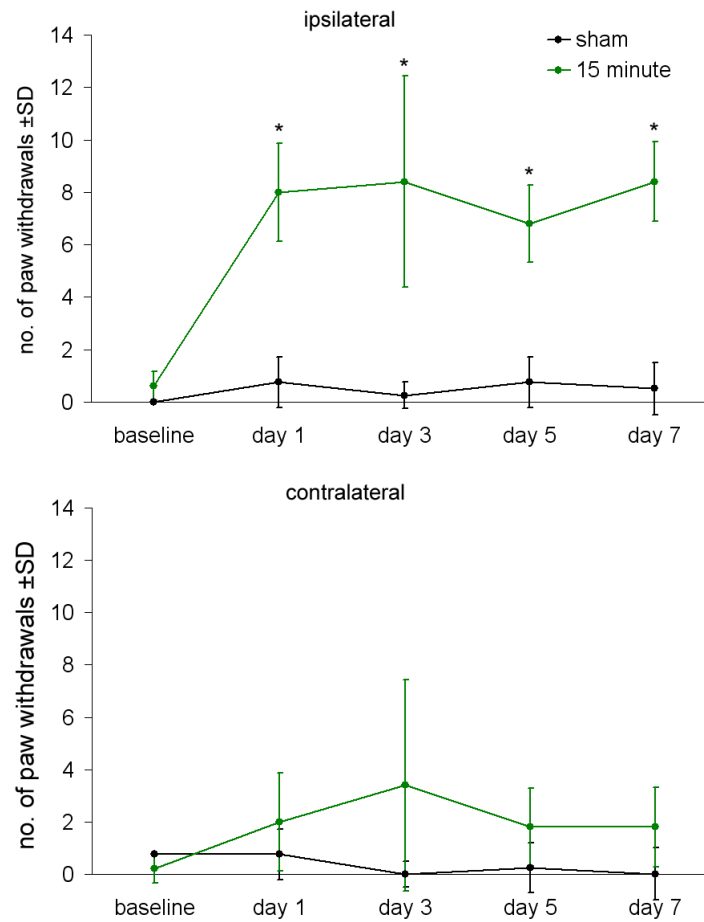


**Fig. 4.2** Average mechanical allodynia assessed in the ipsilateral and contralateral forepaws following sham procedures or a 15 minute compression. On each testing day after compression, the number of withdrawals in the ipsilateral paw significantly increased (\* $p < 0.011$ ) compared to sham.

There were no significant differences in the contralateral forepaw between any group (Figs. 4.1 & 4.2). Specifically, contralateral paw withdrawals were slightly greater following a 10 minute than a 3 minute compression or sham procedures, but this was not significant (Fig. 4.1). The number of contralateral paw withdrawals following the 15 minute compression also was not significantly different from sham. There were no differences in the number of contralateral paw withdrawals from baseline for any injury group. Please see Appendix C for the individual behavioral data for all rats in this study.



## **4.4 Thermal Hyperalgesia After Transient Nerve Root Compressions**

The temporal response of mechanical allodynia after a 15 minute compression (Fig. 4.2) is similar to that produced by a 10 minute compression (Fig. 4.1). Furthermore, the number of paw withdrawals elicited after the 10 and 15 minute compressions were similar. Therefore, in this study, thermal hyperalgesia was evaluated following nerve root compression durations known to either elicit mechanical allodynia (15 minutes) or to produce no changes to the mechanical sensitivity of the rat's forepaw (3 minutes). Thermal hyperalgesia was evaluated at post-operative days 1 and 7, when mechanical allodynia is initiated and maintained, respectively (Figs. 4.1 & 4.2).

### **4.4.1 Methods**

Surgical procedures were as described in Chapter 3 with rats receiving a compression injury to the right C7 nerve root or sham (Hubbard & Winkelstein 2005, Nicholson et al. 2011). Each rat either received a 10gf transient nerve root compression applied for 3 or 15 minutes, or a surgical sham exposure (n=7/group). Bilateral thermal hyperalgesia was evaluated prior to (baseline) and on day 1 and day 7 after injury. Bilateral mechanical allodynia was also measured at baseline and at both post-operative time-points to ensure that the 3 and 15 minute compression conditions were comparable to those reported in Section 4.3. For each testing session, mechanical allodynia was evaluated using the methods described in Section 4.3 and was completed before testing for thermal hyperalgesia.

Thermal hyperalgesia was evaluated by placing rats in a wire mesh cage on a glass surface (Fig. 4.3) and allowed to acclimate to the environment for 20 minutes prior

to testing. Thermal hyperalgesia was measured using a commercially available device (Fig. 4.3; UC San Diego) by applying a radiant heat source (projection bulb) focused on the plantar surface of each forepaw using established methods to quantify withdrawal latency (Dirig et al. 1997, Hargreaves et al. 1988). The projection bulb was positioned under the plantar surface of the forepaw with the assistance of an angled mirror attached to the stimulus. The latency time between when the heat source was first applied and when the paw withdrawal occurred (withdrawal latency) was measured by an automatic timer that was synchronized with the stimulus (Fig. 4.3). On each day of testing, the withdrawal latency was measured three times for each paw, with a 10 minute rest between each measurement, and the average for each of the ipsilateral and contralateral paws across the three rounds was recorded for each rat on each day.

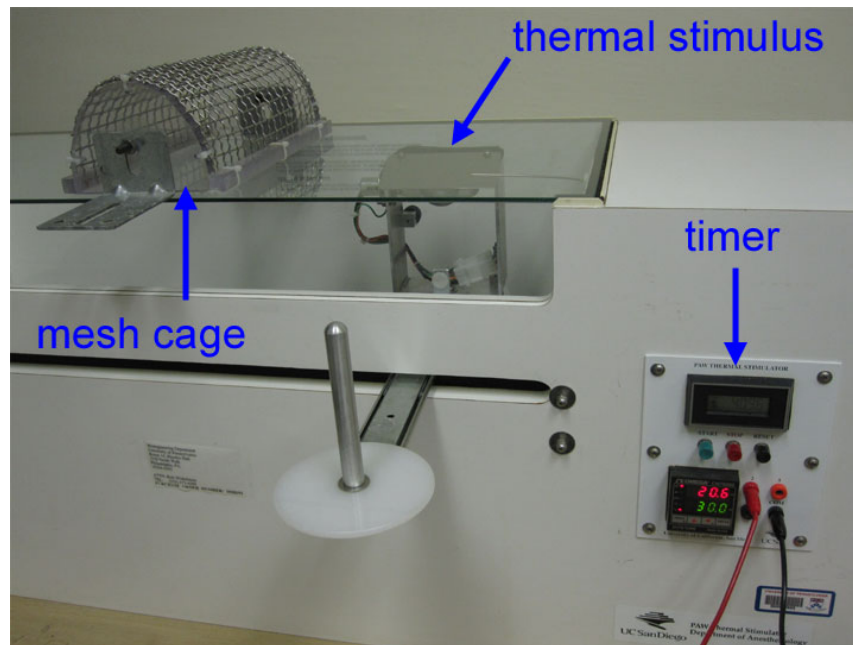


**Fig. 4.3** Device for measuring thermal hyperalgesia in the rat. A rat is placed in the wire mesh cage enclosure on a glass surface and the thermal stimulus is positioned under the forepaw. The timer measures the time between the application of the stimulus and when the paw is withdrawn.

Differences in the withdrawal latency and mechanical allodynia between groups over time was determined by a two-way repeated measures ANOVA for the ipsilateral and contralateral forepaws, separately. At each day, separate one-way ANOVAs with a post-hoc Bonferroni correction tested for differences in the ipsilateral and contralateral forepaws between groups. T-tests compared the number of paw withdrawals elicited in the 3 and 15 minute compression groups to their respective groups in the studies presented in Section 4.3.

#### **4.4.2 Results**

Thermal hyperalgesia varied significantly between groups ( $p < 0.013$ ) only for the ipsilateral forepaw, and only developed following a 15 minute compression (Fig. 4.4). At day 1, the withdrawal latency for the thermal stimulus after a 15 minute compression significant decreased ( $p < 0.020$ ) compared to the latencies after both sham and a 3 minute root compression and remained significantly lower ( $p < 0.010$ ) than both groups at day 7 (Fig. 4.4). Thermal hyperalgesia after a 3 minute compression did not significantly differ from sham procedures at either time-point. Furthermore, the withdrawal latency for both the 3 minute compression and sham groups was not different baseline at either post operative time-point. In the contralateral forepaw, no differences were observed between any group, nor did the withdrawal latency vary from the associated baseline values (Fig. 4.4). The withdrawal latency measured for each rat is summarized in Appendix C.

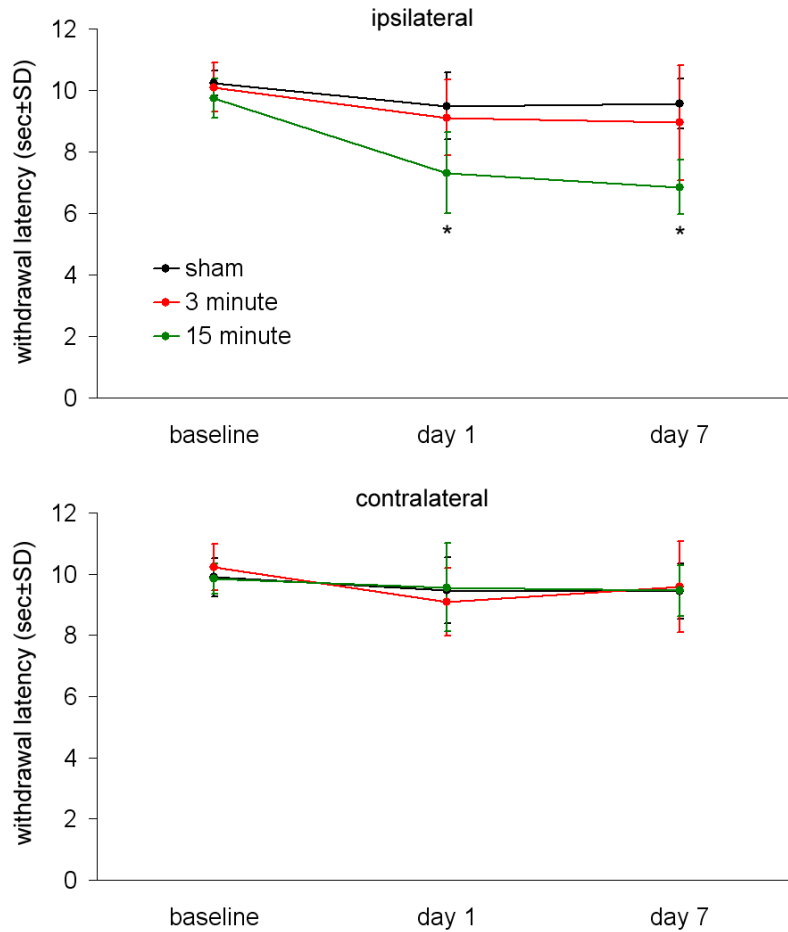


**Fig. 4.4** Thermal hyperalgesia in the forepaw. The thermal latency after a 15 minute compression is significantly (\* $p < 0.020$ ) decreased at both day 1 and day 7 compared to a 3 minute compression and sham. No significant differences in the withdrawal latency were observed in the contralateral forepaw between any group at any time-point.

Like thermal hyperalgesia, mechanical allodynia was only elicited in the ipsilateral forepaw following a 15 minute compression (Fig. 4.5). Within 1 day, the number of paw withdrawals to the 4.0gf filament significantly increased ( $p < 0.001$ ) after a 15 minute compression compared to sham and the 3 minute compression and remained significantly greater ( $p < 0.005$ ) than both groups at day 7 (Fig. 4.5). The 3 minute compression and sham groups did not vary from baseline at either time-point. There were no significant differences in the number of ipsilateral paw withdrawals elicited after a 3 minute compression or a 15 minute compression in the present study compared to the

same compression duration groups presented in Section 4.3 (Figs. 4.1-4.2 & 4.5). Appendix C summarizes the paw withdrawal response for each day for each rat.

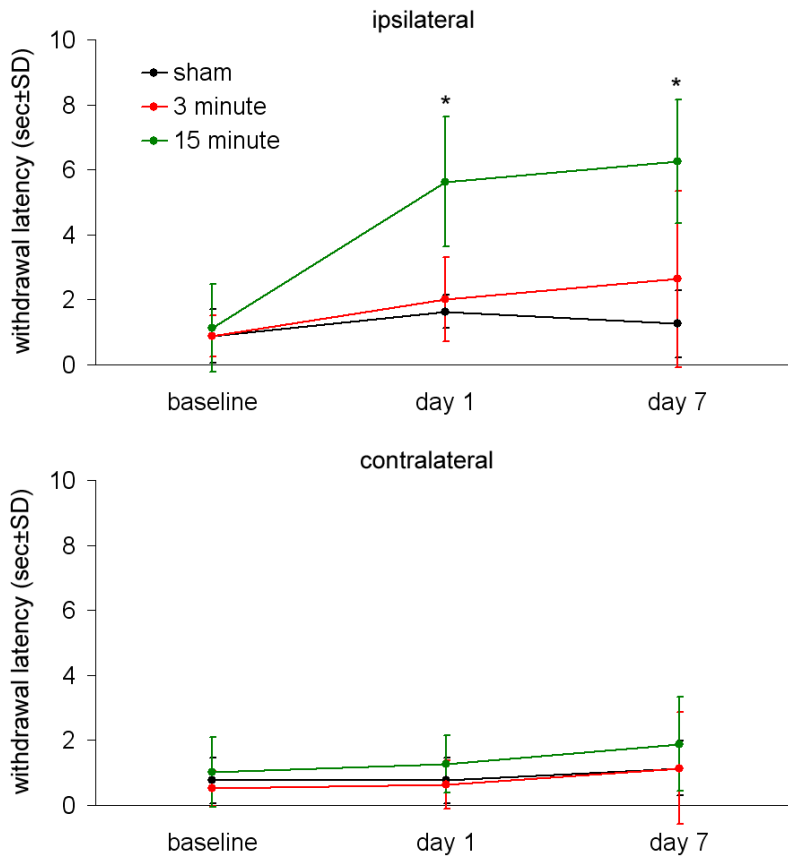


**Fig. 4.5** Mechanical allodynia in the ipsilateral forepaw is significantly elevated ( $*p < 0.005$ ) following a 15 minute compression compared to a 3 minute compression and sham procedures at days 1 and 7.

## 4.5 Discussion

Thermal hyperalgesia only developed following compressions that also elicited mechanical allodynia (Figs. 4.1-4.2 & 4.4-4.5). Furthermore, there were no robust differences in the number of paw withdrawals evoked by the von Frey filament stimulus after the 10 or 15 minute compression durations (Figs. 4.1 & 4.2) indicating that allodynia is not differentiated by compression durations longer than 10 minutes. Previous

studies that applied graded compression magnitudes in the range of 5.30-108.99mN demonstrated that above an applied load of 76.2mN, allodynia is insensitive to the compression duration (Hubbard et al. 2008a). The present study suggests that there is likely a similar duration threshold for eliciting maximum allodynia that lies between 3 and 10 minutes; above 10 minutes, there is no further increase in the mechanical allodynia response (Figs. 4.1 & 4.2). The compression mechanics required to elicit thermal hyperalgesia appear to be similar to, if not the same as, those required to elicit mechanical allodynia (Figs. 4.4 & 4.5). Therefore, like mechanical allodynia, the withdrawal latency is likely not further reduced by compressions applied for durations longer than 15 minutes (Fig. 4.4).

Damage sustained to both the myelinated A $\delta$  fibers and unmyelinated C fibers by a mechanical compression to the nerve root likely underlies the development of mechanical and thermal hyperalgesia in this model (Figs. 4.1-4.2 & 4.3-4.5; Braz et al. 2005, Jensen & Baron 2003). Both types of fibers exhibit axonal swelling and irregular morphology by day 7 after the painful 15 minute compression (Nicholson et al. 2011) and in other animal models of mechanical trauma to the nerve root (Kobayashi et al. 2005a, Kobayashi et al. 2008). To date, nerve root conduction studies have only demonstrated neuronal dysfunction in the fast transmitting, myelinated A fibers during an applied compression (Nicholson et al. 2011, Pedowitz et al. 1992). The development of thermal hyperalgesia (Fig. 4.4), which is mediated by sensitized C fibers (Jensen et al. 2001) suggests that these nociceptive fibers of the nerve root are also susceptible to altered neurotransmission during the applied compression.

The relationship between compression duration and the development of behavioral sensitivity observed here (Figs. 4.1-4.2 & 4.4-4.5) expands our understanding of how the mechanical loading profile of a nerve root compression mediates pain (Huang et al. 2012, Hubbard et al. 2008a, Rothman et al. 2010, Winkelstein et al. 2002). Just as there is a magnitude threshold (Hubbard et al. 2008a), there is also a compression duration threshold between 3 and 10 minutes for eliciting behavioral sensitivity (Figs. 4.1 & 4.2). A recent study reports that compression magnitudes to the nerve root that are 15 times greater than the threshold for inducing *hypersensitivity* will actually induce *hyposensitivity* to mechanical stimuli (Huang et al. 2012, Hubbard et al. 2008a), suggesting that if the mechanical thresholds for eliciting *hypersensitivity*, including the compression duration threshold, are greatly exceeded, sensation may actually decrease and this may be one contributing factors to the paresthesia and numbness that develop in some cases of radiculopathy (Abbed & Coumans 2007). It has previously been reported that the extent of demyelination and degeneration that develops in the root is more extensive after a root compression that elicits *hyposensitivity* than a compression that elicits *hypersensitivity* (Huang et al. 2012). The more severe pathology that accompanies loss of sensation after a root compression suggests that pain may require intact axons whose response to stimuli is exaggerated due to surrounding inflammatory responses in the root itself or the spinal cord, including glial activation, cytokine upregulation and macrophage infiltration (Chang et al. 2011, Colburn et al. 1999, Rothman et al. 2009).

Because the magnitude threshold for reducing mechanical sensitivity in the forepaw is higher than the threshold for developing persistent pain, there may also be a duration threshold greater than the 15 minutes applied here (Fig. 4.4), above which

thermal *hypoalgesia* develops. Given that both the duration and magnitude of compression determine the development of *hypersensitivity* or *hyposensitivity*, the behavioral responses to the mechanical and thermal stimuli observed here (Figs. 4.1-4.2 & 4.4-4.5) expands, but does not complete, our understanding of the complex relationship between the compression mechanics and behavioral outcomes (Figs. 4.1-4.2 & 4.3 & 4.4; Huang et al. 2012, Hubbard et al. 2008a, Rothman et al. 2010). Although additional studies could further define the relationship between nerve root compression mechanics and radicular pain, defining this relationship in the rat has limited applications when extrapolating to human nerve root mechanics. The value of defining compression durations that do and do not elicit pain is that the nonpainful compression provides a study control group for differentiating pathologies that are specific to nerve root-mediated pain from those that may solely be attributed to the effects of mechanical compression of the root.

One limitation of most animal pain models of trauma or injury is that the painful condition is only compared to a surgical control without consideration for the severity of the injury (Mogil et al. 2010). Such study designs may errantly identify chemical and/or anatomical responses that are not necessarily specific to pain (Grace et al. 2010). For example, in the same model of a nerve root compression used in the present study, spinal mGluR5 can be upregulated or unchanged after both painful and nonpainful nerve root compressions, depending on the magnitude of the applied compression (Nicholson et al. 2012). Because of such disparities between pain and physiology or tissue pathology, models that replicate graded pain responses after spinal cord and peripheral nerve injury have been developed to specifically correlate neurochemical, anatomical and



inflammatory responses to the development and maintenance of behavioral sensitivity (Carlson et al. 2003, Grace et al. 2010, Lotz & Chin 2010). In a similar manner, specific radicular pain-associated tissue responses can be determined by utilizing the painful and nonpainful transient cervical nerve root compressions that are defined by the compression duration (Figs. 4.1-4.2 & 4.5).

In addition to defining graded pain responses, characterizing mechanical allodynia and thermal hyperalgesia increases the utility of animal models of pain for pharmacological studies (Mogil et al. 2010, Moloney et al. 2013). Some treatments may only target one modality of sensitivity; thus, analgesic agents must be assessed across many different pain modalities (Hama et al. 2003, Hudson et al. 2002, Wang et al. 2005). The NMDA antagonist, MK-801, for example, alleviates mechanical, but not thermal, hyperalgesia in a rat model of peripheral inflammation (Hama et al. 2003). Characterizing the type(s) of pain present after injury is, therefore, critical for analgesic drug development. Prior to this study, there were limited data regarding the development of thermal hyperalgesia after a transient cervical nerve root injury (Huang et al. 2012). By characterizing the onset and persistence of both mechanical allodynia and thermal hyperalgesia (Figs. 4.3 & 4.4), pharmacological studies in this model can use both of these behavioral assessments to strengthen our understanding of mechanisms driving the different aspects of nerve root-mediated pain.

The present study characterized sensory changes after a transient cervical nerve root compression; yet, motor weakness is also a symptom of radiculopathy (Abbed & Coumans 2007). Although muscle function and strength have been measured in this model of cervical radiculopathy, no motor impairment was observed (Dunk et al. 2011).

The dorsal nerve root only contains afferent neurons. However, it is possible that injury to the ventral root and/or proximal spinal cord may be required to induce the motor impairment that is observed in some models of nerve root injury (Shamji et al. 2009). While there is certainly room to further characterize the sensory and motor deficits associated with a nerve root compression, the present study identified and characterized the development of the two most common types of clinically reported evoked neuropathic pain: mechanical and thermal sensitivity (Figs. 4.1-4.2 & 4.3; Backonja & Stacey 2004). Furthermore, this study demonstrates that the development of mechanical allodynia and thermal hyperalgesia are both mediated by the compression duration, suggesting that duration-mediated neuronal responses in the nerve root during the applied compression may initiate these painful outcomes (Nicholson et al. 2011)

#### **4.6 Integration & Conclusions**

The studies in this chapter demonstrate that duration mediates the development of both mechanical allodynia (Figs. 4.1 & 4.2) *and* thermal hyperalgesia (Fig. 4.4). Specifically, behavioral sensitivity only develops when the compression that is applied to the nerve root is longer than the  $6.6 \pm 3.0$  minute critical duration for reducing electrically-evoked action potentials through the root *during* the applied compression (Nicholson et al. 2011). When compression is applied for times shorter than one standard deviation below (3 minutes) or longer than one standard deviation above (10 minutes) this critical duration, only the 10 minute compression elicited mechanical allodynia (Fig. 4.1). This suggests that the changes that are produced in the electrophysiological properties of the nerve root afferents while the root is compressed may be indicative of the subsequent

development of pain, or may even be *the* initiator of the nerve root-mediated pain that develops (Nicholson et al. 2011).

Studies presented in Chapter 5 will use the painful (15 minute) and nonpainful (3 minute) compression conditions established in this chapter to characterize the relationship between a painful compression to the nerve root and development of hyperexcitability in spinal neurons. Although Chapter 3 measured afferent function *during* an applied compression, neuronal signaling *after* a painful nerve root compression has not been defined at a time-point when behavioral sensitivity persists. Therefore, studies in Chapter 5 will record afferent activity from dorsal horn neurons at day 7 after injury. The studies in Chapter 5 will also characterize the temporal expression of spinal glutamate transporters, which regulate glutamate, the neurotransmitter that underlies excitatory neuronal activity (Tao et al. 2005). In order to further define the role of spinal excitatory signaling in the persistence of nerve root-mediated pain, studies in Chapters 6 and 7 measure behavioral sensitivity and spinal neuronal hyperexcitability after pharmacologically modulating the uptake and release of the excitatory neurotransmitter, glutamate, respectively. Specifically, ceftriaxone is administered to increase glial uptake of extracellular glutamate by upregulating the spinal expression of the glutamate transporter, GLT-1 (Chapter 6). The studies presented in Chapter 7 deliver Riluzole after a painful nerve root injury in order to inhibit glutamate release by pre-synaptic neurons. Because many pharmacological treatments may only alleviate either mechanical or thermal sensitivity, both mechanical allodynia and thermal hyperalgesia are evaluated in those studies of painful nerve root compression treated with ceftriaxone or Riluzole in order to characterize the effect of each treatment on each of these pain modalities.

---

## CHAPTER 5

# Glutamate Transporters & Excitatory Signaling in the Spinal Cord following Painful Nerve Root Compression

---

*Parts of this chapter were adapted from:*

Nicholson KJ, Gilliland TM, Winkelstein BA. “Up-regulation of GLT-1 by Treatment with Ceftriaxone Alleviates Radicular Pain by Reducing Spinal Astrocyte Activation and Neuronal Hyperexcitability” *submitted*.

Zhang S, Nicholson KJ, Smith JR, Syré PP, Gilliland TM, Winkelstein BA. “The Roles of Mechanical Compression and Chemical Irritation in Regulating Spinal Neuronal Signaling in Painful Cervical Nerve Root Injury” *Stapp Car Crash Journal*, submitted.

### 5.1 Overview

The interaction between astrocytes and neurons in the central nervous system is bi-directional and because of this “tripartite synapse,” neuronal function in the central nervous is modulated by the neuron-astrocyte network. Astrocytes not only regulate signaling at neuronal synapses, but also respond to neuronal synaptic activity and, in so doing, they provide neuroprotective support under normal conditions (Markowitz et al. 2007, Perea et al. 2009, Ren & Dubner 2008). Activation of astrocytes, which can be initiated by neurodegeneration, however, can switch the role of astrocytes from that of maintaining normal synaptic transmission to enhancing neuronal excitability (Markowitz et al. 2007, Perea et al. 2009, Ren & Dubner 2008). In particular, glutamate transporters on the cellular membrane of astrocytes regulate excitatory synaptic transmission by

taking up excess extracellular glutamate, the primary excitatory neurotransmitter in the central nervous system (Basbaum et al. 2009, Tao et al. 2005, Rothstein et al. 2005). In many animal models of neural tissue injury or disease, however, the glutamate transporters on both astrocytes and neurons are downregulated, resulting in elevated glutamate concentrations at the synapse which can enhance neuronal excitability (Cata et al. 2006, Rothstein et al. 2005). Although many rodent and canine models of nerve root injury demonstrate that activation of spinal astrocytes and neurodegeneration of primary afferents are associated with persistent behavioral sensitivity (Colburn et al. 1999, Hubbard & Winkelstein 2008, Kobayashi et al. 2008, Rothman & Winkelstein 2007), no study has characterized neuronal excitability in the spinal cord or glutamate transporter expression following painful nerve root compression.

Work presented in this chapter focuses on the experiments outlined in Aims 2a and 2b. Studies implicate dysregulation of spinal neuronal and glial glutamate transporters in the persistence of behavioral sensitivity following trauma both in the peripheral and central nervous systems (Kim et al. 2011, Sung et al. 2003, Xin et al. 2009). Therefore, studies in this chapter investigate the hypothesis that downregulation of spinal glutamate transporters and the development of neuronal hyperexcitability in the dorsal horn are associated with behavioral sensitivity following a painful transient C7 cervical nerve root compression in the rat. As such, the studies presented in Section 5.3 characterize the temporal expression of these transporters following the painful (15 minute) and nonpainful (3 minute) nerve root compressions that were defined in Section 4.4. Specifically, the spinal expression of the glial glutamate transporters, GLT-1 and GLAST, and the neuronal glutamate transporter, EAAC1, are quantified at days 1 and 7

to evaluate their association with the initiation and maintenance of behavioral sensitivity in this radiculopathy model. In a second set of studies (Section 5.4), the frequency of evoked afferent firing in the spinal cord is evaluated at day 7 to define whether a painful nerve root compression leads to excitability of dorsal horn neurons. In that work, separate studies characterize the response of neurons in the superficial and deep laminae to evaluate whether such neuronal hyperexcitability is localized to the region associated with primary synapses of nociceptors (superficial laminae) or to the synapses of neurons that transmit non-noxious mechanical stimuli (deep laminae). Based on the results of this chapter, Chapters 6 and 7 further test the contribution of the glutamatergic system to nerve root-mediated pain and neuronal hyperexcitability in the dorsal horn by administering ceftriaxone to promote GLT-1 expression (Chapter 6) and Riluzole to block pre-synaptic glutamate release (Chapter 7), respectively.

## **5.2 Relevant Background**

The annual incidence for neck pain is reported to be 14-50% and as many as one-half of these cases can persist for more than one year (Côté et al. 2004, Hill et al. 2004, Hogg-Johnson et al. 2008). Injury to the cervical nerve roots is a common source of neck pain due to their mechanical susceptibility from foraminal impingement, disc herniation, direct spinal trauma, and/or foraminal stenosis (Eichberger et al. 2000, Nuckley et al. 2002, Wainner & Gill 2000). Rodent models of nerve root injury have established that behavioral sensitivity develops after mechanical insults to the root (Colburn et al. 1999, Hashizume et al. 2000, Huang et al. 2012, Hubbard & Winkelstein 2005) and that the development of mechanical allodynia and thermal hyperalgesia is sensitive to the

duration of the transient nerve root compression (Chapter 4; Rothman et al. 2010). Furthermore, spinal glial activation is only evident following a painful nerve root compression (Nicholson et al. 2012, Rothman et al. 2010). Due to the role spinal glia play in maintaining normal neuronal synaptic transmission, their activation following a painful root compression suggests that altered neurotransmission in the spinal cord may contribute to nerve root-mediated pain (Paixão & Klein 2010, Ren & Dubner 2008). However, afferent signaling in the spinal cord has not been characterized for painful nerve root compressions nor have the cellular mechanisms by which spinal glia contribute to enhanced nociception after such injuries been defined.

Animal models of pain demonstrate that the neurotransmitters, substance P (SP), calcitonin gene related peptide (CGRP) and glutamate, play an important role in nociception (Basbaum et al. 2009). Elevated concentrations of each of these transmitters in the spinal cord is associated with behavioral sensitivity (Bausbaum et al. 2009, Kuner 2010, Sun et al. 2003) Yet, a mechanical injury to the nerve root decreases SP and CGRP in the superficial dorsal horn, where the primary afferents synapse (Koyashi et al. 2005a, Hubbard et al. 2008a). Because both SP and CGRP are trafficked to the spinal cord from the dorsal root ganglion (DRG), nerve root injuries are thought to disrupt the normal axonal flow of SP and CGRP (Kobayashi et al. 2005a, Hubbard et al. 2008a). Glutamate on the other hand, does not rely on normal transport across the dorsal root because it is synthesized in the pre-synaptic terminal from glutamine, which is released by perisynaptic glial cells (Basbaum et al. 2009, Tao et al. 2005). Despite the central role of glutamate in potentiating synaptic transmission in the central nervous system, its role in nerve root-mediated pain has not been investigated.

Extracellular glutamate concentration is tightly regulated in the spinal cord by neurons and glial cells, which take up synaptic glutamate via glutamate transporters (Rothstein et al. 1996, Tao et al. 2005). In the rat spinal cord there are three glutamate transporters: excitatory amino-acid carrier 1 (EAAC1), glutamate-aspartate transporter (GLAST) and glial glutamate transporter 1 (GLT-1) (Rothstein et al. 2005, Queen et al. 2007, Tao et al. 2005). EAAC1 is predominantly expressed by neurons; GLAST and GLT-1 are expressed by glial cells. After spinal cord and peripheral nerve injuries there is a transient increase in expression of all three transporters within the first day (Kim et al. 2011, Sung et al. 2003, Vera-Portocarrero et al. 2002). However, several models of peripheral nerve injury demonstrate that glutamate transporters decrease within a week, when behavioral sensitivity is established, indicating that a decrease in glutamate transporter expression may contribute to neuropathic pain (Hu et al. 2010, Sung et al. 2003, Tao et al. 2005, Xin et al. 2009). In fact, behavioral sensitivity is alleviated and normal glutamate signaling is restored when glutamate transporters are pharmacologically upregulated (Hu et al. 2010, Ramos et al. 2010, Nie et al. 2010). Although those studies implicate glutamate transporters in pain, it is not known whether a painful nerve root injury also mediates glutamate transporter expression in the spinal cord.

Downregulation of spinal glutamate transporters reduces synaptic glutamate clearance which increases the excitability of spinal neurons in the rat (Cata et al. 2006, Inquimbert et al. 2012, Tao et al. 2005). Increased spontaneous and evoked discharge rates of spinal dorsal horn neurons is associated with pain in rodent models of peripheral inflammation, nerve trauma and spinal cord injury (Asante et al. 2009, Hao et al. 1992,



Hains et al. 2003, Pitcher et al. 2004, Shim et al. 2005). Spinal excitability also mediates behavioral responses in nerve root injury (Ramer et al. 2000, Terashima et al. 2011). Specifically, rodent models of nerve root trauma demonstrate that loss of sensation in the rat forepaw after crush injury of multiple cervical nerve roots is associated with reduced afferent activity in the spinal cord, while enhanced behavioral sensitivity is associated with an increase in the amplitude of excitatory post-synaptic currents (EPSCs) after a lumbar root constriction (Ramer et al. 2000, Terashima et al. 2011). EPSCs were only evaluated in lamina II of the superficial dorsal horn (Terashima et al. 2011); but, the amplitude increase does suggest that post-synaptic neurons in the spinal cord are more likely to propagate an action potential in response to excitatory input, thereby increasing the firing rate of second order neurons in the spinal cord (Cata et al. 2009, Inquimbert et al. 2012, Kuner 2009, Nguyen et al. 2009). However, it has not been determined whether mechanical trauma to the nerve root increases the frequency of evoked action potentials of dorsal horn neurons nor has it been established whether such responses occur in the superficial laminae, where the primary nociceptors synapse, and/or the deep laminae, where many low-threshold mechanoreceptors synapse to polysynaptic neurons that also respond to noxious stimuli (Basbaum et al. 2009, Todd 2010).

These studies test the hypothesis that spinal glutamate transporters and neuronal hyperexcitability contribute to behavioral sensitivity following a transient C7 nerve root compression. As such, the spinal expression of GLT-1, GLAST and EAAC1 were evaluated following compression durations that do (15 minutes) and do not (3 minutes) elicit mechanical allodynia (Rothman et al. 2010). Glutamate transporter expression was assessed at days 1 and 7 (Section 5.3), to evaluate the expression of these transporters at

time-points relevant to the establishment and persistence of both mechanical allodynia and thermal hyperalgesia in this model (Chapter 4). In the second study (Section 5.4), neuronal excitability was evaluated in the spinal cord at day 7 following the same 15 minute and 3 minute compression durations, in separate groups. Extracellular recordings were made in the dorsal horn while a range of mechanical stimuli strengths were applied to the forepaw. Collectively, these studies characterize and identify glutamate transporter and neuronal excitability responses in the spinal cord that are specific to painful nerve root compressions.

### **5.3 Temporal Response of Spinal Glutamate Transporters**

#### **5.3.1 Methods**

Male Holzman rats (275-375g) were housed in USDA- and AAALAC-compliant conditions with a 12–12 hour light–dark cycle and free access to food and water. All studies were IACUC-approved and carried out under the guidelines of the Committee for Research and Ethical Issues of the International Association for the Study of Pain (Zimmermann, 1983).

Rats underwent a C7 nerve root compression applied for 15 minutes or 3 minutes, or sham procedures (n=14/group) (Nicholson et al. 2012, Rothman et al. 2010). Mechanical allodynia and thermal hyperalgesia were evaluated prior to surgery (baseline) and on days 1 and 7 after injury. The rats used for the current study were the same as those presented in Section 4.4; detailed methods for the surgical procedures and behavioral assessments are also described in Chapter 4.

In order to assess the temporal profile of spinal glutamate transporters, C7 spinal cord tissue was harvested at day 1 (n=7/group) and day 7 (n=7/group). Matched spinal cord sections were harvested from normal, naïve rats (n=2) and were included in all assays as controls. Rats were anesthetized with an intraperitoneal injection of 65mg/kg pentobarbital then transcardially perfused with 200ml Dulbecco's Phosphate-Buffered Saline (PBS; Mediatech, Inc.; Manassas, VA) followed by 300ml of 4% paraformaldehyde (Sigma; St. Louis, MO). The C7 spinal cord was removed and post-fixed over night. The samples were then transferred to 30% sucrose for cryoprotection and embedded in OCT media (Sakura Finetek USA, Inc.; Torrance, CA) then stored at -80°C. Each spinal cord tissue was axially sectioned (14µm) and thaw-mounted onto slides.

Sections were labeled for the glial glutamate transporters GLT-1 and GLAST, or the neuronal glutamate transporter, EAAC1, by blocking in 5% normal goat serum (Vector Laboratories; Burlingame, CA) with 0.3% Triton-X100 (Bio-Rad Laboratories; Hercules, CA) and then incubated overnight at 4°C in either rabbit anti-GLT-1 (1:1000; Abcam, Inc.; Cambridge, MA), rabbit anti-GLAST (1:1000; Abcam, Inc.; Cambridge, MA) or rabbit anti-EAAC1 (1:1000; Alpha Diagnostics). The slides were then fluorescently labeled with goat anti-rabbit Alexa Fluor 546 (1:1000; Invitrogen; Carlsbad, CA) and the ipsilateral and contralateral dorsal horns were digitally imaged at 200x from 3-6 sections per slide.

To quantify the expression of each glutamate transporter in the superficial dorsal horn, images were cropped to include laminae I-II and quantitative densitometry was used to measure the percent positive pixels as a measure of positive labeling (Abbadie et

a. 1996, Nicholson et al. 2012, Romer-Sandoval et al. 2008, Rothman et al. 2007). Results are reported relative to the expression of each marker as measured in normal tissue. Ipsilateral and contralateral transporter expression was evaluated separately. A two-way ANOVA tested for differences in the expression of each glutamate transporter over time for each injury group. At each day, a one-way ANOVA tested for differences between each injury group and normal.

### **5.3.2 Results**

As detailed in Chapter 4 and summarized in Appendix C, mechanical allodynia and thermal hyperalgesia were only elicited in the ipsilateral forepaw following the 15 minute compression (Figs. 4.4 & 4.5). At both time-points assessed (days 1 & 7), the number of paw withdrawals following the 15 minute compression was significantly elevated ( $p < 0.005$ ) over both the 3 minute compression and sham groups (Fig. 4.5). Likewise, the withdrawal latency in the 15 minute compression group was significantly shorter ( $p < 0.020$ ) than the groups receiving a 3 minute compression or the sham procedures (Fig. 4.4).

The spinal expression of GLT-1 in the ipsilateral dorsal horn decreased only at day 7 following the 15 minute compression (Fig. 5.1). All groups exhibited GLT-1 expression that was comparable to normal levels at day 1. But, by day 7, the expression of GLT-1 in the ipsilateral superficial dorsal horn after the 15 minute compression ( $0.79 \pm 0.28$  relative to normal) significantly decreased ( $p = 0.002$ ) compared to the expression levels in normal, naïve tissue (Fig. 5.1). Furthermore, this decrease in GLT-1 expression was also significant when compared to sham and the 3 minute compression

( $p < 0.035$ ) at day 7, and also to the GLT-1 expression levels after a 15 minute compression at day 1 ( $p = 0.046$ ). The GLT-1 expression on the side contralateral to the applied nerve root injury was not different between any group or from normal levels at either time point (Fig. 5.1). A detailed summary of the quantification of spinal GLT-1 expression for each rat is provided in Appendix D.

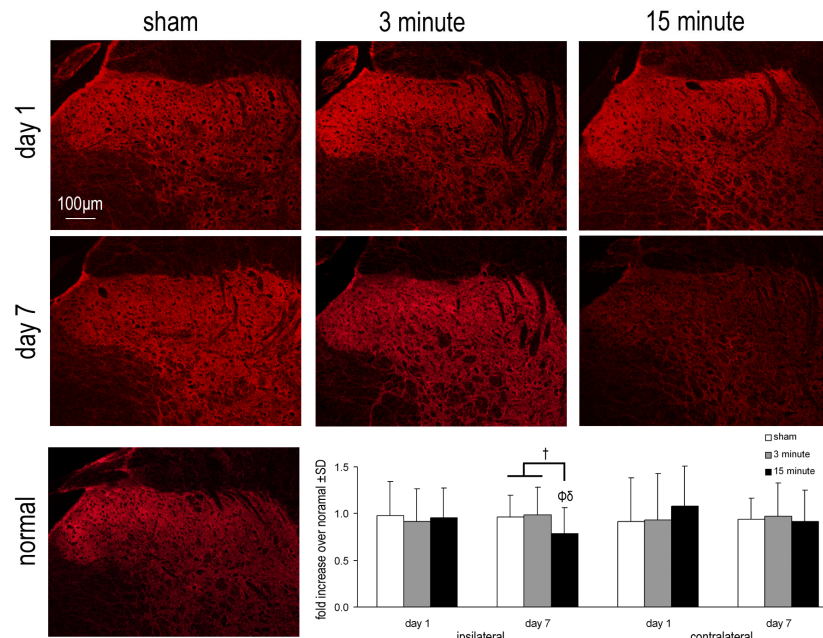


**Fig. 5.1** GLT-1 expression in the superficial laminae of the dorsal horn. GLT-1 expression decreased only at day 7 after a 15 minute compression compared to expression levels in normal tissue ( $\Phi p = 0.002$ ) and expression in the sham and 3 minute compression groups at day 7 ( $\dagger p < 0.035$ ). GLT-1 expression was significantly decreased ( $\delta p = 0.046$ ) from day 1 to day 7. The expression of GLT-1 in the contralateral dorsal horn did not change over time or between injury groups.

The expression of GLAST in the ipsilateral dorsal horn increased in all injury groups at day 1 but this increase remained at day 7 *only* after a 15 minute compression (Fig. 5.2). GLAST expression increased significantly ( $p < 0.033$ ) over normal levels (by 1.2-1.3 fold) on day 1 after all of the surgical procedures, including sham (Fig. 5.2). At day 7, GLAST expression in the ipsilateral dorsal horn after a 15 minute compression remained significantly ( $p = 0.049$ ) elevated over normal, and it significantly decreased

( $p=0.017$ ) after sham between days 1 and 7 (Fig. 5.2). No differences in the expression of GLAST were observed in the contralateral dorsal horn between any injury group at day 1 or day 7 (Fig. 5.2). Appendix D summarizes the detailed spinal expression levels of GLAST for each rat.

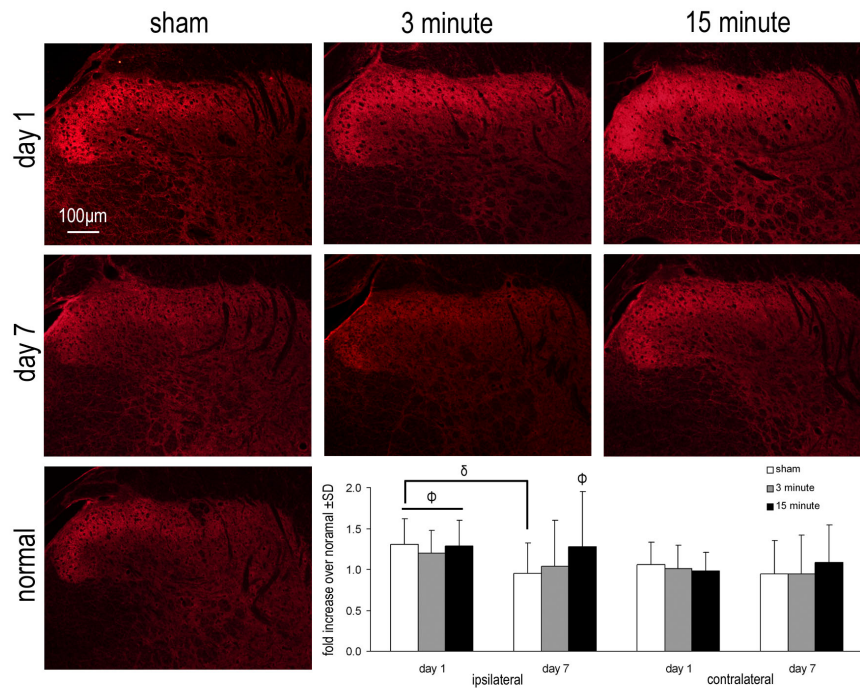


**Fig. 5.2** Spinal GLAST expression after nerve root compressions. At day 1, GLAST significantly increased ( $\Phi p < 0.033$ ) over normal levels in the ipsilateral dorsal horn following sham, 3 minute compression and 15 minute compression. GLAST expression remained significantly elevated over normal ( $\Phi p = 0.049$ ) at day 7 only after a 15 minute compression. GLAST expression significantly decreased ( $\delta p = 0.017$ ) after sham from day 1 to day 7. No differences in the contralateral GLAST expression were observed between any group or over time.

No significant differences in the spinal expression of EAAC1 were observed between any group in both the ipsilateral and contralateral dorsal horns (Fig. 5.3). For each injury group, the expression of EAAC1 was also unchanged over time, from day 1 to day 7. See Appendix D for the spinal expression of EAAC1 for each rat.

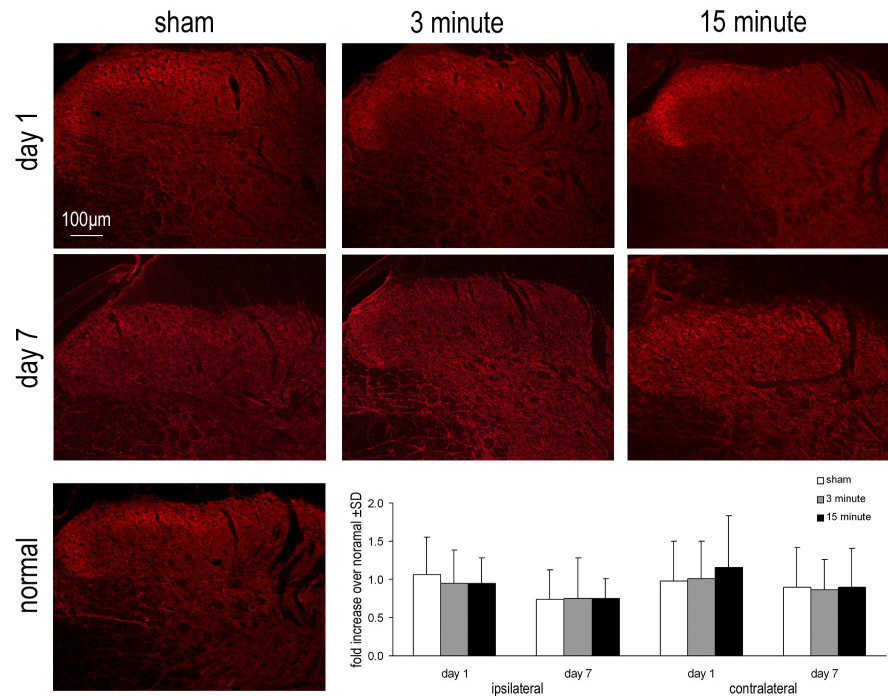


**Fig. 5.3** The spinal expression of EAAC1 after a transient nerve root compression. At days 1 and 7, the bilateral spinal expression of EAAC1 in the superficial laminae was not different from sham or normal levels following a 3 minute or a 15 minute nerve root compression.

## 5.4 Evoked Afferent Signaling in the Spinal Cord

### 5.4.1 Methods

All studies used male Holtzman rats (300-400g; Harlan Sprague–Dawley; Indianapolis, IN). Rats were housed in a 12-12 hour light-dark cycle and given free access to food and water. Studies were approved by our Institutional Animal Care and Use Committee and carried out under the guidelines of the Committee for Research and Ethical Issues of the International Association for the Study of Pain (Zimmermann 1983).

Rats underwent procedures for a C7 nerve root compression applied for 3 minutes (n=2) or 15 minutes (n=13), using the methods described in Chapters 3 and 4 (Hubbard & Winkelstein 2005, Nicholson et al. 2011, Nicholson et al. 2012, Rothman & Winkelstein

2007). A control group that underwent sham procedures was also included (n=13). Bilateral mechanical allodynia was evaluated at day 7 by counting the total number of paw withdrawals elicited by 30 stimulations of a 4.0gf filament applied to the forepaw. Detailed methods for assessing mechanical allodynia are described in Section 4.3 (Hubbard & Winkelstein 2005, Nicholson et al. 2012). Differences in the number of paw withdrawals between each group were determined by a one-way ANOVA with post-hoc Bonferroni correction. At day 7, electrophysiologic recordings were made in the superficial laminae (50-450 $\mu$ m below the pial surface) and the deep laminae (450-1000 $\mu$ m), in separate groups. Recordings were made in the superficial laminae following a 15 minute compression or sham procedures (n=8 rats/group). Recordings were made in the deep laminae following a 15 minute compression (n=5 rats), a 3 minute compression (n=2 rats) and sham procedures (n=5 rats).

In order to record extracellular potentials in the dorsal horn of the spinal cord, rats were anesthetized with 45mg/kg pentobarbital via an intraperitoneal injection. Adequate anesthesia was confirmed by a hind paw pinch and was maintained with an additional dose of pentobarbital (1-5mg/kg i.p.) given approximately every 40-50 minutes, or as needed. The cervical spine was re-exposed at day 7 via a dorsal, midline incision and any scar tissue that had formed over the right C6/C7 spinal cord from the initial surgery was carefully removed. A laminectomy removed any remaining bone at C6 and C7 on the left side to fully expose the spinal cord at those levels; then the dura was removed. The rat was placed on a stereotaxis frame using bilateral ear bars and a clamp to the spinous process of T2. Mineral oil was applied to the spinal cord to maintain its hydration. A thoracotomy was performed to minimize spinal cord motion associated with normal



breathing and respiration was maintained by mechanical ventilation via a mid-cervical tracheotomy (40-50 cycles/min; Harvard Small Animal Ventilator Model 683; Harvard Apparatus; Holliston, MA) (Crosby et al. 2013). Expired CO<sub>2</sub> concentration was continuously monitored (Capnogard; Novamatrix Medical Systems; Wallingford, CT) and the core body temperature was maintained between 35-37°C using a heat plate and a rectal probe (TCAT-2DF; Physitemp Instruments Inc.; Clifton, NJ).

Extracellular spinal cord recordings were acquired using a glass-insulated tungsten probe (<1µm tip; FHC; Bowdoin, ME) inserted vertically into the dorsal spinal cord proximal to the site where the C7 nerve root exits the spinal cord. Recordings were made in both the ipsilateral and contralateral superficial laminae; in the deep laminae, recordings were only made in the ipsilateral dorsal horn. The signal was amplified with a gain of 3000 (ExAmp-20KB; Kation Scientific, Inc.; Minneapolis, MN), processed with a 60Hz noise eliminator (Hum Bug; Quest Scientific; North Vancouver, BC) and digitally stored at 25kHz (MK1401; CED; Cambridge, UK). Mechanoreceptive neurons innervating the forepaw were searched for by lightly brushing the plantar surface of the forepaw and slowly advancing the probe through the dorsal horn (50-450µm or 450-1000µm below the pial surface for the superficial and deep laminae, respectively) until a neuron responsive to the light brushing was found (Crosby et al. 2013, Hains et al. 2003, Quinn et al. 2010). Once a neuron was identified, a sequence of six mechanical stimuli was applied to the forepaw: (1) 10 light brush strokes with a brush applied over 10 seconds; (2-5) a series of four von Frey filaments (1.4, 4.0, 10.0, 26.0gf), each applied five times for 1 second with a 1-second rest between application; and (6) a 10-second,

60gf pinch by a microvascular clip (Roboz, Inc.; Gaithersburg, MD) (Crosby et al. 2013, Quinn et al. 2010).

Voltage recordings were spike-sorted in Spike2 (CED; Cambridge, UK) to count the number of action potentials evoked by each stimulus for individual neurons. For the brush stimulus, the number of action potentials was summed over the period of light brushing. For each von Frey filament application, the number of action potentials was summed over both the stimulation period and the rest period that immediately followed. For both the brush and the von Frey filament stimuli, the baseline number of spikes occurring in the 10-second period prior to the first stimulation was subtracted from the spike counts to identify only the spikes evoked by those stimuli (Hains et al. 2003). For the 60gf pinch, the number of spikes was summed over the 5-second period between 3-8 seconds after the clip was applied, in order to only consider those spikes evoked by the pinch and to exclude the spikes evoked by the application and removal of the clip (Quinn et al. 2010). The number of spikes evoked by the clip stimulus was determined by subtracting the baseline number of spikes that occurred in the 5-second window prior to the first stimulation from the spike count. For statistical analysis, the spike count was log-transformed because of a positive-skew in the distribution of data (Quinn et al. 2010). Separate two-way repeated measures ANOVAs tested for differences in the number of evoked spikes between groups and filament strength for each of the superficial and deep laminae and for the ipsilateral and contralateral dorsal horns, separately. Tukey HSD post-hoc tests compared the number of evoked spikes between groups that were evoked by each filament.

Neurons were classified as either wide dynamic range (WDR), low-threshold mechanoreceptive (LTM) or nociceptive specific (NS) by comparing the spike rate (spikes/sec) evoked by the light brushing and the 60gf clip stimuli (Hains et al. 2003, Laird & Bennett 1993, Saito et al. 2008). Neurons that responded maximally to the light brush were identified as LTM and those that responded in a graded manner were identified as WDR (Hains et al. 2003, Woolf & Fitzgerald 1983). Neurons that responded only to the noxious clip stimulus were classified as NS (Hains et al. 2003). The distribution of WDR, LTM and NS neurons between groups was compared using Pearson's chi-squared tests for the ipsilateral and contralateral neurons and for each of the superficial and deep laminae, separately. All electrophysiology data are expressed as the mean $\pm$ SEM.

#### **5.4.2 Results**

Behavioral sensitivity only developed in the ipsilateral forepaw by day 7 following a 15 minute compression (Fig. 5.4). There was a significant increase in the number of paw withdrawals in the group that received a 15 minute compression compared to both the 3 minute compression ( $p=0.043$ ) and the sham ( $p<0.001$ ) groups. In the contralateral forepaw, there were no differences in the number of paw withdrawals between any of the groups (Fig. 5.4). The number of paw withdrawals that were elicited by each rat are detailed in Appendix C.

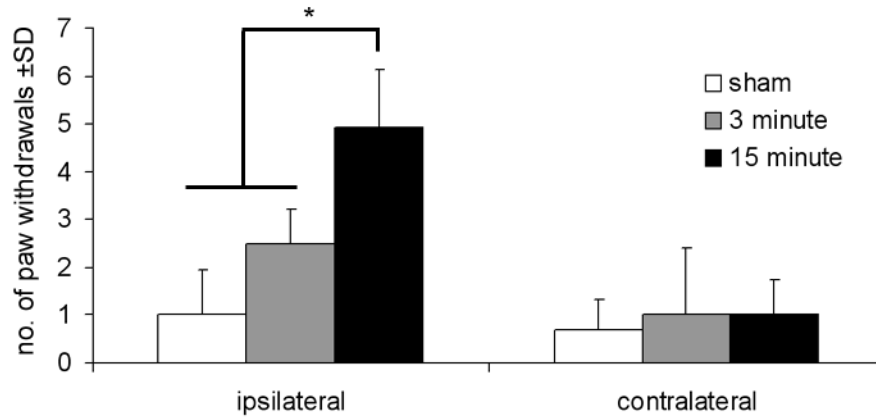


**Fig. 5.4** Mechanical allodynia at day 7 after a 15 minute compression, a 3 minute compression or sham. There was a significant (\* $p < 0.044$ ) increase in the number of paw withdrawals on the ipsilateral side elicited by a 4.0gf filament in the 15 minute compression group compared to the other groups.

A total of 146 neurons were recorded in the superficial laminae ( $266 \pm 86 \mu\text{m}$ ) and 78 neurons were recorded in the deep laminae ( $635 \pm 120 \mu\text{m}$ ). For the neurons recorded in the superficial (Fig. 5.5) and deep (Fig. 5.6) laminae, there were no differences between the depth of recording for each surgical group. The depth of recording and the number of spikes evoked by each filament are summarized for each neuron in Appendix E.

There were no significant differences detected in the number of evoked spikes that were recorded for each group in either the superficial or deep laminae. In both the ipsilateral and contralateral dorsal horns, the frequency of neuronal firing in the superficial laminae after the painful 15 minute compression was comparable to that measured in the sham group (Fig. 5.5). The frequency of neuronal firing in the deep laminae of the ipsilateral dorsal horn was, in general, about 50% higher after the painful nerve root compression (15 minutes) compared to sham (Fig. 5.6), but this was not significant. Yet, neuronal firing in the deep laminae after a 3 minute compression remained near sham levels (Fig. 5.6). For example, the 10gf filament evoked  $33.6 \pm 8.1$

spikes in the 15 minute compression group,  $21.8 \pm 6.7$  spikes in the 3 minute compression group and  $21.0 \pm 4.4$  spikes in the sham group (Fig. 5.6).

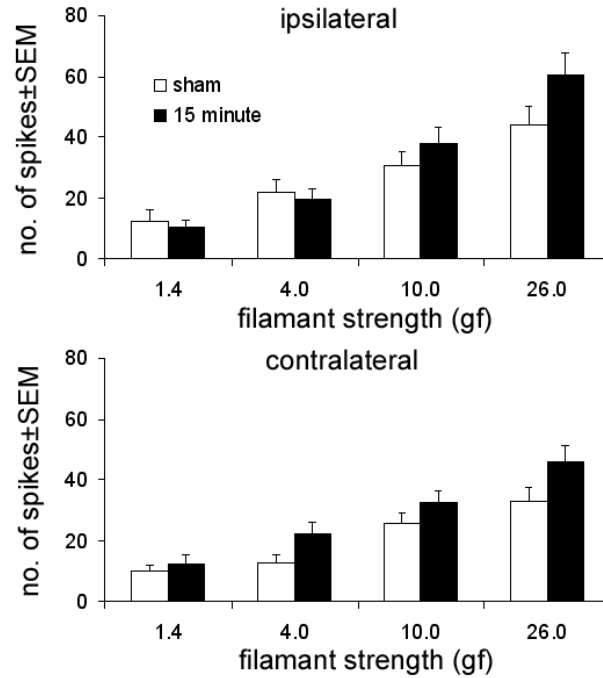


**Fig. 5.5** Frequency of neuronal firing in the ipsilateral and contralateral superficial dorsal horns at day 7.

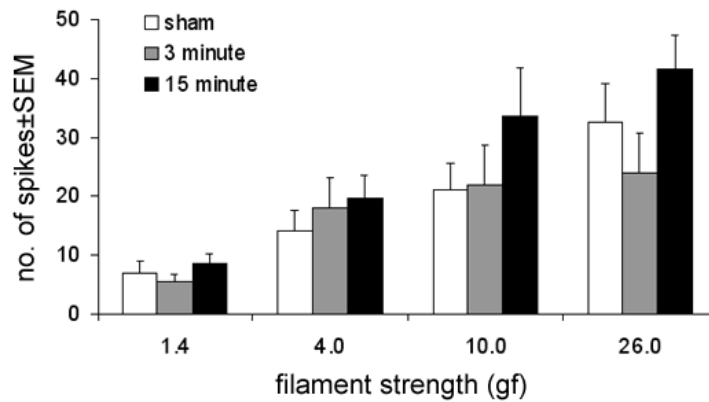


**Fig. 5.6** Total number of spikes in the deep dorsal horn evoked by a range of von Frey filaments applied to the ipsilateral forepaw at day 7.

The proportion of WDR neurons increased only in the ipsilateral superficial dorsal horn after a 15 minute compression (Fig. 5.7). In the ipsilateral spinal cord, 74% of the recorded neurons were classified as WDR in the 15 minute compression group; this

was significantly ( $p=0.002$ ) more than the proportion of WDR neurons identified after sham procedures (43%) (Fig. 5.7). Although the proportion of NS neurons did not change after the 15 minute compression, the proportion of LTM neurons decreased from 38% after sham to 10% after the painful nerve root compression (Fig. 5.7). In the contralateral superficial dorsal horn (Fig. 5.7) and in the ipsilateral deep laminae (Fig. 5.8), the phenotype distribution was unchanged between groups. No NS neurons were identified in the deep laminae of the dorsal horn for any of the groups.

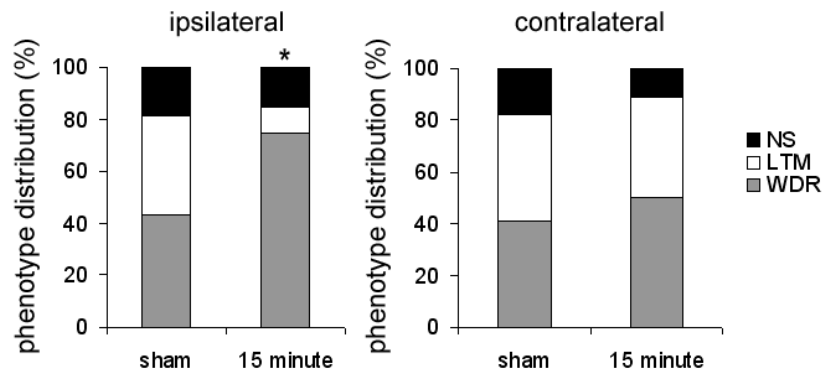


**Fig. 5.7** Neuronal phenotype distribution in the superficial dorsal horn at day 7. The distribution of LTM and WDR neurons in the ipsilateral dorsal horn is significantly different ( $p=0.002$ ) after a painful 15 minute compression than sham. There is also an increase in the proportion of WDR neurons and a decrease in the proportion of LTM neurons. The phenotype distribution in the contralateral dorsal horn does not change.

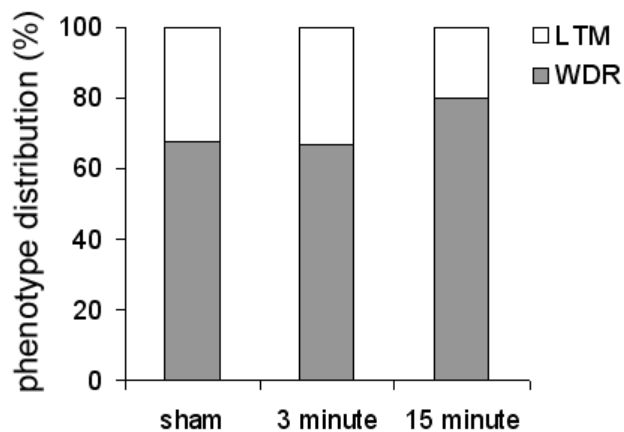


**Fig. 5.8** Neuronal phenotype distribution in the deep laminae is not different between injury groups. No NS neurons were identified in the deep laminae for any group.

## 5.5 Discussion

Downregulation of GLT-1, upregulation of GLAST, neuronal hyperexcitability and an increase in WDR neurons were only observed at day 7 following a painful (15 minute) nerve root compression (Figs. 5.1-5.2 & 5.4-5.7). Like the transient nerve root compression used in the present study, spinal cord and peripheral nerve injuries also mediate spinal cord glutamate transporter expression in the rat (Kim et al. 2011, Sung et al. 2003). However, whether GLT-1, GLAST or EAAC1 is downregulated or upregulated depends on the type of injury sustained (Kim et al. 2011, Sung et al. 2003, Vera-Portocarrero et al. 2002, Xin et al. 2009). Specifically, mechanical trauma to spinal cord, peripheral nerve or nerve root each differentially modulates spinal glutamate transporter expression (Kim et al. 2011, Sung et al. 2003, Vera-Portocarrero et al. 2002, Xin et al. 2009). For example, both GLT-1 and EAAC1 are downregulated and GLAST is unchanged at day 7 after a sciatic nerve ligation (Sung et al. 2003). After a spinal cord contusion, GLT-1 and GLAST are downregulated, and EAAC1 is upregulated (Kim et al. 2011). Therefore, while spinal cord trauma, peripheral nerve injury and nerve root compression are each characterized by neuronal hyperexcitability in the spinal cord (Figs. 5.5 & 5.6; Hains et al. 2003, Hao et al. 1992, Liu et al. 2011, Pitcher et al. 2004) that is associated with dysregulation of spinal glutamate transporter expression (Figs. 5.1-5.3; Kim et al. 2011, Sung et al. 2003, Vera-Portocarrero et al. 2002, Xin et al. 2009), there are likely unique cellular mechanisms that contribute to these spinal responses that depend on the site and/or type of mechanical trauma. It is well-known that neurodegeneration can trigger oxidative stress, but non-injured neurons are protected from this oxidative stress, in part by removal of excess extracellular glutamate

(Markowitz et al. 2007, Tao et al. 2005). Neurodegeneration is localized to distinct regions of the nervous system following painful spinal cord, nerve root and peripheral nerve injuries. Specifically, neurodegeneration is evident in the spinal cord following a spinal cord compression, the central branch of the primary afferents after a nerve root compression, and the distal branch of the primary afferents following a sciatic nerve ligation (Carlton et al. 2009, Chen et al. 1992, Hubbard & Winkelstein 2008, Jancalek & Dubovy et al. 2007, Kobayashi et al. 2008). Therefore, dysregulation of glutamate transporters in the *spinal cord* that is triggered by neurodegeneration is likely determined by whether neurodegeneration is present in the cord itself, the afferents that synapse in the cord or in peripheral regions of the nervous system (Carlton et al. 2009, Chen et al. 1992, Hubbard & Winkelstein 2008, Jancalek & Dubovy 2007, Kobayashi et al. 2008).

The damage to the primary afferents that develops after a painful nerve root injury likely contributes directly to the downregulation of GLT-1 that is observed in our study (Fig. 5.1; Hubbard & Winkelstein 2008, Kobayashi et al. 2008, Nicholson et al. 2011). Such damage, including axonal swelling and loss of axonal transport (Section 3.4), is only evident after the same painful 15 minute compression that was associated with a decrease in spinal GLT-1 here (Fig. 5.1; Hubbard & Winkelstein 2008, Nicholson et al. 2011). Astrocytes require pre-synaptic neuronal signaling in order to express GLT-1 (Ghosh et al. 2011, Yang et al. 2009). This damage extends to the primary synapse in the dorsal horn after a nerve root compression (Kobayashi et al. 2008), which provides a putative mechanism for impairment of the normal afferent signaling to spinal astrocytes and to the downregulation of spinal GLT-1 (Fig. 5.1). At one day after injury, when GLT-1 was unchanged (Fig. 5.1), the primary afferents also retain their normal



morphology in this injury model (Hubbard & Wikelstein 2008); the fact that the temporal profiles of GLT-1 downregulation and afferent degeneration are similar is further evidence that the primary afferents contribute, or are closely related, to the reduction in spinal GLT-1 after painful nerve root injury.

Unlike GLT-1, GLAST expression does not require neuronal signaling, but is regulated by extracellular glutamate via positive feedback by which elevated glutamate concentrations increases GLAST expression (Aronica et al. 2001, Perego et al. 2000). The downregulation of GLT-1 after a painful nerve root compression (Fig. 5.1) likely increases the extracellular glutamate in the dorsal horn, thereby increasing GLAST (Figs. 5.2). Interestingly, GLAST increased at day 1 in *all* groups (Fig. 5.2), suggesting that the surgical procedures alone are sufficient to increase spinal glutamate, but normal glutamate clearance after the non-painful procedures (sham; 3 minute compression) prevented the development of any further imbalances in the glutamatergic system. Even when extracellular glutamate concentrations are elevated in the central nervous system of rats or in neuron cultures, neuronal degeneration and excitotoxicity are prevented if an increase in glutamate uptake activity is able to prevent the sustained over-accumulation of glutamate (Gilad et al. 1990, Sher & Hu 1990, Springer et al. 1997). Even though GLAST remained elevated after the painful root compression, it was not able to compensate for the loss of GLT-1, which dominates glutamate uptake activity in the central nervous system (Danbolt 2001, Holmseth et al. 2012). EAAC1 was unchanged from sham and normal levels following both the nonpainful and painful nerve root compressions in the present study (Fig. 5.3). After a spinal cord contusion, EAAC1 is rapidly upregulated within one hour at the site of injury, but returns to normal levels

within one day (Vera-Portocarrero et al. 2002, Xin et al. 2009). A similar, transient increase in spinal EAAC1 could have also occurred within hours after a nerve root compression, contributing to the initiation of nerve root-mediated pain (Vera-Portocarrero et al. 2002, Xin et al. 2009). By day 7, however, the unchanged expression of spinal EAAC1 after a painful nerve root compression (Fig. 5.3) suggests that this transporter does play a significant role in the maintenance of nerve root-mediated pain. Understanding the pathways that regulate EAAC1 expression in this model, such as protein kinase signaling (Gonzalez et al. 2002, Holmseth et al. 2012), would provide additional insight into whether painful root compression modulates the function of EAAC1.

The frequency of neuronal firing after a painful nerve root compression increased in the deep laminae of the dorsal horn, but was not different from sham responses in the superficial laminae (Figs. 5.5 & 5.6). Few studies have evaluated neuronal firing rates in different laminae regions of the spinal cord in models of pain (Ramer et al. 2000, Seagrove et al. 2004, Urch et al. 2003, Wall et al. 1981). Unlike the present findings (Figs. 5.5 & 5.6), hyperexcitability in the superficial dorsal horn in a rat model of bone cancer pain was more robust than in the deeper laminae (Urch et al. 2003) indicating that different types of chronic pain may be mediated by hyperexcitability of distinct populations of dorsal horn neurons (Fig. 5.6; Urch et al. 2003). After a painful nerve root compression (15 minute), the frequency of neuronal firing in the deep dorsal horn increased by 40-60% compared to sham responses (Fig. 5.6). Specifically, the same 4.0gf filament that elicited mechanical allodynia at day 7 after the 15 minute compression (Fig. 5.4) also evoked 40% more action potentials in the deep laminae compared to sham when

that filament was applied to the forepaw at this same time-point (Fig. 5.6), suggesting that mechanical sensitivity is likely mediated by hyperexcitability of deep dorsal horn neurons. Contrary to this, the frequency of neuronal firing in the superficial dorsal horn evoked by the 4.0gf filament slightly *decreased* after a painful nerve root compression compared to sham responses (Fig. 5.7). Cervical radicular pain is not likely encoded by the frequency of evoked neuronal firing in the superficial laminae due to the fact that the frequency of neuronal signaling evoked by a 4.0gf is unchanged in this region of the spinal cord even though that same filament evokes significantly more paw withdrawals after a painful compression (Figs. 5.4 & 5.5). Future studies should identify the neurochemical properties of deep dorsal horn neurons contributing to hyperexcitability in these neurons; it is possible that such studies may also identify a role for superficial dorsal horn neurons in mediating cervical radicular pain due to the interconnections between spinal neurons across laminae regions.

Treatments to restore normal sensation following a cervical nerve root crush are able to do so by restoring electrically-evoked afferent signaling only in the deep dorsal horn (Ramer et al. 2000). The contribution of deep dorsal horn neurons to normal sensation (Ramer et al. 2000) and behavioral sensitivity (Figs. 5.4 & 5.6) following mechanical injury to the cervical nerve root implicate these neurons in driving nerve root-mediated pain. Spinal circuits between the superficial and deep laminae do, however, suggest that changes to the intrinsic properties of superficial dorsal horn neurons may contribute to the hyperexcitability of the deep dorsal horn neurons (Suzuki et al. 2002, Urch et al. 2003). The increased hyperexcitability of the deep dorsal horn neurons observed in the present study may (Fig. 5.6), therefore, be attributed to an increase in the

amplitude of excitatory post-synaptic currents in laminae II that was reported in a rat model of lumbar root constriction (Terashima et al. 2011). Deep dorsal horn excitability could also be attributed to the increase in the proportion of WDR neurons that was observed in the superficial laminae (Fig. 5.7) given that WDR neurons are thought to mediate neuropathic and inflammatory pain (Hao et al. 1991, Liu et al. 2011, Urch et al. 2003). Even though the present study did not detect any robust changes in the firing rate of superficial dorsal horn neurons (Fig. 5.5), nerve root mediated pain may be driven by changes in the intrinsic properties of neurons in the superficial dorsal horn, including the phenotype shift that was observed here (Fig. 5.7).

An increase in the synaptic strength between neurons in the superficial dorsal horn may contribute to the increase in WDR neurons in this region (Fig. 5.7; Keller et al. 2010, Kohno et al. 2003, Okamoto et al. 2001). Astrocytes modulate synaptic strength, in part, by regulating extracellular glutamate (Paixão & Klein 2010, Tao et al. 2005). After a painful nerve root compression, there was a shift in the spinal expression of both glutamate transporters that are associated with astrocytes (GLT-1, GLAST) (Figs. 5.1 & 5.2) indicating that there was also likely a shift in the neuronal synapse properties that are regulated by astrocytes in the spinal cord (Nguyen et al. 2009, Paixão & Klein 2010, Tao et al. 2005). The shift from LTM to WDR (Fig. 5.8) suggests that normally monosynaptic, LTM, neurons become polysynaptic, forming synapses with nociceptors (Keller et al. 2010). Such plasticity of the spinal neurons could be attributed to enhanced excitability or disinhibition of interneurons, which are predominantly localized to laminae I-III (Basbaum et al. 2009, Todd 2010). Downregulation of GLT-1 at day 7 (Fig. 5.1) indicates that an increase in excitatory signaling in the superficial laminae likely

contributed to the spinal plasticity in this model of radiculopathy (Fig. 5.1; Cata et al. 2006, Inquimbert et al. 2011), but does not rule out the contribution of reduced inhibitory signaling. It should be noted that reduced afferent synaptic connections, an hypothesized mechanism for GLT-1 downregulation (Ghosh et al. 2011, Yang et al. 2009), also may reduce the synaptic strength of inhibitory neurons (Todd 2010). Therefore, a decrease in inhibition along with the increase in excitatory signaling that is associated with GLT-1 downregulation may have both contributed to the neuronal plasticity observed in this model of nerve root-mediated pain (Basbaum et al. 2009, Cata et al. 2006, Inquimbert et al. 2011, Todd 2010). Additional studies of the inhibitory and excitatory circuits after a nerve root compression are necessary to determine the role that each of these neuronal circuits have in nerve root-mediated pain.

In the spinal cord, neuronal excitability and the glial expression of GLT-1 and GLAST at day 7 are each sensitive to the duration of an applied nerve root compression (Figs. 5.1, 5.2 & 5.6). Even though the same 10gf compression was applied to the nerve root for all studies, a compression period of 3 minutes was found to be insufficient to modulate glutamate transporter expression and neuronal excitability in the spinal cord (Figs. 5.1, 5.2 & 5.6). That same 3 minute compression also does not elicit behavioral sensitivity (Fig. 5.4), neuronal pathology in the nerve root or spinal glial activation, all of which are evident by day 7 after a painful 15 minute compression (Nicholson et al. 2011, Rothman et al. 2010). These behavioral, neuronal and glial responses are likely each initiated by the physiological responses of the nerve root tissues that develop *during* the applied compression, such as impaired intraradicular blood flow, nutrient transport and afferent signaling (Kobayashi et al. 2008, Nicholson et al. 2011, Olmarker et al. 1989b,

Pedowitz et al. 1992). Indeed, studies show that the duration of an applied compression mediates the degree of impaired neurotransmission through the root (Nicholson et al. 2011, Pedowitz et al. 1992) and that, in the same model of cervical radiculopathy used here, afferent discharge rates through the root continuously decrease for the first 6.6 minutes of applied compression (Nicholson et al. 2011). Removing compression to the root *before* that critical duration (i.e. 3 minutes), precludes the development of behavioral sensitivity and associated neuronal and glial responses that normally occur after mechanical trauma to the nerve root (Hubbard & Winkelstein 2005, Hubbard et al. 2008a, Rothman et al. 2010). By characterizing spinal glutamate transporters and neuronal excitability for both painful and nonpainful nerve root compressions, the current study suggests that downregulation of GLT-1 and neuronal hyperexcitability are specifically associated with radicular pain (Figs. 5.1 & 5.6). Certainly, additional studies are required to test the contribution of spinal GLT-1 and neuronal excitability to nerve root-mediated pain; however, this is the first study to demonstrate that shifts in glutamate uptake by glia in the superficial laminae are associated with neuronal phenotype switches, which likely mediates neuronal hyperexcitability in the deep dorsal horn (Figs 5.1-5.2 & 5.5-5.7). Together, these studies suggest a role for glia in enhancing spinal excitatory signaling, which mediates radicular pain.

## **5.6 Integration & Conclusions**

Studies reported in this chapter demonstrate that spinal GLT-1 decreases and neuronal excitability is enhanced (Figs. 5.1 & 5.5) only after a 15 minute compression that also elicits behavioral sensitivity (Chapter 4) and inhibits neurotransmission through

the root *during* compression (Chapter 3). Although a *decrease* in the frequency of afferent signaling through the root may initiate the development of behavioral sensitivity (Chapter 3 & 4), radicular pain is likely maintained by an *increase* in neuronal firing in the spinal cord (Fig. 5.6; Chapter 4). In the superficial laminae, neuronal hyperexcitability was unchanged at day 7 following a painful nerve root compression when a 4.0gf filament was applied to the forepaw of the rat despite the fact that the 4.0gf filament elicits more paw withdrawals at day 7 (Fig. 5.5). Yet an increase in the proportion of WDR neurons in the superficial dorsal horn may contribute to neuronal hyperexcitability that develops in the deeper laminae (Figs. 5.6 & 5.7; Suzuki et al. 2002, Urch et al. 2003). The glial glutamate transporter, GLAST, was upregulated at day 7 after a painful nerve root injury (Fig. 5.2). Although most studies would suggest that this upregulation is indicative of elevated glutamate clearance by this transporter, there are data suggesting that an increase in GLAST may also contribute to neuronal hyperexcitability (Niederberger et al. 2006). The downregulation of GLT-1 and the upregulation of GLAST (Figs. 5.1 & 5.2), may therefore, both contribute to neuronal hyperexcitability in nerve root-mediated pain.

The electrophysiological studies in this chapter were performed in parallel with the electrophysiological studies presented in Chapter 7. In the studies presented here (Section 5.4), the frequency of neuronal firing increased by as much as 60% in the deep dorsal horn after a painful nerve root compression (Fig. 5.6). However, this increase was not statistically significant using the current group sizes (n=2-5 rats/group). Despite the small sample size, the robust differences in the deep dorsal horn were sufficient to inform the group sizes required for the Riluzole treatment experiments (Chapter 7) that were

performed concurrently. Therefore, in order to minimize the use of animals, in accordance with guidelines of the Committee for Research and Ethical Issues of the International Association for the Study of Pain (Zimmermann 1983), no additional electrophysiologic studies were conducted using these injury groups alone to characterize neuronal excitability in the spinal cord following 3 minute or 15 minute compression durations (Section 5.4). Instead, two control groups in the Riluzole study received an intraperitoneal injection of  $\beta$ -cyclodextrin as the vehicle on day 1; one group of rats underwent a painful 15 minute compression while the other group received the sham exposure. The electrophysiological recordings made in the deep dorsal horn from those two vehicle-control groups were consistent with those reported here; after a painful nerve root compression there is an increase in frequency of neuronal firing compared to sham responses in the deep laminae of the dorsal horn (Fig. 5.6).

The downregulation of GLT-1 that is only observed following a painful (15 minute) nerve root compression suggests that radicular pain is, in part, mediated by elevated spinal glutamate concentrations (Cata et al. 2006, Inquimbert et al. 2012, Tao et al. 2005). To test this hypothesis, studies in Chapter 6 will lower spinal glutamate concentrations by pharmacologically upregulating GLT-1 with daily intrathecal injections of ceftriaxone after a painful nerve root compression (Rothstein et al. 2005). To reduce spinal glutamate without altering its uptake by GLT-1, studies in Chapter 7 will block pre-synaptic glutamate release by administering Riluzole on day 1 after painful injury. Behavioral sensitivity and neuronal hyperexcitability are assessed in each pharmacological study. Together, Chapters 5-7 define the role of extracellular glutamate



in mediating both neuronal hyperexcitability and behavioral sensitivity following a painful nerve root compression.

---

## CHAPTER 6

# Upregulation of GLT-1 by Ceftriaxone Treatment Alleviates Nerve Root-Mediated Pain

---

*Parts of this chapter have been adapted from:*

Nicholson KJ, Gilliland TM, Winkelstein BA. “Upregulation of GLT-1 by Treatment with Ceftriaxone Alleviates Radicular Pain by Reducing Spinal Astrocyte Activation and Neuronal Hyperexcitability” *submitted*.

### 6.1 Overview

A recent report by the Committee on Advancing Pain Research, Care, and Education of the Institute of Medicine identifies chronic pain as a leading public health issue in the United States (Institute of Medicine 2011). That report cites the fact that most new drugs for chronic pain are variations of existing treatments (i.e. opioids, non-steroidal anti-inflammatory drugs) and suggests that basic science research should focus instead on novel approaches (Institute of Medicine 2011). Although the glutamatergic system has long been targeted for its role in mediating pain and therapies to alleviate neuropathic pain by antagonizing glutamate receptors show promise in animal studies, these drugs have psychosocial and cardiovascular side effects that prohibit their widespread clinical use (Muir & Lees 1995). Therefore, recent efforts to modulate the glutamatergic system have focused on the glutamate transporters, which regulate extracellular glutamate (Amin et al. 2012, Hajhashemi et al. 2012, Verma et al. 2010, Yamada & Jinno 2011). Maintaining normal extracellular glutamate by modulating glutamate transporters has the potential to maintain the normal function of glutamate

signaling in the central nervous system without producing significant deleterious side effects that are associated with many glutamate receptor antagonists (Muir & Lees 1995, Tao et al. 2005). The glutamate transporter, GLT-1, dominates glutamate uptake in the central nervous system of rats, and studies have shown that some antibiotics upregulate the spinal expression of this transporter (Amin et al. 2012, Nie et al. 2010, Rothstein et al. 2005). One such antibiotic, ceftriaxone, relieves neuropathic pain after peripheral nerve injury in many animal models (Amin et al. 2012, Eljaja et al. 2011, Hajhashemi et al. 2012, Hu et al 2010, Ramos et al. 2010). The studies presented in Chapter 5 demonstrate that painful nerve root compression is associated with a significant decrease in the spinal expression of GLT-1 by day 7 after injury, suggesting that this transporter may mediate the persistence of nerve root-mediated pain. To further define the relationship between spinal GLT-1 and cervical radicular pain, ceftriaxone was given intrathecally daily after painful nerve root injury to upregulate spinal GLT-1. In addition to behavioral sensitivity, spinal GLAST, GFAP and neuronal excitability were measured to characterize the contribution of GLT-1 on the astrocytic activation and increased neuronal activity that are normally observed after a painful nerve root compression (Chapter 5; Hubbard & Winkelstein 2005, Rothman et al. 2010).

The work presented in this chapter focuses on the experiments outlined in Aims 3a and 3c. Due to a large number of recent reports implicating GLT-1 downregulation in maintaining neuropathic pain after peripheral nerve injuries, including chronic constriction to the sciatic nerve and a spinal nerve ligation (Amin et al. 2012, Eljaja et al. 2011, Hajhashemi et al. 2012, Hu et al 2010, Ramos et al. 2010), the studies in this chapter test the hypothesis that the downregulation of GLT-1 that is evident by day 7

after a painful nerve root compression (Chapter 5) contributes to the maintenance of mechanical allodynia and thermal hyperalgesia. Ceftriaxone was administered daily, starting on day 1, when the spinal expression of GLT-1 expression remains unchanged (Chapter 5). Spinal GLT-1 was measured at day 7 to assess whether the expression of this transporter is increased by such treatment. Mechanical allodynia and thermal hyperalgesia were measured for 7 days and comparisons were made to evaluate if treatment was effective in attenuating behavioral sensitivity.

There is limited information about the relationship between ceftriaxone and other astrocytic and neuronal responses that normally develop in the spinal cord after a painful nerve root compression, including upregulation of GFAP and GLAST and enhanced neuronal excitability (Sections 5.3 & 5.4; Ramos et al. 2010, Rothman et al. 2010, Trantham-Davidson et al. 2012). Furthermore, few *in vivo* studies have characterized the dose-response of ceftriaxone on behavioral sensitivity (Amin et al. 2012, Hajhashemi et al. 2012, Hu et al. 2010) and, to-date, the dose-response of ceftriaxone on spinal cellular responses has only been reported for GLT-1 expression and pro-inflammatory cytokines levels (Amin et al. 2012). Even though ceftriaxone does reduce pro-inflammatory cytokines after a sciatic nerve constriction injury in the rat, the dose-response of ceftriaxone was only evaluated when given in combination with minocycline, an inhibitor of microglia (Amin et al. 2012, Raghavendra et al., 2003). Astrocytes, rather than microglia, however have a crucial role in the *maintenance* of neuropathic pain (Colburn et al. 1999, Hashizume et al. 2000, Milligan & Watkins 2009, Raghavendra et al. 2003, Wieseler-Frank et al. 2004) and astrocyte activation, along with neuronal activity, is associated with persistent cervical radicular pain (Chapter 5; Nicholson et al. 2012,

Rothman et al. 2010). Therefore, in order to characterize the dose-response of ceftriaxone to spinal astrocytic and neuronal responses that are relevant to chronic pain, two doses of ceftriaxone were administered using concentrations (10 $\mu$ g and 150 $\mu$ g) previously determined to alleviate neuropathic pain in the rat (Hu et al. 2010, Ramos et al. 2010). For each dose, spinal GLT-1, GLAST and GFAP were quantified at day 7 using immunohistochemistry. In separate groups of rats, spinal neuronal hyperexcitability was also measured at day 7 after treatment using electrophysiological techniques.

## **6.2 Relevant Background**

The cervical nerve root is a common source of neck pain due to its susceptibility to injury from foraminal impingement, disc herniation and/or foraminal stenosis (Abbed & Coumans 2007, Carette & Fehlings 2005, Wainner & Gill 2000). In the rat, trauma to the nerve root induces persistent behavioral sensitivity (Colburn et al. 1999, Hashizume et al. 2000, Huang et al. 2012, Hubbard & Winkelstein 2005, Rothman et al. 2010). Glutamate is the primary neurotransmitter in pain signaling and its synaptic concentration is tightly regulated by glutamate transporters (Anderson & Swanson 2000, Basbaum et al. 2009, Gegelashvilia et al. 2000, Tao et al. 2005). Because the glial glutamate transporter, GLT-1, removes as much as 90% of extracellular glutamate in the central nervous system (Danbolt 2001, Holmseth et al. 2012, Rothstein et al. 1996) normal glutamate uptake by this transporter is essential for maintaining the proper extracellular glutamate concentration (Inquimbert et al. 2012, Sung et al. 2003 ). In the spinal cord, GLT-1 has been shown to decrease within a week of a painful transient cervical nerve root compression (Chapter 5) and also peripheral nerve injury in association with behavioral

sensitivity, supporting a decrease in spinal GLT-1 expression as possibly contributing to neuropathic pain (Hu et al. 2010, Sung et al. 2003, Tao et al. 2005, Xin et al. 2009). Furthermore, upregulation of GLT-1 via administration of ceftriaxone has been shown to alleviate behavioral sensitivity and restore the normal spinal concentration of glutamate after painful nerve injury, without directly regulating either of the other two spinal glutamate transporters, EAAC1 and GLAST (Inquimbert et al. 2012, Rothstein et al. 2005). Although those studies implicate GLT-1 in pain, it is not known whether restoring spinal GLT-1 expression would be sufficient to alleviate nerve root-mediated pain.

Astrocytic activation and neuronal hyperexcitability are both mediated in the spinal cord by glutamate signaling and are associated with neuropathic pain (Cata et al. 2006, Gao & Ji 2000, Liaw et al. 2005, Weng et al. 2006). Because astrocytic activation is only induced by transient nerve root compressions that are painful (Nicholson et al. 2012, Rothman et al. 2010), spinal astrocyte activation via elevated glutamate signaling is hypothesized as contributing to nerve root-mediated pain. Increased spinal glutamate also enhances neuronal excitability (Cata et al. 2006, Jourdain et al. 2007, Nguyen et al. 2009, Sung et al. 2003). The amplitude of evoked excitatory post-synaptic currents increases in laminae II of the dorsal horn following a sustained constriction of the lumbar nerve root in the rat (Terashima et al. 2011) suggesting that excitatory neurotransmitters, such as glutamate, increase in the superficial dorsal horn (Jourdain et al. 2007, Nguyen et al. 2009). Elevated glutamate concentrations in the dorsal horn may increase the excitability of the second order neurons that project into the deeper laminae from this region (Suzuki et al. 2000, Todd 2010, Urch et al. 2003), contributing to the neuronal hyperexcitability that develops in this region after a painful nerve root compression (Chapter 5). It is

unknown whether pharmacologic modulation of spinal glutamate by upregulation of GLT-1 would mediate the spinal neuronal signaling and/or astrocytic activation that is evident after a painful nerve root compression (Chapter 5; Hubbard & Winkelstein 2005, Nicholson et al. 2012, Rothman et al. 2010, Terashima et al. 2011).

This study tests the hypothesis that spinal GLT-1 contributes to maintaining behavioral sensitivity following a transient cervical nerve root compression. Using ceftriaxone treatment paradigms previously determined to alleviate behavioral sensitivity following chronic constriction of the sciatic nerve, two doses of ceftriaxone (10 $\mu$ g and 150 $\mu$ g) were administered daily into the intrathecal space (Amin et al. 2012, Eljaja et al. 2011, Hu et al. 2010, Inquimbert et al. 2012, Ramos et al. 2010) after a painful root compression to determine their relative effectiveness in modulating spinal GLT-1 upregulation and/or alleviating nerve root-mediated pain. Because pain is multi-modal (Jensen et al. 2001, Mogil 2009), both mechanical allodynia and thermal hyperalgesia were evaluated in order to define the contribution of GLT-1 on each of these pain modalities. Spinal GFAP and GLAST were evaluated at day 7 after ceftriaxone treatment to evaluate whether restoring GLT-1 also suppresses astrocyte activation and/or restores the normal spinal expression of this glutamate transporter. The effect of ceftriaxone on dorsal horn neuronal excitability also was evaluated by measuring evoked action potentials at day 7 after treatment. Although ceftriaxone has been reported to reduce spinal GFAP expression at a dose that also abolishes neuropathic pain and restores spinal GLT-1 in the rat (Ramos et al. 2010), *in vitro* studies suggest that astrocytic expression of GLT-1 and GFAP is independently modulated across varying concentrations of ceftriaxone (Bachetti et al. 2010, Beller et al. 2011, Lee et al. 2008). Therefore, in order

to define and compare the effectiveness of ceftriaxone *in vivo* on spinal GLT-1 and GFAP, along with its modulation of GLAST expression and neuronal excitability in the spinal cord, each were evaluated following both doses (10 $\mu$ g and 150 $\mu$ g). Collectively, these studies characterize the contribution of spinal GLT-1 to behavioral sensitivity after a painful nerve root compression.

## 6.3 Methods

### 6.3.1 Surgical Procedures & Ceftriaxone Administration

Male Holzman rats (Harlan Sprague-Dawley; Indianapolis, IN; 275-375g) were housed in USDA- and AAALAC-compliant conditions with a 12–12 hour light–dark cycle and free access to food and water. All studies were IACUC-approved and carried out under the guidelines of the Committee for Research and Ethical Issues of the International Association for the Study of Pain (Zimmermann 1983).

Rats underwent a 15 minute compression applied to the nerve root or sham exposure using methods described in Chapter 3 (Hubbard & Winkelstein 2005, Nicholson et al. 2011). Briefly, under isoflurane anesthesia, the right C7 nerve root was compressed by removing the right C6/C7 lamina and applying a 10gf microvascular clip for 15 minutes. Starting on the first day after injury (day 1), rats were randomly assigned to receive either ceftriaxone treatment or the saline vehicle. Within the treatment group, one group of rats received a 40 $\mu$ L intrathecal injection of 10 $\mu$ g ceftriaxone (Wockhardt; Parsippany, NJ) dissolved in saline (*injury+10 $\mu$ g*; n=16); a second group of rats received a 40 $\mu$ L intrathecal injection of 150 $\mu$ g of ceftriaxone dissolved in saline (*injury+150 $\mu$ g*; n=16). In the vehicle treatment group (*injury+saline*; n=15), rats received a 40 $\mu$ L



intrathecal injection of saline alone. The same vehicle treatment was administered to rats that underwent sham procedures (*sham+saline*; n=15). Both the treatment and the vehicle were administered in the intrathecal space between L4 and L5 via a lumbar puncture on days 1-6, immediately following behavioral assessments (Hu et al. 2010, Rothman & Winkelstein 2010).

### **6.3.2 Behavioral Assessments & Immunohistochemistry**

A subgroup of rats from each treatment group was evaluated for behavioral sensitivity (*injury+10 $\mu$ g*, n=8; *injury+150 $\mu$ g*, n=8, *injury+saline*, n=7; *sham+saline*, n=7). Detailed methods are described in Chapter 4 (Dirig et al. 1997, Hubbard & Winkelstein 2005). Bilateral mechanical allodynia was evaluated daily at baseline and on post-operative days 1 through 7 by counting the total number of paw withdrawals elicited (out of 30, for each filament) by a 1.4, a 2.0 and a 4.0gf von Frey filament. Bilateral thermal hyperalgesia also was evaluated by measuring the withdrawal latency to a thermal stimulus at baseline and on post-operative days 1 and 7, when thermal sensitivity is normally initiated and maintained in this model of cervical radiculopathy (Chapter 4). Two-way, repeated measures ANOVAs tested for differences in each behavioral assessment over time for the ipsilateral and contralateral forepaws, separately. At each time-point, a separate one-way ANOVA with post-hoc Bonferroni correction tested for differences between groups in mechanical allodynia and thermal hyperalgesia. The ipsilateral and contralateral forepaws were evaluated separately for all comparisons.

The C7 spinal cord was harvested at day 7 and labeled for the glial glutamate transporters, GLT-1 and GLAST, using the methods described in Chapter 5. In addition,

spinal GFAP expression was also assessed as a marker of activated astrocytes (Colburn et al. 1999, Nicholson et al. 2012). Briefly, spinal sections were labeled for GLT-1, GLAST, or GFAP. Sections were blocked in 5% normal goat serum (Vector Laboratories; Burlingame, CA) with 0.3% Triton-X100 (Bio-Rad Laboratories; Hercules, CA) then incubated overnight at 4°C in rabbit anti-GLT-1 (1:1000; Abcam, Inc.; Cambridge, MA), rabbit anti-GLAST (1:1000; Abcam, Inc.; Cambridge, MA), or mouse anti-GFAP (1:500; Millipore; Bellerica, MA). The slides were then fluorescently labeled with goat anti-rabbit Alexa Fluor 546 (1:1000; Invitrogen; Carlsbad, CA) or goat anti-mouse Alexa Fluor 546 (1:1000; Invitrogen; Carlsbad, CA) and the ipsilateral and contralateral dorsal horns from 3-6 sections per slide were digitally imaged at 200x and then cropped over the superficial dorsal horn (laminae I-II). Positive labeling was quantified using quantitative densitometry (Abbadie et al. 1996, Rothman et al. 2010). Results are reported relative to the expression of each marker measured in tissue samples from normal, naïve rats (n=2). For each labeled protein (GLT-1, GLAST, GFAP), a one-way ANOVA tested for differences between each injury group for the ipsilateral and contralateral dorsal horns, separately.

### **6.3.3 Electrophysiological Recordings**

In separate groups of rats, electrophysiological recordings were made in the spinal cord at day 7 (n=8/group). Bilateral mechanical allodynia was also assessed at baseline and on days 1 and 7 using the methods described in Section 5.4 such that mechanical sensitivity was measured in response to stimulation by the 1.4, 4.0 and 10.0gf filaments in order to match the mechanical stimuli that were applied to the forepaw during the

extracellular recordings. A t-test compared the number of paw withdrawals elicited by the 4.0gf filament at day 7 between each group used for the electrophysiological study and their matched group in the immunohistochemistry study to test that the two studies used comparable conditions at the time of the electrophysiological recordings and tissue harvest, respectively. For statistical analysis, a one-way ANOVA tested for differences in the number of paw withdrawals between groups at each day that were elicited by each filament (1.4, 4.0, 10.0gf), for the ipsilateral and contralateral forepaws, separately.

Extracellular recordings were made in the deep laminae of the spinal cord (400-1000 $\mu$ m). Detailed methods are described in Section 5.4. A glass-insulated tungsten probe (<1 $\mu$ m tip; FHC; Bowdoin, ME) was inserted into the spinal cord proximal to the C7 nerve root in rats anesthetized with an intraperitoneal (i.p.) injection of pentobarbital (45mg/kg, supplemented by 1-5mg/kg doses, as needed). Mechanoreceptive neurons innervating the forepaw were searched for by lightly brushing the plantar surface of the forepaw (Crosby et al. 2013, Hains et al. 2003, Quinn et al. 2010). Once a neuron was identified, a sequence of six mechanical stimuli was applied to the forepaw: (1) 10 light brush strokes with a brush applied over 10 seconds; (2-5) a series of four von Frey filaments (1.4, 4.0, 10.0, 26.0gf), each applied five times for 1 second with a 1-second rest between application; and (6) a 10-second, 60gf pinch by a microvascular clip (Roboz, Inc.; Gaithersburg, MD) (Quinn et al. 2010). There was 60 seconds of rest between the applications of each of the different stimuli.

Voltage recordings were spike-sorted in Spike2 (CED; Cambridge, UK) to count the number of action potentials that was evoked by each stimulus for individual neurons. For the brush stimulus, the number of action potentials was summed over the period of

the light brushing. For each von Frey filament application, the number of action potentials was summed over both the stimulation period and the 1-second rest period that immediately followed. For both the brush and the von Frey filament stimuli, the baseline number of spikes occurring in the 10-second period prior to the first stimulation was subtracted from the spike counts during stimulation in order to identify only the spikes evoked by those stimuli (Hains et al. 2003). For the 60gf pinch, the number of spikes was summed over the 5-second period between 3-8 seconds after the clip was applied, in order to only consider those spikes evoked by the pinch and to exclude the spikes evoked by the application and removal of the clip (Quinn et al. 2010). The number of spikes evoked by the clip stimulus was determined by subtracting the baseline number of spikes that occurred in the 5-second window prior to the first stimulation from the spike count.

Neurons were classified as either wide dynamic range (WDR) or low-threshold mechanoreceptive (LTM) neurons by comparing the spike rate (spikes/sec) evoked by the light brushing and the 60gf clip stimuli (Hains et al. 2003, Laird & Bennett 1993, Saito et al. 2008). Neurons that responded maximally to the light brush were identified as LTM and those that responded in a graded manner were identified as WDR (Hains et al. 2003, Woolf & Fitzgerald 1983).

For statistical analysis, the number of spikes counted in the electrophysiological study was log-transformed because of a positive-skew in the distribution of data (Quinn et al. 2010). Separate mixed-effect one-way ANOVAs with Tukey HSD post-hoc tests compared differences in the number of action potentials that were evoked by each filament between groups; neurons were nested within rats and rats were nested in groups. A mixed-effect one-way ANOVA with the same levels of nesting tested for differences

between groups for the depth at which the neurons were recorded from. The distribution of neurons identified as WDR and LTM was compared between groups using Pearson's chi-squared tests. All electrophysiology data are expressed as the mean±standard error of the mean (SEM).

## 6.4 Results

### 6.4.1 Spinal GLT-1 Upregulation by Ceftriaxone

The expression of GLT-1 in the ipsilateral dorsal horn at day 7 after a painful nerve root compression is increased by both of the 10µg and the 150µg doses of ceftriaxone treatment after a painful nerve root compression (Fig. 6.1). Spinal GLT-1 expression in the ipsilateral dorsal horn decreased significantly ( $p=0.021$ ) from sham (*sham+saline*) following a painful nerve root treated with saline (*injury+saline*); it was also significantly decreased ( $p=0.010$ ) compared to the 150µg ceftriaxone treatment (*injury+150µg*). In fact, the expression of GLT-1 was not different between the *sham+saline* and either of the two ceftriaxone treatment groups (Fig. 6.1). In the contralateral dorsal horn, the expression of GLT-1 was unchanged between all of the groups. Quantification of spinal GLT-1 expression for each rat can be found in Appendix D.

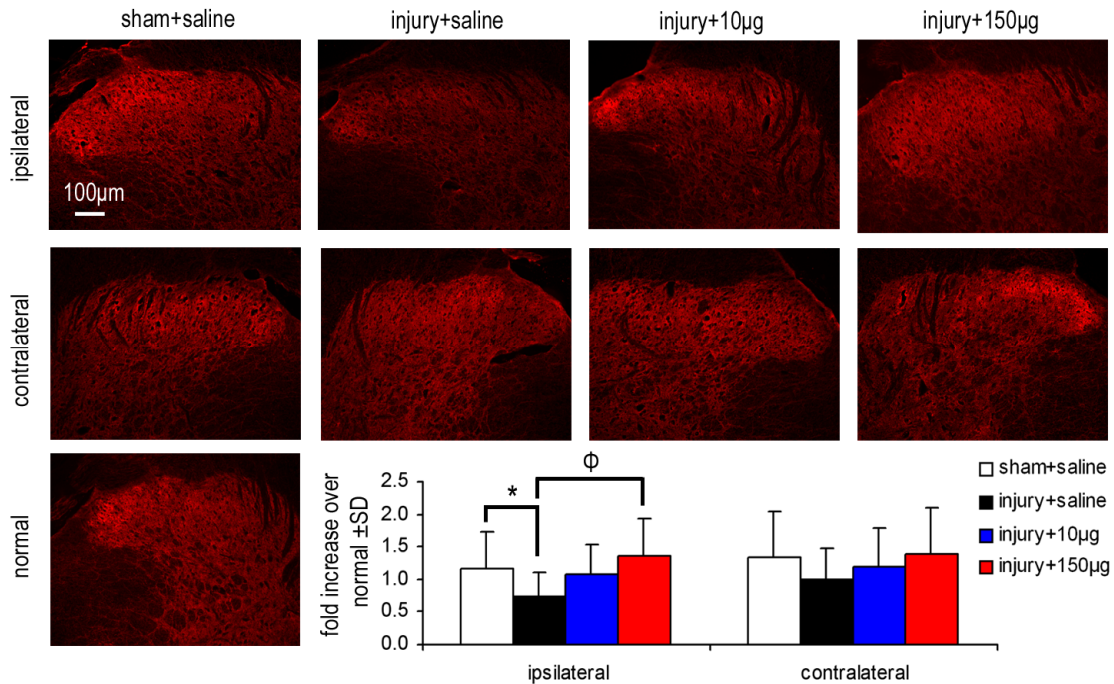


**Fig. 6.1** Spinal GLT-1 at day 7 following root compression treated with 10µg or 150µg of ceftriaxone (*injury+10µg*, *injury+150µg*) or the saline vehicle (*injury+saline*), or following sham procedures (*sham+saline*). In the ipsilateral dorsal horn, the 150µg dose of ceftriaxone (*injury+150µg*) significantly ( $\Phi p=0.010$ ) increased the expression of GLT-1 compared to the vehicle treatment (*injury+saline*). The expression of GLT-1 in the *injury+saline* group was also significantly reduced ( $*p=0.021$ ) compared to *sham+saline* in the ipsilateral dorsal horn.

#### 6.4.2 Behavioral Sensitivity After Ceftriaxone Treatment

Both doses of ceftriaxone abolished mechanical allodynia and thermal hyperalgesia that developed in the ipsilateral forepaw after a painful nerve root compression (Figs. 6.2 & 6.4). Appendix C summarizes the behavioral data for each rat used in this study. At day 1, the number of paw withdrawals elicited by the 4.0gf von Frey filament significantly increased ( $p<0.001$ ) in all of the groups that received a nerve root compression (*injury+saline*, *injury+10µg*, *injury+150µg*) compared to *sham+saline* (Fig. 6.2). However, by day 3 (2 days after the start of treatment), the number of paw withdrawals elicited by the 4.0gf filament in the treatment groups (*injury+10µg*, *injury+150µg*) returned to sham levels and remained significantly less ( $p<0.003$ ) than the

number of paw withdrawals elicited in the vehicle-treated group (*injury+saline*) for the remainder of the study (Fig. 6.2). The number of paw withdrawals in the *sham+saline* group did not significantly differ from baseline at any time-point.

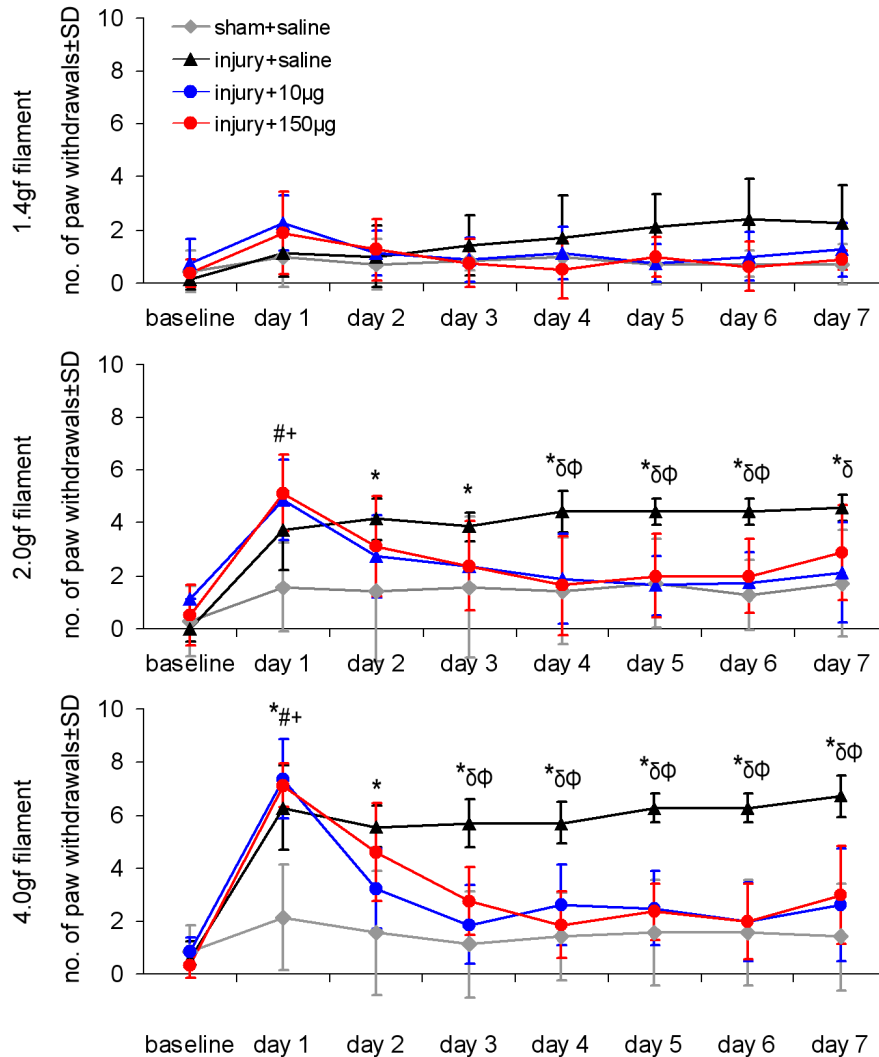


**Fig. 6.2** Mechanical allodynia in the ipsilateral forepaw for daily ceftriaxone treatments starting on day 1, quantified as the number of paw withdrawals for stimulation with a 1.4, 2.0 and 4.0gf filament. Prior to treatment on day 1, the number of paw withdrawals elicited by the 4.0gf filament in the ipsilateral forepaw of each group undergoing root compression (*#injury+10µg*, *+injury+150µg*, *\*injury+saline*) was significantly greater ( $p<0.001$ ) than *sham+saline*. The number of paw withdrawals in the *injury+saline* group was significantly elevated over sham ( $*p<0.001$ ) for all post-operative time-points. Yet, starting on day 3, the number of withdrawals after ceftriaxone treatment significantly decreased ( $\delta p\leq 0.001$ , *injury+10µg*;  $\Phi p\leq 0.002$ , *injury+150µg*) compared to *injury+saline*. The 2.0gf filament responses were similar to those evoked by the 4.0gf filament, but not as robust; the number of paw withdrawals in the *injury+10µg* ( $\delta p=0.012$ ) and *injury+150µg* ( $\Phi p=0.006$ ) groups were significantly less than *injury+saline* starting at day 4.

Testing with the 2.0gf filament elicited similar responses in the ipsilateral forepaw to those elicited by the 4.0gf in all groups (Fig. 6.2). At day 1, the number of paw withdrawals after ceftriaxone treatment (*injury+10 $\mu$ g*, *injury+150 $\mu$ g*) were significantly ( $p<0.005$ ) increased over *sham+saline*; *sham+saline* did not vary from baseline at any time-point. The number of paw withdrawals elicited in the vehicle treatment group (*injury+saline*) was significantly elevated ( $p<0.019$ ) over *sham+saline* on days 2 through 7 (Fig. 6.2). On day 4, the number of paw withdrawals in the *injury+vehicle* group was also significantly elevated over both treatment groups (*injury+10 $\mu$ g*,  $p=0.012$ ; *injury+150 $\mu$ g*,  $p=0.006$ ) and remained significantly elevated over *injury+10 $\mu$ g* ( $p<0.019$ ) through day 7 and *injury+150 $\mu$ g* ( $p<0.005$ ) through day 6 (Fig. 6.2).

The number of withdrawals elicited by the 1.4gf filament applied to the ipsilateral forepaw did not significantly differ from baseline for any group and there were no differences in the number of paw withdrawals between any group (Fig. 6.2). Similarly, for testing with each of the three filaments in the contralateral forepaw, the number of paw withdrawals did not vary over time or between groups (Fig. 6.3).



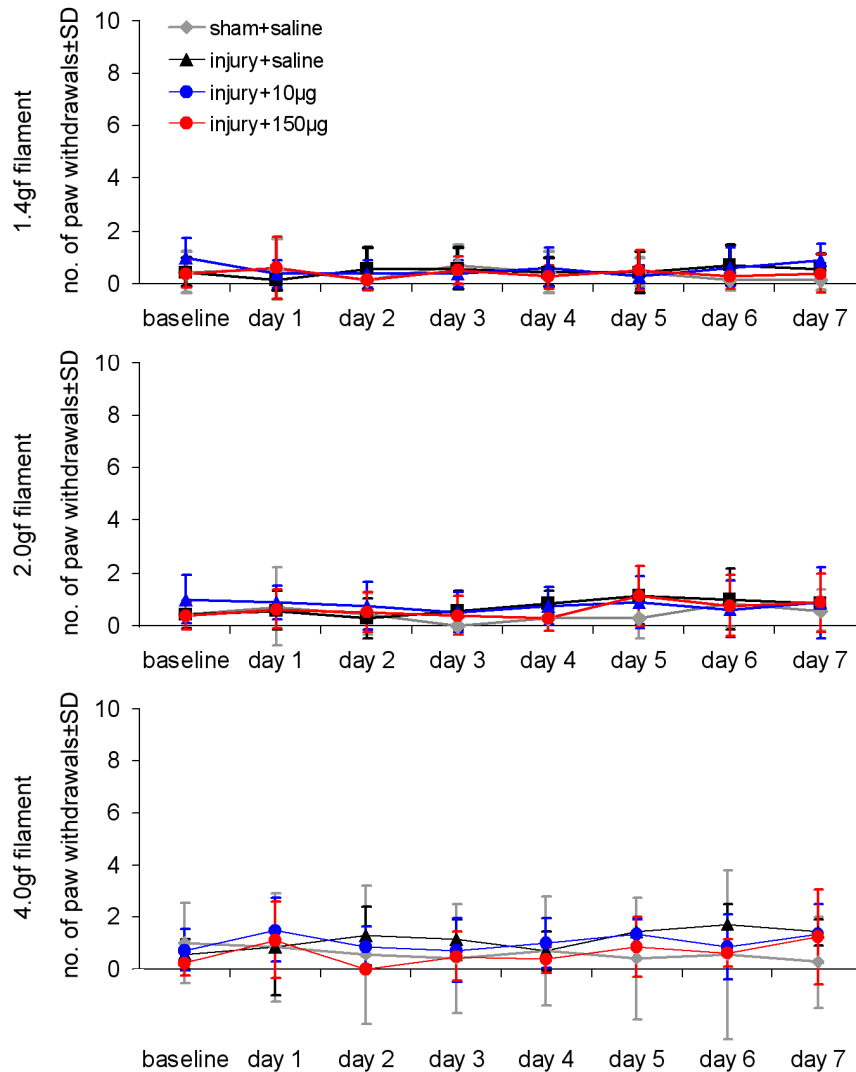


**Fig. 6.3** Mechanical allodynia in the contralateral forepaw for testing with a 1.4, 2.0 and 4.0gf filament did not vary over time or from sham (*sham+saline*) after a nerve root compression treated with ceftriaxone (*injury+10µg*, *injury+150µg*) or the saline vehicle (*injury+saline*).

Like mechanical allodynia, thermal hyperalgesia in the ipsilateral forepaw after the nerve root compression treated with ceftriaxone decreased by day 7, regardless of the dose (Fig. 6.4). At day 1, the withdrawal latency was significantly shorter ( $p < 0.038$ ) after a nerve root compression (*injury+saline*, *injury+10µg*, *injury+150µg*) compared to sham (*sham+saline*) (Fig. 6.4); *sham+saline* did not differ from baseline at either time-point. But, by day 7, the withdrawal latencies in the groups receiving the 10µg ceftriaxone

treatment (*injury+10 $\mu$ g*, 10.1 $\pm$ 3.2 seconds) and the 150 $\mu$ g ceftriaxone treatment (*injury+150 $\mu$ g*, 10.4 $\pm$ 2.1 seconds) were significantly greater ( $p<0.003$ ) than the latency for the vehicle-treated group (*injury+saline*, 5.8 $\pm$ 0.7 seconds) and was not different from *sham+saline* (9.4 $\pm$ 1.1 seconds) (Fig. 6.4). Thermal hyperalgesia in the contralateral paw was unchanged from baseline for all groups (Fig. 6.4).

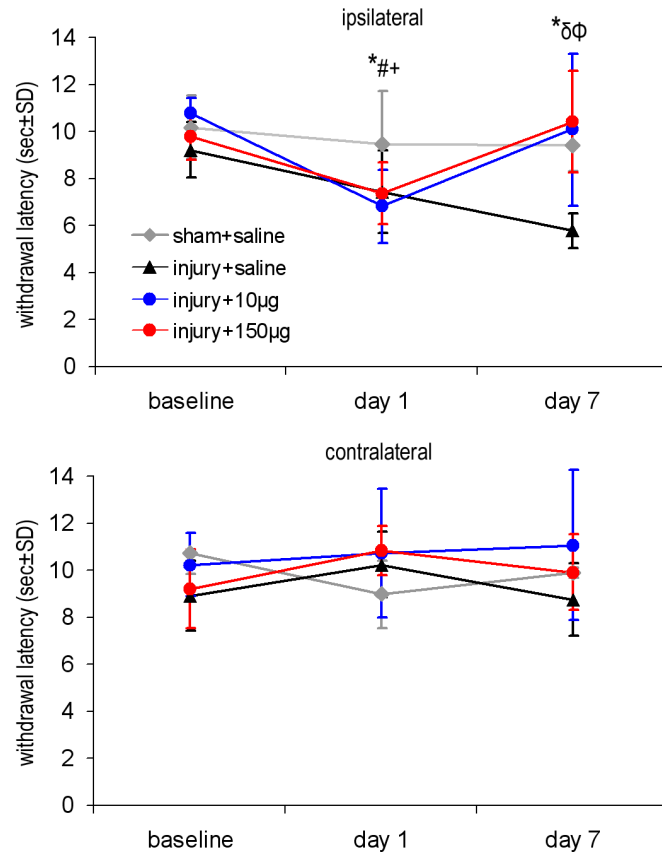


**Fig. 6.4** Thermal hyperalgesia prior to (baseline, day 1) and after (day 7) daily treatments of ceftriaxone, starting on day 1. On day 1, there was a significant decrease in the withdrawal latency in the ipsilateral forepaw in each of the three groups undergoing root compression ( $\#p=0.007$ , *injury+10 $\mu$ g*;  $+p=0.027$ , *injury+150 $\mu$ g*;  $*p=0.038$ , *injury+saline*) compared to *sham+saline*. By day 7, the withdrawal latency significantly increased in each of the groups receiving the ceftriaxone treatment ( $\delta p=0.002$ , *injury+10 $\mu$ g*;  $\Phi p=0.001$ , *injury+150 $\mu$ g*) compared to *injury+saline*. The withdrawal latency in *injury+saline* group remained significantly lower ( $*p=0.014$ ) than *sham+saline* at day 7.

### 6.4.3 Effect of Ceftriaxone on Spinal GLAST & GFAP Expression

Only the 10 $\mu$ g dose of ceftriaxone treatment (*injury+10 $\mu$ g*) decreased the expression of GFAP that was upregulated after the vehicle treatment (*injury+saline*) (Fig. 6.5). The expression of GFAP in the ipsilateral dorsal horn was significantly elevated ( $p<0.004$ ) after a nerve root compression with vehicle treatment (*injury+saline*) and 150 $\mu$ g of ceftriaxone (*injury+150 $\mu$ g*) compared to *sham+saline*. In the *injury+10 $\mu$ g* group, the ipsilateral expression of GFAP was not different from any group (Fig. 6.5).

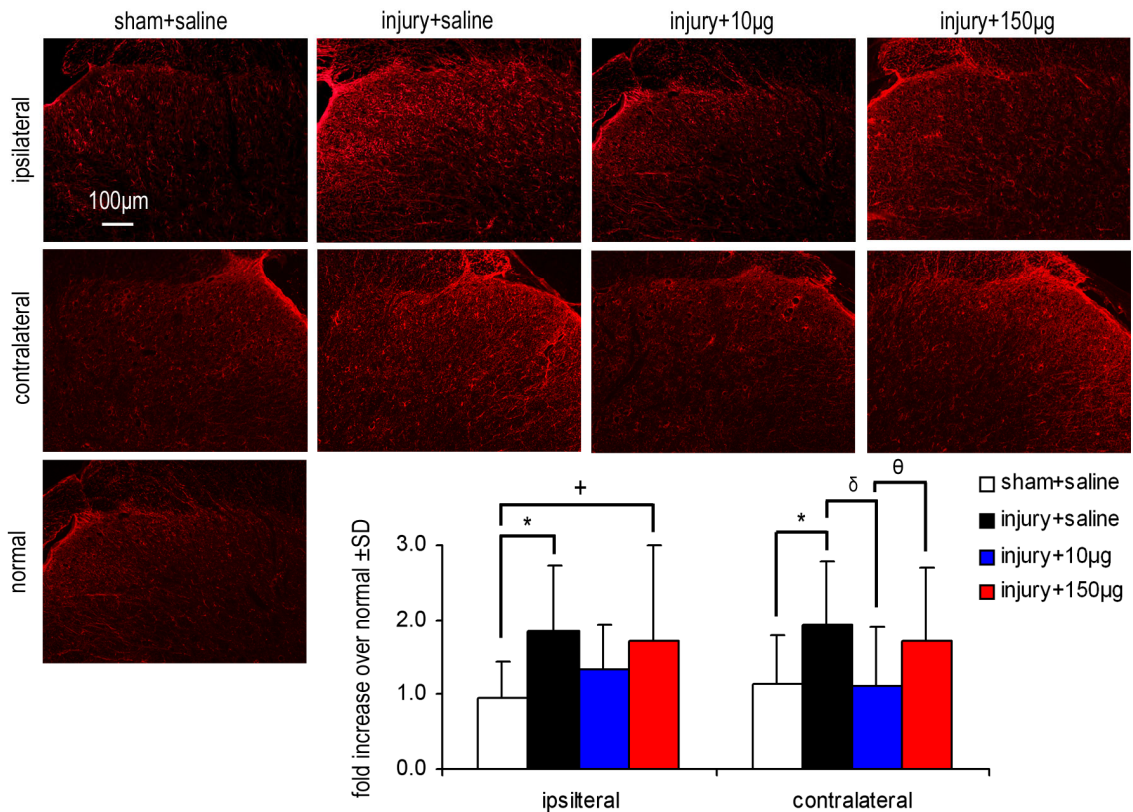


**Fig. 6.5** Ceftriaxone dose-dependently modulated bilateral spinal expression of GFAP at day 7. In the ipsilateral dorsal horn, the expression of GFAP was significantly elevated in the *injury+saline* ( $*p=0.001$ ) and the *injury+150 $\mu$ g* ( $+p=0.003$ ) groups compared to *sham+saline*. The expression of GFAP in the *injury+10 $\mu$ g* group was not different from any other group in the ipsilateral dorsal horn. In the contralateral dorsal horn, the expression of GFAP was also elevated after *injury+saline* compared to both *sham+saline* ( $*p=0.001$ ) and *injury+10 $\mu$ g* ( $\delta p<0.001$ ). After treatment with ceftriaxone, the expression of GFAP in the contralateral dorsal horn significantly increased ( $\theta p=0.012$ ) in *injury+150 $\mu$ g* compared to *injury+10 $\mu$ g*.

In the contralateral dorsal horn, GFAP expression was significantly elevated ( $p < 0.002$ ) in the vehicle treatment group (*injury+saline*) compared to both the *sham+saline* and *injury+10 $\mu$ g* groups (Fig. 6.5). Following treatment with 150 $\mu$ g of ceftriaxone (*injury+150 $\mu$ g*), the expression of GFAP was significantly elevated ( $p = 0.012$ ) over the 10 $\mu$ g treatment group (*injury+10 $\mu$ g*) (Fig. 6.5).

Both doses of ceftriaxone returned the ipsilateral expression of GLAST to sham levels at day 7 after a nerve root injury (Fig. 6.6). After a nerve root compression treated with the saline vehicle (*injury+saline*), the expression of GLAST in the ipsilateral dorsal horn was significantly increased ( $p = 0.047$ ) over *sham+saline*. For each ceftriaxone

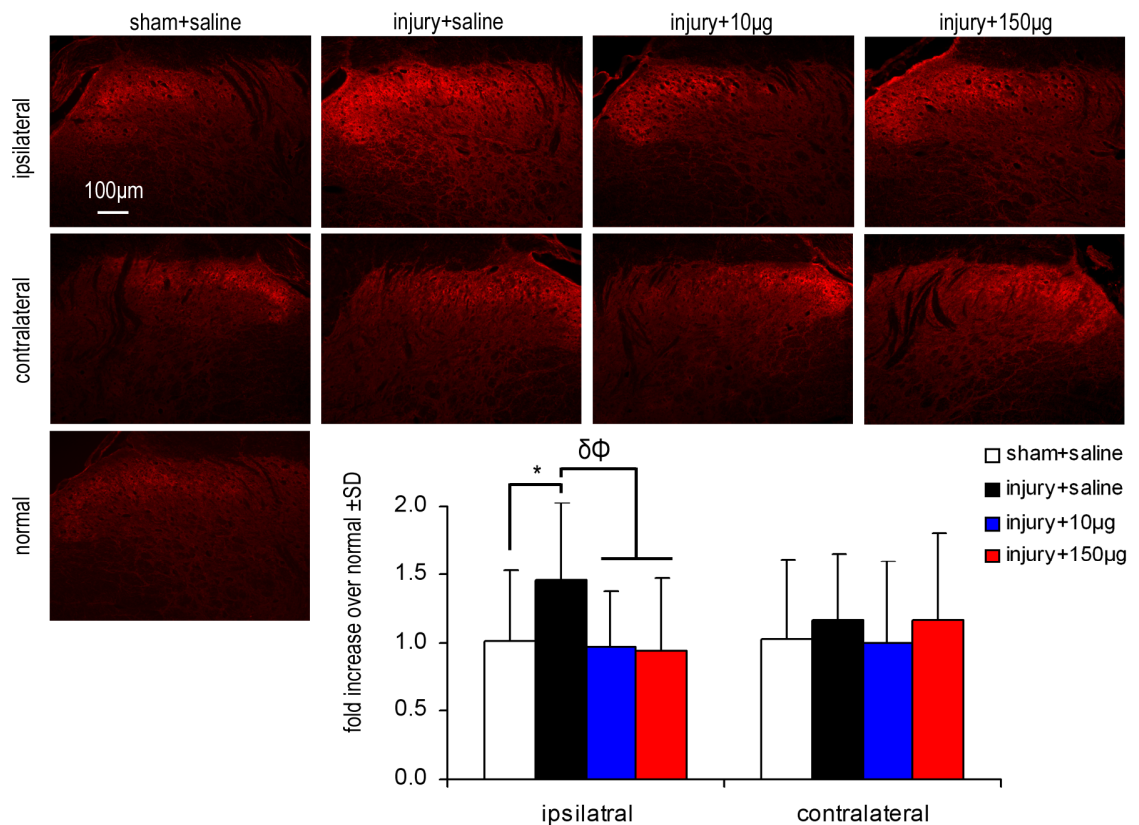


**Fig. 6.6** Spinal GLAST expression at day 7 after a root compression treated with ceftriaxone (*injury+10 $\mu$ g*, *injury+150 $\mu$ g*) and the saline vehicle (*injury+saline*), and sham exposure (*sham+saline*). The expression of GLAST only increased in the ipsilateral dorsal horn after *injury+saline* compared to *injury+10 $\mu$ g* ( $\delta p = 0.033$ ), *injury+150 $\mu$ g* ( $\Phi p = 0.042$ ) and *sham+saline* ( $*p = 0.047$ ).

treatment dose, GLAST expression in the ipsilateral dorsal horn was significantly reduced (*injury+10 $\mu$ g*,  $p=0.033$ ; *injury+10 $\mu$ g*,  $p=0.042$ ) compared to *injury+saline*, and not different from sham levels (Fig. 6.6). The expression of GLAST in the contralateral dorsal horn was unchanged between all groups. Appendix D summarizes the quantification of spinal GFAP and GLAST for the individual rats in this study.

#### **6.4.4 Evoked Action Potentials in the Spinal Cord After Ceftriaxone Treatment**

As with the behavioral sensitivity and spinal GLAST responses (Figs. 6.2, 6.4 & 6.6), ceftriaxone reduced the neuronal hyperexcitability that develops in the ipsilateral spinal dorsal horn after a nerve root compression. As was observed in the rats used in the immunohistochemical study (Fig. 6.2), the number of paw withdrawals elicited by the 4.0 filament at day 7 was significantly elevated in the vehicle treated group (*injury+saline*;  $p<0.001$ ) over both of the ceftriaxone treatment groups (*injury+10 $\mu$ g*, *injury+150 $\mu$ g*) and the sham exposure (*sham+saline*) (Fig. 6.7). Likewise, for testing with the 10.0gf filament at day 7, a significant increase ( $p<0.001$ ) in the number of ipsilateral paw withdrawals was observed in the *injury+saline* group compared to the *injury+10 $\mu$ g*, *injury+150 $\mu$ g* and *sham+saline* groups (Fig. 6.7). There were no differences in the number of paw withdrawals elicited by the 1.4gf filament between any group; no differences were observed in the contralateral forepaw between groups for testing with any filament (Fig. 6.7). Please see Appendix C for a summary of the behavioral data for each rat.

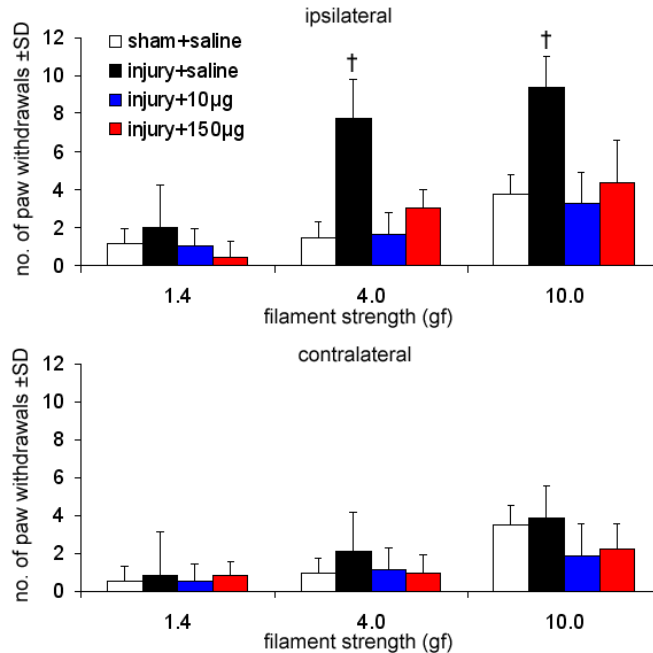


**Fig. 6.7** Bilateral mechanical allodynia at day 7 after a painful root compression treated with ceftriaxone (*injury+10µg*, *injury+150µg*) or vehicle (*injury+saline*), or sham procedures (*sham+saline*). The number of withdrawals elicited in the ipsilateral forepaw by the 4.0 and 10.0gf filaments in the *injury+saline* group was significantly elevated (<sup>†</sup> $p < 0.001$ ) over all other groups.

A total of 273 neurons were recorded for all four groups, at an average depth of  $646 \pm 138 \mu\text{m}$ . The average depth of neurons that was recorded for each group was not significantly different from each other. The recording depth and spike counts for each neuron are summarized in Appendix E.

Similar to the behavioral responses, the number of action potentials evoked by the 4.0, 10.0 and 26.0gf filaments increased significantly ( $p < 0.024$ ) in the *injury+saline* group compared to sham (*sham+saline*) and the 10µg treatment group (*injury+10µg*) (Fig. 6.8). The number of evoked spikes in the 150µg treatment group (*injury+150µg*) was only significantly elevated over *sham+saline* ( $p < 0.042$ ) for testing with the 10.0 and 26.0gf filaments (Fig. 6.8). On average, the number of spikes evoked in the *injury+saline* group was 2-3 times greater than the number of spikes evoked in any other group. For

example, for stimulation by the 10.0gf filament, the number of evoked spikes in the *injury+saline* group was  $51.3 \pm 8.6$ , which was significantly greater than the number of spikes evoked by that filament for the *sham+saline* ( $17.5 \pm 3.3$ ;  $p=0.002$ ), the *injury+10 $\mu$ g* ( $24.2 \pm 2.8$ ;  $p=0.023$ ) and the *injury+150 $\mu$ g* ( $28.8 \pm 5.0$ ;  $p=0.041$ ) groups. Although the

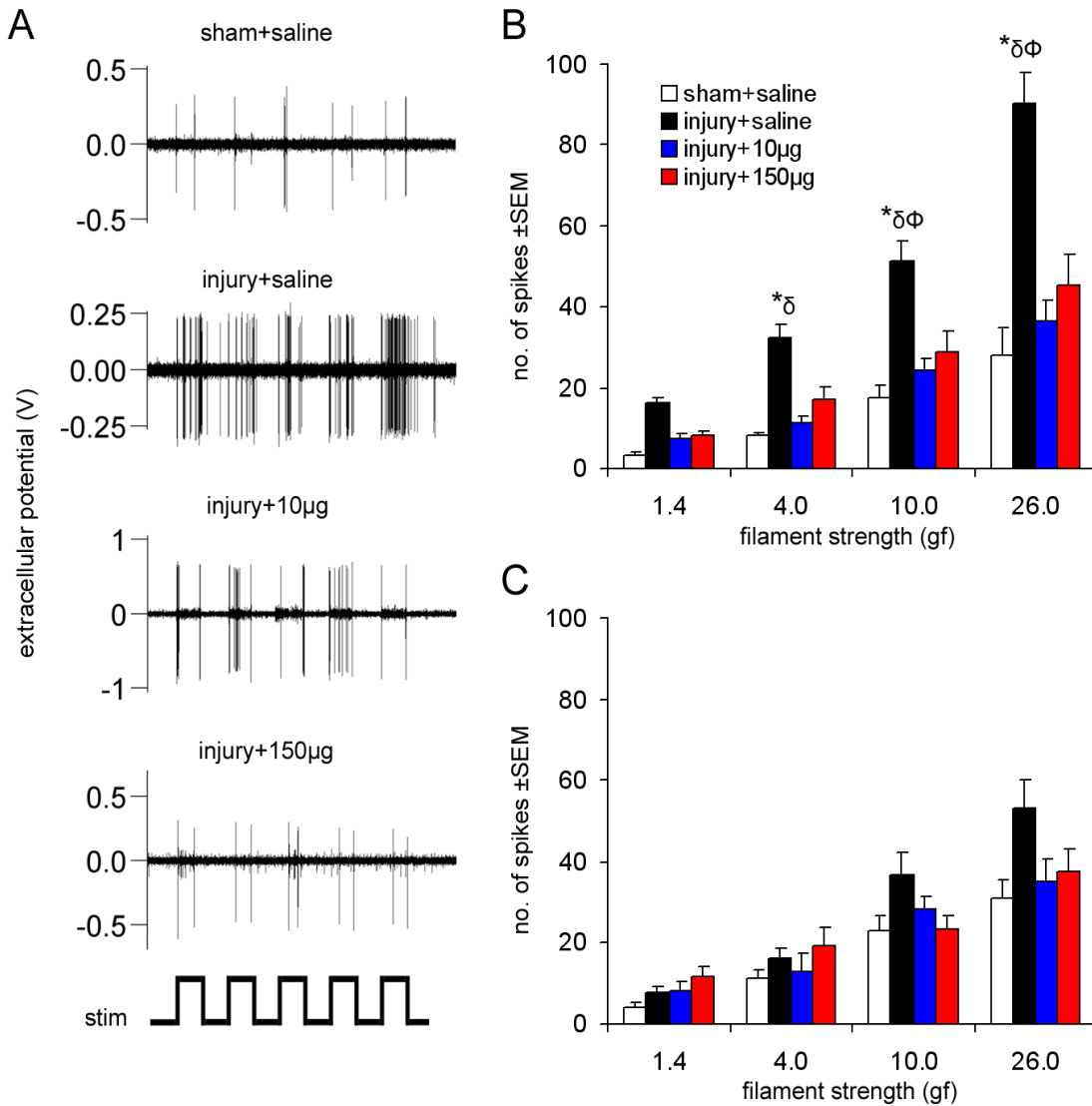


**Fig. 6.8** Ceftriaxone reduces neuronal hyperexcitability in the spinal cord at day 7 after injury (*injury+10 $\mu$ g*, *injury+150 $\mu$ g*) compared to vehicle (*injury+saline*). **(A)** Representative extracellular potentials recorded in the ipsilateral spinal cord for each group during application of the 4.0gf filament stimulus (stim) are shown. **(B)** The number of spikes evoked in the ipsilateral spinal cord by the 4.0, 10.0 and 26.0gf filaments applied to the paw was significantly elevated in *injury+saline* compared to *sham+saline* ( $*p<0.008$ ), *injury+10 $\mu$ g* ( $\delta p<0.024$ ) and *injury+150 $\mu$ g* (the 10.0 and 26.0gf filaments only,  $\Phi p<0.042$ ). **(C)** Contralateral neuronal excitability was not different between any group.

number of spikes elicited by the 1.4gf was elevated in the *injury+saline* group, this increase was not significant. Similarly, the small increase in the number of spikes in the contralateral dorsal horn that was evoked in the *injury+saline* group by stimulation using the 10.0 and 26.0gf filaments was not statistically different from *sham+saline*, *injury+10μg* or *injury+150μg* (Fig. 6.8). In addition, the proportion of WDR neurons identified in the ipsilateral spinal cord that were recorded from in the *injury+saline* group (91%) was significantly greater ( $p < 0.015$ ) than the proportion of WDR neurons recorded in ipsilateral dorsal horn of any of the other groups (Fig. 6.9): *sham+saline* (60%), *injury+10μg* (64%), *injury+150μg* (67%). The proportion of WDR neurons in the contralateral dorsal horn (63-72%) did not differ between any of the groups (Fig. 6.9).

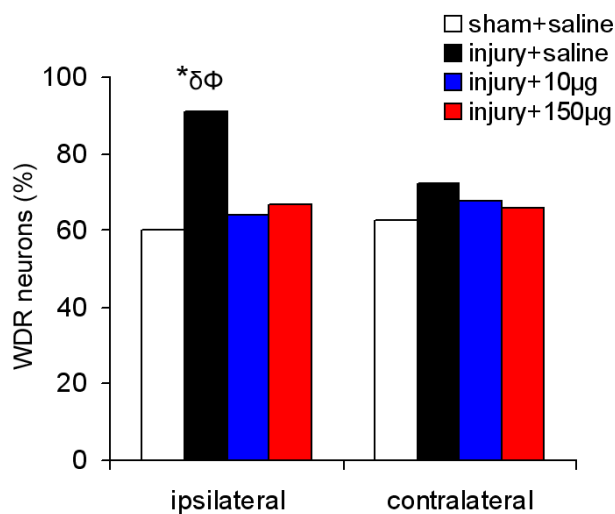


**Fig. 6.9** Both 10μg and 150μg of ceftriaxone reduced the proportion of WDR neurons detected in the spinal cord at day 7 after injury (*injury+10μg*, *injury+150μg*) compared to vehicle (*injury+saline*) and sham (*sham+saline*). The percent of WDR neurons after *injury+saline* increased only in the ipsilateral spinal cord compared to *sham+saline* ( $*p=0.004$ ), *injury+10μg* ( $\delta p=0.008$ ) and *injury+150μg* ( $\Phi p=0.014$ ).



## 6.5 Discussion

Ceftriaxone treatment restored GLT-1 expression in the spinal cord while also abolishing behavioral sensitivity and the associated GLAST upregulation and neuronal hyperexcitability that normally develop at day 7 (Figs. 6.1-6.4 & 6.6-6.9; Chapter 5). The spinal astrocytic activation that develops after a painful nerve root compression (Nicholson et al. 2012, Rothman et al. 2010) was abolished by the 10 $\mu$ g dose of ceftriaxone, but not by the 150 $\mu$ g dose (Fig. 6.5). Although this is the first study to demonstrate that daily intrathecal injection of ceftriaxone in the lumbar region of the rat upregulates GLT-1 in the cervical region, it is not the first to show that pharmacological agents delivered to the lumbar region can mediate cellular outcomes in the cervical spinal cord. In this same painful injury model, cervical spinal inflammation was attenuated by cytokine antagonists delivered via lumbar puncture (Rothman & Winkelstein 2010). Daily lumbar punctures of ceftriaxone, as was done in the current study, increases GLT-1 expression in the lumbar cord, but has no effect on behavioral sensitivity in the hindpaw of normal rats (Hu et al. 2010). It is, therefore, unlikely that the delivery method chosen for the current study changed behavioral sensitivity in the hindpaw, which was not measured.

This is the first study to demonstrate that upregulation of GLT-1 by daily intrathecal injection of ceftriaxone abolishes radicular pain and, for the 10 $\mu$ g dose, associated spinal astrocyte activation (Figs. 6.1-6.5). In response to varying magnitudes and durations of nerve root compression, spinal astrocyte activation is evident *only* when behavioral sensitivity also develops, supporting the role of reactive astrocytes in providing substantial contributions to the persistence of behavioral sensitivity (Nicholson

et al. 2012, Rothman et al. 2010). Although it has been reported that glial activation is necessary for the maintenance of pain (Weiseler-Frank et al. 2004), the results of this study indicate that astrocyte activation alone is not sufficient to induce behavioral sensitivity due to the fact that the 150 $\mu$ g dose of ceftriaxone *did* reduce behavioral sensitivity in the absence of a reduction in spinal GFAP expression (Figs. 6.2 & 6.5). In addition to their role in taking up extracellular glutamate, the activated spinal glia also contribute to pain by modulation of neuronal synapse strength and neuronal excitability through the release of neurotransmitters, neuropeptides and cytokines (Milligan & Watkins 2009, Wieseler-Frank et al. 2004). Glia likely mediate radicular pain by a combination of their functions; however, the results of this study indicate that maintenance of normal GLT-1 uptake of glutamate by glial cells is, in itself, sufficient to abolish nerve root-mediated pain, with or without, a reduction in spinal astrocyte activation (Figs. 6.1-6.5). Many studies demonstrate that cervical radicular pain is associated with activated astrocytes in the spinal cord (Hubbard & Winkelstein 2005, Nicholson et al. 2012, Rothman et al. 2010) and that astrocytes contribute to chronic neuropathic pain by releasing pro-inflammatory cytokines, ATP, nitric oxide and prostaglandin E<sub>2</sub> (Markowitz et al. 2007, Milligan & Watkins 2009, Perea et al. 2009, Ren & Dubner 2008). Although previous reports suggest that astrocytes contribute to the *initiation* of nerve root-mediated pain by releasing pro-inflammatory cytokines (Rothman et al. 2009b, Rothman & Winkelstein 2010), this is the first study to identify a potential cellular mechanism (GLT-1) by which these astrocytes contribute to the *maintenance* of cervical radicular pain (Figs. 6.1-6.5).

Ceftriaxone modulates the astrocytic expression of GFAP and GLT-1 *in vitro* through the NF- $\kappa$ B signaling pathway (Bachetti et al. 2010, Lee et al. 2008, Yamada & Jinno 2011). In cultured astrocytes, ceftriaxone decreases GFAP promoter activity and suppresses GFAP upregulation by reducing NF- $\kappa$ B activity, but increases the expression of GLT-1 by *promoting* NF- $\kappa$ B signaling (Bachetti et al. 2010, Lee et al. 2008, Yamada & Jinno 2011). There is a dose-dependent relationship between ceftriaxone and NF- $\kappa$ B activity, which may explain the divergent effects of ceftriaxone on astrocytes (Bachetti et al. 2010, Lee et al. 2008, Yamada & Jinno 2011). In separate studies, low concentrations of ceftriaxone activate NF- $\kappa$ B and increases GLT-1 promoter activity *in vitro* (Ghosh et al. 2011, Lee et al. 2008) while higher concentrations are required to suppress the activity NF- $\kappa$ B and reduce GFAP promoter activity in cultured astrocytes (Bachetti et al. 2010, Yamada & Jinno 2011). Although GLT-1 expression has not been evaluated under conditions required for ceftriaxone to reduce NF- $\kappa$ B signaling and GFAP promoter activity, it is likely that GLT-1 is reduced or unchanged at these higher concentrations due to its dependence on NF- $\kappa$ B activation (Bachetti et al. 2010, Lee et al. 2008, Yamada & Jinno 2011). Taken together, these *in vitro* studies suggest that both the 10 $\mu$ g and 150 $\mu$ g doses used in the present study were sufficiently low to up-regulate GLT-1 (Fig. 6.1) by promoting the NF- $\kappa$ B signaling pathway (Ghosh et al. 2011, Lee et a. 2008). It is, therefore, likely that ceftriaxone did not directly modulate GFAP expression (Fig. 6.5). It could be hypothesized then, that the decrease in GFAP expression that is evident after the 10 $\mu$ g treatment (Fig. 6.5) was a consequence of reduced extracellular glutamate. This would not explain why GFAP remained elevated after treatment with the 150 $\mu$ g dose (Fig. 6.5), however. Although previous studies demonstrate that ceftriaxone alleviates

behavioral sensitivity and reduces astrocyte activation while promoting GLT-1 expression in peripheral nerve injury and multiple sclerosis (Ramos et al. 2010), the current study demonstrates that there is no clear relationship between ceftriaxone and its effects on GLT-1 and GFAP. Additional *in vitro* and *in vivo* studies are needed to clarify the mechanism(s) by which ceftriaxone modulates the expression of GLT-1 and GFAP in order to fully understand how astrocytes contribute to the maintenance of nerve root-mediated pain.

Spinal GLAST expression and neuronal hyperexcitability are both mediated, in part, by extracellular glutamate activation of metabotropic glutamate (mGluRs) and N-methyl-D-aspartate (NMDA) receptors (Aronica et al. 2003, Jourdain et al. 2007, Ren & Dubner 2008, Tilleux & Hermans 2007). The reduction in both spinal GLAST expression and neuronal hyperexcitability that was observed after painful root compression treated with ceftriaxone (Figs. 6.6 & 6.8) serve as proxies suggesting reduced spinal glutamate signaling (Aronica et al. 2003, Jourdain et al. 2007, Ren & Dubner 2008, Tilleux & Hermans 2007). Very few studies have evaluated the effects of ceftriaxone on GLAST expression or neuronal hyperexcitability (Mimura et al. 2011, Rothstein et al. 2005, Trantham-Davidson et al. 2012). Ceftriaxone has no effect on GLAST in both normal rats and brain-injured neonate pups (Mimura et al. 2011, Rothstein et al. 2005), indicating that the downregulation of spinal GLAST at day 7 after the ceftriaxone treatment (Fig. 6.6) was not likely a direct consequence of ceftriaxone. Excitatory signaling in the nucleus accumbens of the rat after cocaine administration is also reduced by upregulating GLT-1 with ceftriaxone (Knackstedt et al. 2010, Trantham-Davidson et al. 2012). Although that study, along with our results (Fig. 6.8), indicates that ceftriaxone can

modulate neuronal excitability, it is not clear whether neuronal signaling is *directly* modulated by ceftriaxone or by GLT-1 regulation of extracellular glutamate in the spinal cord. Interestingly, inhibition of spinal GLAST in the rat reduces extracellular glutamate and excitatory neuronal signaling, which is contrary to the notion that glutamate transporter inhibition would increase excitatory signaling (Niederberger et al. 2006). Although it is not clear how GLAST regulates excitatory signaling, the downregulation of GLAST after ceftriaxone treatment may also contribute to reducing the spinal neuronal hyperexcitability (Figs. 6.6 & 6.8) (Niederberger et al. 2006).

Ceftriaxone also reduced the distribution of WDR neurons in the spinal cord after injury (Fig. 6.9). There is an increase in neurons exhibiting a WDR phenotype after a painful root compression (Fig. 6.9); this is consistent with rodent models of spinal cord hemisection, facet joint distraction and sciatic nerve compression (Hains et al. 2003, Keller et al. 2007, Quinn et al. 2010) and may be a functional reorganization of afferents in the dorsal horn such that normally monosynaptic neurons become polysynaptic (Baba et al. 2003, Keller et al. 2007, Kohno et al. 2003, Okamoto et al. 2001). Specifically, the shift from LTM to WDR neurons (Fig. 6.9), suggests that after injury, high threshold A $\delta$  and C fibers form synapses with neurons that normally only synapse with low-threshold A $\beta$  fibers (Basbaum et al. 2009, Keller et al. 2007, Okamoto et al. 2001). Alternatively, the phenotypic shift could indicate enlarged WDR neuron receptive fields after injury (Hanai et al. 1996, Konodo et al. 2003, Suzuki et al. 2000), increasing the likelihood of finding this type of neuron using the search protocol employed in this study. However, increased receptive field size is also attributed to central reorganization of afferents in the spinal cord after nerve injury (Konodo et al. 2003, Suzuki et al. 2000). Regardless,

whether the phenotypic shift observed here reflects an increase in the number of WDR neurons or an increase in WDR receptive field sizes, it does indicate plasticity in the spinal cord after a painful nerve root injury (Baba et al. 2003, Keller et al. 2007, Kohno et al. 2003, Konodo et al. 2003, Okamoto et al. 2001, Suzuki et al. 2000). Enhanced excitability of excitatory neurons is believed to be responsible for such reorganization (Keller et al. 2007, Kohno et al. 2003). The intrathecal injection of ceftriaxone, which has been shown to reduce excitatory glutamate signaling in the spinal cord (Hu et al. 2010, Inquimbert et al. 2012), restored the distribution of WDR neurons after injury to the cervical nerve root (Fig. 6.9). These two effects of ceftriaxone indicate that enhanced excitatory signaling, rather than reduced inhibitory signaling, contributes, at least in part, to spinal reorganization after a painful nerve root injury (Baba et al. 2003, Keller et al. 2007, Kohno et al. 2003, Okamoto et al. 2001).

Both doses of ceftriaxone (10 $\mu$ g, 150 $\mu$ g) abolished mechanical allodynia and thermal hyperalgesia in the forepaw after a painful nerve root compression (Figs. 6.2 & 6.4). Contrary to these findings, mechanical allodynia has been reported to exhibit a graded decrease for doses from 50 $\mu$ g to 100 $\mu$ g after a sciatic nerve injury in the rat; at least 100 $\mu$ g is required to abolish behavioral sensitivity when treatment begins at day 9 (Hu et al. 2010). Even though that study, like the one presented here, administered ceftriaxone daily by lumbar puncture, there was a 10-fold increase in the amount of ceftriaxone required to abolish mechanical allodynia produced by a peripheral nerve injury (100 $\mu$ g vs. 10 $\mu$ g; Fig. 6.2) (Hu et al. 2010). The different dose-response of ceftriaxone on behavioral sensitivity between that neuropathic pain model and the radicular pain model used here could be attributed to differences between nerve- and

nerve root-mediated pain, but is more likely due to the earlier time of intervention (day 1) that was used in the current study. In that same painful nerve injury model, 50 $\mu$ g of ceftriaxone (the lowest dose tested), administered at the time of injury, completely prevented the development of mechanical allodynia (Hu et al. 2010). Twice as much ceftriaxone (100 $\mu$ g) was required to abolish behavioral sensitivity when treatment did not begin until day 9 (Hu et al. 2010), demonstrating that higher doses of ceftriaxone are needed to effectively alleviate pain when treatment is delayed until after the injury or pain has already been established. Because people often delay medical treatment for neck pain until it is severe enough to interfere with everyday activities (Côté et al. 2001), clinically-relevant doses of ceftriaxone for alleviating nerve root-mediated pain may be higher than the 10 and 150 $\mu$ g that were administered at day 1 in the current study. However, it is worth noting that daily, intrathecal injections of 150 $\mu$ g of ceftriaxone can alleviate behavioral sensitivity even if administration is not started until 12 days after a chronic constriction injury of the sciatic nerve in the rat (Ramos et al. 2010). Although additional studies are required to determine whether ceftriaxone can similarly attenuate radicular pain when treatment is administered at later time-points, the study by Ramos et al. (2010) does suggest that ceftriaxone can alleviate cervical radicular pain in the rat even if treatment begins at a late time after persistent behavioral sensitivity is established (Ramos et al. 2010).

The current study did not determine whether the analgesic effects of ceftriaxone persist even after treatment is discontinued. The half-life of a single dose of ceftriaxone in the cerebrospinal fluid (CSF) of rodents is estimated to be 7-8 hours (Lutsar et al. 1998); so within 3 days, less than 1% of the ceftriaxone would remain in the CSF after

the last treatment is given. Yet, after a chronic constriction to the sciatic nerve of the rat, ceftriaxone alleviates mechanical allodynia for at least 7 days after the final dose (Amin et al. 2012, Hajhashemi et al. 2012, Hu et al. 2010). These studies suggest that if ceftriaxone is administered until behavioral sensitivity resolves, pain symptoms will remain attenuated even after treatment is discontinued (Amin et al. 2012, Hajhashemi et al. 2012, Hu et al. 2010). It is likely, therefore, that ceftriaxone would have long lasting effects of abolishing mechanical allodynia and thermal hyperalgesia out to at least day 13 in the current study, had behavioral testing been continued. Unlike its effects on behavioral sensitivity and GLT-1 expression (Hu et al. 2010, Ramos et al. 2010, Rothstein et al. 2005), few studies have characterized the effects of ceftriaxone on spinal inflammation, neuronal signaling or the expression of other glutamate transporters involved in pain. These results help to define the effects of ceftriaxone by evaluating spinal astrocytic activation, GLAST expression and neuronal hyperexcitability after treatment in a model of painful nerve root compression (Figs. 6.5, 6.6 & 6.8). Although the present study did not directly measure glutamate clearance in the spinal cord, ceftriaxone specifically increases the expression of the membrane-bound, dimer form of GLT-1, which is the only functionally active form of GLT-1 and also increases the activity of GLT-1 even when the transporter's expression is unchanged in the rat (Haugeto et al. 1996, Lipski et al. 2007, Ramos et al. 2010). Therefore, the upregulation of GLT-1 by ceftriaxone (Fig. 6.1) strongly suggests that glutamate uptake also increases. By restoring the normal balance of glutamate uptake via GLT-1, ceftriaxone alleviates nerve root-mediated pain by reducing spinal hyperexcitability and also normalizing the spinal expression of GLAST and distribution of WDR neurons.



## 6.6 Integration & Conclusions

Downregulation of spinal GLT-1 after a nerve root compression is only evident when behavioral sensitivity is also present (Chapters 4 & 5). Pharmacologic upregulation of this transporter with ceftriaxone alleviates both the mechanical allodynia and thermal hyperalgesia that develop after a painful nerve root compression (Figs. 6.2 & 6.4), suggesting that spinal GLT-1 *contributes* to radicular pain in this model and is not simply an indicator of a painful nerve root compression (Section 5.3). Interestingly, ceftriaxone also reduces spinal GLAST expression (Fig. 6.6), despite the fact that ceftriaxone does not alter the expression of GLAST in the central nervous system of normal, naïve rats (Rothstein et al. 2005). It is likely that ceftriaxone reduces spinal GLAST in this study by reducing glutamate concentration in the spinal cord, due to the increase in glutamate uptake by spinal GLT-1 (Figs. 6.1 & 6.6; Aronica et al. 2003, Jourdain et al. 2007, Ren & Dubner 2007, Tilleux & Jinn 2007). Therefore, even though studies in Chapter 5 show that a painful nerve root compression is associated with an increase in the expression of GLAST in the spinal dorsal horn (Figure 5.2), this upregulation is likely an indicator of, but is not a contributor to, nerve root-mediated pain (Aronica et al. 2003, Jourdain et al. 2007, Ren & Dubner 2007, Rothstein et al. 2005, Tilleux & Jinn 2007). In fact, *in vitro* studies demonstrate that GLAST is neuroprotective when rapidly upregulated by extracellular glutamate and that upregulation of GLAST by glial cell-line-derived neurotrophic factor (GDNF) prevents axotomy-induced apoptosis *in vivo* (Duan et al. 1999, Koeberle & Bähr 2008). Although its effects on spinal GLAST were not determined, GDNF also attenuates nerve root-mediated pain when it is applied directly to the affected root in this model (Hubbard et al. 2009). In addition to those studies

demonstrating the neuroprotective effects of GLAST, it should also be noted that spinal GLAST is upregulated at day 1 in the model of cervical radiculopathy used here even after the non-painful nerve root exposure (sham) and non-painful 3 minute root compression (Figure 5.2), indicating that GLAST upregulation in the spinal cord is not, by itself, sufficient for the development of behavioral sensitivity in the forepaw of the rat.

Both doses (10 $\mu$ g and 150 $\mu$ g) of ceftriaxone abolished behavioral sensitivity after a painful nerve root compression (Figs. 6.2 & 6.4). Previous studies suggest that higher doses of ceftriaxone are required to alleviate behavioral sensitivity if treatment does not begin until after spinal GLT-1 is downregulated after the painful nerve injury (Hu et al. 2010). Because the current study administered ceftriaxone at day 1, when spinal GLT-1 is unchanged after a painful nerve root compression (Figure 5.1), the 10 $\mu$ g dose may not be sufficient to reduce pain if it is administered at later time-points (Hu et al. 2010); even a larger dose (50 $\mu$ g) has been shown not to be sufficient to abolish behavioral sensitivity after a sciatic nerve constriction when it is administered at day 9 (Hu et al. 2010). However, 150 $\mu$ g of ceftriaxone does alleviate behavioral sensitivity after a painful sciatic nerve injury in the rat, even when treatment begins as late as day 12 (Ramos et al. 2010). If ceftriaxone is administered later than day 1 after a painful nerve root compression, it is possible that *only* the 150 $\mu$ g dose would be sufficient to alleviate behavioral sensitivity. Therefore, even though the 10 $\mu$ g dose does alleviate nerve root-mediated pain, it may not be a clinically-relevant dose for treating cervical radiculopathy, which is often not diagnosed until symptoms have already persisted for many months (Côté et al. 2001).

Unlike its effects on behavioral sensitivity, the two doses of ceftriaxone (10 $\mu$ g and 150 $\mu$ g) did differentially modulate spinal GFAP expression (Fig. 6.5). Specifically,

astrocyte activation decreased after the 10 $\mu$ g treatment, but remained significantly elevated over sham levels after treatment with 150 $\mu$ g of ceftriaxone. Although ceftriaxone may have directly modulated spinal GFAP (Fig. 6.5), separate studies of ceftriaxone's mechanisms of action in cultured astrocytes suggest that the concentrations of ceftriaxone required to upregulate GLT-1 have no effect on GFAP promoter activity (Bachetti et al. 2010, Beller et al. 2011, Lee et al. 2008). Those *in vitro* studies suggest that the spinal expression of GFAP observed in the current study was likely a consequence of reduced extracellular glutamate resulting from the upregulation of GLT-1 (Bachetti et al. 2010, Beller et al. 2011, Lee et al. 2008). Contradicting this hypothesis, however, is the 150 $\mu$ g dose of ceftriaxone, had no effect on spinal GFAP expression, but did restore the expression of GLT-1 in the dorsal horn (Figs. 6.1 & 6.6). To date, no study has *directly* compared the dose-response of ceftriaxone on the promoter activities of GLT-1 and GFAP promoter activity. Future *in vitro* studies that further define ceftriaxone-mediated NF $\kappa$ B modulation of GLT-1 and GFAP may provide additional insight into the differential effects of ceftriaxone on spinal GFAP that were observed in the current study (Fig. 6.6).

The concentration of extracellular glutamate in the central nervous system is a function of its release by neurons and its uptake by glutamate transporters (Tao et al. 2005). The present study demonstrated that an increase in spinal GLT-1 alleviates nerve root-mediated pain (Figs. 6.2 & 6.4), presumably by decreasing extracellular glutamate in the spinal cord (Haugeto et al. 1996, Inquimbert et al. 2012, Lipski et al. 2007, Ramos et al. 2010). Spinal glutamate levels are also reduced by blocking its release from pre-synaptic neurons using sodium-channel inhibitors (Blackburn-Munro et al. 2002,

Lamanauskas & Nistri 2008, MacIver et al. 1996). Because the present study abolished mechanical allodynia and thermal hyperalgesia by increasing spinal GLT-1, blocking pre-synaptic glutamate release may also alleviate behavioral sensitivity after a painful nerve root compression. To test this hypothesis, the studies in Chapter 7 administer the sodium channel blocker, Riluzole (Kuo et al. 2006, Lamanauskas & Nistri 2008, Staffstrom et al. 2007, Wang et al. 2004), to test whether reducing spinal glutamate by blocking its release also attenuates behavioral sensitivity in this model of cervical radiculopathy.

---

## CHAPTER 7

# Riluzole Treatment of Nerve Root-Mediated Pain

---

*Parts of this chapter have been adapted from:*

Nicholson KJ, Zhang S, Gilliland TM, Winkelstein BA. “Riluzole abolishes behavioral sensitivity & prevents the development of axonal damage and spinal modifications that are evident after painful nerve root compression,” *submitted*.

### 7.1 Overview

Neck pain is often attributed to an injury of the cervical roots (Abbed & Couman 2002, Carette & Fehlings 2005, Krivickas & Wilbourn 2000, Wainner & Gill 2000). Mechanical compression to the nerve root reduces axonal flow and induces degeneration of the primary afferents in both rodent and canine models (Hubbard & Winkelstein 2008, Kobayashi et al. 2005a). Riluzole, an FDA-approved drug for the treatment of the neurodegenerative disease, amyotrophic lateral sclerosis (ALS), inhibits the loss of motor function and the development of spinal motor neuron degeneration that are associated with that disease (Bellingham 2011, Doble 1996). Riluzole has also been shown to inhibit neurodegeneration, promote normal motor function and mitigate behavioral sensitivity in animal models after spinal cord trauma, ventral nerve root avulsion and chronic constriction of the sciatic nerve (Coderre et al. 2007, Hama & Sagen 2011, Pintér et al. 2010, Schwartz & Fehlings 2001, Sung et al. 2003, Wu et al. 2013). Like the

dorsal nerve root, peripheral nerves enclose primary afferents (Basbaum et al. 2009). However, the regenerative properties of the distal axons in peripheral nerve differ from those of the central axons in the nerve root (Di Maio et al. 2011, Jancalek & Dubovy 2007). No study has determined whether Riluzole's effects on pain from neural tissue pathologies in the periphery (Coderre et al. 2007, Sung et al. 2003) are also effective in mitigating pain mediated by a compression injury to the axons of the nerve root.

Riluzole alleviates behavioral sensitivity even when it is administered after pain develops in rodent models of spinal cord trauma and sciatic nerve compression (Hama & Sagen 2011, Sung et al. 2003). However, Riluzole's ability to attenuate behavioral sensitivity after it is already established has only been evaluated for up to 48 hours after treatment (Sung et al. 2003). Because Riluzole has a half-life of up to 31 hours in the rat (Wu et al. 2013) it is not known whether Riluzole can continue to alleviate pain long after it is cleared from the spinal cord. A single dose of Riluzole immediately after spinal cord compression improves motor function, reduces spinal cord tissue loss and preserves axonal transport in the descending pathways of the spinal cord for at least six weeks (Schwartz & Fehlings 2011). Therefore, a single dose of Riluzole within minutes of injury appears to be sufficient to provide lasting neuroprotection for at least six weeks (Schwartz & Fehlings 2011). However, that study did not determine whether a single dose of Riluzole can simultaneously alleviate persistent behavioral sensitivity and limit the development of neuropathology if behavioral sensitivity is already established before Riluzole is administered.

The work in this chapter correspond to Aims 3a and 3c of the overall thesis and evaluate the analgesic and neuroprotective properties of a single dose of Riluzole that is

administered after the initiation of nerve root-mediated pain. The studies detailed here test the hypothesis that Riluzole can alleviate nerve root-mediated pain by reducing the neuropathology that normally develops in the nerve root after a root compression (Kobayashi et al. 2005a, Hubbard & Winkelstein 2008, Nicholson et al. 2011). Behavioral sensitivity was measured for seven days to evaluate the time-course of mechanical allodynia and thermal hyperalgesia for six days after treatment. The studies in Chapters 3 and 5 demonstrate that extensive axonal damage develops in the nerve root and that the excitability of dorsal horn neurons in the spinal cord is enhanced at day 7 after a painful nerve root compression (Nicholson et al. 2011). Therefore, in order to evaluate the neuroprotective properties of Riluzole after a painful C7 nerve root compression in the rat, neuropathology in the root and neuronal excitability in the spinal cord were both evaluated at day 7. Neuropathology was assessed by evaluating the morphology of the myelinated and unmyelinated axons in the root and also by assessing axonal transport through the root. Myelinated axons were labeled for NF200, while the unmyelinated axons were labeled for calcitonin-gene related peptide (CGRP) and isolectin-B4, labeling the peptidergic and nonpeptidergic populations, respectively. The spinal expression of CGRP was also quantified in order to evaluate axonal transport of this neuropeptide through the root, which is normally impaired after a painful nerve root compression (Hubbard et al. 2008a).

## 7.2 Relevant Background

Neck pain affects nearly one-half of the adult population annually (Côté et al. 2004, Hogg-Johnson et al. 2008). Injury to the cervical nerve root is a common source of pain and can result from disc herniation, spinal stenosis or neck trauma (Abbed & Coumans 2007, Carette and Fehlings 2005, Krivickas et al. 2008, Wainner & Gill 2000). In animal models of root compression, axonal degeneration develops in the root and extends towards the synapses in the dorsal horn, where axon terminals become enlarged and neurotransmitter levels are altered (Hubbard et al. 2008a, Hubbard & Winkelstein 2008, Kobayashi et al. 2008). Although these spinal modifications that are documented after painful root compression suggest that injury may mediate afferent signaling, the signaling properties of spinal neurons have not been evaluated after a painful nerve root compression.

Neuronal hyperexcitability is associated with neural tissue damage, including axonal injury – a hallmark of nerve root compression injuries – and altered phenotypic behavior in the spinal cord (Hubbard & Winkelstein 2008, Inquimbert et al. 2012, Kobayashi et al. 2008, Neugebauer et al. 1996). Sensitization of wide dynamic range (WDR) neurons, in particular, is thought to drive neuronal hyperexcitability and behavioral sensitivity after spinal cord ischemia and spinal nerve ligation (Hao et al. 1992, Liu et al. 2011). Although increased calcitonin gene-related peptide (CGRP) and associated signaling contribute to neuronal hyperexcitability after painful neural trauma (Bennett et al. 2000, Neugebauer et al. 1996), painful root compression decreases CGRP in the superficial dorsal horn (Hubbard et al. 2008a, Kobayashi et al. 2005a). No study



has evaluated CGRP expression in the deep laminae, despite the known involvement of neurons in that region of the dorsal horn in pain from peripheral nerve injuries (Chao et al. 2008, Kerr & David 2007).

Riluzole is an anticonvulsant that has neuroprotective properties in animal models of neurodegenerative disease and neural tissue injury, which are attributed to its inhibition of presynaptic glutamate release by blocking voltage-gated sodium channels (Bellingham 2011, Coderre et al. 2007, Doble 1996, Jehle et al. 2000, Siniscalchi et al. 1997). Riluzole decreases the size of spinal cord lesions, promotes motor function recovery, and restores the electrophysiological properties of spinal neurons after spinal cord compression (Schwartz & Fehlings 2001, Stutzmann et al. 1996, Wu et al. 2013). It also mitigates axonal degeneration and promotes axonal regeneration after nerve injury (Costa et al. 2007, Pintér et al. 2010, Vorwerk et al. 2004). Those studies suggest that Riluzole may inhibit the axonal degeneration that is induced after a painful root compression (Hubbard & Winkelstein 2008, Nicholson et al. 2011). Although regeneration of dorsal roots after their crush injury restores normal sensation (Ramer et al. 2000) and Riluzole is anti-allodynic for neuropathic pain (Coderre et al. 2007, Sung et al. 2003), it is not known if, and to what extent, Riluzole may preserve the normal axonal structure and afferent signaling and alleviate the pain that develops after compression of the nerve root. It is also unclear whether a single dose of Riluzole is sufficient to provide sustained pain relief when administered early after pain has developed (Hama & Sagen 2011).

This study investigates whether a single dose of Riluzole can eliminate behavioral sensitivity and axonal damage in the injured root, as well as prevent the spinal changes

that develop after a painful root compression. We hypothesized that Riluzole would abolish behavioral sensitivity by preserving axonal morphology and would abate the spinal modifications of CGRP and neuronal excitability that are observed after painful root compression. Mechanical allodynia and thermal hyperalgesia were assessed after injury, with and without Riluzole treatment, or a sham surgical procedure. The morphology of myelinated, peptidergic and nonpeptidergic axons in the root and spinal CGRP were evaluated at day 7 using immunohistochemistry. At that same time-point, electrophysiological recordings were made in the spinal cord to evaluate the effect of Riluzole on neuronal firing evoked by peripheral stimuli to the paw after a painful root compression.

### **7.3 Methods**

All studies used male Holtzman rats (300-400g; Harlan Sprague–Dawley; Indianapolis, IN). Rats were housed in a 12-12 hour light-dark cycle and given free access to food and water. Studies were approved by our Institutional Animal Care and Use Committee and carried out under the guidelines of the Committee for Research and Ethical Issues of the International Association for the Study of Pain (Zimmermann 1983).

#### **7.3.1 Surgical Procedures & Riluzole Administration**

The C7 dorsal nerve root was compressed under isoflurane inhalation anesthesia (4% for induction, 2% for maintenance). The rat was placed in a prone position and an incision was made along the midline over the cervical spine from the base of the skull to

the spinous process of the second thoracic vertebra (Hubbard & Winkelstein 2005, Nicholson et al. 2011, Rothman et al. 2005, Rothman et al. 2010). The C6 and C7 vertebrae were exposed by carefully separating the overlying musculature and a hemilaminectomy and partial facetectomy on the right side were performed at C6/C7 to expose the right C7 nerve root. A small incision was made in the dura over the C7 nerve root and a 10gf microvascular clip (World Precision Instruments; Sarasota, FL) was placed on the dorsal root for 15 minutes and then removed. A surgical control group received sham procedures, which included all of the same procedures as the surgical manipulation and nerve root exposures, but without any compression applied. Wounds were closed using 3-0 polyester sutures and surgical staples and rats were monitored while they recovered in room air.

On day 1 after compression, rats were randomly assigned to receive either Riluzole or its vehicle carrier. The Riluzole treatment group (*inj+Ril*; n=7) received a 1ml intraperitoneal (i.p.) injection of 3mg/kg Riluzole (Sigma; St. Louis, MO) dissolved in the vehicle 10%  $\beta$ -cyclodextrin (Sigma; St. Louis, MO). In the group receiving vehicle treatment (*inj+veh*; n=7), a 1ml injection of 10%  $\beta$ -cyclodextrin dissolved in saline was given. The same vehicle treatment was also given on day 1 to the rats that had received a sham surgery (*sham+veh*; n=7). All injections were administered after behavioral assessments were performed on day 1.

### **7.3.2 Behavioral Assessments**

Bilateral mechanical allodynia and thermal hyperalgesia were assessed in the forepaw as measures of behavioral sensitivity. Mechanical allodynia was measured prior

to (baseline) and on post-injury days 1, 2, 3, 5, and 7 (Hubbard & Winkelstein 2005, Rothman et al. 2005). After a 20 minute period of acclimation, the 1.4, 2.0 and 4.0gf von Frey filaments (Stoelting Co.; Wood Dale, IL) were each applied to the plantar surface of each forepaw 10 times, in three rounds, separated by 10 minutes of rest between rounds. For each filament, the total number of paw withdrawals for each forepaw and for each rat was summed for the three rounds on each day and averaged across groups.

Thermal hyperalgesia was measured at baseline and on days 1 and 7 using established methods (Dirig et al. 1997, Hargreaves et al. 1988). After a 20 minute acclimation period, the thermal stimulus was focused on the plantar surface of each forepaw using a radiant heat source until a withdrawal response was provoked. A positive response was taken if the withdrawal was a sudden and quick movement and/or the rat licked, shook, curled or looked at the paw. The time period during which the thermal stimulus was applied to the forepaw until a positive response was observed was recorded as the withdrawal latency. On each testing day, the withdrawal latency time was measured for each forepaw three times, separated by 10 minutes of rest. For each forepaw, the average latency across the rounds for each day was recorded for each rat and averaged for each group. For each behavioral assessment (mechanical allodynia, thermal hyperalgesia), a two-way repeated measures ANOVA tested for differences between groups over time for the ipsilateral and contralateral forepaws, separately. To determine differences between groups at each day, separate one-way ANOVAs with post-hoc Bonferroni correction were performed, with significance for all tests at  $p < 0.05$ .

### 7.3.3 Immunohistochemistry

The dorsal nerve root and spinal cord at C7 were harvested on day 7 after behavioral testing to assess axonal morphology in the ipsilateral nerve root and bilateral expression of CGRP in the superficial and deep laminae of the dorsal horn. Rats were anesthetized via an intraperitoneal injection of 65mg/kg pentobarbital and transcardially perfused with 200ml Dulbecco's PBS followed by 300ml of 4% paraformaldehyde. The C7 cervical spinal cord and adjacent nerve roots were harvested, post-fixed overnight, transferred to 30% sucrose for cryoprotection and then embedded in OCT media (Sakura Finetek USA, Inc.; Torrance, CA). Samples were cryosectioned at 14 $\mu$ m, such that the spinal cord tissue was sectioned axially and the adjacent nerve roots were sectioned along their longitudinal axis, and thaw-mounted onto slides. Each slide contained six non-adjacent sections spanning a region at the centerline of the nerve root. For comparison, matched tissue samples also were harvested from normal, naïve rats (n=2) and included in tissue processing.

Sections were colabeled for neurofilament-200 (NF200), CGRP and isolectin-B4 (IB4) to label myelinated, peptidergic and non-peptidergic neurons, respectively. Sections were blocked in 10% normal goat serum (Vector Laboratories; Burlingame, CA) with 0.3% Triton-X100 (Bio-Rad Laboratories; Hercules, CA) then incubated overnight at 4°C in mouse anti-NF200 (1:500; Sigma; St. Louis, MO), rabbit anti-CGRP (1:1000; Peninsula Laboratories; Sancarlos, CA) and biotinylated IB4 (5 $\mu$ g/ml; Sigma; St. Louis, MO). Sections were then fluorescently labeled with secondary antibodies for goat anti-mouse Marina Blue (1:200; Invitrogen; Carlsbad, CA), goat anti-rabbit Alexa Fluor 546

(1:1000; Invitrogen; Carlsbad, CA) and fluorescein (DTAF) conjugated streptavidin (1:500; Jackson ImmunoResearch, Inc.; West Grove, PA), respectively.

Axonal morphology in the affected nerve root was evaluated by digitally imaging NF200, CGRP, and IB4 in the root at 200x (3-6 sections per sample). Two independent reviewers who were blinded to the sample groups assessed the extent of axonal abnormalities for each of the types of labeled axons, separately, using customary methods (Hubbard & Winkelstein 2008, Nicholson et al. 2011, Serbest et al. 2007, Singh et al. 2006). Nerve roots that did not differ from normal uncompressed roots were assigned (-), indicating the absence of axonal pathology. Nerve roots that contained any evidence of axonal swelling or discontinuous labeling were assigned a positive (+) score. If the abnormalities extended across the entire length of the root, that section was assigned a positive score of (++), indicating extensive damage. For each rat, the ratings were averaged across the tissue sections, and between both reviewers, such that each nerve root was assigned a single score on a five-point scale: (-), (-/+), (+), (+/++) or (++).

Axonal transport to the spinal cord was evaluated by quantifying the CGRP labeling in uniform sized regions of interest (ROI) in the superficial and deep laminae of the dorsal horn. The dorsal horn was imaged at 200x (ROI of 1360x1024 pixels) and images were separately cropped over the superficial laminae (I-II; ROI of 750x150 pixels) and deeper laminae (IV-V; ROI of 696x380 pixels) in the ipsilateral and contralateral dorsal horns, separately. CGRP expression was measured in at least three sections from each rat using quantitative densitometry and reported as a percent of the expression in normal tissue (Abbadie et al. 1996, Kerr & David 2007, Romero-Sandoval et al. 2008, Rothman et al. 2010). Differences in the expression of CGRP between groups

in the superficial and deep laminae were tested by separate mixed-effect ANOVAs with sections nested by rat and rats nested within groups for the ipsilateral and contralateral dorsal horns, separately. Differences between the groups were determined by post-hoc Tukey HSD tests.

#### **7.3.4 Electrophysiology**

In a separate group of rats, neuronal hyperexcitability was measured in the deep laminae of the spinal cord at day 7. Rats underwent a C7 nerve root compression or sham procedure and were assigned to the same treatment paradigms as described above (n=7 per group): *inj+Ril*, *inj+veh* or *sham+veh*. Bilateral mechanical allodynia was measured in the forepaws before injury (baseline) and on day 7, using stimulation by 1.4, 4.0 and 10.0gf von Frey filaments, as described above. For each filament, a one-way ANOVA with post-hoc Bonferroni correction tested for differences in response between groups for the ipsilateral and contralateral forepaws, separately. A t-test compared the number of paw withdrawals elicited by the 4.0gf filament between each group used for this electrophysiological study and the matched group in the immunohistochemistry study (Section 7.3.1) to test that the studies used comparable injury and behavioral conditions.

Following behavioral testing on day 7, rats were anesthetized with 45mg/kg pentobarbital via i.p. injection. Adequate anesthesia was confirmed by a hind paw pinch and was maintained with an additional dose of pentobarbital (1-5mg/kg i.p.) given approximately every 40-50 minutes, or as needed. The cervical spine was re-exposed via a dorsal, midline incision and any scar tissue that formed over the right C6/C7 spinal cord from the initial surgery was carefully removed. A laminectomy removed any remaining

bone at C6 and C7 on the left side to fully expose the spinal cord at those levels and the dura was then removed. The rat was placed on a stereotaxis frame using bilateral ear bars and a clamp on the spinous process of T2. Mineral oil was applied to the spinal cord to maintain hydration. A thoracotomy was performed to minimize spinal cord motion associated with normal breathing and respiration was maintained by mechanical ventilation via a mid-cervical tracheotomy (40-50 cycles/min; Harvard Small Animal Ventilator Model 683; Harvard Apparatus; Holliston, MA) (Crosby et al. 2013). Expired CO<sub>2</sub> concentration was continuously monitored (Capnogard; Novamatrix Medical Systems; Wallingford, CT) and the core body temperature was maintained between 35-37°C using a heat plate and a rectal probe (TCAT-2DF; Physitemp Instruments Inc.; Clifton, NJ).

Extracellular spinal cord recordings were acquired using a glass-insulated tungsten probe (<1µm tip; FHC; Bowdoin, ME) inserted vertically into the dorsal spinal cord proximal to the site where the C7 nerve root exits the spinal cord. In order to measure action potentials evoked by mechanical stimuli to the ipsilateral forepaw, the probe was placed proximal to the ipsilateral (right) C7 nerve root. Likewise, the probe was placed proximal to the contralateral (left) C7 nerve root to record action potentials evoked by mechanical stimulation to the contralateral forepaw. The signal was amplified with a gain of 3000 (ExAmp-20KB; Kation Scientific, Inc.; Minneapolis, MN), processed with a 60Hz noise eliminator (Hum Bug; Quest Scientific; North Vancouver, BC) and digitally stored at 25kHz (MK1401; CED; Cambridge, UK). Mechanoreceptive neurons innervating the forepaw were searched for by lightly brushing the plantar surface of the forepaw and slowly advancing the probe through the deep laminae (400-1000µm below



the pial surface) until a neuron responsive to the light brushing was found (Crosby et al. 2013, Hains et al. 2003, Quinn et al. 2010). Once a neuron was identified, a sequence of six mechanical stimuli was applied to the forepaw: (1) 10 light brush strokes with a brush applied over 10 seconds, (2-5) a series of four von Frey filaments (1.4, 4.0, 10.0, 26.0gf), each applied five times for 1 second with a 1-second rest between application, and (6) a 10-second, 60gf pinch by a microvascular clip (Roboz, Inc.; Gaithersburg, MD) (Quinn et al. 2010). There was 60 seconds of rest between applications of each of the different stimuli.

Voltage recordings were spike-sorted in Spike2 (CED; Cambridge, UK) to count the number of action potentials evoked by each stimulus for individual neurons. For the brush stimulus, the number of action potentials was summed over the period of light brushing. For each von Frey filament application, the number of action potentials was summed over both the stimulation period and the rest period that immediately followed. For both the brush and the von Frey filament stimuli, the baseline number of spikes occurring in the 10-second period prior to the first stimulation was subtracted from the spike counts to identify only the spikes evoked by those stimuli (Hains et al. 2003). For the 60gf pinch, the number of spikes was summed over the 5-second period between 3-8 seconds after the clip was applied, in order to only consider those spikes evoked by the pinch and to exclude the spikes evoked by the application and removal of the clip. The number of spikes evoked by the clip stimulus was determined by subtracting the baseline number of spikes that occurred in the 5-second window prior to the first stimulation from the spike count. For statistical analysis, the spike count was log-transformed because of a positive-skew in the distribution of data that is common with these experiments (Quinn et

al. 2010). Separate mixed-effect one-way ANOVAs with Tukey HSD post-hoc tests compared differences in the number of action potentials that were evoked by each filament between groups for the ipsilateral and contralateral neurons, separately; neurons were nested within rats and rats were nested in groups. A mixed-effect one-way ANOVA with the same levels of nesting tested for differences between groups for the depth at which the neurons were recorded from.

Neurons were classified as either wide dynamic range (WDR) or low-threshold mechanoreceptive (LTM) neurons by comparing the spike rate (spikes/sec) evoked by the light brushing and the 60gf clip stimuli (Hains et al. 2003, Laird & Bennett 1993, Saito et al. 2008). Neurons that responded maximally to the light brush were identified as LTM and those that responded in a graded manner were identified as WDR (Hains et al. 2003, Woolf & Fitzgerald 1983). The distribution of WDR and LTM neurons between groups was compared using Pearson's chi-squared tests for the ipsilateral and contralateral neurons, separately. All electrophysiology data are expressed as the mean $\pm$ SEM.

## 7.4 Results

Sustained behavioral sensitivity is attenuated within one day after a single i.p. injection of Riluzole (Fig. 7.1 & 7.2). There is a significant difference ( $p < 0.001$ ) in the number of ipsilateral paw withdrawals in response to the 2.0 and 4.0gf mechanical stimuli between the groups over time (Fig. 7.1). At day 1, the number of paw withdrawals elicited by the 2.0 and 4.0gf in the ipsilateral forepaw is significantly ( $p < 0.004$ ) elevated over sham responses for both groups undergoing a nerve root compression (*inj+veh*,

*inj+Ril*). However, at day 2 after compression, the number of paw withdrawals elicited by the 4.0gf is reduced to sham levels with Riluzole treatment (Fig. 7.1), which is a significant decrease compared to injury with vehicle treatment ( $p=0.014$ ). The number of paw withdrawals in the *inj+veh* group remains significantly greater than both the *inj+Ril* and *sham+veh* groups at all time points after day 1 ( $p<0.003$ ), for testing with the 4.0gf filament. For testing with the 2.0gf filament, the number of paw withdrawals elicited in the *inj+Ril* is significantly less ( $p=0.034$ ) than the *inj+veh* group only on day 5. There are no differences between the *sham+veh* and *inj+Ril* groups at any time point after treatment on day 1, for testing with both the 2.0 and 4.0gf filaments (Fig. 7.1). No differences were detected between any group for testing with the 1.4gf filament. In the contralateral forepaw, there were no differences in the number of paw withdrawals between any group for any filament strength. Appendix C details the number of paw withdrawals elicited by each filament for each rat in this study.

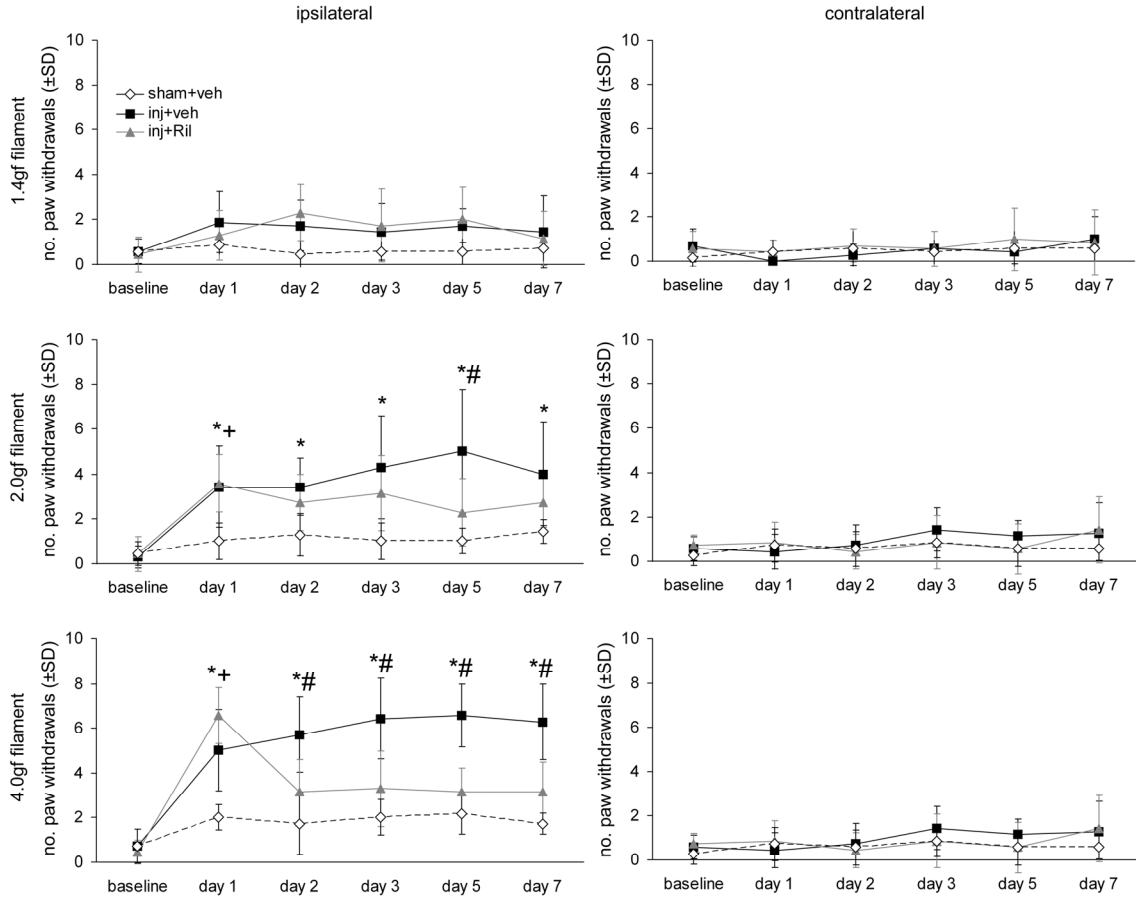


**Fig. 7.1** Mechanical allodynia tested with the 1.4, 2.0 and 4.0gf filaments after nerve root compression with and without Riluzole treatment in the ipsilateral and contralateral forepaws. Prior to treatment (day 1), mechanical allodynia is significantly greater than sham (*sham+veh*) in both the vehicle-treated (*inj+veh*; \*) and Riluzole-treated (*inj+Ril*; +) root compression groups, for testing with the 2.0 and 4.0gf filaments. For those same filaments, mechanical allodynia remains significantly greater in the *inj+veh* group than the *sham+veh* (\*) group but is also increased over the treatment group (*inj+Ril*; #) for all subsequent days for testing with the 4.0gf filament. No differences are detected between any group for testing with the 1.4gf filament or in the contralateral forepaw for any filament strength.

Similarly, Riluzole also attenuates the thermal hyperalgesia that is evident after a nerve root compression (Fig. 7.2). At day 1, the withdrawal latency in the ipsilateral forepaw for both of the nerve root compression (*inj+Ril* & *inj+veh*) groups is significantly ( $p < 0.025$ ) shorter than that of sham (Fig. 7.2). After Riluzole is given, however, the withdrawal latency at day 7 in the injury group ( $6.6 \pm 0.9$  seconds; *inj+veh*) is significantly shorter than the withdrawal latency for either the Riluzole treatment group

( $8.3 \pm 1.2$  seconds; *inj+Ril*;  $p=0.044$ ) or the sham group ( $9.6 \pm 1.3$  seconds; *sham+veh*;  $p=0.001$ ) groups (Fig. 7.2). There is no difference in latency between the *inj+Ril* and *sham+veh* groups at day 7 (Fig. 7.2). There are no differences latency time in the contralateral forepaw between any group (Fig. 7.2). The withdrawal latency recorded for each rat is summarized in Appendix C.

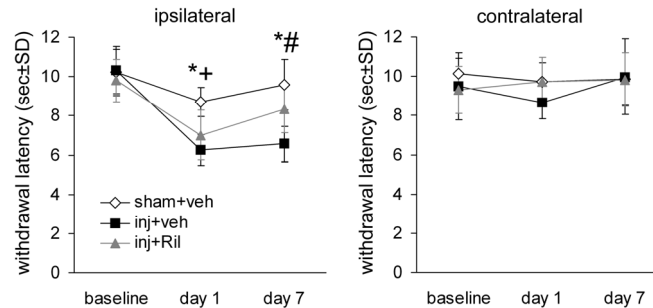


**Fig. 7.2** Thermal hyperalgesia after nerve root compression with and without Riluzole treatment in the ipsilateral and contralateral forepaws. At day 1, the withdrawal latency from a thermal stimulus significantly decreases in both compression groups (*inj+veh*; \*, *inj+Ril*; +) compared to *sham+veh*. After treatment, the withdrawal latency at day 7 is significantly less for *inj+veh* than both *inj+Ril* (#) and *sham+veh* (\*). No differences are detected in the contralateral forepaw for any group.

Riluzole treatment after a painful nerve root compression partially prevents the axonal swelling, thinning of the myelinated axons and axon disorganization in the nerve root that is typically evident at day 7 after a painful root compression (Fig. 7.3 & Table 7.1). The nerve root for one sample in the *inj+veh* group (#157) was damaged at the time of harvest so it was not evaluated (Table 7.1). After a painful nerve root compression, there are regions of discontinuous NF200 immunoreactivity along the length of the nerve root (Fig. 7.3). Axonal swelling is also evident for all three types of labeled axons (Fig. 7.3), such that the diameter of the axons labeled for NF200, CGRP, and IB4 varies along the length of the root (Fig. 7.3). In the nerve roots harvested from three rats in the vehicle-treated injury group (#156, #163, #198), axonal injury extends across the

majority of the root in at least two of the three types of labeled axons (Table 7.1). In contrast, the NF200-labeled axons remain uniform in diameter along the length of the root and are evenly distributed along the width of the root in the *sham+veh* group (Fig. 7.3). The unmyelinated axons (CGRP & IB4) are also uniform in their distribution within the root and are noticeably smaller in diameter than the myelinated axons (NF200). Although there is some evidence of axonal swelling in some of the axons of some of the rats in the *inj+Ril* group, the diameter of the axons remains relatively consistent across the length of the root (Fig. 7.3). Furthermore, only one root (#161) exhibits substantial axonal damage across the entire length of the root, and only in the NF200-labeled axons (Table 7.1). In two of the nerve roots in the *inj+Ril* group (#149, #160) there is no indication of injury in any of the NF200-, CGRP- or IB4-labeled neurons (Table 7.1).

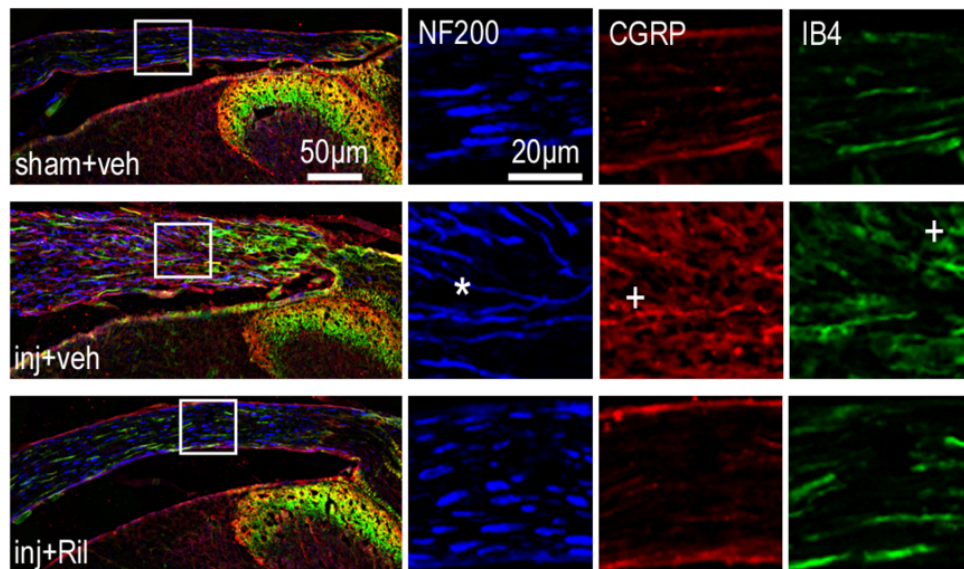


**Fig. 7.3** Representative images of C7 nerve roots labeled for myelinated (NF200), peptidergic (CGRP) and nonpeptidergic (IB4) axons at day 7 for *sham+veh*, *inj+veh*, or *inj+Ril*. The region within the box is enlarged to show each of the three labels separately for clarity. After sham, axons are evenly labeled for NF200, CGRP and IB4 and are uniformly distributed throughout the root. After a painful root compression (*inj+veh*), axons exhibit regions of swelling (+) and the NF200-labeled axons, in particular, appear to thin (\*). These hallmarks are not evident in the *inj+Ril* group, which exhibits characteristics similar to sham.

**Table 7.1** Summary of the NF200, CGRP, and IB4 ratings.

Group	ID	NF200	CGRP	IB4
sham+vehicle	162	-	-	-
	193	-	-	-
	195	-	-	-/+
	196	-	-	-
	200	-	-	-
	211	-	-	-
	212	-	-	-
	inj+vehicle	156	+ /+++	+
157		*	*	*
163		+ /+++	+	++
194		+	+	+
198		++	+ /+++	+ /+++
199		- /+	+	- /+
210		- /+	- /+	-
inj+Riluzole		147	- /+	+
	148	+	+	+
	149	-	-	-
	158	- /+	- /+	-
	159	+	- /+	+
	160	-	-	-
	161	+ /+++	+	+

- No abnormalities  
+ Regions of axons exhibit abnormalities  
++ Abnormalities across most of the root  
\* No data due to damaged specimen

Similar to the neuroprotective effects of Riluzole on nerve root morphology that are observed at day 7 (Fig. 7.3 & Table 7.1), the expression of CGRP in the ipsilateral superficial laminae of the spinal cord is increased and the expression of this neurotransmitter in the deep laminae of the ipsilateral dorsal horn is reduced with Riluzole treatment (Fig. 7.4). CGRP expression in the dorsal horn of the *inj+veh* group is significantly decreased ( $p=0.009$ ) in the superficial laminae compared to the sham group (Fig. 7.4B). In the deep laminae, CGRP significantly increased ( $p=0.003$ ) after compression (*inj+veh*) compared to the *sham+veh* group (Fig. 7.4C). With Riluzole

treatment, however, there are no differences in the expression of CGRP in either the superficial or deep laminae compared to either the *sham+veh* or the *inj+veh* groups (Fig. 7.4). CGRP expression in the contralateral dorsal horn is unchanged from *sham+veh* for both the *inj+veh* and *inj+Ril* groups in both the superficial and deep laminae (Fig. 7.4). In Appendix D, the quantification of CGRP in the superficial and dorsal laminae for each rat is provided.

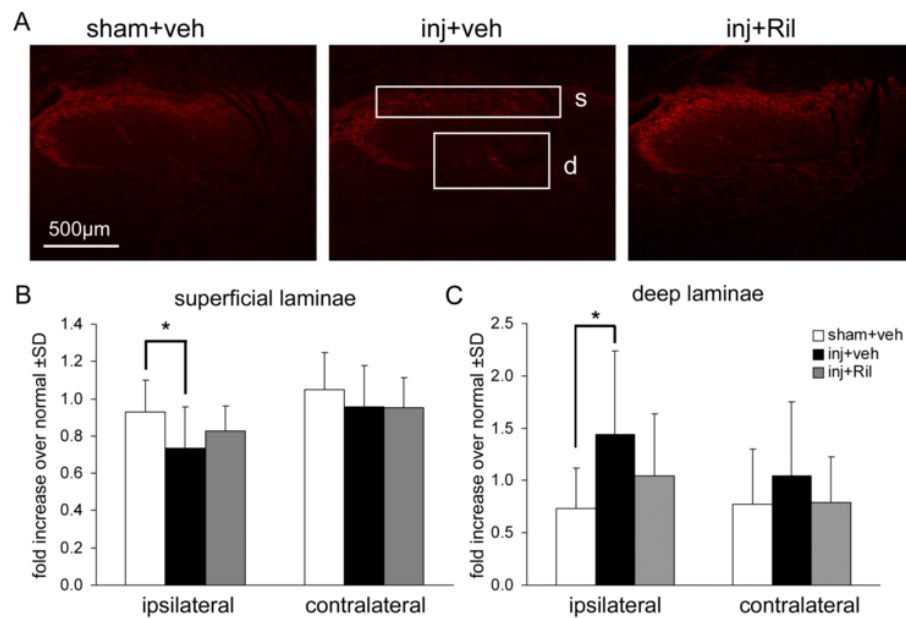


**Fig. 7.4** CGRP expression in the dorsal horn at day 7. **(A)** Representative images of CGRP-labeled dorsal horns in the ipsilateral superficial (s) and deep (d) laminae after sham (*sham+veh*), nerve root compression with vehicle (*inj+veh*) and with Riluzole (*inj+Ril*). **(B-C)** Quantification of CGRP labeling demonstrates that nerve root compression significantly (\*) decreases only in the ipsilateral superficial dorsal horn **(B)** and increases only in the ipsilateral deep dorsal horn **(C)** after a painful nerve root compression compared to sham, but is not changed from sham with Riluzole treatment.

Riluzole also abates the hyperexcitability of the deep dorsal horn neurons that is observed in the ipsilateral spinal cord following a painful nerve root compression. Similar to the lack of mechanical allodynia observed in the ipsilateral forepaw at day 7 after Riluzole treatment (Fig. 7.1), the number of paw withdrawals elicited by the 4.0 and



10.0gf filaments is also decreased compared to vehicle treatment (Fig. 7.5A). No significant differences are observed between any groups for testing with the 1.4gf filament in the ipsilateral forepaw (Fig. 7.5A) or for testing with any filament strength in the contralateral forepaw (Fig. 7.5B).

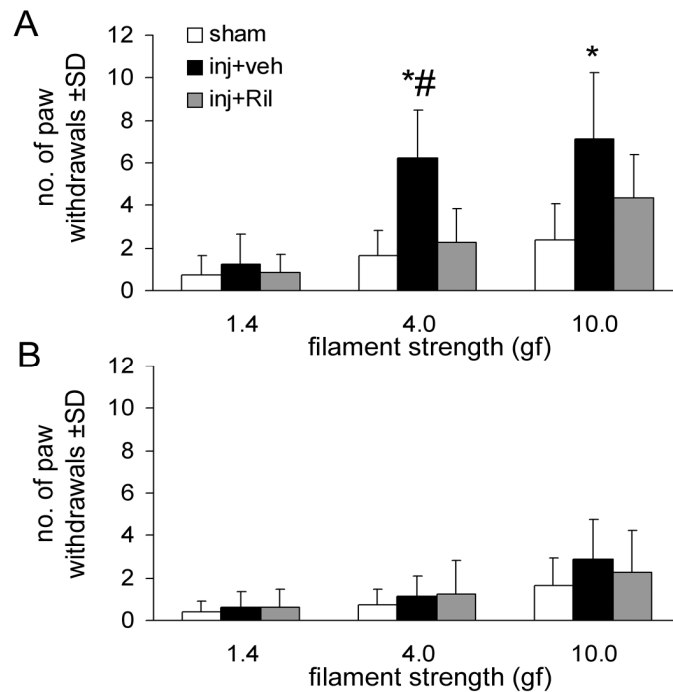


**Fig. 7.5** Bilateral mechanical allodynia at day 7 for testing with the 1.4, 4.0 and 10.0gf filaments. **(A)** The number of paw withdrawals in the ipsilateral forepaw is significantly increased ( $p < 0.002$ ) in the *inj+veh* group compared to *sham+veh* (\*; for 4.0 and 10.0gf filaments) and *inj+Ril* (#; 4.0gf). **(B)** Contralateral allodynia is unchanged from *sham+veh* for both the *inj+veh* and *inj+Ril* groups.

Extracellular recordings were made from 215 neurons at an average depth of  $640 \pm 140 \mu\text{m}$  and no significant differences are detected in the recording depth between groups. The depth of recording, the number of evoked spikes and the phenotype of each neuron is summarized in Appendix E. The number of spikes evoked by each of the 4.0, 10.0 and 26.0gf filaments in the *inj+veh* group significantly increases ( $p < 0.045$ ) by nearly two-fold over the number of spikes evoked for *sham+veh* (Fig. 7.6B). After

Riluzole treatment, the spike counts decrease to sham levels for each filament (Fig. 7.6B). Specifically, for stimulation with the 4.0gf filament, the number of spikes in the *inj+veh* group ( $19\pm 4$  spikes) is significantly greater than the number evoked in the *sham+veh* group ( $11\pm 2$ ;  $p=0.0337$ ) and the *inj+Ril* group ( $12\pm 2$ ;  $p=0.0421$ ) (Fig. 7.6). No differences are detected in the number of spikes evoked by the 1.4gf filament between any of the groups. Regardless of the filament strength, no differences are detected in the number of evoked spikes in the contralateral spinal cord between any of the groups (Fig. 7.6C).

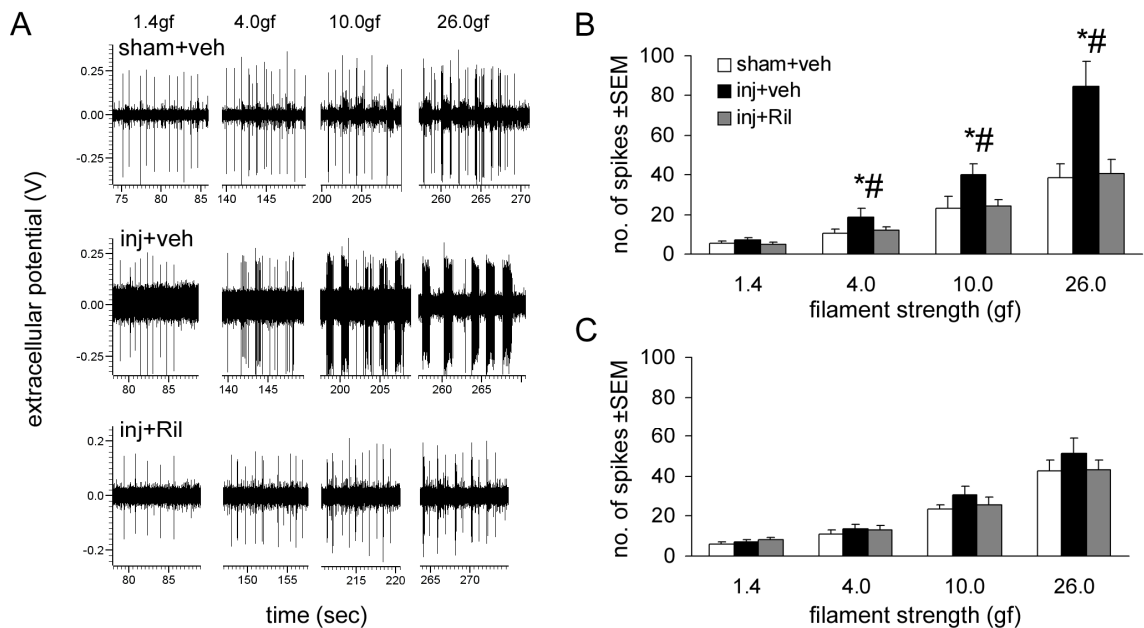


**Fig. 7.6** Neuronal excitability at day 7 in the spinal cord. **(A)** Representative extracellular recordings for each group during the 1.4, 4.0, 10.0 and 26.0gf filament stimuli applied to the ipsilateral forepaw. **(B)** Neuronal excitability in the ipsilateral dorsal horn is significantly elevated in the *inj+veh* group compared to both *sham+veh* (\*) and *inj+Ril* (#) in response to paw stimulation by the 4.0, 10.0 and 26.0gf filaments. **(C)** In the contralateral dorsal horn, the number of evoked spikes is unchanged between all groups.

Riluzole treatment reduces the number of WDR neurons in the ipsilateral deep dorsal horn (Table 7.2). A total of 147 WDR neurons and 68 LTM neurons were identified in all groups. In the ipsilateral dorsal horn, there is a significantly greater proportion of WDR neurons (83%) in the *inj+veh* group than the *sham+veh* (61%;  $p=0.030$ ) and *inj+Ril* groups (61%;  $p=0.042$ ) (Table 7.2). The distribution of the neuron phenotypes in the contralateral dorsal horn is unchanged across all groups (Table 7.2). In general, the WDR neurons respond to the light brush and noxious pinch in a graded manner. The frequency of evoked firing to the light brush in the WDR and LTM neurons is  $2.7\pm 0.8$  spikes/sec and  $2.0\pm 0.7$  spikes/sec, respectively, and not different between the two neuron populations. During the noxious pinch, however, there is a significant increase ( $p<0.042$ ) in the frequency of evoked firing by the WDR neurons compared to the LTM neurons (Fig. 7.7). Specifically, the frequency of evoked firing in the WDR neurons ( $5.7\pm 3.5$  spikes/sec) is more than three times the frequency of evoked firing in LTM neurons ( $1.7\pm 1.5$  spikes/sec) (Fig. 7.7).

**Table 7.2** Distribution of WDR and LTM neuron

location	group	neuron phenotype distribution (%)	
		WDR	LTM
ipsilateral	sham+vehicle *	61	39
	injury+vehicle *#	83	17
	injury+Riluzole #	61	39
contralateral	sham+vehicle	67	33
	injury+vehicle	74	26
	injury+Riluzole	65	35

\*significant difference between injury+vehicle & sham+vehicle

#significant difference between injury+vehicle & injury+Riluzole

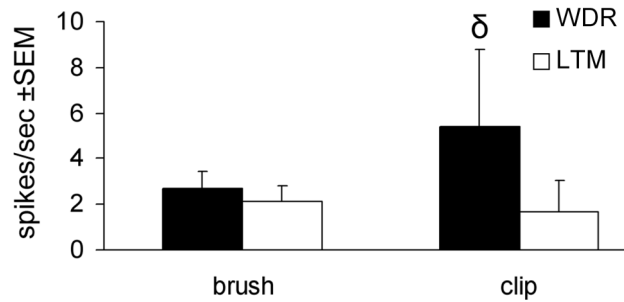


**Fig. 7.7** The firing rate of WDR and LTM neurons in the spinal cord in response to light brushing and a noxious clip applied to the forepaw on day 7. WDR neurons exhibit a graded response, while the LTM neurons primarily respond to light brushing. During the noxious clip, the frequency of neuronal firing in WDR neurons is significantly greater ( $\delta$ ) than that of LTM neurons.

## 7.5 Discussion

This is the first study to demonstrate that a single dose of Riluzole delivered early after the onset of nerve root-mediated pain is sufficient to immediately abolish the mechanical and thermal sensitivity that develop otherwise, along with a prevention of the development of neuronal pathology and spinal hyperexcitability at a later time-point (Figs. 7.1-7.6). Riluzole mitigated the axonal damage of primary afferents that is normally observed after painful root compression (Fig. 7.3) and restored the normal CGRP expression in the dorsal horn, where many of those afferents synapse (Fig. 7.4). Further, the frequency of neuronal firing in the deeper laminae ( $640 \pm 140 \mu\text{m}$ ) and the proportion of WDR neurons also returned to sham levels after Riluzole treatment (Fig. 7.6 & Table 7.2). Given that Riluzole abolished both behavioral and spinal neuronal sensitivity to the 4.0 and 10.0gf stimuli of the forepaw (Figs. 7.5 & 7.6), this study provides the first evidence that dorsal horn neuron sensitization contributes to forepaw sensitivity in this model of cervical radicular pain. The neuronal hyperexcitability that is observed in response to both non-noxious (4.0gf) and noxious (10.0 & 26.0gf) stimuli

(Fig. 7.6) (Hubbard & Winkelstein 2005, Quinn et al. 2010) suggests that sensitization of WDR neurons, in particular, may drive nerve root-mediated pain since these neurons encode stimuli intensities across both input ranges, unlike the LTM neurons (Hains et al. 2003, Urch & Dickenson 2003). The increase in the number of WDR neurons after injury (Table 7.2) further supports this notion that pain after root injury is mediated by WDR neurons. Interestingly, neuronal hyperexcitability and behavioral sensitivity were both completely abolished by Riluzole (Figs. 7.1, 7.2, 7.5 & 7.6), even though axonal swelling was still evident in some samples (Table. 7.1 & Fig. 7.3) and spinal CGRP expression did not completely return to sham levels (Table 7.1 & Fig. 7.4).

Inhibiting neuronal signaling in the brain may be essential to Riluzole's antinociceptive properties (Hama & Sagen 2011) and may augment its effects to produce the pronounced reduction in behavioral sensitivity and neuronal signaling despite the presence of axonal swelling and discontinuities in neurofilament labeling (Figs. 7.1-7.3 & 7.6). Riluzole has been shown previously to cross the blood-brain barrier rapidly and to reduce spinal glutamate and mechanical hyperalgesia within one hour after an i.p. injection (Coderre et al. 2007, Hama & Sagen 2011, Wu et al. 2013). After spinal cord contusion, Riluzole alleviates pain when it is systemically administered via an i.p. injection or when it is administered directly into the brain by an intracerebroventricular (i.c.v.) injection; yet, it is ineffective in alleviating behavioral sensitivity when it is directly administered into the intrathecal (i.t.) space of the spinal cord (Hama & Sagen 2011). Therefore, the effects of Riluzole on supraspinal glutamate appear to play a critical role in reducing pain associated with spinal cord injury. Since the supraspinal signaling after a painful root injury has not been well-defined, it is unclear whether such

supraspinal effects also contribute to the reduced behavioral sensitivity that is observed here (Figs. 7.1 & 7.2).

Systemic delivery of Riluzole mitigated mechanical sensitivity within one day of its administration and maintained its analgesic effect on both mechanical and thermal sensitivity for at least six days after that single injection (Figs. 7.1 & 7.2). To date, Riluzole's effects on behavior have been evaluated only for 2 hours after a single treatment and for four days after the final dose of daily repeated injections (Hama & Sagen 2011, Sung et al. 2003). Accordingly, this is the first study to demonstrate that a single dose, given *after* the development of pain has long-lasting effectiveness on behavioral sensitivity *and* nociceptive responses. Modulation of the glutamatergic system has long been considered a primary target for pain treatment (Bleakman & Nisenbaum 2006, Kwon et al. 2010, Tao et al. 2005). Although spinal glutamate was not measured here, *in vivo* and *in vitro* studies demonstrate that Riluzole inhibits pre-synaptic glutamate release by blocking sodium channels (Bellingham 2011, Blackburn-Munro et al. 2002, Sung et al. 2003). Regulation of spinal glutamate may, therefore, provide more comprehensive relief than antagonists to specific glutamate receptors, like the metabotropic glutamate receptor 5 (Bellingham 2011, D'Antoni et al. 2008, Mao et al. 2002), which only alleviate mechanical allodynia, but not thermal sensitivity, in neuropathy models (Dogrul et al. 2000, Hudson et al. 2002). Additional studies that identify activity of glutamate and its receptor following Riluzole treatment could better identify those mechanisms by which Riluzole alleviates radicular pain (Figs. 7.1 & 7.2).

Although Riluzole promotes cell survival and neurite outgrowth *in vitro* (Shortland et al. 2006), this is the first *in vivo* study demonstrating that Riluzole reduces

damage to primary afferents after a compression injury (Fig. 7.3). Riluzole not only mitigated axonal damage in the compressed nerve root, but also restored CGRP transport to the superficial dorsal horn (Figs. 7.3 & 7.4A). In models of neuropathic pain, there is a positive correlation between spinal CGRP expression and behavioral sensitivity (Bennett et al. 2000, Kerr & David 2007, Neugebauer et al. 1996). Despite that, Riluzole reduced behavioral sensitivity while also increasing superficial dorsal horn expression of CGRP (Figs. 7.1, 7.2 & 7.4A); yet, CGRP transport is only one indicator of neuronal function. In addition to reduced CGRP transport in those models, myelin degeneration and reduced axonal conduction were also reported (Chang & Winkelstein 2011, Hubbard & Winkelstein 2008, Kobayashi et al. 2008, Pedowitz et al. 1992). Riluzole inhibits the development of both of these injury markers after nerve and spinal cord injury (Costa et al. 2007, Stutzmann et al. 1996). Therefore, in addition to preserving axonal morphology and CGRP expression in the superficial dorsal horn in this study (Figs. 7.3 & 7.4A), Riluzole likely also inhibited the development of myelin degeneration and changes to the conduction properties of the axons that normally develop after painful nerve root compressions (Chang & Winkelstein 2008, Hubbard & Winkelstein 2008, Kobayashi et al. 2008, Pedowitz et al. 1992).

The reduced expression of CGRP that was observed in the deep laminae after Riluzole treatment (Fig. 7.4C) may be secondary to the improved neuronal health that is maintained after Riluzole treatment (Figs. 7.3). *In vitro* studies demonstrate that Riluzole has the opposite effect of increasing CGRP expression in neurons, together with promoting neurite growth (Leinster et al. 2010, Shortland et al. 2006). Therefore, it is likely that the reduced CGRP expression in the deep dorsal horn is an indirect

consequence of Riluzole. Aberrant sprouting of fibers from the superficial dorsal horn is thought to increase the expression of CGRP in the deeper laminae (Kerr & David 2007, Krenz & Weaver 1997). Extending those findings to the current study, the increased expression of CGRP after a painful nerve root compression (Fig. 7.4C) may indicate an increase in the number of CGRP-labeled fibers that do not normally extend into the deeper laminae. In fact, aberrant sprouting in the dorsal horn occurs when the nerve root is transected and primary afferents degenerate (McMahon & Kett-White 1991), suggesting that compression to the root may also induce similar sprouting. By preserving axonal morphology in the root, concurrent axonal degeneration is mitigated and aberrant sprouting of neurons into the deep dorsal horn is also prevented after Riluzole treatment.

In the spinal cord, neurotransmission of CGRP is essential for enhancing neuron excitability in models of painful knee joint inflammation and spinal cord injury (Bennett et al. 2000, Neugebauer et al. 1996). Therefore, the elevated expression of CGRP in the deep dorsal horn after a painful nerve root compression likely contributed to the neuronal hyperexcitability observed in this same region (Figs. 7.4C & 7.6). In the rat spinal cord, anti-NGF reduces neuronal hyperexcitability by preventing CGRP-labeled afferents from aberrant sprouting after a spinal cord injury (Christensen & Hulsebosch 1997, Gwak & Hulsebosch 2011). Accordingly, Riluzole may have reduced neuronal hyperexcitability in the current study by similarly reducing the expression of CGRP in the deep laminae (Figs. 7.4C & 7.6).

Our findings show, for the first time, that neuronal hyperexcitability and a shift in the phenotypic properties of dorsal horn neurons is evident following a painful transient root compression (Fig. 7.6 & Table 7.2). In contrast, a painful nerve root ligation does not



alter the frequency of evoked post-synaptic neuronal firing in the superficial dorsal horn (Terashima et al. 2011). That same study also reported that the amplitude of post-synaptic excitatory currents increases, which the authors suggested to be amplification of input from primary afferents by spinal neurons (Terashima et al. 2011). This amplification may be attributed to the increase in the number of WDR neurons observed in our study (Table 7.2), which reflects an increase in the number of neurons that respond to noxious stimuli (Hains et al. 2003, Jensen et al. 2001, Quinn et al. 2010). The observed increase in the frequency of neuronal firing to both noxious and non-noxious stimuli after a transient nerve root compression (Fig. 7.6) is consistent with other studies of neuropathic pain (Pitcher et al. 2010, Shim et al. 2005, Sung et al. 2003). Hyperexcitability of WDR neurons, in particular, underlies pain after neural injury (Hains et al. 1993, Hao et al. 1992). Furthermore, WDR neurons, but not LTM neurons, enhance their firing rate in response to increased CGRP signaling (Bennett et al. 2000, Hao et al. 1992, Liu et al. 2011). It is possible that the increased number of WDR neurons together with the elevated CGRP in the deep laminae may act together to enhance the neuronal excitability that develops after a painful root compression (Figs. 7.4C, 7.6 & Table 7.2).

Riluzole has been reported to bind to voltage-gated sodium channels and inhibit the persistent sodium current, reducing the frequency of repetitive firing of neurons (Bellingham 2011, Jehle et al. 2000, Siniscalchi et al. 1997). This is consistent with the lower frequency of firing that was observed after its administration in this study (Fig. 7.6). However, the effects of a single dose of Riluzole on the temporal response of neuronal signaling was not investigated here, nor were the specific relationships determined between axonal morphology, CGRP expression, and the frequency of

neuronal firing. Considering that an i.p. injection of Riluzole in the rat has a half-life up to 25-31 hours and, at high doses has sedative effects that last for only four hours (Liboux et al. 1999, Manz et al. 1992, Wu et al. 2013), it is likely that Riluzole has peak effects on glutamate signaling in the present study within the first day after its injection. By administering Riluzole at day 1, it may have prevented the development of tissue pathology in the root and spinal cord, thereby also preventing the development of heightened spinal neuronal firing even after the effects of Riluzole had worn off (Figs. 7.1, 7.2 & 7.6) (Manz et al. 1992, Wu et al. 2013). At day 1 after the same painful compression, CGRP in the superficial dorsal horn is not modified from sham controls and axonal injury in the root is absent (Hubbard & Winkelstein 2008, Kobayashi et al. 2005a, Rothman et al. 2005). By administering Riluzole at this time-point, it likely inhibited, but did not reverse, the development of axonal pathology in the root and loss of CGRP transport to the spinal cord. Additional studies measuring the temporal responses in the glutamatergic system for nerve root-mediated pain are needed to fully understand the mechanism(s) by which Riluzole may be acting. Nonetheless, this study establishes that even a single dose of Riluzole administered after the onset of behavioral sensitivity can inhibit the evoked neuronal signaling in the spinal cord that develops in association with attenuation of thermal and mechanical behavioral sensitivity.

## **7.6 Integration & Conclusions**

This study supports the hypothesis that a systemic injection of Riluzole at day 1 can alleviate behavioral sensitivity and reduce neuronal pathology that develops in the

nerve root and spinal cord. The known action of Riluzole decreasing the extracellular glutamate in the central nervous system suggests that an early increase in extracellular glutamate after a nerve root compression contributes to neuronal dysfunction and degeneration, consistent with cascades associated with traumatic brain and spinal cord injuries (Lau & Tymianski 2010). Therefore, even though spinal glutamate transporter expression is unchanged at day 1 following a painful nerve root compression (Chapter 5), elevated glutamate signaling at that time-point likely does contribute to the development of nerve root-mediated pain. The results of the current study suggest that nerve root-mediated pain may initially be maintained by an increase in glutamate release, which is inhibited by Riluzole (Doble 1996, Kuo et al. 2006). By day 7, however, behavioral sensitivity is maintained by impaired glutamate uptake that is attributed to a decrease in the spinal expression of the glutamate transporter, GLT-1 (Chapters 5 & 6). Certainly, additional studies are needed to test this hypothesis. However, taken together, the studies in Chapters 5 and 6 and this current chapter, are the first to indicate that glutamate may contribute to both the initiation and the maintenance of nerve root-mediated pain.

Unlike the wealth of animal studies demonstrating Riluzole's ability to prevent motor impairment and to promote improvements in motor function after injury (Bellingham 2011, Cifra et al. 2012, Doble 1996, Janahmadi et al. 2009, Kwon et al. 2010, Pintér et al. 2010, Schwartz & Fehlings 2001, Simard et al. 2012, Wu et al. 2013), the current study is one of only a handful of studies demonstrating that Riluzole also improves sensory function (Coderre et al. 2007, Hama & Sagen 2011, Sung et al. 2003). Contrary to the present findings, however, Riluzole does not alleviate hyperalgesia associated with a burn injury applied to the lower leg of human subjects (Hammer et al.

1999), suggesting that it may only be effective in treating pain associated with direct trauma to neural tissues (Coderre et al. 2007, Hama & Sagen 2011, Sung et al. 2003). The current study provides new insight into how Riluzole may alleviate nerve root-mediated pain by protecting the morphology of injured afferents, limiting redistribution of spinal neurotransmitters, and abolishing afferent hyperexcitability in the spinal cord.

---

## CHAPTER 8

### Summary, Synthesis & Future Work

---

#### 8.1 Introduction

Compression to the nerve root is a well-established mechanism for producing radiculopathy, and animal models have identified inflammatory and neuronal responses in both the nerve root and affected axons, as well as the spinal cord, that are associated with different painful nerve root compressions (Colburn et al. 1999, Garfin et al. 1990, Hubbard & Winkelstein 2005, Kobayashi et al. 2008, Olmarker et al. 1989a, Rothman et al. 2009a,b). Furthermore, compression magnitude and duration thresholds for eliciting behavioral sensitivity after a C7 transient root compression in the rat are associated with spinal inflammation and modifications to spinal neuropeptide expression by day 7 (Hubbard & Winkelstein 2005, Hubbard et al. 2008a, Nicholson et al. 2012, Rothman et al. 2010). Those studies suggest a role for nerve root biomechanics in modulating spinal neuronal signaling, which is normally regulated, in part, by the glutamatergic system. However, prior to the studies in this thesis, it was not known whether the duration of a painful nerve root compression modulates the signaling patterns of neurons in the affected nerve root or the spinal cord or whether those neuronal responses have direct effects on modifying the glutamatergic system. Therefore, the purpose of this thesis was

to define the role of one injury parameter, compression duration, for inducing neuronal dysfunction in the nerve root *during* a painful root compression and to identify those neuronal and glutamatergic changes in the spinal cord that are relevant to persistent radicular pain.

The key findings of this thesis are presented in this chapter, together with several considerations regarding the study design and the methodologies that were chosen (Section 8.2). The key findings from this collection of studies is then discussed in the context of the broader literature on nerve root and axonal compression, nociception and the biomechanics of nerve root tissues (Section 8.3). Finally, Section 8.4 outlines areas for future work that, based on the work in this thesis, would further define the role of neuronal and glutamatergic signaling in mediating pain after a cervical nerve root compression and also potential targets for alleviating the associated radicular pain.

## **8.2 Summary**

Electrophysiological data demonstrate that mechanical compression to the C7 nerve root induces immediate neuronal dysfunction in the axons of the nerve root in the rat (Fig. 8.1) (Nicholson et al. 2011). When a 10gf compression is applied to the nerve root, the number of action potentials that are electrically evoked in the periphery (at the forepaw) and recorded in the spinal cord decrease by 52-68% compared to pre-compression levels within 3 minutes of the compression. On average, the number of action potentials recorded from each neuron continues to decrease until  $6.6 \pm 3.0$  minutes into the compression period, after which there are no further changes in

neurotransmission through the root (Fig. 8.1). Even though a 3 minute compression is sufficient to reduce the number of evoked action potentials that are transmitted through the root by more than 50%, axonal conduction returns to pre-compression levels within 10 minutes if the compression is removed within 3 minutes (Nicholson et al. 2011). Conversely, when compression to the root is applied for 15 minutes, the number of

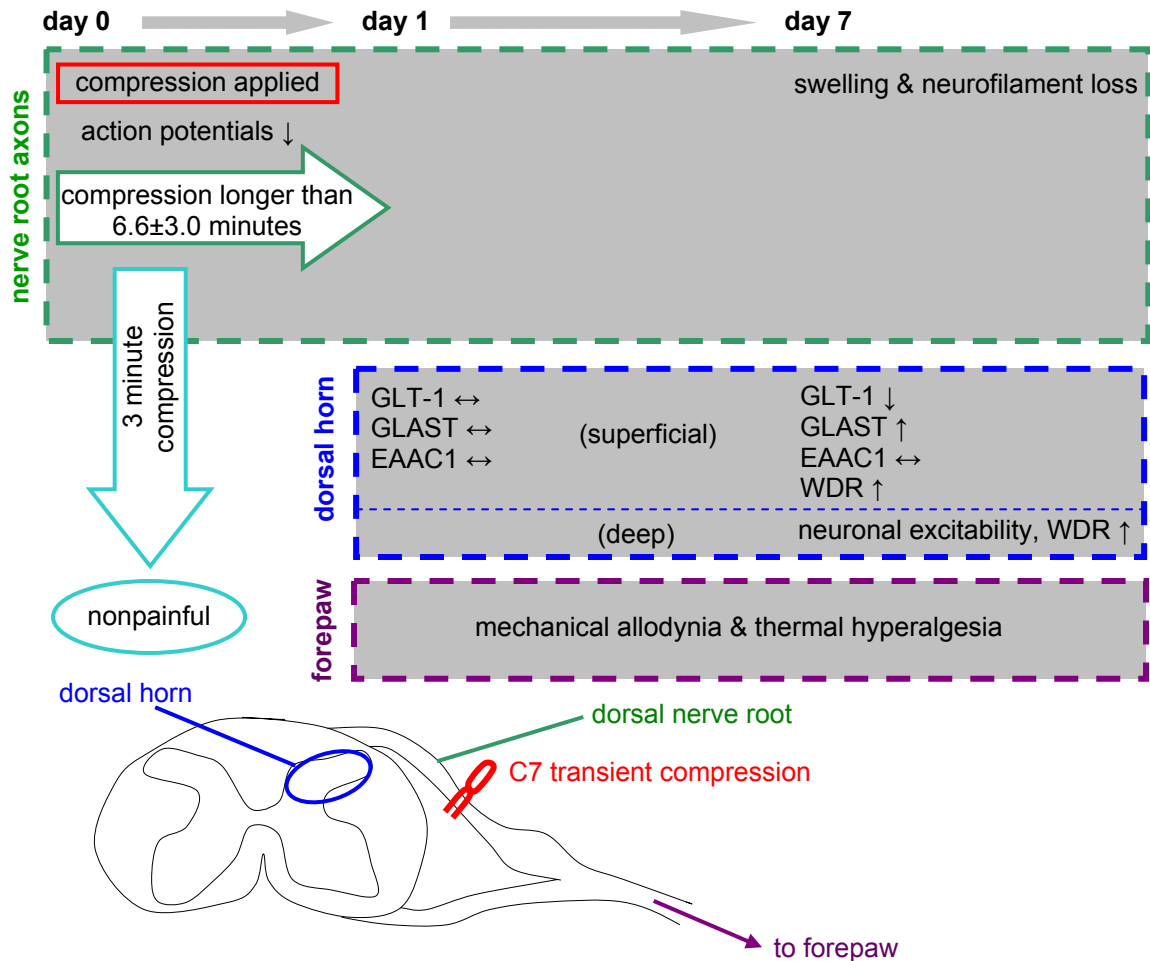


**Fig. 8.1** Compression to the dorsal nerve root immediately decreases (↓) the rate of evoked action potentials through the root until a critical duration of  $6.6 \pm 3.0$  minutes, after which there are no further changes in the discharge rate. Following a compression applied to the root for a period longer (15 minutes) than this critical duration, mechanical allodynia and thermal hyperalgesia both develop in the forepaw by day 1, but the expression of spinal glutamate transporters, GLT-1, GLAST and EAAC1, is unchanged (↔) in the superficial laminae at day 1. At day 7, behavioral sensitivity is still evident and extensive axonal damage is evident in injured root. In the spinal cord at day 7, the expression of GLT-1 decreases (↓), while GLAST expression and deep dorsal horn neuronal excitability both increase (↑).

electrically-evoked action potentials recorded in the spinal cord remains at  $58\pm 25\%$  lower than pre-compression levels for at least 10 minutes after the compression is removed. This sustained change in the conduction properties of the nerve root axons after the 15 minute compression suggests that the  $6.6\pm 3.0$  is a critical duration for inhibiting neurotransmission through the nerve root during an applied compression (Fig. 8.1).

The conduction properties of an individual axon have been shown to vary with the amount of stress it undergoes *in vivo* in the spinal cord and peripheral nerve of rodents (Hosmane et al. 2011, Shi 2004, Shi & Whitebone 2006, Wall et al. 1992). However, when a peripheral nerve is held under compression, stress is not uniformly distributed across the individual axons (Strain & Olson 1975), and this is likely true for the nerve root as well. Therefore, the conduction properties of each axon within a compressed nerve root likely vary between axons, depending on the local stress gradients. The critical compression duration of 6.6 minutes was determined by averaging the critical duration determined for *individual* axons, defined as the duration required to block, or maximally reduce, the number of action potentials evoked in the spinal cord by a peripheral stimulus for each of the recorded neurons (Nicholson et al. 2011). That average critical duration of 6.6 minutes may be biased by the search protocol used to identify afferents in the forepaw of the rat and may not reflect the conduction properties of the entire population of the nerve root axons. Specifically, mechanically sensitive, but not heat sensitive fibers were identified. Most afferent fibers are both thermally and mechanically sensitive, however (Basbaum et al. 2009). Because thermoreceptors are comprised of C and A $\delta$  fibers, which are less vulnerable to mechanical injury than A $\beta$  mechanoreceptors (Basbaum et al. 2009, Jancalék & Dubovy 2007, Mosconi & Kruger 1997, Strain & Olson 1975), the duration



threshold of 6.6 minutes is likely a conservative indicator of injury across all axons in the root. An alternative method for assessing axonal conduction through the root is to measure the collective response of all axons in the nerve root by measuring compound action potentials. Although studies have, in fact, measured compound action potentials through the nerve roots of the porcine cauda equina (Pedowitz et al. 1992, Rydevik et al. 1992), those authors concede that it was not possible to exclude possible efferent conduction through the ventral nerve root from their recordings (Rydevik et al. 1992).

Since the goal of this thesis was to evaluate *afferent* function during a dorsal nerve root compression known to elicit pain, spinal recordings were made in the superficial dorsal horn, where these afferent fibers synapse. Although it cannot be conclusively determined whether the neurons recorded in this thesis represent the average conduction properties of all axons in the compressed nerve root, the search protocol used here randomly selected mechanoreceptors of the forepaw (Nicholson et al. 2011), where mechanical allodynia is established after a painful nerve root compression. As such, the  $6.6\pm 3.0$  minute critical duration likely reflects the response of afferents that innervate the region where sensitivity develops in this rat model of cervical radiculopathy.

That same critical duration ( $6.6\pm 3.0$  minute) for decreasing the rate of evoked action potentials through the root also approximates the compression duration threshold for eliciting sustained behavioral sensitivity in the forepaw of the rat (Chapter 4; Nicholson et al. 2012). Compression to the nerve root only induces mechanical allodynia when compression is applied longer than (10 minutes) that critical duration and not after a shorter (3 minute) compression. Although the development of mechanical allodynia was only determined for testing with a 4.0gf filament, a 2.0gf filament has elicited similar

trends in the responses to those reported in this thesis after nerve root compression durations of 3 and 15 minutes (Rothman et al. 2010). Furthermore, previous studies establish that the stimulation magnitude threshold for eliciting a paw withdrawal response decreases from 13.0-15.0gf using Chaplan's up-down threshold method (Chaplan et al. 1994) to 2.0-4.0gf after a 15 minute nerve root compression (Hubbard & Winkelstein 2005). It is possible that a 3 minute compression also induces mechanical hyperalgesia, but the threshold for eliciting a painful response lies between 4.0gf and 13.0gf. By only testing for mechanical allodynia with a 4.0gf filament, the studies presented here did not determine whether a 3 minute compression to the nerve root in the rat enhances the sensitivity of the forepaw to stimuli greater than a 4.0gf. However, a 3 minute compression does not lower the threshold for eliciting a painful response to a thermal stimulus (Chapter 4). The fact that a 3 minute compression does not lower that thermal response or increase the withdrawal frequency to mechanical stimuli (Nicholson et al. 2013a), together support the hypothesis that there is a compression duration threshold, near  $6.6 \pm 3.0$  minutes, for eliciting behavioral sensitivity after a nerve root compression of 10gf in the rat.

The duration threshold for eliciting behavioral sensitivity after nerve root compression likely varies with the load magnitude. Although the studies presented in this thesis demonstrate that there is a duration threshold between 3 and 10 minutes for eliciting mechanical allodynia after a 10gf nerve root compression (Chapter 4; Nicholson et al. 2012), Sekiguchi et al. (2009) report that persistent mechanical hyperalgesia can develop after a nerve root compression applied for as short as 3 seconds in the rat. The magnitude of compression was not defined for that short, 3 second nerve root

compression, but was described as a *crush* injury by those authors (Sekiguchi et al. 2009) and was likely much higher than the 10gf applied in the studies presented throughout this thesis. In fact, even a compression load as high as 60gf applied for 3 minutes to the cervical nerve root in the rat is insufficient to elicit mechanical allodynia (Nicholson et al. 2012), indicating that Sekiguchi et al. (2009) likely compressed the nerve root with load magnitudes much higher than 60gf. Although the magnitude of compression required to elicit behavioral sensitivity after a 3 second nerve root compression has not been defined, it is clear that the duration threshold for eliciting behavioral sensitivity that is near  $6.6 \pm 3.0$  minutes after a 10gf compression far exceeds the duration threshold that lies between 0 and 3 seconds after a *crush* injury to the nerve root (Nicholson et al. 2011, 2012, Sekiguchi et al. 2009). Therefore, the duration threshold for inhibiting neurotransmission through the root *during* compression and for the development of behavioral sensitivity is only applicable to a 10gf C7 nerve root compression in the rat (Chapters 3 & 5) (Nicholson et al. 2011, 2012).

Blocking pre-synaptic glutamate release in the central nervous system (CNS) with a single injection of Riluzole or upregulating spinal GLT-1 with daily intrathecal injections after the development of behavioral sensitivity (day 1) both abolish behavioral sensitivity (Fig. 8.2; Chapters 6 & 7) (Nicholson et al. 2013a,b). It is well-established that Riluzole inhibits glutamate release by pre-synaptic neurons and decreases the overall extracellular concentration of glutamate in the spinal cord (Coderre et al. 2007, Hama et al. 2011, MacIver et al. 1996, Wang et al. 2004). Riluzole abolished mechanical allodynia for at least six days and preserved the normal morphology of the nerve root axons at day 7 even though it was only administered on day 1 (Fig. 8.2) (Chapter 7; Nicholson et al.

2013b). These sustained behavioral and neuroprotective effects of Riluzole long after Riluzole would already have been metabolically cleared from the CNS (Wu et al. 2013), indicates that glutamatergic neurotransmission in the CNS at day 1 after a painful nerve root compression has an essential role for the subsequent development of *sustained* nerve root-mediated pain. Conversely, without modifying the *release* of glutamate, but increasing spinal glutamate uptake by upregulating GLT-1 with a daily ceftriaxone injection, nerve root-mediated pain is also abolished (Fig. 8.2) (Chapter 6; Nicholson et al. 2013a). By day 7, ceftriaxone restored spinal GLT-1 expression, which is normally downregulated at this time-point after a painful nerve root compression (Fig. 8.2; Chapter 5). Therefore, findings from that ceftriaxone study suggest that glutamate signaling in the

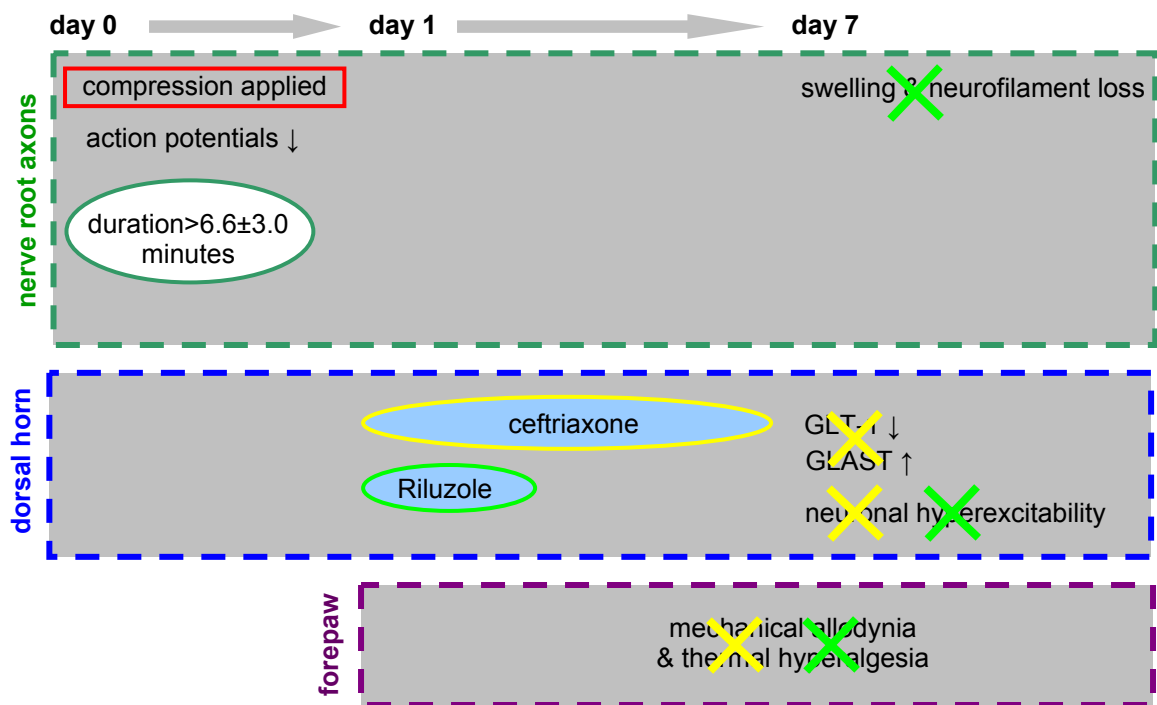


**Fig. 8.2** Daily treatment with ceftriaxone on days 1 through 6, or a single treatment with Riluzole on day 1, both abolish behavioral sensitivity and neuronal hyperexcitability in the spinal cord by day 7. After ceftriaxone treatment, the spinal expression of GLT-1 and GLAST both return to normal at day 7. The axons of the nerve root also retain their normal morphology after treatment with Riluzole at day 7.

spinal cord likely contributes to the *maintenance* of behavioral sensitivity at day 7 due to the impaired glutamate uptake by GLT-1 after a painful nerve root compression. Notably, neuronal hyperexcitability in the deep laminae of the spinal cord that normally develops by day 7 was reduced by both Riluzole and ceftriaxone (Nicholson et al. 2013a,b) implicating spinal neuronal hyperexcitability as one underlying mechanism mediating behavioral sensitivity. Together, the studies that administered Riluzole or ceftriaxone indicate that, by day 1, the glutamatergic system is essential to initiating the cellular mechanisms in the CNS associated with *persistent* behavioral sensitivity that is maintained, in part, by downregulation of GLT-1 in the spinal cord.

In the superficial laminae of the dorsal horn, the expression of the neuronal glutamate transporter, EAAC1, was unchanged at days 1 and 7 after a painful nerve root compression, but may have mediated the phenotypic shift from low threshold mechanoreceptors (LTMs) to wide dynamic range (WDR) neurons that develops by day 7 (Chapter 5; Jarzylo & Man 2012, Kondo et al. 2002, Lim et al. 2006, Nicholson et al. 2013a, Zhang et al. 2013). Previous studies report that upregulation of AMPA receptors on post-synaptic LTM neurons in the spinal cord change the response characteristics of these neurons to that of WDR neurons after a painful sciatic nerve constriction injury in the rat (Kondo et al. 2002, Lim et al. 2006). The distribution of AMPA receptors on post-synaptic neurons is determined, in part, by EAAC1 (Jarzylo & Man 2012), suggesting that EAAC1 may have increased the proportion of WDR neurons after a painful nerve root compression by trafficking AMPA receptors to the synapse of LTM neurons in the spinal cord. Unlike the glial glutamate transporters, as much as 70-80% of EAAC1 is intracellular, but can traffic to the plasma membrane in response to aberrant neuronal

firing (Holmseth et al. 2012, Ross et al. 2011). It has previously been reported that spontaneous firing increases in the superficial laminae after a chronic constriction root injury (Terashima et al. 2011), which provides one mechanism by which EAAC1 may be trafficked to the plasma membrane, thereby upregulating AMPA receptors (Jarzylo & Man 2012) and contributing to the phenotypic shift of neurons in this region of the spinal dorsal horn (Chapter 5).

Downregulation of spinal GLT-1 after a painful nerve root compression is likely sufficient to increase spinal neuronal excitability even in the absence of any change in the expression of the neuronal glutamate transporter, EAAC1, in the dorsal horn (Chapter 5). The contribution of EAAC1 to overall glutamate uptake is thought to be minimal (Holmseth et al. 2012, Rothstein et al. 1996) and, in fact, it has been reported that a 78% reduction in EAAC1 expression in the rat brain does not change the concentration of extracellular glutamate (Rothstein et al. 1996). In contrast, downregulating GLT-1 by 58% produces a 32-fold increase in extracellular glutamate in the rat brain (Rothstein et al. 1996). This large increase in extracellular glutamate due to impaired glutamate uptake by GLT-1 is sufficient to increase neuronal hyperexcitability (Cata et al. 2006, Inquimbert et al. 2012). Together, those studies suggest that downregulation of EAAC1 is not required to increase extracellular glutamate and the associated neuronal excitability that is observed after a painful nerve root compression (Chapter 5; Cata et al. 2006, Inquimbert et al. 2012, Rothstein et al. 1996). However, it should be noted that due to the low expression of EAAC1, immunohistochemistry may not be sensitive enough to detect subtle changes in the expression of this glutamate transporter after a painful nerve root compression (Chapter 5). Although immunoblotting may be more discriminating in

detecting EAAC1 concentrations (Holmseth et al. 2012, Sung et al. 2003), immunohistochemistry was chosen because this method provides spatial resolution. Furthermore, the same immunohistochemical methods used to quantify spinal EAAC1 expression in this thesis are sensitive enough to detect changes in the spinal expression of EAAC1 following a painful facet joint distraction (Dong et al. 2012). In the studies presented here, no trends were observed in the spinal expression of EAAC1 after a painful nerve root compression (Chapter 5), indicating that more sensitive methods for quantifying EAAC1 protein concentrations would also likely not detect any robust modifications to the spinal expression of this transporter associated with radicular pain. This would suggest that AMPA receptor-mediated phenotypic shifts in the superficial dorsal horn after a painful nerve root compression may be due to increased *activity* of EAAC1 or increased glutamate activation of AMPA receptors due to impaired glutamate uptake by GLT-1 (Chapters 5 & 6; Nicholson et al. 2013a).

There is a compression duration threshold between 3 and 15 minutes for inducing axonal damage in the nerve root, upregulating spinal GLT-1, downregulating spinal GLAST and enhancing neuronal hyperexcitability in the deep laminae, all of which develop by day 7 and are associated with persistent behavioral sensitivity after a transient C7 nerve root compression (Chapters 3-5). It is possible that the 6.6 minute critical duration for inhibiting electrically-evoked action potentials from the forepaw to the spinal cord also defines the duration threshold for eliciting these neuronal and glutamatergic responses at day 7. However, the studies in this thesis did not explicitly test that hypothesis. Instead, compression durations of 3 minutes and 15 minutes were used for all immunohistochemical and electrophysiologic studies. The 15 minute compression

duration was specifically chosen in order to compare the outcomes of this thesis with the broader existing literature in nerve root compression since there is a wealth of literature already defining inflammatory, neurotrophic, neuropeptidergic, neurodegenerative and behavioral responses after a 10gf, 15 minute C7 nerve root compression in the rat (Hubbard & Winkelstein 2005, Hubbard & Winkelstein 2008, Hubbard et al. 2008a, Rothman et al. 2007, Rothman et al. 2010). By only applying compressions for a duration of 15 minutes, the findings and implications from this thesis are limited. Further, the hypothesis that there is a relationship between the neuronal responses *during* a nerve root compression and the neuronal, glutamatergic and behavioral responses that develop was not explicitly tested. However, the compression duration threshold for eliciting mechanical allodynia and the development of astrocytic activation at day 7 is between 3 and 10 minutes (Nicholson et al. 2012, Rothman et al. 2010). The  $6.6 \pm 3.0$  minute duration threshold for inhibiting neurotransmission through the root *during* compression does, therefore, approximate and, may even define, the duration threshold for eliciting behavioral sensitivity and spinal inflammation. Both of these are associated with downregulation of spinal GLT-1, increased firing rates of spinal neurons and the development of neuropathology in the nerve root after a transient cervical nerve root injury in the rat (Hubbard & Winkelstein 2008, Nicholson et al. 2011, 2012, 2013a,b). Therefore, the studies in this thesis do support the hypothesis that the 6.6 minute critical duration for inhibiting neurotransmission through the root *during* compression also defines the duration threshold for downregulating spinal GLT-1, eliciting neuronal hyperexcitability and inducing neuropathology in the nerve root. These studies are the first to establish a role for nerve root biomechanics in dysregulating spinal glutamate



transporter expression, enhancing spinal neuronal excitability and reducing cytoskeletal protein expression in the nerve root (Nicholson et al. 2011, 2013a,b).

Mechanical compression to the nerve root by a herniated disc can also irritate the nerve root chemically due to contact with the nucleus pulposus of the disc (Abbed & Coumans 2007, Wainner & Gill 2000). Animal models that compare the cellular cascades in the peripheral and central nervous systems that are associated with a mechanical or chemical insult to the root demonstrate that each type of these root injuries (i.e. chemical, mechanical) may mediate radicular pain via different pathways (Chang et al. 2011, Maves et al. 1993, Rothman et al. 200b). Therefore, the conclusions in this study also may only be applicable to nerve root injuries that are solely attributed to its mechanical deformation. However, the incidence rate of a disc herniation in cervical radiculopathy is reported to be only 25-30% (Carrette & Fehlings 2005, Radhakrishnan et al. 1994, Thoomes et al. 2012). The model of cervical nerve root compression used in the studies here is, therefore, clinically relevant for the remaining 70-75% of reported cases of cervical radiculopathy.

The studies here did not look at time-points later than day 7. Rodent models of both chronic and transient nerve root compressions demonstrate that behavioral sensitivity can persist for up to 3-4 weeks (Rothman et al. 2007). Although pain symptoms are fully established by day 7 (Rothman et al. 2007), the cellular mechanisms that *maintain* behavioral sensitivity may differ over time. For example, after a painful nerve root compression, the neuropeptide, substance P (SP), is downregulated in the dorsal root ganglion (DRG) at day 7, but upregulated in the DRG at day 14, despite the fact that behavioral responses are similar to each other at both time-points (Chang et al.

2011, Hubbard et al. 2008a). SP is specifically associated with nociceptors in the DRG, suggesting that the mechanism underlying nociception continuously shift even after radicular pain is established at day 7. Therefore, even though day 7 is considered relevant to chronic pain in the rat (DeLeo & Winkelstein 2002), the behavioral, neuronal and glutamatergic responses demonstrated at day 7 in the studies presented here may not necessarily reflect the maintenance of pain at later time-points due to the temporal dynamics of neuronal cytoskeletal proteins, neuronal signaling and glutamate transporters, which undergo continuous modifications for weeks to months after neural tissue trauma (Chen et al. 1992, Kim et al. 2011, Serbest et al. 2007, Yoshizawa et al. 1995).

### **8.3 Synthesis**

Graded magnitudes of compression to axons produce graded decreases in axonal transport and axonal conduction *in vivo* and *in vitro* (Chen et al. 1992, Garfin et al. 1990, Gallant 1992, Pedowitz et al. 1992). As was observed during *in vivo* compression to the cervical nerve root in the rat (Nicholson et al. 2011) and in the nerve roots of the cauda equina in the pig (Garfin et al. 1990, Pedowitz et al. 1992), *in vitro* compression to an isolated squid axon inhibits electrically-evoked action potentials through the compressed region both *during* and immediately *after* a transient compression is applied (Gallant 1992). Furthermore, those studies demonstrate that axonal conduction only recovers if the plasma membrane of the axon remains intact (Gallant 1992). After a 15 minute nerve root compression, spinal action potentials evoked by an electrical stimulus to the forepaw do

not recovery for at least 10 minutes (Nicholson et al. 2011), demonstrating that impaired axonal conduction is sustained well after the original insult (compression) is no longer present. Given the relationship between plasma membrane damage and impaired neurotransmission (Gallant 1992), the sustained decrease in axonal conduction that is evident after a 15 minute compression (Nicholson et al. 2011), suggests that a 10gf, 15 minute compression compromises the plasma membrane of afferents in the nerve root.

Even though the number of evoked action potentials from the periphery to the superficial dorsal horn decreases during a painful nerve root compression (Nicholson et al. 2011), the frequency of neuronal evoked firing rates in that same region of the dorsal horn is unchanged at day 7 (Chapter 5; Zhang et al. 2013). Unlike the electrophysiologic studies that measured neurotransmission *during* a nerve root compression, the studies that recorded evoked spinal neuronal activity from the forepaw at day 7 did not determine whether those action potentials were associated with the C7 or C8 nerve root, both of which innervate the rat forepaw (Takahashi & Nakajima 1996). Therefore, based on the studies presented in this thesis, it cannot be determined whether neurotransmission through the C7 nerve root to the superficial dorsal horn remains impaired or recovers by day 7 after a painful nerve root compression. The neuropathology in the C7 nerve root that develops by day 7 after a painful transient nerve root compression in the rat (Hubbard & Winkelstein 2008, Nicholson et al. 2011) and the loss of primary afferent synaptic contact in the superficial dorsal horn after canine or rat lumbar nerve root compression (Kobayashi et al. 2008, Terashima et al. 2011) suggest that neurotransmission from the periphery to the spinal cord does not recover in at least a subset of primary afferents in the affected root after its compression. In fact, Terashima et

al. (2011) report that there are “silent” spinal neurons in the superficial dorsal horn that have no identifiable receptive field after a painful lumbar nerve root ligation in the rat due to lost synaptic contact with the primary afferents that normally synapse onto these second-order neurons (Terashima et al. 2011). There may be similarly “silent” neurons in the superficial laminae after a painful transient cervical nerve root injury that were not recorded in the electrophysiologic studies of this thesis because all neurons were identified by applying a mechanical stimulus to the forepaw (Chapters 5-7) (Zhang et al. 2013). Therefore, the frequency of evoked neuronal firing rates in the dorsal horn at day 7 only reflects the response of those neurons that maintained at least one synaptic connection with a primary afferent innervating the forepaw (Chapter 5; Zhang et al. 2013). Even though there may be an overall decrease in evoked neuronal firing in the superficial dorsal horn due to “silent” neurons (Terashima et al. 2011), for the spinal neurons that do maintain at least one primary synapse, the frequency of firing is unchanged in the superficial laminae at day 7 after a painful nerve root compression (Chapter 5; Terashima et al. 2011, Zhang et al. 2013).

Downregulation of GLT-1 in the *superficial* laminae of the dorsal horn may contribute to the neuronal hyperexcitability that develops in the *deep* laminae by day 7 after a painful nerve root compression (Chapter 5; Nicholson et al. 2013a, Zhang et al. 2013). *In vivo* patch clamp studies in the rat confirm that the *frequency* of post-synaptic excitatory currents does not increase in the superficial dorsal horn after a painful lumbar ligation (Terashima et al. 2011). That same study does report, however, that the *amplitude* of post-synaptic excitatory currents does increase (Terashima et al. 2011), which could be attributed to increased glutamate receptor activation on these post-

synaptic neurons due to impaired glutamate uptake by GLT-1 on perisynaptic glia (Chapter 5; Inquimbert et al. 2012, Nicholson et al. 2013a). Most primary afferents synapse onto an interneuron in the dorsal horn (Todd 2010) and patch clamp recordings on spinal cord slices reveal that primary nociceptors synapse onto excitatory interneurons in laminae I and II and that these interneurons increase the excitability of neurons in laminae III-V (Nakatsuka et al. 2002, Petitjean et al. 2012). An increase in the amplitude of excitatory currents on these post-synaptic interneurons in lamina II after a painful nerve root ligation (Terashima et al. 2011), potentially due to downregulation of GLT-1 (Chapter 5; Nicholson et al. 2013a), may increase excitatory neurotransmission in the deep laminae (Nakatsuka et al. 2002, Petitjean et al. 2012), increasing the firing rate of deep dorsal horn neurons after a painful transient cervical nerve root compression (Chapter 5; Zhang et al. 2013). In this scenario, spinal GLT-1 has a pivotal role in amplifying interlaminar neuronal circuits by enhancing the excitability of dorsal horn neurons in the deep laminae.

A violation of the plasma membrane of compressed axons due to an applied compression is associated with increased release of intracellular glutamate, raising the extracellular glutamate concentration (LaPlaca & Prado 2010). Riluzole may have restored normal extracellular glutamate concentrations at day 1 by inhibiting glutamate release in the central nervous system (Chapter 7). After a single injection of Riluzole, the neuronal hyperexcitability in the spinal cord and axonal pathology in the nerve root that are normally evident at day 7 after a painful nerve root compression were both abolished (Chapters 3, 5 & 7). This suggests that the elevated extracellular concentration of glutamate in the central nervous system at day 1 (Fig. 8.1) is essential for the neuronal

pathophysiology that develops in both the spinal cord and the nerve root by day 7 (Nicholson et al. 2011, 2013b). In fact, an over-accumulation of synaptic glutamate can sensitize neurons and, if the concentration is high enough, cause glutamate-mediated neurotoxicity (Cargill & Thibault 1996, Geddes & Cargill 2001, LaPlaca & Prado 2010). Riluzole may have inhibited the development of neuronal hyperexcitability in the spinal cord and neuropathology in the nerve root at day 7 by reducing extracellular glutamate in the spinal cord at day 1. Even though Riluzole was administered after behavioral sensitivity developed in the forepaw (day 1), that time-point is likely early enough to mitigate the development of robust pathology in the nerve root because axonal degeneration develops sometime between days 1 and 7 (Hubbard & Winkelstein 2008). Therefore, the neuroprotective effects of Riluzole observed here may not be applicable if Riluzole is administered at later time-points, after the development of axonal degeneration in the nerve root.

Early inflammatory responses after a painful C7 nerve root compression in the rat may also contribute to increased synaptic glutamate (Nie et al. 2010, Rothman et al. 2009b, Rothman & Winkelstein 2010, Zou & Crews 2005). Within one hour of a painful C7 compression in the rat, pro-inflammatory cytokines, including TNF $\alpha$ , are upregulated in the spinal cord (Rothman & Winkelstein 2010). TNF $\alpha$  dose-dependently inhibits glutamate uptake in hippocampal slices by up to 25% (Zou & Crews 2005) and, in doing so, may have increased glutamate concentrations within one hour of a painful root compression (Rothman & Winkelstein 2010). Antagonizing TNF $\alpha$  with the soluble TNF receptor-1 attenuates, but does not abolish, radicular pain in this model (Rothman & Winkelstein 2010), suggesting that TNF $\alpha$  may work synergistically with the hypothesized

increase in pre-synaptic glutamate release to elevate synaptic glutamate. Minocycline also prevents the development of pain after a C7 nerve root compression in the rat by suppressing microglial activation and associated pro-inflammatory cytokine release by these cells (Amin et al. 2010, Rothman et al. 2009a, Yamada & Jinno 2011). It has also been shown that minocycline reduces NMDA receptor activation in the spinal cord by upregulating spinal glial glutamate transporters after a painful sciatic nerve ligation in the rat (Nie et al. 2010). Notably, spinal glutamate transporters are unchanged at day 1 after a painful nerve root compression (Chapter 5) and upregulating GLT-1 with ceftriaxone does not abolish behavioral sensitivity until day 3, two days after the initial treatment (Chapter 6). Therefore, even though minocycline also upregulates spinal glial glutamate transporters (Nie et al. 2010), it is more likely that minocycline prevents the development of radicular pain by suppressing microglial activation and associated TNF $\alpha$  release (Amin et al. 2010, Rothman et al. 2009a). Together, the studies that administered Riluzole, ceftriaxone, minocycline or the soluble TNF receptor-1 suggest that increased glutamate release along with microglial activation and associated glutamate uptake inhibition by TNF $\alpha$  likely mediate the *initiation* of nerve root-mediated pain while downregulation of GLT-1 contributes to the *maintenance* of radicular pain.

The compression duration threshold for both the development of neuropathology in the nerve root and downregulation of spinal GLT-1 lies between 3 and 15 minutes after a C7 nerve root compression in the rat (Chapter 5; Nicholson et al. 2011). Astrocytic expression of GLT-1 is tightly regulated by pre-synaptic neurons (Ghosh et al. 2011, Yang et al. 2009). As such, the neuropathology in the nerve root that develops after painful compression (Hubbard & Winkelstein 2008, Nicholson et al. 2011) may mediate

the downregulation of this transporter in the spinal cord after a painful nerve root compression. As demonstrated in this thesis and previously reported, the axons of the nerve root are sensitive to both the magnitude *and* duration of compression (Hubbard & Winkelstein 2008, Garfin et al. 1990, Nicholson et al. 2011, Pedowitz et al. 1992). Furthermore, the load magnitude to induce neuropathology in the nerve root likely varies with the duration of compression. Above 3.2gf, the axonal cytoskeletal protein, NF200, is significantly reduced in the nerve root after a 15 minute compression (Hubbard & Winkelstein 2008). Yet, if a suprathreshold (10gf) compression is applied to the root for only 3 minutes, the axons retain their normal morphology (Nicholson et al. 2011). Axonal pathology *only* develops in the root after a painful nerve root compression (Hubbard & Winkelstein 2008, Nicholson et al. 2011) and even a 60gf compression is not sufficient to elicit behavioral sensitivity if applied for 3 minutes (Nicholson et al. 2012) suggesting that a 60gf, 3 minute compression also could not induce axonal degeneration in the nerve root (Hubbard & Winkelstein 2008, Nicholson et al. 2011). If, indeed, spinal expression of GLT-1 requires normal afferent input from the nerve root, the duration threshold for downregulating this transporter in the dorsal horn that is between 3 and 15 minutes after a 10gf compression likely also varies with the compression magnitude. Furthermore, the magnitude and duration thresholds for producing injury in the nerve roots of the cauda equina in a porcine model decrease with increasing rates of compression (Olmaker et al. 1989a). Given that the nerve root axons are sensitive to the combined contribution of the duration, magnitude and rate of compression and that damage to these axons likely precipitates the downregulation of spinal GLT-1 that results after a nerve root compression (Ghosh et al. 2011, Yang et al. 2009), this transporter may also be sensitive



to these mechanical parameters. The relationship between the primary afferents and spinal GLT-1, may have a central role in transducing the biomechanics of the nerve root tissues into the pain symptoms that develop.

The neuropathology in the nerve root that is normally evident at day 7 after a painful nerve root compression does not develop when sodium channel-dependent glutamate release is blocked at day 1 by Riluzole (Chapter 7). The proposed relationship between the neuropathology in the afferents of the nerve roots and the downregulation of spinal GLT-1 suggests that when these afferents retain their normal morphology after Riluzole treatment, spinal GLT-1 also would not be downregulated. Unlike Riluzole, which rapidly reduces spinal glutamate concentration within 30 minutes of an intraperitoneal injection (Coderre et al. 2007), ceftriaxone did not abolish behavioral sensitivity until day 3 (Chapter 6; Nicholson et al. 2013a), suggesting ceftriaxone does not significantly modify synaptic glutamate concentration until this time-point. Therefore, it is possible that even though ceftriaxone presumably reduces extracellular glutamate, it only directly upregulates spinal GLT-1 without modifying the normal course of the associated neuropathologic responses in the nerve root after painful nerve root compression. Preliminary studies do support this hypothesis; when the nerve root axons retain their normal morphology after a nerve root compression treated with Riluzole, spinal GLT-1 expression is comparable to that in normal tissue (Fig. 8.3). Conversely, if spinal GLT-1 is upregulated by ceftriaxone, extensive axonal pathology *is* apparent in the nerve root (Fig. 8.3), indicating that maintaining spinal GLT-1 expression is not sufficient to mitigate damage to the primary afferents. These preliminary data support the studies in the rest of this thesis that suggest that neurodegeneration in the nerve root

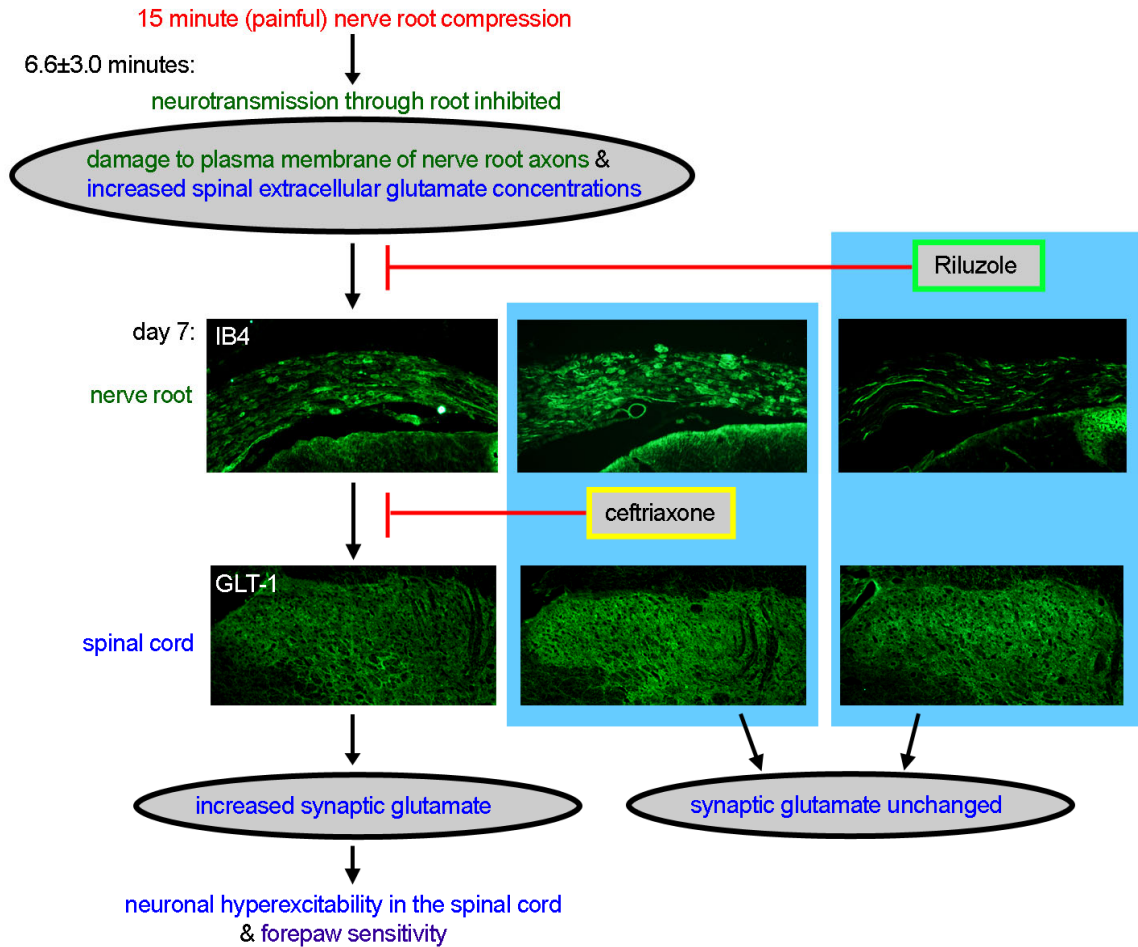


**Fig. 8.3** Proposed schema of the neuronal and glutamatergic responses in the nerve root and spinal cord after a painful 15 minute compression. Longitudinal sections of the nerve root labeled for IB4 and axial sections of the dorsal horn labeled for GLT-1 show that for a compression duration longer than 6.6±3.0 minutes, there is a sustained decrease in neurotransmission through the root, which may be indicative of damage to the plasma membrane of the nerve root axons and may increase glutamate release in the spinal cord. By day 7, there is extensive axonal pathology in the nerve root associated with downregulation of GLT-1 in the dorsal horn, where those axons synapse. Downregulation of GLT-1 increases synaptic glutamate and the firing rate of spinal neurons. Hyperexcitability of spinal neurons in the deep laminae of the dorsal horn mediates behavioral sensitivity. Ceftriaxone and Riluzole both abolish cervical radicular pain by maintaining normal spinal glutamate uptake by GLT-1. Ceftriaxone directly upregulates the expression of spinal GLT-1, while Riluzole prevents the development of neuropathology, thereby maintaining spinal GLT-1 expression.

cause spinal glia to downregulate the expression of GLT-1 (Ghosh et al. 2011, Nicholson et al. 2011, 2013a, Yang et al. 2009).

The studies in this thesis, taken together with the literature, suggest that a 15 minute, 10gf compression damages the plasma membrane of the axons *during* a

sufficiently long applied compression, causing the axons contained within it to release excess synaptic glutamate in the spinal cord (Fig. 8.3). Elevated glutamate concentration in the spinal cord at day 1 after a painful nerve root compression contributes to changes in the neuronal circuits in the spinal cord at day 7 (Fig. 8.3). Specifically, the cytoskeleton of the injured axons in the nerve root is compromised and the firing rate of post-synaptic spinal neurons increases in the deep laminae of the dorsal horn (LaPlaca & Prado 2010, Nicholson et al. 2011). In response to the neurodegeneration that develops in the nerve root after a painful nerve root compression, spinal glial cells in the dorsal horn downregulate their expression of GLT-1 at day 7 (Fig. 8.3) (Nicholson et al. 2013a, Yang et al. 2009). Because GLT-1 is the dominant transporter responsible for glutamate uptake, impaired glutamate uptake by it may sensitize the spinal neurons, increasing the firing rate of these neurons (Fig. 8.3). Finally, evoked spinal neuronal hyperexcitability at day 7 likely mediates the persistence of behavioral sensitivity at this same time-point.

## **8.4 Future Work**

Although this thesis refers to nerve root compressions that elicit mechanical and thermal sensitivity as *painful*, it is not known whether a nerve root compression in this model elicits on-going, spontaneous pain and, if so, whether the presence of the evoked reflexes (mechanical and thermal sensitivity) that are used here, serve as an appropriate proxy for spontaneous pain. The pain field has, for decades, pursued the development of new pain assays that can reliably quantify on-going pain, which is the most-often reported clinical symptom of neuropathic pain (Backonja & Stacey 2004, Mogil et al.

2010). Future studies should investigate potential methods, such as place aversion (LaBuda & Fuchs 2000) that could assess ongoing pain better than evoked reflex tests.

Measuring spontaneous activity of spinal afferents could also serve as a proxy for evaluating spontaneous pain after a cervical transient nerve root compression. The field potential recordings and the search protocol used in this thesis are not robust methods for quantifying spontaneous activity due to the fact that spontaneous neuronal firing can make it difficult to identify an evoked response. Because the goal of the studies in this thesis were to measure evoked firing of spinal neurons in response to the same mechanical stimuli that elicits mechanical allodynia, the electrophysiologic studies were optimized to evaluate *evoked* but not *spontaneous* neuronal firing rates. *In vivo* patch clamp techniques are a more robust method to measure spontaneous neuronal activity and can also identify the cellular mechanisms contributing to the neuronal firing patterns observed by extracellular recordings, such as excitatory and inhibitory post-synaptic currents (Covey et al. 1996, Takeda et al. 2010). Studies employing *in vivo* patch clamp techniques in the spinal cord to assess spontaneous neuronal activity would define the spinal neuronal firing at the synaptic level after a painful nerve root compression and further define the role of glutamate in nerve root-mediated pain by characterizing excitatory neuronal circuits in the dorsal horn.

Neurotransmission through the root is sensitive to both the compression magnitude and the length of time that the compression is applied (Garfin et al. 1990, Nicholson et al. 2011, Pedowitz et al. 1992). The studies in this thesis suggest that impaired axonal conduction during an applied compression is an indicator, or even an initiator, of the subsequent behavioral sensitivity that develops (Nicholson et al. 2011,

2012). Impaired axonal conduction has been associated with structural damage to the axonal plasma membrane (Gallant 1992, LaPlaca et al. 2009). The structural integrity of the plasma membrane can be breached by mechanical overloading and/or an insufficient blood supply (Dyck et al. 1992, Gallant 1992, LaPlaca et al. 2009). Studies have established that intraradicular blood flow continuously decreases with increasing periods of compression to the nerve root (Olmarker et al. 1989b, Yoshizawa et al. 1989), and that ischemia alone is sufficient to reduce axonal conduction through the nerve root (Kobayashi et al. 2008). Therefore, with increasing durations of root compression, ischemic conditions may increasingly compromise the axons' ability to maintain or repair their plasma membranes (LaPlaca et al. 2009). At the same time, the magnitude of an applied compression also modulates the degree of intraradicular ischemia and the extent of axonal plasma membrane damage within the nerve root (Garfin et al. 1990, Kobayashi et al. 2008, Olmarker et al. 1989a). Therefore, there are likely additive effects of compression magnitude and duration on the degree of intraradicular blood flow impairment and axonal membrane damage that develops during a nerve root compression.

Superimposed upon these physiologic responses in the nerve root are the biomechanical properties of the nerve root tissue itself (Hubbard et al. 2008b). Because of its viscoelastic properties, the magnitude of an applied compression will continuously decrease when it is held under a constant deformation as can occur with foraminal stenosis or disc herniation. Conversely, when the compression magnitude is held constant, strain throughout the nerve root will continuously increase. Therefore, the loading conditions of a nerve root compression must be considered when determining the

relative effects of magnitude and duration on mediating circulatory and neuronal responses during compression. Future studies should further define the relative contributions of compression magnitude and duration on impaired axonal conduction by also evaluating intraradicular blood flow and the structural integrity of the axonal plasma membrane during a nerve root compression. Such studies would give further insight into role of nerve root biomechanics in mediating the pathophysiology that develops in root *at the time of injury*.

Recent *in vitro* studies suggest that transcriptional regulation of both GLT-1 and GFAP by ceftriaxone is mediated by NF- $\kappa$ B (Bachetti et al. 2010, Ghosh et al. 2011, Lee et al. 2008, Yang et al. 2009). Both the 10 $\mu$ g and the 150 $\mu$ g dose of ceftriaxone upregulated spinal GLT-1, but only the 10 $\mu$ g dose reduced the normal upregulation of spinal GFAP after a painful nerve root compression (Nicholson et al. 2013a). To date, no study has directly compared the dose-response of ceftriaxone on transcriptional regulation of GLT-1 and GFAP in cultured astrocytes. Studies that further elucidate the mechanism(s) by which ceftriaxone modulates astrocytic GLT-1 and GFAP expression would help to further define the role of astrocytes after a painful nerve root compression and could potentially aid clinicians and pharmacologists in developing more potent therapeutic agents for alleviating radicular pain.

Because Riluzole is already FDA-approved for the treatment of amyotrophic lateral sclerosis (ALS) and is currently in clinical trials as a treatment for spinal cord injury (Fehlings et al. 2012), it has foreseeable potential to be translated from animal studies into clinical use for other types of neural tissue trauma, including nerve root compression. However, there are some important considerations regarding its use as a

treatment for cervical radicular pain. Although *in vitro* studies suggest that Riluzole may enhance neuronal survival and even promote neuronal growth, Riluzole's effects *in vivo* suggest that this drug can only prevent and/or inhibit neuronal degeneration (Coderre et al. 2007, Fehlings et al. 2012, Sung et al. 2003, Wu et al. 2013). Based on these animals studies, Riluzole is unlikely capable of restoring normal axonal morphology or function once degeneration has fully developed after a painful nerve root compression at day 7 (Coderre et al. 2007, Hubbard & Winkelstein 2008, Sung et al. 2003, Wu et al. 2013). In fact, because of this, the previously reported clinical trial design for Riluzole administered it within 12 hours after a traumatic spinal cord injury (Fehlings et al. 2012). For radiculopathy, particularly those cases with a slow onset associated with foraminal spondylosis or a bulging disc, it is not feasible to identify or implement treatment over such a short treatment window. Determining whether there is a therapeutic window for Riluzole treatment in nerve root-mediated pain after a C7 transient cervical nerve root compression would be beneficial.

The studies presented in this thesis suggest that elevated synaptic glutamate due to impaired glutamate uptake contributes to the maintenance of cervical radicular pain (Nicholson et al. 2013a). However, synaptic glutamate concentrations were not measured nor was glutamate receptor activity evaluated. As such, alternative hypotheses could explain the findings in this thesis. Downregulation of spinal GLT- after a painful nerve root compression could reflect increased glutamate receptor activity at day 7 (Dong & Winkelstein 2010, Gwak & Hulsebosch 2005, Hudson et al. 2002, Lea & Faden 2001, Nicholson et al. 2012). Elevated glutamate receptor activity would decrease synaptic glutamate, which in turn, would downregulate GLT-1 (Aronica et al. 2003, Benediktsson

et al. 2012, Perego et al. 2000). Under that paradigm, there is no impaired glutamate uptake and the upregulation of GLT-1 with ceftriaxone increases the competition for synaptic glutamate between GLT-1 and the glutamate receptors, reducing the available glutamate that can activate those receptors (Inquimbert et al. 2012, Sung et al. 2003). Even though the increased expression of spinal GLAST at day 7 after a painful nerve root compression (Chapter 6; Nicholson et al. 2013a) may indicate that spinal glutamate concentrations are, indeed, elevated after a painful nerve root compression (Perego et al. 2000), identifying the relative contributions of glutamate transporters and glutamate receptors in mediating radicular pain are needed. Furthermore, the extracellular concentration of glutamate should be measured at days 1 and 7, which are the time-points identified here when elevated synaptic glutamate may perpetuate the development of axonal damage in the nerve root and when impaired glutamate uptake likely increases synaptic glutamate, respectively.

In summary, the studies presented in this thesis begin to define how the biomechanics of a nerve root compression can modify neuronal circuits in the primary afferents and in the dorsal horn that are relevant to persistent radicular pain. Although these studies lay the groundwork for defining the role of spinal excitatory signaling via glutamate in nerve root-mediated pain, the contribution of inhibitory signaling remains undefined for radicular pain. The primary afferents receive direct axo-axonic inhibitory input from GABAergic neurons (Todd 2010). Therefore, it is possible that the damage sustained to these afferents directly modulates inhibitory neuronal circuits in addition to modulating spinal glutamate transporter expression. Future studies that characterize both the excitatory *and* inhibitory circuits and the contribution of glial cells to each may be



useful to fully define the nociceptive pathways of nerve root-mediated pain. Overall, the studies in this thesis help guide future work understanding the excitatory system in the spinal cord and may also identify potential proteins for therapeutic targeting of radicular pain.

---

## APPENDIX A

### Protocol to Count Electrically-Evoked Action Potentials

---

This appendix details the spike counting methods used in the study described in Chapter 3. Spinal neurons in the superficial dorsal horn (150-350 $\mu$ m below the pial surface) of the C7 spinal cord were electrically evoked by a pair of stimulation probes inserted into the forepaw of the rat (Khan et al. 2002, LaPiro et al. 2009, Nicholson et al. 2011, Urch et al. 2003). After data acquisition, single units were isolated from the extracellular recordings through spike sorting in Spike2 (CED; Cambridge, UK). A post-stimulus histogram was generated in Spike2 to quantify the number of action potentials that were evoked within 10-40msec after application of the electrical stimulus (post-stimulus latency) (Fig. A.1). The 10-40 millisecond post-stimulus latency period was selected in order to exclude any artifact due to the stimulus and also to exclude spontaneous action potentials. Detailed methods for the surgical exposure, instrumentation and recording protocols are described in Chapter 3.

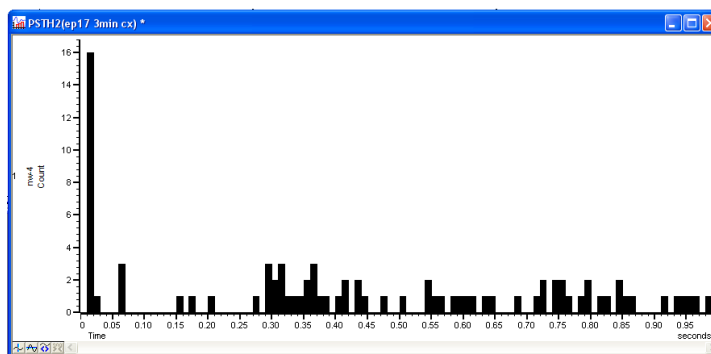


**Fig. A.1** Screen shot showing an example post-stimulus histogram generated by Spike2. The plot illustrates the number of spikes (vertical axis) that are counted in each 0.01 second bin for the first 1.0 second after the stimulus.

A detailed tutorial for spike-sorting and generating post-stimulus histograms is provided in the Spike2 Training Course Manual. This appendix provides additional details on data analysis, in particular, how to generate a post-stimulus histogram using the extracellular recordings collected in Chapter 3 (Appendix B). The first step is to spike-sort the channel that contains the extracellular recording. Once spike-sorting is complete, create a new channel for each WaveMark code that Spike2 generates corresponding to each recorded neuron. Next, the channel that contains the recording from the stimulus needs to be spike-sorted in order to make an Event+ channel using the same methods to spike-sort action potentials from the extracellular recordings.

Each WaveMark code must be analyzed separately in order to quantify the number of evoked action potentials for each firing unit. To create the post-stimulus histogram, select “Stimulus histogram” under the “New results view” in the “Analysis” menu. A “Settings” dialogue will appear (Fig. A.2).

- 1 – Select the WaveMark channel containing the firing unit of interest from the “Channels” drop-down menu.

- 2 – Set the analysis width to 1.0 seconds and the bin size to 0.01 in order to count the number of spikes that occur within each 10 millisecond bin for the first 1.0 second period after the stimulus.
- 3 – Select the Event+ channel from the “Trigger” drop-down menu.
- 4 – Press “Change” to apply the above settings.

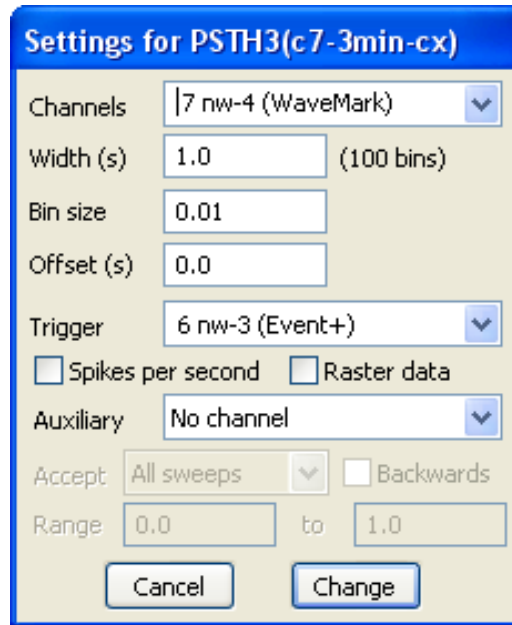


**Fig. A.2** Dialogue box specifying the settings for a post-stimulus histogram in Spike2. The WaveMark channel that contains the firing of a single unit is selected for “Channels” and the Event+ channel that contains the stimulus events is selected at the “Trigger.” The “width” of analysis identifies the period during which Spike2 analyzes the WaveMark after each stimulus and the “bin size” specifies the width of time into which spikes are binned.

With the settings in place, the next step is to quantify the number of spikes that were evoked by each stimulus. A post-stimulus histogram can be generated for the entire data or a subset of the data. To analyze a subset of the data, return to the window containing the data channels and place one vertical cursor on either end of data to be analyzed (Fig. A.3).

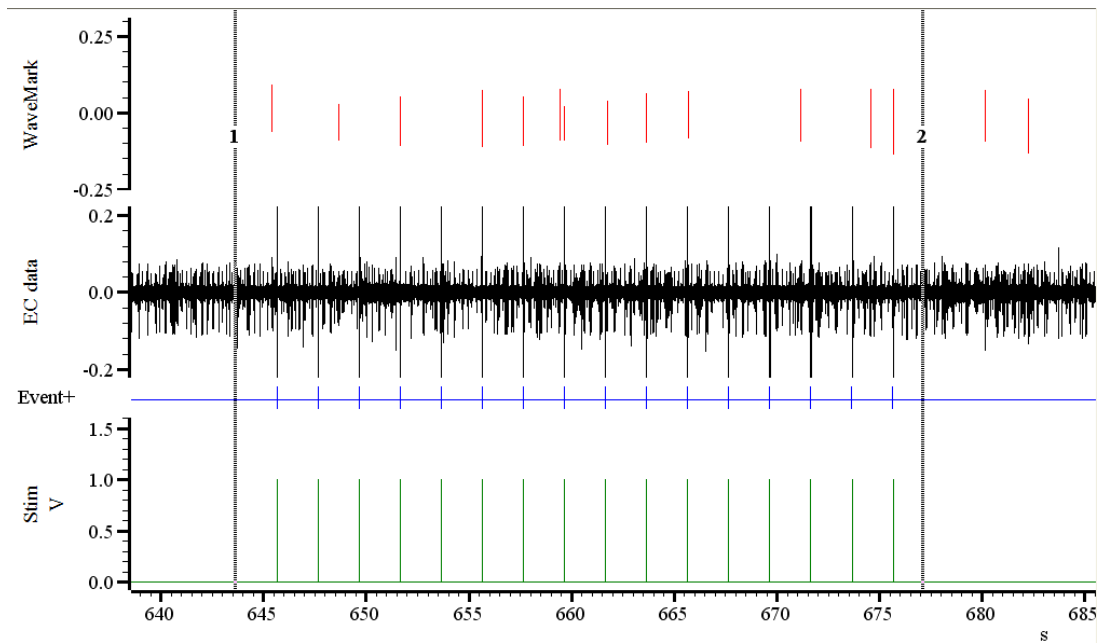


**Fig. A.3** Screen showing a 16-train stimulus (Stim) applied to the forepaw of the rat and extracellular potentials (EC data) recorded in the spinal cord. Also shown is the “Event+” and “WaveMark” channels generated by Spike2 to identify the onset time of each stimulus and the action potentials associated with a single neuron, respectively. Spike2 will generate a post-stimulus histogram for the data enclosed by two vertical cursors (1 & 2).

Return to the post-stimulus histogram window and open the “Process” dialogue box (Fig. A.4)

- 5 – Select the vertical cursor from the “Start time” drop-down menu that was placed at the beginning of the stimulus period.
- 6 – Select the vertical cursor from the “End time” drop-down menu that was placed at the end of the stimulus period.
- 7 – Make sure that the options to “Process all data” and “Clear result data before process” are selected.
- 8 – Select “Process” to generate the post-stimulus histogram (Fig. A.1).
- 9 – Copy the data (either from the “edit” menu or by pressing ctrl+c) and paste the data into an excel spread sheet. The first column will contain the post-

stimulus latency time (in 10 millisecond bins) and the second column will contain the number of spikes that occurred in that 10 millisecond period.

10 – Move the two vertical cursors to the next 16-train stimulus period and repeat steps 5-9 until each stimulus period is analyzed.

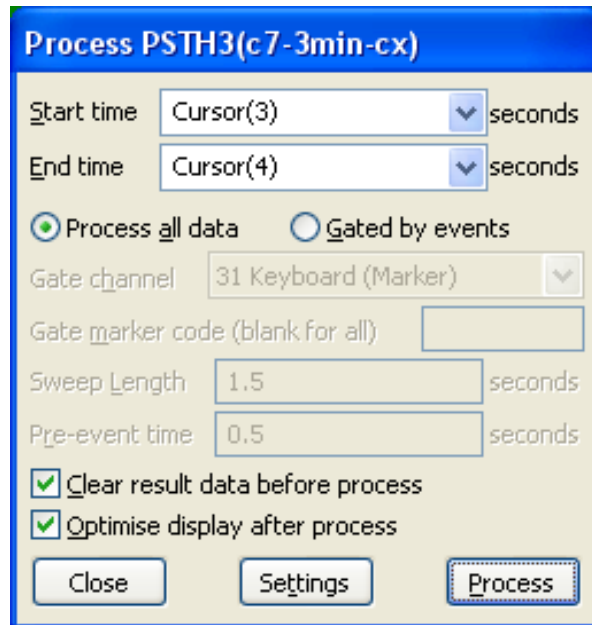


**Fig. A.4** The Spike2 Process dialogue for generating a post-stimulus histogram for the data within the identified “Start time” and “End time.”

---

## APPENDIX B

### **Electrically-Evoked Action Potential Counts During a Nerve Root Compression**

---

This appendix provides a summary of the number of action potentials for each neuron in the electrophysiologic studies presented in Chapter 3, for the sham and compression groups in the 15 minute (Table A.1) and 3 minute (Table A.2) studies. In each table, each neuron that is included is indicated by the rat number followed by a letter to distinguish neurons from the same rat.

**Table B.1** Number of action potentials evoked at each time-point starting with baseline (BL) and running through the compression (C) times and post-compression (P) times for each neuron in the 15 minute study.

time-point	group	sham n=4 neurons (1 rat)				compression n=10 neurons (3 rats)									
	neuron	3A	3B	3C	3D	5A	5B	5C	6A	6B	7A	7B	7C	7D	7E
	BL-1	6	12	2	7	1	4	3	1	2	3	4	8	2	3
	BL-2	4	19	1	12	2	4	5	2	1	5	7	0	4	6
	BL-3	7	9	7	6	2	6	5	0	0	0	6	5	3	4
	BL-4	6	12	6	8	2	6	2	0	1	2	3	3	3	2
	BL-5	7	16	4	7	1	6	3	1	1	1	1	4	3	1
	C1	1	10	2	12	1	4	1	1	2	0	3	4	4	1
	C2	4	14	1	9	1	3	2	2	1	0	3	1	3	0
	C3	6	12	0	10	2	2	1	1	1	0	3	1	1	0
	C4	3	12	4	5	4	4	3	1	2	0	2	1	2	0
	C5	1	15	1	14	1	2	1	2	1	0	2	1	1	0
	C6	6	12	2	5	1	1	2	1	3	0	2	1	1	0
	C7	5	16	3	7	2	1	0	1	0	0	3	1	0	0
	C8	3	15	2	2	4	1	1	1	0	0	1	0	0	0
	C9	5	7	1	9	0	4	0	1	2	0	1	0	0	0
	C10	4	16	1	9	0	1	0	2	0	0	4	0	0	0
	C11	3	8	1	10	0	1	2	0	0	0	2	0	0	0
	C12	7	11	2	11	2	6	4	0	1	0	1	0	1	0
	C13	7	13	2	10	1	4	3	0	2	0	3	0	0	1
	C14	6	15	4	10	1	11	2	0	2	0	1	1	0	0
	C15	9	16	2	11	6	7	6	0	0	0	1	0	1	0
	P1	9	12	1	10	1	6	3	0	1	0	0	0	2	0
	P2	7	13	1	11	1	5	2	1	0	0	2	0	0	1
	P3	6	14	1	11	0	9	2	1	2	0	1	0	1	0
	P4	8	13	1	13	2	1	2	2	1	0	0	0	1	0
	P5	4	15	1	9	2	5	0	1	1	0	1	0	0	0
	P6	7	10	0	19	0	1	1	1	0	0	2	0	2	0
	P7	7	15	1	15	0	3	3	0	1	0	1	0	1	0
	P8	9	14	2	11	0	3	3	1	2	0	1	0	3	0
	P9	5	15	1	10	1	5	1	0	0	0	0	1	1	0
	P10	6	18	2	12	4	2	1	0	1	0	0	0	0	0



**Table B.2** Number of action potentials evoked at each time-point starting with baseline (BL) and running through the compression (C) times and post-compression (P) times for each neuron in the 3 minute study.

time-point	group	sham n=3 neurons (1 rat)			compression n=9 neurons (6 rats)								
	neuron	16A	16B	16C	13A	14A	15F	17A	17B	18A	19A	19C	19D
	BL-1	70	4	1	4	3	5	20	2	2	1	1	3
	BL-2	52	6	2	7	2	1	23	0	1	0	1	1
	BL-3	50	3	1	16	4	2	20	1	0	1	1	2
	BL-4	56	10	1	11	0	2	28	0	0	1	0	0
	BL-5	47	10	1	10	3	2	23	0	2	1	1	0
	C1	37	3	1	11	3	2	14	0	0	1	0	0
	C2	43	6	1	8	3	1	23	1	0	0	0	0
	C3	52	8	1	13	2	0	16	0	0	0	0	0
	P1	39	6	1	7	0	0	14	0	0	0	3	1
	P2	53	8	2	10	3	0	16	0	0	1	0	0
	P3	63	8	3	9	0	1	11	0	0	0	1	2
	P4	74	4	1	9	1	1	8	0	2	0	0	1
	P5	64	6	1	6	2	2	15	1	1	0	1	1
	P6	73	5	1	12	1	0	37	0	0	0	0	0
	P7	75	3	0	9	3	0	23	0	1	0	1	0
	P8	85	5	0	11	0	2	17	0	2	1	2	1
	P9	70	3	1	8	1	0	22	1	2	1	1	0
	P10	78	6	0	7	2	0	12	2	0	1	1	1

---

## APPENDIX C

### Mechanical Allodynia & Thermal Hyperalgesia

---

The tables within this appendix detail the individual behavioral responses for mechanical allodynia and thermal hyperalgesia for each rat included in the behavioral studies in Chapters 4-7. Mechanical allodynia is reported as the number of responses evoked by 30 stimulations with 1.4, 2.0, 4.0 or 10gf von Frey filaments, as noted in each table. Thermal hyperalgesia is reported as the amount of time (seconds) that a thermal stimulus was applied to the forepaw before the rat withdrew the paw from the stimulus (withdrawal latency). For each testing session, the withdrawal latency was measured three times and the average is reported here. Mechanical allodynia and thermal hyperalgesia are reported for the ipsilateral and contralateral forepaws, separately in each table.

The behavioral data for each group is arranged by each chapter. Responses are reported for baseline (BL) and post-injury day 1 (D1) through day 7 (D7). Individual responses at each day are shown in Tables C.1-C.4 for all of the rats that are presented in the studies in Chapter 4. Tables C.1 and C.2 summarize mechanical allodynia following a 3, 10 or 15 minute compression, or sham exposure (Section 4.3). Thermal hyperalgesia and mechanical allodynia following a 3 or a 15 minute compression or sham procedures (Section 4.4) are shown in Tables C.3 and C.4, respectively. The behavioral data in

Tables C.3 and C.4 also correspond to the rats used in the glutamate transporter characterization study presented in Chapter 5. Table C.5 details the individual mechanical allodynia responses for the rats used in the electrophysiology study presented in Chapter 5 following a 3 or a 15 minute compression or the sham exposure.

Tables C.6 and C.7 show individual mechanical allodynia and thermal hyperalgesia responses, respectively, following a painful compression treated with 10 $\mu$ g or 150 $\mu$ g of ceftriaxone (*injury+10 $\mu$ g*, *injury+105 $\mu$ g*) or the saline vehicle (*injury+saline*) or sham procedures treated with saline (*sham+saline*). Those studies are reported in Chapter 6. Table C.8 details the individual mechanical allodynia responses for the rats in those same ceftriaxone treatment groups (*injury+10 $\mu$ g*, *injury+150 $\mu$ g*, *injury+saline*, *sham+saline*) that were used in the electrophysiology study (Chapter 6). Tables C.9-C.11 detail the individual responses for the rats used in the Riluzole study (Chapter 7). Specifically, mechanical allodynia and thermal hyperalgesia are shown in Tables C.9 and C.10, respectively, for the rats used in the immunohistological study after a painful compression treated with Riluzole (*injury+Riluzole*) or the vehicle ( $\beta$ -cyclodextrin; *injury+vehicle*), or sham procedures treated with  $\beta$ -cyclodextrin (*sham+vehicle*). For those same injury groups, (*injury+Riluzole*, *injury+vehicle*, *sham+vehicle*), mechanical allodynia responses are itemized for the rats that spinal electrophysiological recordings were made from (Table C.11).

**Table C.1** Mechanical allodynia (number of paw withdrawals) for testing with a 4.0gf filament following a 3 minute or 10 minute nerve root compression, or sham procedures (corresponding to Section 4.3).

group	rat ID	ipsilateral					contralateral				
		BL	D1	D3	D5	D7	BL	D1	D3	D5	D7
sham	11	0	1	1	1	0	2	0	0	1	0
	29	0	2	0	2	2	1	2	0	0	0
	79	0	1	1	2	2	0	0	0	0	1
	80	0	0	1	1	2	0	0	1	1	1
	104	0	0	1	0	0	0	0	1	0	0
	105	2	2	3	2	2	1	0	2	1	2
3 minute	44	2	4	4	3	3	0	0	0	1	2
	49	0	1	0	0	1	0	0	0	1	1
	52	0	4	4	1	1	0	1	2	1	0
	98	0	1	0	1	2	0	0	0	0	0
	99	0	1	2	1	1	0	0	1	1	2
	103	0	1	0	1	1	1	1	0	0	0
10 minute	22	0	5	4	4	3	1	1	0	1	1
	26	1	7	4	5	5	1	2	1	1	0
	28	0	3	9	3	7	1	1	1	0	1
	90	1	6	8	9	9	0	0	0	0	0
	93	0	7	6	4	7	0	1	0	0	2
	94	1	14	8	6	7	1	7	7	5	5

**Table C.2** Mechanical allodynia (number of paw withdrawals) for testing with a 4.0gf filament following a 15 minute nerve root compression or sham procedures (corresponding to Section 4.3).

group	rat ID	ipsilateral					contralateral				
		BL	D1	D3	D5	D7	BL	D1	D3	D5	D7
sham	14	0	0	0	0	0	0	1	0	0	0
	15	0	1	1	1	0	2	0	0	1	0
	19	0	0	0	0	0	0	0	0	0	0
	21	0	2	0	2	2	1	2	0	0	0
15 minute	12	1	11	15	7	10	0	6	8	3	3
	13	0	6	8	6	9	0	0	3	2	2
	16	0	8	4	7	6	0	2	1	0	0
	17	1	8	7	5	8	0	0	2	0	0
	18	1	7	8	9	9	1	2	3	4	4

**Table C.3** Thermal hyperalgesia (average latency time in seconds) following a 3 minute or a 15 minute nerve root compression or sham procedures (corresponding to studies in Sections 4.4 & 5.3).

group	rat ID	ipsilateral			contralateral		
		BL	D1	D7	BL	D1	D7
sham	216	9.79	10.69	9.36	9.39	11.35	11.12
	220	10.46	10.60	10.12	9.11	9.13	9.30
	226	10.80	10.29	10.15	10.40	9.69	8.75
	228	10.77	10.02	8.80	9.49	10.42	9.63
	229	10.10	9.16	10.46	9.92	8.86	10.26
	234	9.85	7.92	8.36	10.98	8.77	9.41
	238	10.31	9.19	8.87	10.27	7.87	8.58
	109	10.45	9.25	--	10.07	10.85	--
	113	11.10	11.96	--	9.25	10.64	--
	254	10.05	9.09	--	10.52	9.86	--
	258	8.29	9.28	--	10.73	11.39	--
	280	9.12	9.08	--	8.77	9.52	--
	281	10.83	10.74	--	10.88	12.98	--
	282	9.57	8.35	--	9.92	9.49	--
	3 minute	218	9.94	6.55	6.54	10.71	9.09
223		9.82	8.76	9.03	11.39	10.01	9.42
225		11.34	9.92	9.84	11.05	10.46	11.01
227		9.30	9.65	9.14	10.04	8.70	11.06
231		10.97	10.27	9.34	9.93	10.23	10.77
235		9.58	8.49	6.54	9.57	7.97	8.18
236		10.62	9.10	8.82	9.85	7.35	9.41
251		11.48	9.54	--	9.02	12.09	--
253		10.29	9.11	--	10.35	8.09	--
255		8.10	11.23	--	10.21	9.80	--
275		12.07	12.36	--	10.76	11.79	--
276		11.77	8.99	--	9.80	12.29	--
277		10.53	8.34	--	8.67	12.75	--
278		8.23	10.01	--	10.88	10.80	--
15 minute		213	9.95	5.95	8.16	8.80	9.72
	214	10.24	5.22	5.76	10.14	10.01	9.93
	217	10.22	7.01	5.53	9.56	6.91	10.22
	224	10.73	8.27	6.98	10.38	10.48	9.34
	230	9.38	9.51	7.32	10.04	9.25	8.74
	233	9.56	7.75	6.98	10.24	8.13	8.28
	237	8.95	7.29	7.52	9.74	10.73	10.42
	106	8.18	6.15	--	8.14	8.62	--
	107	8.08	5.36	--	8.08	9.77	--
	108	9.96	7.91	--	9.59	9.73	--
	111	12.03	7.39	--	10.71	10.67	--
	112	8.04	7.83	--	8.24	12.75	--
	252	10.04	4.89	--	8.05	8.78	--
	256	8.09	5.76	--	9.01	12.34	--

**Table C.4** Mechanical allodynia (number of paw withdrawals) for a testing with a 4.0gf filament following a 3 minute or a 15 minute nerve root compression or sham procedures (corresponding to studies in Sections 4.4 & 5.3).

group	rat ID	ipsilateral			contralateral		
		BL	D1	D7	BL	D1	D7
sham	216	2	1	3	1	0	2
	220	0	1	0	0	0	1
	226	1	2	1	1	1	2
	228	0	2	2	1	1	0
	229	2	1	2	1	1	2
	234	0	2	0	2	2	0
	238	1	2	1	0	0	1
	109	0	1	--	1	1	--
	113	0	1	--	0	0	--
	254	1	2	--	1	1	--
	258	1	3	--	0	2	--
	280	2	1	--	0	1	--
	281	1	0	--	0	3	--
	282	1	0	--	1	2	--
	3 minute	218	1	3	1	0	0
223		1	0	1	0	1	1
225		0	1	1	1	0	0
227		1	2	2	0	0	1
231		0	1	1	0	1	0
235		2	3	9	1	2	5
236		1	4	3	1	0	0
251		0	1	--	1	0	--
253		0	3	--	1	1	--
255		1	2	--	0	1	--
275		2	1	--	1	2	--
276		3	3	--	2	1	--
277		0	2	--	0	3	--
278		1	1	--	2	1	--
15 minute	213	0	4	3	1	1	1
	214	0	7	7	0	1	0
	217	0	7	5	1	1	2
	224	3	7	9	3	3	5
	230	1	3	5	0	0	1
	233	2	8	8	1	1	2
	237	3	3	7	2	2	2
	106	1	8	--	0	2	--
	107	0	6	--	0	0	--
	108	1	6	--	0	2	--
	111	1	5	--	1	0	--
	112	0	6	--	0	0	--
	252	1	8	--	1	1	--
	256	2	4	--	2	2	--

**Table. C.5** Mechanical allodynia (number of paw withdrawals) in the forepaw for testing with a 4.0gf filament following compression applied for 3 minutes or 15 minutes, or sham procedures (corresponding to studies in Section 5.4).

group	id	ipsilateral			contralateral		
		BL	D1	D7	BL	D1	D7
sham	125	0	2	2	1	1	2
	154	0	1	1	0	1	1
	186	0	1	1	1	1	1
	189	1	3	0	2	2	0
	190	2	1	1	3	2	1
	201	2	1	2	2	1	1
	204	0	2	1	0	1	1
	205	0	2	0	1	1	0
	JRS 7	0	0	0	0	1	0
	JRS 9	0	1	3	2	0	1
	JRS 11	0	0	1	0	1	0
	JRS 42	0	0	1	1	1	1
	JRS 43	0	0	0	1	0	0
	3 minute	315	1	2	2	0	1
316		1	1	3	0	1	0
15 minute	122	1	7	6	0	0	2
	126	0	3	2	0	0	0
	127	0	6	6	0	0	1
	153	0	5	5	0	0	1
	188	2	4	4	1	1	1
	192	1	7	6	1	0	0
	203	0	4	5	0	1	0
	206	1	6	5	0	0	1
	JRS 8	4	3	5	0	1	2
	JRS 10	4	3	5	1	0	1
	JRS 30	4	6	7	1	1	1
	JRS 34	3	4	8	0	1	3
	JRS 41	3	1	0	1	0	0

**Table C.6** Mechanical allodynia (number of paw withdrawals) for daily treatments with 10µg or 150µg ceftriaxone or saline after injury (*injury+10µg*, *injury+150µg*, *injury+saline*) or sham (*sham+saline*) (corresponding to studies in Chapter 6).

	group	rat ID	ipsilateral							contralateral								
			BL	D1	D2	D3	D4	D5	D6	D7	BL	D1	D2	D3	D4	D5	D6	D7
1.4gf filament	sham+saline	131	0	1	1	1	1	1	1	0	1	0	0	1	0	1	0	0
		171	2	3	2	1	1	0	1	2	2	3	1	2	2	0	0	1
		175	0	1	0	1	1	2	0	1	0	1	0	1	0	1	0	0
		178	1	0	2	1	1	1	0	1	0	0	0	0	0	0	0	0
		179	0	2	0	0	1	0	1	0	0	0	0	0	0	0	0	0
		183	0	0	0	1	1	0	1	0	0	0	0	1	0	0	1	0
		184	0	0	0	1	1	1	1	1	0	0	0	0	1	1	0	0
	injury+saline	128	0	2	0	2	3	4	5	3	0	0	0	0	1	0	2	1
		129	0	2	2	3	4	3	4	5	1	0	1	1	1	1	0	1
		130	0	1	0	1	0	1	1	1	0	0	0	0	0	0	1	0
		164	0	0	1	0	0	1	1	1	1	0	2	2	0	0	1	0
		165	1	1	3	2	3	3	2	2	1	1	1	1	1	0	1	1
		174	0	2	0	0	1	1	2	2	0	0	0	0	0	0	0	1
		182	0	0	1	2	1	2	2	2	0	0	0	0	0	2	0	0
	injury+10µg	138	2	2	1	0	0	0	1	1	0	0	0	1	1	1	1	0
		139	0	2	0	1	1	1	1	1	2	1	0	0	0	0	0	1
		140	0	1	0	0	0	0	1	1	1	0	0	0	0	0	1	1
		141	2	3	1	2	1	0	1	3	2	1	1	0	1	1	2	2
		168	1	4	2	2	3	1	3	2	0	1	1	0	2	0	0	1
		169	0	2	2	0	2	1	0	0	1	0	0	1	1	0	0	1
		176	1	1	1	1	1	1	0	0	1	0	0	1	0	0	0	0
177	0	3	2	1	1	2	1	2	1	0	1	0	0	0	1	1		
injury+150µg	136	0	0	0	0	0	1	0	0	0	0	0	0	0	0	0	0	
	142	0	0	0	0	0	2	2	1	0	0	0	0	0	2	0	0	
	143	1	1	2	2	1	2	2	1	1	2	0	1	0	1	0	2	
	167	0	2	3	0	0	1	0	1	0	0	0	0	1	0	1	1	
	172	1	2	0	1	0	0	0	1	1	0	0	1	0	0	0	0	
	173	0	4	2	1	0	1	0	1	0	0	0	1	0	0	0	0	
	180	1	2	1	0	0	0	0	1	1	0	1	0	0	0	1	0	
181	0	4	2	2	3	1	1	1	0	3	0	1	1	1	0	0		
2.0gf filament	sham+saline	131	0	0	1	1	2	2	1	2	0	1	0	0	1	0	1	1
		171	1	4	1	2	2	2	2	2	1	4	2	0	1	2	2	2
		175	0	2	3	2	1	2	1	1	1	0	1	0	0	0	0	0
		178	0	0	2	2	0	2	2	2	0	0	0	0	0	0	1	1
		179	0	3	1	1	2	2	1	2	0	0	0	0	0	0	0	0
		183	0	1	1	2	1	1	1	1	0	0	0	0	0	0	2	0
		184	1	1	1	1	2	1	1	2	1	0	0	0	0	0	0	0
	injury+saline	128	0	2	3	5	6	5	6	5	0	1	0	1	1	3	2	1
		129	0	5	6	5	7	5	5	5	1	2	1	1	2	1	1	2
		130	0	2	3	2	3	3	5	4	0	1	0	0	1	0	2	0
		164	0	4	2	1	2	3	3	2	0	0	1	0	1	1	0	0
		165	0	3	5	4	4	6	3	3	1	0	0	1	0	2	1	1
		174	0	4	4	5	5	5	4	5	0	0	0	0	0	1	0	1
		182	0	6	6	5	4	4	5	8	1	0	0	1	1	0	1	1
injury+10µg	138	2	4	2	2	1	1	2	2	1	0	0	0	0	1	0	1	
	139	1	5	0	1	1	0	1	0	1	1	0	0	1	0	1	0	
	140	0	3	1	2	0	0	0	2	1	0	0	0	0	0	0	0	



		ipsilateral							contralateral									
group	rat ID	BL	D1	D2	D3	D4	D5	D6	D7	BL	D1	D2	D3	D4	D5	D6	D7	
2.0gf filament (cont.)	injury+10µg (cont.)	141	3	4	2	2	0	2	2	6	3	1	2	1	0	3	3	4
		168	2	5	4	1	3	1	2	3	1	2	2	2	1	1	0	0
		169	0	7	3	1	1	1	0	1	0	1	1	0	1	0	0	1
		176	0	4	6	5	4	4	3	1	0	1	1	1	2	1	0	0
		177	1	7	4	5	5	4	4	2	1	1	0	0	1	1	1	1
	injury+150µg	136	0	6	2	1	0	1	0	3	0	1	0	0	0	2	0	2
		142	0	2	4	2	1	2	3	2	0	0	1	2	1	2	2	0
		143	2	4	3	3	0	4	3	5	1	0	0	0	0	3	3	3
		167	0	4	3	3	2	2	3	2	0	1	0	0	0	1	0	1
		172	1	6	2	1	3	0	1	1	1	0	0	0	0	0	1	0
		173	1	5	4	4	2	3	2	3	0	1	1	0	0	0	0	0
		180	0	5	2	2	2	1	1	3	0	0	0	0	0	0	0	0
		181	0	9	5	3	3	3	3	4	1	2	2	1	1	1	0	1
	sham+saline	131	0	2	2	2	2	1	2	2	1	0	1	0	1	0	0	0
		171	2	5	2	2	2	2	2	2	2	5	3	2	2	1	2	1
		175	1	2	2	1	1	2	1	1	1	0	0	0	0	0	0	0
		178	0	2	2	2	0	2	2	2	1	1	0	0	0	0	1	0
		179	1	3	1	0	2	2	1	0	1	0	0	0	0	0	0	1
183		1	0	2	0	1	1	2	1	1	0	0	1	1	1	1	0	
184		1	1	0	1	2	1	1	2	0	0	0	0	1	1	0	0	
4.0gf filament		injury+saline	128	0	6	6	6	8	8	9	8	0	0	1	2	2	2	3
	129		1	8	7	8	7	7	7	10	2	3	2	3	2	2	2	3
	130		1	4	3	3	4	4	6	4	0	2	1	1	0	1	2	1
	164		0	5	6	5	4	6	6	5	1	0	2	0	0	2	3	0
	165		1	6	6	6	6	7	6	7	1	1	2	2	0	1	2	1
	174		0	7	4	6	5	5	4	5	0	0	1	0	0	1	0	1
	182		1	8	7	6	6	7	6	8	0	0	0	0	1	1	0	1
	injury+10µg	138	2	8	2	1	1	2	0	1	2	0	0	0	0	1	0	2
		139	0	6	1	1	2	1	1	0	0	1	1	0	2	0	1	0
		140	0	6	2	1	0	1	1	2	1	2	1	0	0	0	1	0
		141	2	7	2	2	2	5	3	7	2	2	1	1	1	5	3	7
		168	1	8	6	3	5	2	3	3	0	1	2	3	1	1	1	1
		169	1	8	2	1	2	1	1	2	0	3	1	0	1	2	0	0
		176	0	7	6	3	4	4	3	3	0	1	1	1	2	1	0	0
		177	1	9	5	3	5	4	4	3	1	2	0	1	1	1	1	1
	injury+150µg	136	0	8	1	2	1	2	0	0	0	4	0	0	0	1	0	0
		142	0	6	5	1	0	3	2	4	0	1	0	0	0	2	1	3
		143	1	7	7	3	2	3	4	6	1	0	0	2	1	3	1	5
167		0	6	6	4	2	3	1	3	0	2	0	2	1	1	0	1	
172		0	7	4	1	3	0	1	1	0	0	0	0	0	0	1	0	
173		1	8	4	4	2	3	2	3	0	0	0	0	0	0	0	0	
180		1	7	4	3	1	2	2	3	0	0	0	0	0	0	1	0	
181		0	8	6	4	4	3	4	4	1	2	0	0	1	0	1	1	

**Table C.7** Thermal hyperalgesia (average latency time in seconds) for daily treatments with 10 $\mu$ g or 150 $\mu$ g ceftriaxone after injury (*injury+10 $\mu$ g*, *injury+150 $\mu$ g*) or the saline vehicle after injury (*injury+saline*) or sham procedures (*sham+saline*) (corresponding to studies in Chapter 6).

	rat ID	ipsilateral			contralateral		
		BL	D1	D7	BL	D1	D7
sham+saline	131	10.68	11.91	8.20	9.92	8.76	10.35
	171	9.54	7.98	9.40	10.56	7.50	9.65
	175	8.89	10.54	8.01	12.01	10.35	9.76
	178	10.54	6.74	10.78	10.10	8.39	9.88
	179	12.54	6.74	8.92	11.31	7.01	9.96
	183	10.50	11.87	10.51	11.45	10.31	9.88
	184	8.56	10.49	10.08	9.72	10.51	9.77
injury+saline	128	7.87	10.55	5.52	7.74	10.28	8.56
	129	10.37	8.09	5.83	10.22	11.23	7.73
	130	8.48	6.52	5.52	9.94	7.39	8.18
	164	8.51	8.34	5.97	7.44	10.80	8.16
	165	8.56	6.57	4.63	7.78	10.52	7.41
	174	9.79	6.95	5.91	8.07	9.71	9.22
	182	11.04	5.07	7.10	11.18	11.62	12.03
injury+10 $\mu$ g	138	10.71	8.00	12.71	11.09	9.47	13.20
	139	11.65	8.91	13.08	8.43	15.13	10.93
	140	10.37	4.66	14.39	10.43	13.58	17.90
	141	11.72	7.94	9.47	8.97	12.54	10.06
	168	10.29	5.99	10.51	9.94	8.66	10.14
	169	10.53	7.63	7.50	12.64	8.12	7.75
	176	10.08	6.42	8.33	10.83	10.80	9.30
	177	11.08	5.00	4.68	9.56	7.73	9.17
injury+150 $\mu$ g	136	7.91	8.08	12.77	8.77	12.07	13.30
	142	9.63	8.37	13.80	6.79	10.43	8.91
	143	9.44	8.14	10.24	11.40	11.03	8.46
	167	11.22	5.05	7.53	10.10	9.15	8.65
	172	10.46	8.43	8.85	11.23	11.32	9.35
	173	9.40	7.80	10.01	7.35	10.13	9.25
	180	9.56	5.61	8.73	8.56	10.33	10.51
	181	10.60	7.48	11.43	9.68	12.31	10.85

**Table C.8** Mechanical allodynia (number of paw withdrawals) for daily treatments with 10µg or 150µg ceftriaxone or saline after injury (*injury+10µg*, *injury+150µg*, *injury+saline*) or sham (*sham+saline*) (corresponding to studies in Chapter 6).

		ipsilateral			contralateral			
group	rat ID	BL	D1	D7	BL	D1	D7	
1.4gf filament	sham+saline	301	1	1	0	0	2	0
		302	2	0	1	2	0	1
		303	0	0	2	1	1	0
		304	2	1	0	0	0	1
		305	1	2	1	1	1	2
		306	0	2	2	0	0	0
		313	0	0	2	2	0	0
		314	2	0	1	1	0	0
	injury+saline	287	1	2	0	1	2	0
		288	0	1	0	1	0	1
		297	1	2	5	2	1	1
		298	1	8	6	1	1	2
		299	1	4	2	1	2	0
		300	0	3	1	0	1	2
		307	2	1	1	1	0	0
		308	1	1	1	1	1	1
	injury+10µg	285	0	2	2	1	1	1
		286	0	1	2	1	0	0
		290	0	0	1	2	0	0
		293	0	1	2	2	0	1
		294	1	0	0	0	0	1
		296	0	0	0	1	1	0
		311	0	3	1	1	0	0
		312	0	1	0	0	0	1
	injury+150µg	283	1	3	0	0	0	2
		284	1	1	0	1	1	1
		289	0	1	0	0	1	1
		291	1	0	0	0	0	0
292		1	4	1	1	1	1	
295		0	4	0	0	0	0	
309		1	1	2	1	0	1	
310		2	4	0	2	0	1	
2.0gf filament	sham+saline	301	2	2	2	0	1	0
		302	1	1	1	1	1	1
		303	2	3	2	1	2	2
		304	0	0	1	0	0	2
		305	0	3	0	0	2	0
		306	2	1	2	2	2	2
		313	3	1	2	2	0	0
		314	4	2	2	3	1	1
	injury+saline	287	2	7	5	0	2	1
		288	1	8	6	2	1	0
		297	3	9	8	1	2	3
		298	2	11	11	2	3	4
		299	1	9	8	1	3	3
		300	0	5	10	0	0	2
307	2	7	6	0	1	1		

		ipsilateral			contralateral				
group	rat ID	BL	D1	D7	BL	D1	D7		
2.0gf filament (cont.)	injury+saline	308	3	7	8	2	1	3	
	injury+10µg	285	1	7	2	1	2	1	
		286	2	6	2	2	1	0	
		290	0	7	1	1	2	2	
		293	2	8	4	1	0	1	
		294	0	7	1	1	1	2	
		296	1	8	0	1	1	0	
		311	0	8	1	0	2	2	
		312	1	6	2	2	0	1	
		injury+150µg	283	2	5	4	1	1	1
	284		2	6	2	2	0	1	
	289		1	8	4	1	0	3	
	291		1	5	5	2	1	0	
	292		2	7	2	1	1	0	
	295		1	6	3	0	0	1	
	309		0	5	3	1	1	1	
	310		1	9	1	2	2	1	
	4.0gf filament	sham+saline	301	2	4	3	2	4	5
302			3	3	5	4	4	4	
303			2	5	4	1	5	3	
304			1	3	2	2	3	3	
305			6	8	5	5	5	4	
306			3	6	4	4	6	3	
313			1	0	4	1	0	3	
314			5	3	3	4	4	3	
injury+saline		287	2	8	7	2	4	4	
		288	3	11	7	2	5	3	
		297	5	11	9	4	3	4	
		298	3	13	11	4	7	5	
		299	2	15	11	2	8	4	
		300	1	11	11	1	5	5	
		307	4	11	9	1	2	2	
		308	3	7	10	4	1	4	
		injury+10µg	285	3	9	2	3	5	0
			286	3	9	3	3	3	2
290			2	10	2	3	3	2	
293			3	12	6	3	6	3	
294			1	8	5	2	3	3	
296			3	8	1	4	2	1	
311			1	11	3	2	5	2	
312			3	9	4	4	2	2	
injury+150µg		283	3	8	8	3	4	4	
		284	3	5	4	2	2	3	
		289	2	10	5	4	4	2	
		291	3	7	6	2	3	3	
		292	3	8	4	2	3	2	
		295	3	11	2	2	4	0	
	309	2	7	4	3	2	3		
	310	2	10	2	1	5	1		

**Table C.9** Mechanical allodynia (number of paw withdrawals) after a painful nerve root compression treated with Riluzole (*injury+Riluzole*) or the vehicle (*injury+vehicle*) or sham (*sham+vehicle*) (corresponding to studies in Chapter 7).

	group	rat ID	ipsilateral					contralateral						
			BL	D1	D2	D3	D5	D7	BL	D1	D2	D3	D5	D7
1.4gf filament	sham+vehicle	162	0	1	1	1	0	1	0	0	0	0	0	1
		193	1	1	1	0	1	1	0	0	2	1	0	1
		195	0	1	0	0	1	1	1	0	0	0	1	0
		196	1	1	0	1	0	0	0	1	1	0	0	0
		200	1	0	0	1	0	1	0	1	1	0	1	1
		211	0	1	0	0	0	0	0	0	0	1	0	1
		212	1	1	1	1	2	1	0	1	0	1	2	0
	injury+vehicle	156	1	1	2	1	1	4	0	0	0	0	1	1
		157	0	2	1	3	3	0	1	0	0	1	1	0
		163	1	4	3	3	2	3	2	0	1	1	0	3
		194	1	3	3	2	2	0	1	0	0	0	0	1
		198	0	1	2	1	2	2	0	0	0	2	0	1
		199	1	0	0	0	1	1	1	0	0	0	1	0
		210	0	2	1	0	1	0	0	0	1	0	0	1
	injury+Riluzole	147	0	0	2	0	1	0	0	0	0	0	0	1
		148	0	0	2	1	0	1	0	0	1	0	0	0
		149	2	3	5	5	4	3	1	0	1	1	3	4
		158	0	2	2	1	2	2	0	1	0	0	0	0
159		0	1	1	2	1	0	1	1	0	1	1	0	
160		0	1	2	1	3	0	0	0	1	0	0	0	
161		1	2	2	2	3	2	2	1	2	2	3	1	
2.0gf filament	sham+vehicle	162	0	0	2	2	1	2	0	0	0	0	0	1
		193	0	2	2	0	1	1	0	0	1	1	1	1
		195	1	1	2	1	2	1	0	1	1	1	1	0
		196	1	0	0	0	1	1	1	0	1	1	1	0
		200	0	1	2	2	1	2	1	1	1	0	2	0
		211	0	1	0	1	1	2	0	1	0	0	1	2
		212	1	2	1	1	0	1	1	0	1	0	1	0
	injury+vehicle	156	0	4	3	2	5	7	0	0	0	0	2	0
		157	0	6	4	6	4	4	1	0	1	2	1	1
		163	1	5	3	6	5	4	0	3	0	3	0	3
		194	0	4	3	5	5	1	0	0	1	2	0	0
		198	1	1	6	7	9	6	1	0	1	1	2	1
		199	0	2	3	3	7	5	1	0	1	1	1	0
		210	0	2	2	1	0	1	0	1	0	0	1	1
	injury+Riluzole	147	0	2	1	2	2	3	1	1	0	0	0	1
		148	0	2	2	1	1	1	0	1	1	0	0	1
		149	2	5	4	6	4	4	1	2	1	2	2	2
		158	0	5	4	2	3	3	0	0	0	0	2	1
159		0	4	2	3	0	2	1	1	1	0	0	0	
160		0	4	4	4	4	2	0	0	2	1	1	0	
161		1	3	2	4	2	4	1	1	1	3	1	3	

		ipsilateral						contralateral						
group	rat ID	BL	D1	D2	D3	D5	D7	BL	D1	D2	D3	D5	D7	
4.0gf filament	sham+vehicle	162	1	2	3	3	1	2	1	1	1	0	0	1
		193	0	2	3	2	3	2	0	1	0	1	1	1
		195	1	3	1	3	3	1	0	0	0	1	0	1
		196	0	2	0	1	2	2	0	0	0	0	0	0
		200	1	2	2	2	1	2	1	2	1	1	0	0
		211	0	1	0	1	2	1	0	0	2	2	2	1
		212	2	2	3	2	3	2	0	1	0	1	1	0
	injury+vehicle	156	0	4	4	6	7	8	0	0	0	1	1	1
		157	0	7	5	8	6	4	1	0	0	2	1	0
		163	2	2	5	8	7	8	1	0	2	3	1	4
		194	0	6	7	7	8	8	1	0	2	2	2	0
		198	1	4	9	8	8	6	1	0	1	1	2	2
		199	1	7	5	4	6	5	0	2	0	1	0	1
		210	1	5	5	4	4	5	0	1	0	0	1	1
	injury+Riluzole	147	0	6	2	3	2	3	1	1	0	0	0	0
		148	0	7	3	2	4	2	0	1	0	0	0	2
		149	1	9	6	6	4	4	1	2	2	2	3	4
		158	1	6	3	1	4	4	1	0	0	0	0	0
		159	0	7	2	3	2	1	1	0	0	1	1	0
		160	0	5	4	3	4	3	0	0	1	0	0	2
		161	1	6	2	5	2	5	1	2	0	3	0	2

**Table C.10** Thermal hyperalgesia (average withdrawal latency in seconds) after a painful nerve root compression treated with Riluzole (*injury+Riluzole*) or the vehicle (*injury+vehicle*), or sham (*sham+vehicle*) (corresponding to studies in Chapter 7).

	rat ID	ipsilateral			contralateral		
		BL	D1	D7	BL	D1	D7
sham+vehicle	162	8.80	8.24	8.79	11.30	8.88	9.03
	193	10.17	7.80	10.14	10.06	11.32	10.37
	195	11.24	9.55	11.59	9.34	9.87	11.39
	196	11.25	9.42	9.20	10.62	9.17	10.57
	200	8.46	8.56	8.25	9.60	9.45	7.96
	211	11.21	8.74	8.60	10.87	10.46	9.13
	212	10.41	7.52	8.81	9.24	7.31	8.84
injury+vehicle	156	10.26	5.29	8.07	6.59	9.18	13.39
	157	10.23	5.54	5.98	9.75	9.51	10.42
	163	10.80	6.39	5.62	10.36	9.09	10.44
	194	10.01	6.15	6.05	11.83	7.17	8.09
	198	9.07	7.46	6.51	8.08	8.27	8.75
	199	9.28	6.66	7.12	9.59	8.79	8.80
	210	12.66	5.06	7.95	10.32	9.59	11.55
injury+Riluzole	147	9.35	7.76	6.47	9.58	9.34	8.39
	148	9.47	6.60	9.86	9.38	9.49	10.88
	149	11.62	7.39	8.35	11.10	8.54	9.69
	158	10.95	7.04	9.46	9.54	12.03	8.61
	159	8.45	5.06	8.69	9.92	9.98	11.82
	160	9.25	6.09	8.34	7.22	10.46	8.58
	161	9.65	9.06	7.10	8.48	8.30	10.88

**Table C.11** Mechanical allodynia (number of paw withdrawals) after a painful nerve root compression treated with Riluzole (*injury+Riluzole*) or the vehicle (*injury+vehicle*), or sham (*sham+vehicle*) (corresponding to studies in Chapter 7).

	group	rat ID	ipsilateral				contralateral			
			BL	D1	D2	D7	BL	D1	D2	D7
1.4gf filament	sham+vehicle	259	1	0	1	1	1	0	1	0
		261	0	2	3	0	0	1	0	1
		263	1	0	2	2	0	0	0	1
		265	0	0	1	1	0	0	1	0
		268	1	0	0	0	0	0	0	0
		269	1	1	0	0	1	1	2	0
		271	0	0	2	2	0	0	1	1
		274	1	1	1	0	1	1	0	0
	injury+vehicle	244	0	0	3	0	0	1	0	1
		246	0	3	1	2	1	1	0	0
		247	0	0	1	0	0	0	1	0
		249	0	3	3	0	1	1	2	1
		264	0	1	4	1	0	0	2	2
		266	1	2	4	2	1	0	1	1
		272	1	4	4	4	1	0	1	0
		273	0	0	0	1	0	1	0	0
	injury+Riluzole	243	1	2	2	2	1	2	2	1
		245	0	0	1	0	1	0	1	1
		248	0	5	2	0	0	0	1	0
		250	1	1	1	0	1	1	1	0
		260	0	1	2	1	0	0	0	1
262		0	3	4	1	1	0	0	1	
267		0	2	1	1	0	1	0	0	
270		0	0	1	2	1	0	0	1	
4.0gf filament	sham+vehicle	259	1	2	1	2	1	1	1	0
		261	0	3	3	0	0	0	0	1
		263	0	2	2	3	0	2	0	1
		265	1	0	1	1	1	1	1	0
		268	0	1	1	2	0	0	1	1
		269	1	1	1	2	2	2	1	2
		271	0	1	3	3	0	0	1	1
		274	0	2	2	0	1	1	1	0
	injury+vehicle	244	0	6	6	9	1	0	2	1
		246	1	5	8	8	0	0	1	3
		247	0	8	7	2	1	2	2	0
		249	1	7	5	6	1	4	1	1
		264	2	5	4	4	2	1	2	2
		266	0	3	4	7	0	1	1	1
		272	2	9	10	7	3	2	4	0
		273	2	2	5	7	2	0	0	1
	injury+Riluzole	243	0	10	7	4	1	4	4	4
		245	0	5	3	0	0	1	1	0
		248	1	8	4	5	0	3	0	2
		250	1	8	3	2	1	2	0	0
		260	0	3	2	2	1	0	0	1
262		1	5	4	2	1	0	0	1	
267		0	5	3	1	1	0	1	2	



	group	rat ID	ipsilateral				contralateral			
			BL	D1	D2	D7	BL	D1	D2	D7
10.0gf filament	sham+vehicle	270	2	6	3	2	0	1	2	0
		259	2	2	0	2	1	1	0	0
		261	1	3	2	0	0	0	1	0
		263	1	1	3	3	0	0	1	2
		265	0	2	2	1	1	0	0	1
		268	2	3	2	3	2	1	3	2
		269	2	4	2	5	1	2	1	4
		271	3	1	5	4	3	1	4	2
		274	2	1	3	1	3	0	2	2
	injury+vehicle	244	0	5	8	8	0	2	2	5
		246	2	6	10	9	1	2	2	4
		247	1	7	9	1	0	2	4	0
		249	0	10	10	7	1	2	4	4
		264	2	4	5	4	1	0	1	0
		266	1	5	4	8	1	1	0	3
		272	3	10	9	10	2	6	4	4
		273	2	5	6	10	2	2	3	3
	injury+Riluzole	243	3	11	7	6	2	4	6	5
		245	0	5	5	3	0	0	1	2
		248	1	9	6	8	0	1	3	4
		250	2	8	5	3	2	2	2	0
		260	1	5	3	2	1	1	1	0
		262	2	7	4	3	2	1	0	2
		267	1	7	4	5	1	3	1	2
		270	0	7	3	5	0	1	1	3

---

## APPENDIX D

### Quantification of Spinal Protein Using Immunohistochemistry

---

This appendix summarizes the immunolabeling of the dorsal horn of the spinal cord that was quantified in studies presented in Chapters 5-7. For all studies, densitometry was performed using Matlab to quantify the positively-labeled pixels in each image. The Matlab code is provided in Appendix F. Images are identified by the rat ID followed by the image number (ID-number). All data are expressed relative to the expression of each protein in normal tissue. The expression of each protein is quantified for the ipsilateral and contralateral dorsal horns separately, and is indicated in the “dorsal horn” column of each table. Spinal cord tissue was harvested at days 1 and 7, as indicated by each table.

Tables D.1-D.3 summarize the spinal expression of the glutamate transporters, GLT-1, GLAST and EAAC1, at days 1 and 7 after a 3 or 15 minute compression, or sham procedures (Chapter 5). The spinal expression of GLT-1, GFAP, and GLAST at day 7 after a 15 minute compression treated with 10 $\mu$ g or 150 $\mu$ g ceftriaxone (*injury+10 $\mu$ g*, *injury+150 $\mu$ g*) or the saline vehicle (*injury+saline*) or sham procedures (*sham+saline*) is provided in Tables D.4-D.6 (Chapter 6). Table D.7 and Table D.8 list the spinal expression of CGRP at day 7 in the superficial and deep laminae, respectively

(Chapter 7). CGRP was quantified after a 15 minute nerve root compression treated with Riluzole (*injury+Ril*) and in a group of rats that received the matching vehicle treatment (10%  $\beta$ -cyclodextrin) after that same 15 minute compression (*injury+veh*) or sham procedures (*sham+veh*).

**Table D.1** Quantification of GLT-1 in the superficial laminae at days 1 and 7 (Chapter 5).

dorsal horn	group	time-point	image	GLT-1 (fold increase over normal)
ipsilateral	sham	day 1	109-1	1.14
			109-2	1.44
			109-3	1.23
			109-4	0.73
			109-5	1.34
			109-6	0.77
			113-1	1.63
			113-2	1.06
			113-3	1.43
			113-4	1.38
			113-5	1.23
			113-6	1.50
			254-1	0.78
			254-2	1.29
			254-4	0.47
			258-1	0.62
			258-5	0.54
			258-6	0.79
			280-2	1.38
			280-3	0.40
			280-5	0.88
			281-1	0.55
			281-2	0.41
			281-4	0.62
			281-6	1.03
			282-1	0.78
			282-2	0.70
			282-4	0.84
		282-5	0.89	
		282-6	1.49	
		day 7	216-1	0.53
		216-2	0.79	
		216-3	0.80	
		216-4	0.82	
216-5	0.94			
220-1	0.85			
220-2	0.90			
220-3	0.57			
220-4	0.68			
220-5	0.75			
220-6	1.08			
226-2	1.23			
226-3	1.06			
226-4	0.95			
226-5	1.51			
226-6	0.98			
228-1	0.93			

dorsal horn	group	time-point	image	GLT-1 (fold increase over normal)
ipsilateral (cont.)	sham	day 7	228-2	1.01
			228-3	0.90
			228-4	1.11
			228-5	0.92
			228-6	0.81
			229-1	1.09
			229-2	1.20
			229-3	1.41
			229-4	0.97
			229-5	0.88
			229-6	1.02
			234-1	0.93
			234-2	0.63
			234-3	1.05
			234-4	0.87
			234-5	0.76
			238-1	1.62
			238-2	0.78
			238-3	1.07
			238-4	1.05
	238-5	1.16		
	238-6	1.11		
	3 minute	day 1	251-2	0.99
			251-3	1.14
			251-4	0.70
			251-5	1.25
			253-2	0.98
			253-3	1.20
			253-4	0.90
			253-5	0.88
			253-6	1.18
			255-2	0.70
			255-3	0.23
			255-6	0.68
			275-2	0.91
			275-4	0.83
275-6			0.70	
276-1			0.70	
276-2	1.31			
276-5	0.95			
276-6	2.26			
277-1	0.89			
277-2	0.74			
277-6	0.88			
278-2	0.44			
278-4	0.55			
278-6	0.88			
	day 7	218-1	0.93	
		218-2	0.79	
		218-3	0.77	

dorsal horn	group	time-point	image	GLT-1 (fold increase over normal)
ipsilateral (cont.)	3 minute	day 7	218-5	0.80
			218-6	0.38
			223-2	1.16
			223-3	0.71
			223-4	1.02
			223-5	1.08
			223-6	1.04
			225-1	1.46
			225-3	1.10
			225-4	1.05
			227-1	0.88
			227-2	1.47
			227-3	1.12
			227-4	1.34
			227-5	1.12
			227-6	1.40
			231-1	0.46
			231-2	0.48
			231-3	0.52
			231-4	0.76
			231-6	0.53
			235-1	0.63
			235-2	0.80
			235-3	0.73
			235-4	1.24
			235-5	1.40
			235-6	0.83
	236-1	1.07		
	236-2	1.07		
	236-3	0.74		
	236-4	1.10		
	236-5	1.08		
	236-6	1.14		
15 minute	day 1	106-1	0.63	
		106-3	0.79	
		106-4	0.61	
		106-5	0.64	
		106-6	0.69	
		107-1	1.09	
		107-2	1.20	
		107-3	0.94	
		107-6	1.02	
		108-1	1.24	
		108-2	1.34	
		108-3	1.27	
		108-5	0.90	
		111-1	1.35	
		111-2	1.46	
		111-3	0.85	
111-4	1.45			

dorsal horn	group	time-point	image	GLT-1 (fold increase over normal)
ipsilateral (cont.)	15 minute	day 1	111-5	0.98
			111-6	0.96
			112-1	1.13
			112-3	1.14
			112-5	1.04
			112-6	0.88
			252-2	1.12
			252-3	0.70
			252-5	1.16
			256-1	0.18
			256-2	0.60
		256-5	0.23	
		day 7	213-1	0.92
			213-2	0.91
			213-3	0.97
			213-5	0.64
			214-1	0.43
			214-2	0.38
			214-4	0.61
			214-5	0.83
			214-6	1.01
			217-1	1.24
			217-3	0.93
			217-4	1.01
			217-5	0.89
			217-6	0.73
			224-1	1.36
			224-2	1.09
			224-4	0.94
			224-5	1.23
			224-6	1.03
			230-1	0.39
			230-2	0.69
			230-3	0.70
			230-4	0.22
			230-5	1.00
230-6	0.96			
233-1	1.07			
233-2	0.93			
233-3	1.09			
233-4	0.54			
233-5	0.96			
233-6	0.78			
237-1	0.86			
237-2	0.95			
237-3	0.49			
237-4	0.64			
237-5	0.83			
237-6	0.98			

dorsal horn	group	time-point	image	GLT-1 (fold increase over normal)
contralateral	sham	day 1	109-1	0.98
			109-2	1.75
			109-3	0.67
			109-4	0.88
			109-5	1.59
			109-6	0.81
			113-1	0.91
			113-2	0.61
			113-3	0.85
			113-4	1.18
			113-5	1.07
			113-6	0.83
			254-2	0.93
			254-3	0.92
			254-4	0.81
			254-6	1.13
			258-3	0.99
			258-5	0.68
			258-6	1.13
			280-2	0.47
			280-4	0.07
			280-6	0.11
			281-1	0.96
			281-2	0.41
			281-4	0.69
			281-6	0.55
			282-2	1.77
		282-3	1.05	
		282-4	0.96	
		282-5	1.93	
		day 7	216-1	0.91
			216-2	1.11
			216-4	1.00
			216-5	0.75
			220-1	0.89
			220-2	0.90
220-3	0.90			
220-4	1.09			
220-5	0.87			
220-6	0.91			
226-1	1.28			
226-2	0.89			
226-3	1.17			
226-5	0.83			
226-6	0.82			
228-1	1.06			
228-3	1.22			
228-4	0.85			
228-5	0.98			
228-6	1.04			



dorsal horn	group	time-point	image	GLT-1 (fold increase over normal)
contralateral (cont.)	sham	day 7	229-2	1.15
			229-3	0.84
			229-5	0.73
			229-6	1.82
			234-1	0.91
			234-2	0.64
			234-4	0.66
			234-5	0.71
			234-6	0.88
			238-2	0.87
			238-4	0.67
			238-5	0.94
	238-6	0.83		
	3 minute	day 1	251-2	1.29
			251-3	1.04
			251-4	0.71
			253-2	1.58
			253-3	1.20
			253-4	1.35
			253-5	1.44
			253-6	1.32
			255-1	0.33
			255-2	0.54
			255-3	0.41
			255-4	0.41
			255-6	0.73
			275-1	0.47
			275-2	1.06
			275-4	1.11
			276-1	1.58
			276-2	0.88
			276-4	1.50
			276-6	0.19
277-3			1.71	
277-4	2.06			
277-5	1.05			
278-1	0.32			
278-2	0.26			
278-3	0.23			
day 7	218-1	0.95		
	218-2	1.47		
	218-3	1.05		
	218-4	1.50		
	218-5	0.75		
	218-6	0.95		
	223-1	1.06		
	223-2	1.92		
	223-3	0.58		
223-4	0.45			
223-5	1.01			

dorsal horn	group	time-point	image	GLT-1 (fold increase over normal)	
contralateral (cont.)	3 minute	day 7	223-6	0.94	
			225-1	1.22	
			225-2	1.62	
			225-3	0.76	
			227-1	0.79	
			227-2	1.17	
			227-3	1.15	
			227-4	1.23	
			227-5	1.06	
			227-6	1.06	
			231-1	0.56	
			231-2	0.82	
			231-3	0.74	
			231-4	0.26	
			231-5	0.34	
			231-6	0.88	
			235-1	1.21	
			235-2	0.83	
			235-3	1.02	
			235-4	1.40	
			235-5	0.81	
			235-6	1.18	
			236-1	0.49	
			236-2	0.56	
	236-3	0.82			
	236-4	0.58			
	236-5	0.62			
	236-6	0.65			
		15 minute	day 1	106-1	1.29
				106-2	0.83
	106-3			0.57	
	106-4			1.08	
	106-5			0.87	
	106-6			1.35	
	107-2			0.95	
	107-3			1.47	
	107-4			1.38	
	107-5			1.36	
	108-1			1.44	
	108-2			1.62	
	108-3			1.52	
	108-4			1.52	
	108-5	1.58			
	108-6	0.97			
	111-2	1.06			
	111-3	0.44			
	111-4	0.30			
	111-5	0.36			
	112-1	1.33			
	112-2	1.30			

dorsal horn	group	time-point	image	GLT-1 (fold increase over normal)
contralateral (cont.)	15 minute	day 1	112-4	0.83
			112-5	1.77
			112-6	0.60
			252-2	1.82
			252-3	0.51
			252-5	0.62
			256-3	0.43
			256-5	0.67
		256-6	1.17	
		day 7	213-1	0.79
			213-2	1.06
			213-3	0.89
			213-4	1.10
			213-5	1.16
			213-6	0.33
			214-1	1.12
			214-2	0.53
			214-3	1.43
			214-4	1.29
			214-5	0.61
			214-6	1.25
			217-1	1.22
			217-2	0.71
			217-3	0.72
			217-4	0.85
			217-5	0.88
			217-6	0.88
			224-3	1.57
			224-4	1.15
			224-5	1.52
			224-6	1.53
			224-7	1.51
			230-1	0.95
			230-2	1.31
			230-3	1.12
			230-5	0.86
230-6	1.41			
233-1	0.73			
233-2	0.68			
233-3	0.95			
233-4	0.86			
233-5	0.77			
233-6	0.70			
237-1	0.31			
237-2	0.38			
237-3	0.54			
237-4	0.96			
237-5	0.69			
237-6	0.82			

**Table D.2** Quantification of GLAST in the superficial at days 1 and 7 (Chapter 5).

dorsal horn	group	time-point	image	GLAST (fold increase over normal)
ipsilateral	sham	day 1	109-1	1.71
			109-3	1.82
			109-4	1.39
			109-5	1.22
			109-6	1.52
			113-1	1.97
			113-3	1.74
			113-4	1.46
			113-5	0.85
			113-6	0.96
			254-1	1.50
			254-2	1.28
			254-3	0.56
			254-4	0.84
			258-1	0.84
			258-2	1.01
			258-3	1.31
			258-4	1.12
			258-5	1.19
			258-6	0.92
			280-1	1.11
			280-3	1.22
			280-5	1.11
			280-6	1.44
			281-1	1.41
			281-2	1.17
		281-3	1.76	
		281-4	1.41	
		281-5	1.42	
		281-6	1.53	
		282-2	1.44	
		282-4	1.39	
		282-5	1.43	
		282-6	1.33	
day 7	216-1	0.46		
	216-2	0.72		
	216-3	1.18		
	216-4	0.74		
	216-5	1.47		
	216-6	1.09		
	220-1	0.87		
	220-2	1.06		
220-3	0.62			
220-4	0.93			
220-5	0.58			
220-6	1.05			
226-2	0.52			
226-4	0.51			

dorsal horn	group	time-point	image	GLAST (fold increase over normal)	
ipsilateral (cont.)	sham	day 7	226-5	1.07	
			226-6	0.75	
			228-1	0.33	
			228-2	1.57	
			228-3	1.91	
			228-4	0.61	
			228-5	1.39	
			228-6	0.93	
			229-1	1.14	
			229-2	0.69	
			229-3	1.68	
			229-4	0.59	
			229-5	1.10	
			229-6	0.89	
			234-1	1.08	
			234-2	1.23	
			234-3	1.29	
			234-4	1.33	
			234-5	0.96	
			234-6	1.18	
	238-1	0.76			
	238-2	0.92			
	238-3	1.20			
	238-4	0.84			
	238-5	0.08			
	238-6	0.79			
		3 minute	day 1	251-1	0.83
				251-2	0.96
				251-3	0.77
	251-4			1.30	
	251-6			1.41	
	253-2			0.90	
	253-4			0.99	
	253-5			0.85	
	253-6			0.88	
	255-1			1.09	
	255-2			0.92	
	255-3			0.81	
	255-4			1.20	
	255-5			1.11	
	275-1	1.15			
	275-3	1.30			
	275-5	1.29			
	275-6	1.11			
	276-1	1.70			
	276-3	0.93			
	276-4	1.48			
	276-6	1.15			
	277-2	1.38			
	277-4	1.35			

dorsal horn	group	time-point	image	GLAST (fold increase over normal)
ipsilateral (cont.)	3 minute	day 1	277-5	0.97
			277-6	1.28
			278-1	1.25
			278-2	1.35
			278-3	1.91
			278-4	1.74
			278-5	1.57
		278-6	1.47	
		day 7	218-1	0.60
			218-2	1.03
			218-3	0.53
			218-4	1.04
			218-5	0.22
			218-6	0.60
			223-1	0.45
			223-3	0.55
			223-4	0.16
			223-5	0.60
			223-6	0.19
			225-1	0.61
			225-2	2.37
			225-4	2.12
			225-5	2.50
		225-6	1.25	
		227-1	1.05	
		227-2	2.22	
		227-3	0.24	
		227-4	1.01	
	227-5	0.19		
	227-6	1.13		
	231-1	0.96		
	231-2	1.09		
	231-3	1.29		
	231-4	1.25		
	231-5	1.24		
	231-6	0.88		
	235-1	0.87		
	235-2	0.85		
	235-3	0.76		
	235-4	1.01		
	235-5	0.93		
	235-6	0.78		
236-1	1.20			
236-3	0.95			
236-4	1.16			
236-5	1.06			
236-6	1.04			
15 minute	day 1	106-3	0.70	
		106-5	1.25	
		106-6	1.11	

dorsal horn	group	time-point	image	GLAST (fold increase over normal)
ipsilateral (cont.)	15 minute	day 1	107-1	1.34
			107-2	1.58
			107-3	1.53
			107-4	2.17
			108-1	1.71
			108-3	1.30
			108-4	1.47
			108-5	1.31
			111-1	1.32
			111-2	0.66
			111-3	1.03
			111-4	0.78
			112-2	1.07
			112-3	1.16
			112-4	1.29
			112-6	1.73
			252-2	1.21
			252-3	1.26
			252-4	1.25
			252-5	1.57
			252-6	1.18
			256-1	1.43
			256-2	1.40
			256-3	1.47
		256-4	1.01	
		256-5	1.04	
		256-6	0.99	
		day 7	213-1	0.56
			213-2	0.86
			213-3	1.45
			213-4	0.67
			213-5	1.11
			213-6	1.39
			214-2	0.72
			214-3	0.90
			214-4	0.42
214-5	0.97			
214-6	1.50			
217-1	0.99			
217-2	1.80			
217-3	1.62			
217-4	1.23			
217-5	1.29			
224-1	0.98			
224-2	2.03			
224-3	2.01			
224-4	0.91			
224-5	0.98			
224-6	1.89			
230-1	0.78			

dorsal horn	group	time-point	image	GLAST (fold increase over normal)
ipsilateral (cont.)	15 minute	day 7	230-2	1.94
			230-3	2.79
			230-4	2.49
			230-5	3.61
			230-6	3.07
			233-1	1.09
			233-2	1.25
			233-3	0.59
			233-4	0.55
			233-5	1.24
			233-6	0.67
			237-1	0.94
			237-2	1.27
			237-3	1.24
			237-4	0.92
237-5	1.09			
237-6	0.89			
contralateral	sham	day 1	109-2	1.15
			109-3	1.37
			109-4	1.17
			113-1	0.90
			113-3	0.82
			113-4	0.82
			113-5	0.99
			254-1	0.96
			254-2	1.37
			258-1	0.96
			258-2	0.84
			258-3	0.68
			258-4	0.71
			258-5	0.99
			258-6	0.69
		280-1	0.94	
		280-3	1.06	
		280-5	1.15	
		280-6	1.02	
		281-1	1.57	
		281-3	1.55	
		281-4	1.25	
		281-5	1.65	
		282-2	1.28	
		282-3	0.81	
		282-4	0.88	
		day 7	216-1	0.53
216-2	1.16			
216-3	1.30			
216-4	0.91			
216-5	1.13			
216-6	0.67			
220-1	1.19			



dorsal horn	group	time-point	image	GLAST (fold increase over normal)
contralateral (cont.)	sham	day 7	220-2	1.61
			220-3	1.06
			220-4	0.98
			220-5	0.92
			220-6	0.63
			226-2	1.69
			226-3	1.45
			226-4	0.46
			226-5	1.38
			226-6	0.65
			228-1	0.60
			228-2	1.75
			228-3	1.14
			228-4	0.32
			228-5	1.64
			228-6	1.31
			229-1	1.08
			229-2	0.91
			229-3	2.00
			229-4	0.18
			229-5	0.84
			229-6	0.65
			234-1	0.74
			234-2	0.79
			234-3	0.69
			234-4	0.53
			234-5	0.69
			234-6	0.72
	234-7	0.64		
	234-8	0.80		
	238-1	0.76		
	238-2	0.61		
	238-3	1.11		
238-4	0.48			
238-5	0.91			
3 minute		day 1	251-2	1.03
			251-3	1.10
			251-4	1.16
			251-5	1.19
			251-6	1.14
			253-2	0.96
			253-4	1.08
			253-5	0.64
			253-6	0.80
			255-2	0.73
255-3	0.94			
255-5	0.68			
255-6	1.22			
275-1	0.91			
275-2	0.90			

dorsal horn	group	time-point	image	GLAST (fold increase over normal)
contralateral (cont.)	3 minute	day 1	275-3	0.81
			275-5	0.77
			275-6	0.98
			276-1	1.44
			276-2	1.48
			276-3	0.59
			276-6	0.80
			277-2	1.25
			277-3	0.81
			277-4	1.32
			277-5	0.77
			278-1	1.40
			278-3	1.66
			278-4	0.83
		278-5	1.55	
		278-6	0.97	
		day 7	218-1	0.87
			218-2	1.41
			218-3	0.84
			218-4	0.74
			218-5	0.92
			218-6	0.19
			223-1	0.77
			223-2	0.72
			223-3	1.31
			223-4	0.70
			223-5	1.01
			223-6	0.11
			225-1	1.09
			225-3	1.07
			225-4	2.34
			225-5	0.98
			227-1	0.97
			227-2	1.88
			227-4	2.15
			227-5	0.58
227-6	0.73			
231-1	0.54			
231-2	0.67			
231-3	0.25			
231-4	0.27			
231-5	0.48			
231-6	0.74			
235-1	0.60			
235-2	0.50			
235-3	0.92			
235-4	0.94			
235-5	0.69			
235-6	0.86			
236-1	0.86			

<b>dorsal horn</b>	<b>group</b>	<b>time-point</b>	<b>image</b>	<b>GLAST (fold increase over normal)</b>
contralateral (cont.)	3 minute	day 7	236-2	0.62
			236-3	0.73
			236-4	1.30
			236-5	0.68
			236-6	0.89
	15 minute	day 1	106-1	1.07
			106-2	1.08
			106-5	1.00
			106-6	0.81
			107-2	0.70
			107-3	0.88
			107-4	0.77
			108-2	0.55
			108-3	1.36
			108-5	1.46
			108-6	0.91
			111-1	1.31
			111-2	0.93
			111-3	0.88
			111-4	1.32
			112-1	1.02
			112-2	0.98
			112-3	0.99
			112-4	1.08
			252-2	0.77
			252-3	0.89
			252-4	1.16
			252-5	0.73
			252-6	1.17
			256-1	1.02
			256-2	0.74
			256-3	0.59
			256-4	1.02
256-5	0.85			
256-6	1.35			
day 7	213-2	1.21		
	213-3	1.24		
	213-4	0.87		
	213-5	0.92		
	213-6	1.00		
	214-2	0.98		
	214-3	0.69		
	214-4	0.91		
	214-5	1.29		
	217-1	1.84		
	217-2	1.59		
	217-3	1.86		
217-4	1.00			
217-5	1.64			
217-6	0.78			

<b>dorsal horn</b>	<b>group</b>	<b>time-point</b>	<b>image</b>	<b>GLAST (fold increase over normal)</b>
contralateral (cont.)	15 minute	day 7	224-2	0.94
			224-3	2.32
			224-5	1.49
			224-6	1.02
			230-2	1.89
			230-4	1.51
			230-6	1.79
			233-1	0.95
			233-2	1.21
			233-3	1.17
			233-4	1.13
			233-5	1.06
			233-6	1.07
			237-1	1.10
			237-2	0.56
			237-3	0.94
			237-4	0.86
			237-5	0.55
237-6	0.91			

**Table D.3** Quantification of EAAC1 in the superficial laminae at days 1 and 7 (Chapter 5).

dorsal horn	group	time-point	image	EAAC1 (fold increase over normal)
ipsilateral	sham	day 1	109-1	1.80
			109-2	0.90
			109-3	0.65
			109-5	1.07
			109-6	0.61
			113-1	0.83
			113-1	0.55
			113-2	1.59
			113-3	1.40
			113-4	0.96
			113-5	0.87
			113-6	0.87
			254-1	1.23
			254-2	1.26
			254-3	0.88
			258-2	1.15
			258-3	1.25
			258-5	0.59
			258-6	1.20
			280-2	0.69
			280-4	0.49
			280-5	0.61
			281-1	0.15
			281-2	0.56
		281-4	2.42	
		282-1	1.89	
		282-2	1.64	
		282-3	0.77	
		282-4	1.36	
		day 7	216-1	0.96
			216-2	0.83
			216-3	0.73
			216-5	1.09
			216-6	0.77
220-1	0.86			
220-2	0.46			
220-4	0.24			
220-5	0.94			
226-1	0.21			
226-2	0.89			
226-3	0.84			
226-4	0.43			

dorsal horn	group	time-point	image	EAAC1 (fold increase over normal)
ipsilateral (cont.)	sham	day 7	226-5	0.16
			226-6	0.28
			228-1	0.53
			228-2	0.51
			228-3	0.44
			228-4	0.33
			228-5	1.02
			228-6	1.04
			229-3	0.53
			229-4	1.60
			229-5	1.04
			229-6	1.53
			234-2	0.42
			234-3	1.04
			234-4	0.43
			234-5	1.46
			234-6	0.28
			238-1	0.70
			238-3	0.73
			238-4	0.56
	238-5	0.91		
	238-6	1.24		
	3 minute	day 1	251-3	0.81
			251-4	1.12
			251-5	1.02
			253-3	1.20
			253-4	1.28
			253-6	1.20
			255-1	1.15
			255-3	1.16
			255-5	0.95
			275-2	0.49
			275-3	0.32
			275-4	0.32
276-1			1.46	
276-2			0.37	
276-3	0.99			
276-4	0.94			
276-5	1.20			
276-6	1.46			
277-1	0.62			
277-2	1.59			
277-3	0.55			
277-5	1.95			
277-6	0.67			

dorsal horn	group	time-point	image	EAAC1 (fold increase over normal)
ipsilateral (cont.)	3 minute	day 1	278-2	1.65
			278-3	0.77
			278-4	0.63
			278-5	0.62
		day 7	218-1	0.11
			218-2	0.23
			218-3	0.38
			218-4	0.68
			218-5	0.85
			218-6	0.22
			223-1	0.31
			223-2	0.28
			223-3	0.23
			223-4	0.23
			225-1	0.97
			225-2	2.48
			225-4	1.88
			227-1	0.54
			227-2	0.71
			227-4	2.04
			231-1	1.18
			231-2	0.76
			231-3	0.57
			231-4	0.71
	231-5	1.51		
	235-1	1.29		
	235-2	0.53		
	235-3	0.68		
	235-4	0.36		
	235-6	0.77		
	236-1	0.73		
	236-2	0.81		
	236-3	0.38		
	236-4	0.48		
236-6	0.46			
15 minute	day 1	106-1	1.21	
		106-2	0.94	
		106-3	1.08	
		106-4	1.26	
		106-5	0.81	
		106-6	0.84	
		107-2	1.43	
		107-3	1.74	
		107-4	1.20	
		108-1	1.18	

dorsal horn	group	time-point	image	EAAC1 (fold increase over normal)
ipsilateral (cont.)	15 minute	day 1	108-2	1.38
			108-3	1.37
			108-4	0.87
			108-5	0.96
			108-6	1.07
			111-1	0.73
			111-2	1.00
			111-3	0.54
			111-4	0.66
			111-5	1.03
			111-6	0.79
			112-1	0.69
			112-2	0.59
			112-3	0.52
			112-4	0.40
			112-5	1.28
			112-6	0.81
			252-1	0.63
			252-3	0.97
			252-5	1.40
		256-2	0.46	
		256-4	0.36	
		256-6	0.77	
		day 7	213-1	0.65
			213-2	0.99
			213-3	0.41
			213-4	0.50
			213-5	0.47
			213-6	0.63
			214-1	0.08
			214-2	0.89
			214-3	0.49
			214-4	0.76
			214-5	1.15
214-6	0.84			
217-1	0.78			
217-2	0.80			
217-3	0.68			
217-5	0.79			
217-6	1.08			
224-1	0.58			
224-2	0.71			
224-3	1.24			
224-4	0.92			
224-5	0.78			



dorsal horn	group	time-point	image	EAAC1 (fold increase over normal)
ipsilateral (cont.)	15 minute	day 7	224-6	0.91
			230-1	0.61
			230-2	0.72
			230-4	0.82
			230-5	0.72
			233-1	0.74
			233-2	1.04
			233-3	0.96
			233-4	0.63
			233-5	0.46
			233-6	0.59
			237-1	0.68
			237-2	0.62
			237-3	0.95
			237-4	0.41
237-5	0.42			
contralateral	sham	day 1	109-1	1.03
			109-2	1.05
			109-5	0.84
			109-6	1.05
			113-2	0.69
			113-3	0.81
			113-5	1.01
			113-6	0.70
			254-1	1.68
			254-2	0.73
			254-3	0.57
			258-2	0.64
			258-3	0.69
			258-4	0.80
			258-6	1.14
			280-2	0.59
			280-3	1.02
			280-4	0.41
			280-5	0.41
			280-6	0.35
281-2	0.17			
281-3	1.97			
281-4	1.88			
282-1	0.94			
282-2	2.18			
282-3	1.98			
282-4	1.18			
282-5	0.86			

dorsal horn	group	time-point	image	EAC1 (fold increase over normal)
contralateral (cont.)	sham	day 7	216-1	0.35
			216-2	0.50
			216-6	0.93
			220-1	0.68
			220-2	1.76
			220-3	0.80
			220-5	0.64
			220-6	1.67
			226-1	1.45
			226-2	0.61
			226-3	0.49
			226-4	0.17
			226-5	0.10
			226-6	0.54
			228-1	2.06
			228-2	1.42
			228-3	0.91
			228-4	1.34
			228-5	1.37
			228-6	2.10
			229-3	0.79
			229-4	0.97
			229-5	0.86
			229-6	1.71
			234-1	1.10
			234-3	0.55
			234-4	0.44
	234-5	1.01		
	234-6	1.01		
	238-1	0.91		
	238-4	0.51		
	238-5	1.00		
	238-6	0.95		
	3 minute	day 1	251-1	0.96
			251-2	0.20
			251-3	0.89
			251-6	0.55
			253-1	1.02
			253-2	0.35
			253-5	1.59
			253-6	1.16
			255-1	0.76
	255-3	0.87		
	255-5	0.94		
	255-6	0.58		

dorsal horn	group	time-point	image	EAAC1 (fold increase over normal)
contralateral (cont.)	3 minute	day 1	275-2	1.11
			275-4	1.20
			275-5	0.39
			276-1	0.51
			276-2	1.18
			276-3	0.37
			276-5	1.56
			277-1	0.68
			277-2	0.74
			277-3	0.57
			277-4	1.14
			277-5	1.97
			277-6	0.77
			278-2	2.02
			278-3	0.65
			278-4	2.08
			278-5	1.49
			day 7	218-2
		218-3		0.53
		218-4		1.10
		218-5		0.82
		218-6		0.82
		223-1		0.85
		223-2		1.59
		223-3		0.32
		223-4		1.13
		225-1		0.68
		225-2		0.89
		225-4		1.34
		227-1		0.93
		227-3		1.45
		227-4		1.74
		231-1		0.68
		231-4		0.54
		231-5		0.67
		231-6	0.70	
235-1	0.53			
235-3	0.96			
235-4	0.99			
235-5	0.80			
235-6	0.75			
236-1	1.60			
236-2	1.74			
236-3	0.39			
236-4	0.87			

dorsal horn	group	time-point	image	EAAC1 (fold increase over normal)
contralateral (cont.)	3 minute	day 7	236-5	1.06
			236-6	0.47
	15 minute	day 1	106-1	1.32
			106-2	1.47
			106-3	1.13
			106-4	1.23
			106-5	1.83
			106-6	1.21
			107-1	0.69
			107-2	1.12
			107-3	0.74
			107-4	0.97
			108-1	1.10
			108-2	1.03
			108-3	1.03
			108-4	1.13
			108-5	1.22
			111-1	0.44
			111-2	0.65
			111-3	0.71
			111-4	0.67
			111-5	0.68
			111-6	0.93
			112-1	1.29
			112-2	0.81
			112-3	0.88
			112-4	1.15
			112-5	1.16
			112-6	1.06
			252-1	0.67
			252-2	0.61
			252-3	0.61
			252-4	1.84
			256-2	3.40
			256-3	0.82
	256-4	3.81		
	256-6	0.74		
	day 7	213-1	2.10	
		213-2	1.05	
		213-3	0.32	
213-4		1.04		
213-5		0.97		
213-6		1.17		
214-1		0.21		
214-2	0.26			

<b>dorsal horn</b>	<b>group</b>	<b>time-point</b>	<b>image</b>	<b>EAC1 (fold increase over normal)</b>
contralateral (cont.)	15 minute	day 7	214-3	0.32
			214-4	0.56
			214-5	0.13
			214-6	0.82
			217-1	0.59
			217-3	0.73
			217-4	0.97
			217-6	0.50
			224-1	0.51
			224-2	1.02
			224-3	1.21
			224-4	2.58
			224-5	0.80
			224-6	1.98
			230-1	0.63
			230-3	1.08
			230-4	1.09
			230-5	0.83
			230-6	0.50
			232-1	1.80
			233-1	1.14
			233-2	0.61
			233-3	1.34
			233-4	1.28
			233-5	1.28
			237-1	0.45
			237-2	0.85
237-3	0.77			
237-4	0.46			
237-5	1.16			

**Table D.4** Quantification of GLT-1 in the superficial laminae at day 7 after a painful compression treated with of ceftriaxone (*injury+10 $\mu$ g*, *injury+150 $\mu$ g*) or the saline vehicle (*injury+saline*), or sham treated with the saline (*sham+saline*) (Chapter 6).

dorsal horn	group	image	GLT-1 (fold increase over normal)
ipsilateral	sham+saline	131-1	1.44
		131-2	0.39
		131-4	0.97
		131-6	1.39
		171-2	2.02
		171-4	1.43
		171-6	1.32
		175-1	0.27
		175-2	0.22
		175-5	0.20
		178-2	1.06
		178-3	1.06
		178-5	0.65
		178-6	1.43
		179-4	1.02
		179-5	0.75
		179-6	1.64
		183-2	0.97
		183-4	0.80
		183-5	0.82
		183-6	1.10
		184-2	2.07
		184-3	1.96
		184-4	1.51
	184-5	2.14	
	184-6	1.83	
	injury+saline	128-2	0.12
		128-3	0.06
		128-4	0.03
		128-5	0.02
		128-6	0.18
		129-1	1.04
		129-2	0.84
		129-4	0.94
129-5		0.69	
129-6		0.93	
130-1		1.04	
130-2		0.48	
130-3		0.84	
130-4		0.67	
164-1	0.80		
164-2	1.14		
164-3	1.11		
164-4	1.01		
164-5	0.86		
164-6	1.04		

dorsal horn	group	image	GLT-1 (fold increase over normal)
ipsilateral (cont.)	injury+saline	165-1	0.84
		165-2	1.13
		165-4	1.01
		165-5	0.88
		165-6	0.97
		174-1	0.51
		174-3	0.73
		174-5	0.70
		174-6	0.67
		182-1	0.35
		182-3	1.10
	182-5	1.19	
	injury+10 $\mu$ g	138-1	1.83
		138-2	0.46
		138-3	0.59
		138-4	1.03
		139-2	0.48
		139-3	1.86
		139-5	0.50
		140-1	0.31
		140-2	0.30
		140-3	0.33
		141-1	1.74
		141-2	1.06
		141-4	1.65
		141-6	1.57
		168-1	1.36
		168-2	1.03
		168-4	1.02
		168-6	0.75
		169-2	1.44
		169-3	1.00
		169-4	1.37
	169-5	0.73	
	169-6	1.67	
	176-2	1.23	
	176-3	1.28	
	176-4	1.19	
	176-5	1.11	
	176-6	1.01	
	177-3	0.87	
	177-4	1.19	
177-5	1.23		
177-6	1.13		
injury+150 $\mu$ g	136-2	0.56	
	136-3	0.54	
	136-4	1.88	
	136-5	1.52	
	142-1	1.33	
	142-2	1.39	
	142-3	1.24	

dorsal horn	group	image	GLT-1 (fold increase over normal)
ipsilateral (cont.)	injury+150µg	142-5	1.03
		143-1	2.02
		143-3	1.99
		143-4	2.21
		143-5	1.58
		167-2	2.03
		167-4	1.89
		167-6	2.05
		172-1	1.22
		172-2	1.20
		172-3	1.11
		172-4	0.88
		172-6	0.60
		173-2	0.60
		173-3	0.60
		173-5	0.81
		173-6	0.66
		180-1	2.01
		180-2	2.12
		180-3	2.12
180-4	2.14		
181-3	1.19		
181-4	0.58		
181-5	1.34		
181-6	0.79		
contralateral	sham+saline	131-1	0.72
		131-2	0.67
		131-4	1.75
		131-6	1.01
		171-2	1.64
		171-3	0.49
		171-4	0.92
		175-1	0.70
		175-2	0.71
		175-6	0.11
		178-2	1.64
		178-4	1.31
		178-5	0.44
		179-4	1.20
		179-5	0.35
		179-6	1.43
		183-1	0.98
		183-2	1.78
		183-3	1.47
		183-4	1.59
184-1	2.24		
184-2	2.22		
184-3	2.44		
184-4	2.27		
184-5	2.43		
184-6	2.24		



dorsal horn	group	image	GLT-1 (fold increase over normal)
contralateral (cont.)	injury+saline	128-1	0.34
		128-2	0.28
		128-3	0.77
		128-4	0.67
		128-5	0.40
		128-6	0.22
		129-1	1.19
		129-2	1.14
		129-4	0.51
		129-5	0.60
		129-6	0.15
		130-1	1.27
		130-2	1.25
		130-3	0.67
		130-4	1.20
		164-1	0.92
		164-2	1.21
		164-3	1.02
		164-4	1.17
		164-5	1.12
		164-6	1.31
		165-1	1.11
		165-2	1.28
		165-4	1.14
		165-5	1.00
		165-6	1.27
		174-1	0.69
		174-2	0.96
		174-3	0.60
		174-4	1.00
		174-5	0.67
		174-6	0.56
		182-1	2.03
		182-3	2.10
	182-5	2.06	
	182-6	1.84	
	injury+10 $\mu$ g	138-1	2.26
		138-3	2.53
		138-4	1.49
		138-5	0.88
139-2		1.34	
139-3		1.81	
139-5		0.91	
140-1		0.23	
140-2		0.15	
140-3		0.19	
140-6		0.16	
141-1		1.27	
141-4		1.01	
141-6		0.81	
168-1		1.96	

<b>dorsal horn</b>	<b>group</b>	<b>image</b>	<b>GLT-1 (fold increase over normal)</b>
contralateral (cont.)	injury+10µg	168-2	0.24
		168-3	0.70
		169-1	0.92
		169-2	1.45
		169-3	1.80
		169-4	1.38
		169-6	1.08
		176-1	1.00
		176-2	1.70
		176-3	1.24
		176-4	1.55
		177-3	1.35
		177-4	1.39
		177-5	1.40
	177-6	1.28	
	injury+150µg	136-3	0.36
		136-4	1.03
		136-5	0.27
		136-6	0.97
		142-1	0.45
		142-2	0.81
		142-3	1.73
		142-6	0.72
		143-1	2.62
		143-3	2.53
		143-4	2.87
		143-5	2.32
		167-2	2.71
		167-4	1.60
		167-6	1.97
		172-1	1.16
		172-2	1.13
		172-3	1.11
		172-4	0.64
		172-6	0.42
		173-1	0.83
173-2		1.48	
173-3	1.08		
173-4	1.60		
173-6	1.35		
180-1	1.91		
180-2	2.07		
180-3	2.10		
180-4	2.02		
181-1	0.73		
181-2	0.98		
181-4	1.41		
181-5	1.42		
181-6	1.26		

**Table D.5** Quantification of GFAP in the superficial laminae at day 7 after a painful compression treated with ceftriaxone (*injury+10 $\mu$ g*, *injury+150 $\mu$ g*) or the saline vehicle (*injury+saline*), or sham treated with the saline (*sham+saline*) (Chapter 6).

dorsal horn	group	image	GFAP (fold increase over normal)	
ipsilateral	sham+saline	131-1	1.66	
		131-2	1.14	
		131-6	1.45	
		171-2	1.21	
		171-4	1.21	
		171-5	0.49	
		171-6	1.23	
		175-2	0.68	
		175-3	0.41	
		175-6	0.55	
		178-1	0.44	
		178-2	0.74	
		178-3	0.66	
		178-4	1.02	
		178-5	0.53	
		178-6	0.78	
		179-1	0.50	
		179-2	0.54	
		179-3	0.66	
		179-4	0.98	
		179-5	0.91	
		179-6	0.98	
		183-1	0.49	
		183-2	1.27	
	183-4	1.57		
	183-5	2.41		
	184-1	0.72		
	184-2	1.55		
	184-3	0.42		
	184-4	1.54		
	184-5	0.40		
	184-6	1.41		
		injury+saline	128-1	2.15
			128-2	2.06
			128-3	3.60
			128-4	3.78
	130-1		1.64	
	130-2		1.01	
	130-3		3.22	
	130-4		2.67	
	129-1		1.62	
	129-4		2.95	
	129-5		0.51	
	129-6		1.79	

dorsal horn	group	image	GFAP (fold increase over normal)
ipsilateral (cont.)	injury+saline	164-1	0.48
		164-2	0.96
		164-3	0.84
		164-4	1.85
		164-5	2.53
		164-6	2.69
		165-2	1.87
		165-4	1.94
		165-6	2.02
		174-2	1.02
		174-4	1.39
		174-6	1.06
		182-1	1.61
		182-2	2.27
		182-3	1.34
		182-4	1.81
		182-6	1.09
		injury+10 $\mu$ g	138-1
	138-2		2.46
	138-3		2.82
	138-4		1.52
	140-1		0.82
	140-2		0.85
	140-3		0.91
	140-6		1.27
	139-2		1.56
	139-3		0.57
	139-5		1.73
	141-2		1.37
	141-4		1.33
	141-6		1.41
	168-2		0.63
	168-3		1.17
	168-4		1.74
	168-5		1.35
	168-6	1.13	
169-1	0.88		
169-2	1.62		
169-4	2.17		
169-5	0.92		
169-6	2.19		
176-2	1.17		
176-4	1.04		
176-6	0.99		
177-1	0.80		
177-2	1.08		
177-3	0.77		
177-4	0.87		
177-5	1.02		

dorsal horn	group	image	GFAP (fold increase over normal)
ipsilateral (cont.)	injury+10 $\mu$ g	177-6	0.77
	injury+150 $\mu$ g	136-2	5.92
		136-3	4.89
		136-4	4.12
		136-5	3.43
		136-6	2.73
		142-1	1.04
		142-2	0.47
		142-3	3.09
		142-5	1.41
		142-6	1.58
		143-3	1.52
		143-4	2.36
		143-5	1.18
		167-1	1.31
		167-2	2.82
		167-4	2.27
		167-5	2.32
		167-6	2.27
		172-1	1.00
		172-2	1.20
		172-3	0.97
		172-4	0.71
		172-6	1.13
		173-2	0.51
		173-4	0.41
		173-5	0.49
		180-1	0.50
		180-2	0.29
	180-3	0.71	
180-4	1.01		
181-1	1.17		
181-2	1.15		
181-3	1.06		
181-4	1.48		
181-5	1.92		
181-6	1.29		
contralateral	sham+saline	131-1	0.79
		131-2	1.34
		131-4	1.24
		131-6	1.19
		171-3	1.98
		171-4	0.55
		171-5	1.88
		175-1	0.19
		175-2	0.51
		175-6	0.51
178-1	0.47		
178-2	1.17		

<b>dorsal horn</b>	<b>group</b>	<b>image</b>	<b>GFAP (fold increase over normal)</b>
contralateral (cont.)	sham+saline	178-3	0.41
		178-4	0.71
		178-5	0.58
		179-1	0.43
		179-2	0.57
		179-3	0.77
		179-4	1.22
		179-5	0.93
		179-6	1.15
		183-1	1.27
		183-2	2.40
		183-4	2.30
		183-5	2.59
		184-1	1.57
		184-2	2.13
		184-3	0.52
		184-4	1.49
		184-5	0.54
	184-6	1.87	
	injury+saline	128-1	3.80
		128-2	1.63
		128-3	2.32
		128-6	3.02
		130-1	2.01
		130-2	2.78
		130-3	2.05
		130-4	3.84
		129-1	1.69
		129-2	1.92
		129-4	0.71
		129-5	0.72
		129-6	1.17
		164-2	2.41
		164-3	1.24
		164-4	2.15
		164-5	1.76
164-6		2.54	
165-2	3.08		
165-4	2.38		
165-6	1.56		
174-2	1.37		
174-4	0.98		
174-5	0.98		
174-6	1.00		
182-1	2.13		
182-2	2.62		
182-3	1.29		
182-4	2.30		
182-6	0.69		

dorsal horn	group	image	GFAP (fold increase over normal)
contralateral (cont.)	injury+10 $\mu$ g	138-1	1.97
		138-2	3.39
		138-3	3.42
		138-4	2.08
		138-5	2.61
		140-1	0.36
		140-2	0.40
		140-3	0.66
		140-6	0.94
		139-2	1.27
		139-3	0.61
		139-5	1.49
		141-1	0.17
		141-4	1.15
		141-6	1.22
		168-1	0.10
		168-2	0.62
		168-3	1.17
		168-4	0.67
		168-5	0.90
		168-6	1.14
		169-1	0.55
		169-2	0.52
		169-3	0.31
		169-4	1.84
		169-6	1.89
	176-2	1.03	
	176-4	0.94	
	176-6	0.62	
	177-1	0.85	
	177-2	0.60	
	177-3	0.93	
	177-4	0.85	
	177-5	1.04	
177-6	0.76		
	injury+150 $\mu$ g	136-2	2.22
		136-3	2.33
		136-4	4.99
		136-5	1.93
		136-6	3.65
		142-1	0.34
		142-2	0.43
		142-3	2.04
		142-5	1.11
		142-6	1.55
	143-3	1.74	
	143-4	3.11	
	143-5	2.13	
	167-1	1.15	

<b>dorsal horn</b>	<b>group</b>	<b>image</b>	<b>GFAP (fold increase over normal)</b>
contralateral (cont.)	injury+150µg	167-2	3.30
		167-4	2.45
		167-5	1.96
		167-6	2.18
		172-1	1.18
		172-2	1.52
		172-3	0.96
		172-4	0.84
		172-6	0.70
		173-1	0.52
		173-2	0.92
		173-4	1.18
		173-6	0.99
		180-2	0.50
		180-3	1.03
		180-4	2.08
		181-1	1.41
		181-2	1.59
		181-3	1.65
		181-4	1.99
181-5	2.36		
181-6	1.74		



**Table D.6** Quantification of GLAST in the superficial laminae at day 7 after a painful compression treated with ceftriaxone (*injury+10 $\mu$ g*, *injury+150 $\mu$ g*) or the saline vehicle (*injury+saline*), or sham treated with the saline (*sham+saline*) (Chapter 6).

dorsal horn	group	image	GLAST (fold increase over normal)
ipsilateral	sham+saline	131-1	0.61
		131-2	0.71
		131-3	0.45
		131-4	0.42
		131-6	0.74
		171-2	1.91
		171-5	2.53
		171-6	1.97
		174-1	0.61
		174-3	0.74
		174-5	0.93
		174-6	0.59
		175-1	1.00
		175-2	0.68
		175-3	0.90
		175-6	0.71
		178-1	1.08
		178-2	0.68
		178-4	0.61
		178-5	1.08
		183-2	1.22
		183-3	0.75
		183-4	0.94
		183-6	1.20
	184-1	0.78	
	184-2	0.91	
	184-4	1.82	
	184-5	1.72	
	injury+saline	128-2	1.41
		128-4	1.38
		128-5	1.09
		128-6	1.85
		129-3	1.13
		129-4	1.33
		129-6	2.76
		130-2	1.24
130-3		1.28	
130-4		1.20	
164-2		0.63	
164-4		1.14	
164-6	2.24		
165-1	2.06		
165-2	2.02		

dorsal horn	group	image	GLAST (fold increase over normal)
ipsilateral (cont.)	injury+saline	165-4	2.20
		174-2	0.92
		174-3	0.77
		174-4	1.01
		182-1	2.62
		182-2	1.68
		182-3	1.64
		182-4	2.62
		182-5	2.97
	injury+10µg	138-1	0.64
		138-2	0.54
		138-3	0.67
		138-6	1.14
		139-1	0.71
		139-2	1.00
		139-4	0.67
		139-6	1.42
		140-2	0.40
		140-4	0.28
		140-6	0.54
		141-2	0.90
		141-3	1.57
		141-4	0.64
		168-1	0.53
		168-2	0.75
		168-4	1.75
		168-6	1.64
		169-1	1.11
		169-2	1.04
		169-3	1.40
		169-4	0.84
		169-5	0.78
		176-1	0.95
		176-3	0.73
		176-4	0.40
		176-5	0.66
	176-6	0.98	
	177-1	1.05	
	177-3	1.21	
	177-4	1.38	
	177-5	1.38	
	177-6	1.94	
injury+150µg	136-1	1.24	
	136-2	1.36	
	136-4	2.05	
	142-2	0.72	
	142-3	1.75	

dorsal horn	group	image	GLAST (fold increase over normal)
ipsilateral (cont.)	injury+150µg	142-5	1.40
		143-1	1.66
		143-2	0.21
		143-3	0.53
		143-4	1.20
		167-1	0.27
		167-3	0.79
		167-4	0.28
		167-5	0.57
		172-1	1.23
		172-2	0.31
		172-3	0.64
		172-5	0.69
		173-2	0.10
		173-3	0.54
		173-4	1.51
		180-1	1.06
		180-2	0.61
		180-3	1.64
		180-4	1.85
180-5	0.63		
181-1	0.35		
181-2	1.20		
181-3	0.91		
181-4	0.62		
181-5	1.12		
contralateral	sham+saline	131-1	0.92
		131-2	1.04
		131-3	1.43
		131-4	0.61
		131-5	1.50
		171-4	1.99
		171-5	1.53
		171-6	1.40
		174-1	0.44
		174-3	0.73
		174-6	0.69
		175-3	0.69
		175-4	0.23
		175-6	0.23
		178-1	0.95
		178-3	0.35
		178-4	0.48
		178-5	0.65
		178-6	1.19
		183-2	1.66
183-3	0.99		

<b>dorsal horn</b>	<b>group</b>	<b>image</b>	<b>GLAST (fold increase over normal)</b>
contralateral (cont.)	sham+saline	183-4	0.71
		184-1	1.93
		184-4	1.94
		184-5	1.60
	injury+saline	128-2	1.53
		128-4	2.59
		128-6	0.86
		129-3	1.07
		129-4	0.94
		129-6	1.49
		130-2	1.37
		130-3	0.88
		130-4	1.32
		130-5	0.66
		130-6	1.53
		164-2	0.75
		164-4	0.68
		164-6	1.33
		165-1	1.73
		165-2	1.53
		165-4	1.52
		174-1	1.11
		174-2	1.22
		174-3	0.43
		174-4	0.31
		174-5	0.22
		182-3	1.40
		182-4	1.58
	182-5	1.30	
	inj+10 $\mu$ g	138-1	1.36
		138-2	0.74
		138-6	0.63
		139-1	1.99
		139-2	2.14
		139-4	0.73
		139-6	1.26
140-2		0.21	
140-4		0.37	
140-6		0.27	
141-2		0.27	
141-3		0.20	
141-4		0.70	
168-1		1.68	
168-2		1.69	
168-4		0.40	
168-6		0.42	
169-1		1.80	

dorsal horn	group	image	GLAST (fold increase over normal)
contralateral (cont.)	inj+10 $\mu$ g	169-2	1.38
		169-4	0.79
		169-5	0.44
		176-1	1.41
		176-2	0.85
		176-3	1.20
		176-4	0.55
		177-1	1.81
		177-2	1.56
		177-4	1.12
	injury+150 $\mu$ g	136-1	0.29
		136-2	1.63
		136-3	0.37
		136-4	1.63
		142-1	1.10
		142-2	1.34
		142-3	0.32
		142-4	0.42
		142-5	1.29
		143-1	1.34
		143-3	2.23
		143-4	0.88
		167-1	2.51
		167-2	0.98
		167-3	0.78
		172-1	2.55
		172-2	1.97
		172-3	0.44
		172-5	1.01
		173-2	1.12
		173-3	0.40
		173-4	1.79
		180-1	1.28
180-3	0.71		
180-4	0.86		
180-5	0.84		
181-1	1.92		
181-3	1.28		
181-4	0.65		
181-5	0.81		

**Table D.7** Quantification of CGRP in the superficial dorsal horn at day 7 following a 15 minute compression treated with Riluzole (*inj+Ril*) or the vehicle (*inj+veh*), or sham procedures treated with the vehicle (*sham+veh*) (Chapter 7).

dorsal horn	group	image	CGRP (fold increase over normal)
ipsilateral	sham+veh	162-3	1.07
		162-4	0.96
		162-5	0.73
		162-6	0.68
		193-2	1.13
		193-3	0.86
		193-4	1.24
		195-2	0.77
		195-3	0.83
		195-5	1.04
		195-6	1.15
		196-1	1.02
		196-2	0.82
		196-3	1.04
		196-4	0.86
		196-6	1.11
		200-1	1.06
		200-3	1.04
		200-4	0.96
		200-6	1.22
		211-1	0.72
		211-2	1.00
		211-3	0.90
		211-4	1.20
		211-5	0.73
		211-6	0.94
		212-1	0.57
		212-2	0.83
	212-3	0.76	
	212-4	0.79	
	212-5	0.81	
	212-6	0.93	
	inj+veh	156-1	0.41
		156-2	0.85
156-5		1.00	
156-6		1.08	
157-1		0.42	
157-2		0.55	
157-4		0.65	
163-1	0.53		
163-3	0.84		
163-5	0.70		
163-6	0.82		
194-1	0.49		

dorsal horn	group	image	CGRP (fold increase over normal)
ipsilateral (cont.)	sham+veh	194-2	0.71
		194-4	0.62
		194-5	0.72
		198-2	1.30
		198-3	1.03
		198-4	1.12
		198-5	0.67
		198-6	0.92
		199-1	0.66
		199-2	1.01
		199-3	0.54
		199-4	0.82
		199-5	0.36
		199-6	0.50
		210-1	0.73
		210-2	0.79
		210-3	0.64
		210-4	0.69
		210-5	0.59
		210-6	0.70
	inj+Ril	147-1	0.90
		147-2	0.97
		147-3	0.85
		148-1	0.83
		148-2	0.98
		148-3	0.82
		148-4	0.81
		149-1	0.84
		149-2	0.84
		149-3	0.75
		149-4	0.84
		158-1	0.64
		158-2	0.68
		158-3	0.80
158-4	0.96		
158-5	0.74		
158-6	0.93		
159-2	1.13		
159-3	0.78		
159-4	1.12		
159-6	0.68		
160-2	0.74		
160-4	0.50		
160-6	0.95		
161-2	0.83		
161-3	0.73		
161-4	0.80		
161-6	0.71		

dorsal horn	group	image	CGRP (fold increase over normal)
contralateral	sham+veh	162-1	1.03
		162-2	1.10
		162-3	1.06
		193-2	1.39
		193-3	0.71
		193-4	0.68
		195-2	1.05
		195-4	1.27
		195-5	0.82
		195-6	1.17
		196-1	0.77
		196-2	0.84
		196-6	0.85
		200-1	0.92
		200-2	0.73
		200-3	0.84
		200-4	0.95
		211-1	1.18
		211-2	1.30
		211-3	1.25
		211-4	1.25
		211-5	1.10
		211-6	1.17
		212-1	1.18
	212-2	1.19	
	212-3	1.21	
	212-4	1.21	
	212-5	1.04	
	212-6	1.16	
	inj+veh	156-2	0.72
		156-3	0.57
		156-4	1.06
		156-5	1.27
		156-6	1.20
		157-1	0.65
		157-2	0.67
157-3		0.99	
157-4		0.65	
163-1		0.58	
163-2		1.23	
163-3		0.76	
163-4	1.23		
163-5	0.89		
163-6	1.07		
194-4	0.61		
194-5	0.78		
194-6	1.15		
198-2	1.17		
198-3	0.97		



dorsal horn	group	image	CGRP (fold increase over normal)
contralateral (cont.)	inj+veh	198-4	1.19
		198-5	1.01
		198-6	1.28
		199-1	0.70
		199-2	1.23
		199-3	0.89
		199-4	1.02
		199-5	0.73
		199-6	1.07
		210-1	0.87
		210-2	0.96
		210-3	1.03
		210-4	0.97
		210-5	1.19
	210-6	1.15	
	inj+Ril	147-1	1.05
		147-2	1.02
		147-3	1.06
		147-5	1.04
		148-1	0.70
		148-2	0.97
		148-3	0.76
		148-4	0.90
		149-1	0.87
		149-2	0.99
		149-3	0.97
		149-4	0.93
		149-5	1.05
		149-6	1.17
		158-1	0.77
		158-2	0.95
		158-3	0.88
		158-4	1.24
		159-1	0.81
		159-2	0.99
		159-3	0.82
159-4		1.04	
159-6	1.39		
160-1	0.92		
160-2	0.83		
160-4	0.92		
160-5	1.03		
160-6	1.19		
161-1	0.80		
161-2	1.09		
161-3	0.60		
161-4	0.83		
161-6	0.80		

**Table D.8** Quantification of CGRP in the deep dorsal horn at day 7 following a 15 minute compression treated with Riluzole (*inj+Ril*) or the vehicle (*inj+veh*), or sham procedures treated with the vehicle (*sham+veh*) (Chapter 7).

dorsal horn	group	image	CGRP (fold increase over normal)
ipsilateral	sham+veh	162-2	0.69
		162-3	1.07
		162-4	0.52
		162-5	0.59
		193-1	1.62
		193-4	1.31
		193-5	0.69
		195-1	1.03
		195-3	0.66
		195-4	0.78
		195-5	1.82
		196-4	1.02
		200-1	0.77
		200-2	0.16
		200-3	0.78
		200-4	0.34
		200-5	0.20
		211-1	0.74
		211-2	0.91
		211-3	0.72
		211-4	0.34
		211-5	0.62
		211-6	0.54
		212-1	0.37
		212-2	0.52
		212-3	0.78
		212-4	0.37
		212-6	0.59
	inj+veh	156-1	2.34
		156-2	2.33
		156-4	2.54
		156-5	1.53
		156-6	2.22
		157-1	1.59
157-3		1.06	
157-4		0.78	
163-1		1.21	
163-2		0.57	
163-4		0.78	
163-5		0.53	
163-6		0.75	
194-1		2.84	
194-3		1.28	
194-5		1.69	
198-1	1.56		
198-3	1.54		

dorsal horn	group	image	CGRP (fold increase over normal)
ipsilateral (cont.)	inj+veh	198-5	1.84
		199-1	2.54
		199-4	2.38
		199-6	1.10
		210-2	0.60
		210-4	0.31
		210-5	0.50
		210-6	0.78
	inj+Ril	147-1	1.04
		147-2	1.83
		147-3	1.65
		147-4	1.86
		148-1	1.63
		148-2	0.93
		148-3	1.22
		149-3	2.01
		149-4	1.30
		149-5	2.35
		149-6	2.05
		158-1	0.50
		158-3	0.22
		158-4	0.74
		158-6	0.90
		159-2	0.57
		159-3	0.35
		159-4	0.83
		159-6	0.53
		160-1	0.55
		160-2	0.69
		160-3	0.28
		160-4	0.89
		160-5	0.70
161-1	0.64		
161-3	1.01		
161-5	0.90		
contralateral	sham+veh	162-1	0.50
		162-3	0.61
		162-4	0.39
		162-5	0.95
		162-6	0.81
		193-1	2.41
		193-2	2.48
		193-4	1.17
		193-5	1.73
		195-1	0.58
		195-2	0.38
		195-3	0.77
		195-4	0.73
		195-5	1.09
195-6	0.83		

dorsal horn	group	image	CGRP (fold increase over normal)
contralateral (cont.)	sham+veh	196-1	0.40
		196-4	1.00
		196-5	0.92
		200-1	0.75
		200-2	0.95
		200-3	0.42
		200-4	0.39
		200-6	0.32
		211-1	0.51
		211-2	0.39
		211-3	0.45
		211-4	0.66
		211-5	0.58
		211-6	0.54
		212-1	0.63
		212-2	0.75
		212-3	0.35
		212-4	0.62
	212-5	0.36	
	inj+veh	156-1	1.73
		156-2	1.69
		156-3	2.05
		156-4	1.44
		156-5	1.51
		156-6	2.54
		157-1	0.26
		157-2	0.34
		157-3	0.16
		157-4	0.37
		163-3	0.36
		163-4	0.70
		163-5	0.53
		163-6	0.71
		194-1	1.80
		194-3	1.18
		194-4	0.60
		198-2	0.50
		198-3	2.82
		198-5	2.39
		199-2	1.13
		199-3	0.74
		199-4	0.46
210-2		0.85	
210-3	0.87		
210-4	0.48		
210-5	0.83		
210-6	0.98		
inj+Ril	147-1	0.92	
	147-2	1.44	
	147-3	0.91	

<b>dorsal horn</b>	<b>group</b>	<b>image</b>	<b>CGRP (fold increase over normal)</b>
contralateral (cont.)	inj+Ril	147-4	1.48
		147-5	1.11
		147-6	0.93
		148-3	0.87
		148-4	1.19
		148-5	1.46
		148-6	1.05
		149-1	1.14
		149-2	1.21
		149-3	1.85
		149-4	1.25
		158-1	0.67
		158-2	0.36
		158-3	0.37
		158-4	0.45
		158-5	0.69
		158-6	0.47
		159-3	0.24
		159-5	0.14
		159-6	0.33
		160-2	0.58
		160-3	0.62
		160-4	0.86
		160-5	0.36
		160-6	0.27
		161-1	0.55
161-4	0.22		
161-5	0.61		
161-6	0.67		

---

## APPENDIX E

### Quantification of Evoked Action Potentials in the Dorsal Horn

---

This appendix provides a summary of the number of action potentials that were evoked during forepaw stimulation for individual neuron recordings in the dorsal horn on day 7 for studies in Chapters 5, 6 and 7. Specifically, recordings were made in the superficial (Table E.1) and deep (Table E.2) laminae at day 7 following compressions having durations of 3 minutes (deep laminae only), 15 minutes, or sham procedures for the studies presented in Chapter 5. Similarly, spinal recordings in the deep laminae were made at day 7 following ceftriaxone (Chapter 6; Table E.3) or Riluzole treatment (Chapter 7; Table E.4). For the ceftriaxone treatment study, rats underwent a painful compression (10gf, 15 minutes) that was treated with 10 $\mu$ g or 150 $\mu$ g ceftriaxone (*injury+10 $\mu$ g*, *injury+150 $\mu$ g*) or the saline vehicle (*injury+saline*) on days 1 through 6. A separate group of rats received the sham exposure and vehicle treatment (*sham+saline*), also on days 1 through 6. For the Riluzole treatment study, rats were either treated with Riluzole (*injury+Ril*) or the vehicle which was 10%  $\beta$ -cyclodextrin in saline (*injury+veh*), on day 1 after a painful nerve root compression (10gf, 15 minutes). In a control group for that study, rats underwent sham procedures and were treated with the vehicle (*sham+veh*).

In the tables of this appendix, the neuron ID identifies the rat in which the neuron was identified and the order that each neuron was found for that animal (*rat#-neuron order*). For each neuron, the table summarizes the depth (in  $\mu\text{m}$ ) at which it was located from the pial surface and the number of action potentials that were evoked by application of each of four different von Frey filament strengths (1.4, 4.0, 10.0, 26.0gf). The phenotype of each neuron was identified as either wide dynamic range (WDR), low threshold mechanoreceptor (LTM) or nociceptive specific (NS), based on their response to the graded stimuli (Haines et al. 2003, Quinn et al. 2010, Saito et al. 2002).

**Table E.1** Spinal neuronal firing in the superficial laminae at day 7.

side	group	ID	depth	1.4	4.0	10.0	26.0	phenotype
ipsilateral	sham	125-1	400	0	31	25	69	WDR
		125-2	360	12	24	43	41	LTM
		125-3	200	2	15	15	92	WDR
		125-4	430	108	116	108	99	LTM
		125-5	380	13	39	46	88	WDR
		154-1	160	1	42	46	118	WDR
		154-2	240	0	12	15	20	WDR
		154-3	180	0	8	10	18	WDR
		186-1	150	11	9	11	22	LTM
		186-2	200	19	15	28	35	LTM
		186-3	300	0	1	36	30	NS
		186-4	300	4	9	33	28	WDR
		189-1	230	4	5	6	10	WDR
		189-2	340	15	29	30	28	LTM
		189-3	330	2	5	7	1	LTM
		189-4	190	59	57	38	18	LTM
		189-5	310	0	0	7	12	NS
		189-6	290	1	0	2	15	NS
		190-1	350	10	18	43	138	WDR
		190-2	310	48	71	127	137	WDR
		190-3	150	25	46	42	38	LTM
		190-4	200	14	20	42	65	LTM
		190-5	330	1	6	11	14	WDR
		190-6	250	3	5	16	15	NS
		201-2	370	0	7	35	50	WDR
		201-3	250	12	16	15	8	LTM
		201-4	140	0	0	19	25	NS
		204-1	330	0	5	14	48	WDR
		204-2	215	52	80	51	82	LTM
		204-3	260	0	57	74	83	WDR
		204-4	325	9	11	19	10	LTM
		204-5	330	3	8	32	23	LTM
	205-1	365	13	9	18	11	LTM	
	205-2	130	4	6	12	27	WDR	
	205-3	270	6	12	44	85	WDR	
	205-4	340	1	3	11	9	NS	
	205-5	115	2	0	5	12	NS	
	15 minute compression	122-1	60	30	45	55	116	WDR
		122-2	370	52	97	127	119	WDR
		122-3	250	20	19	50	70	WDR
126-1		370	6	3	24	92	WDR	
126-2		250	9	18	175	172	NS	
126-3		350	5	28	48	59	LTM	
126-4		110	1	1	8	53	WDR	
126-5		340	11	10	28	65	WDR	
127-1		350	27	66	59	99	WDR	
127-2		400	61	78	78	112	LTM	
127-3		310	2	6	2	4	LTM	
127-4		310	6	10	27	28	WDR	
127-5		410	8	15	30	112	WDR	



side	group	ID	depth	1.4	4.0	10.0	26.0	phenotype		
ipsilateral (cont.)	15 minute compression (cont.)	153-1	300	5	12	47	61	WDR		
		153-2	150	13	20	19	47	WDR		
		153-3	300	0	1	19	23	NS		
		153-4	270	3	6	19	21	WDR		
		188-1	50	1	5	60	103	NS		
		188-2	250	3	8	21	17	LTM		
		188-3	170	1	7	12	18	WDR		
		188-4	150	6	16	22	60	WDR		
		188-5	160	19	25	45	100	WDR		
		188-6	220	9	32	75	199	WDR		
		192-1	310	0	1	50	60	NS		
		192-2	240	1	8	22	33	WDR		
		192-3	250	0	1	25	46	NS		
		192-4	230	15	40	29	79	WDR		
		192-5	290	4	17	19	30	WDR		
		203-1	305	5	9	20	23	WDR		
		203-2	230	6	39	75	71	WDR		
		203-3	300	13	8	17	23	WDR		
		203-4	160	0	0	0	18	WDR		
		203-5	285	16	19	21	52	WDR		
		206-1	365	7	20	45	49	WDR		
		206-2	340	2	13	20	23	WDR		
		206-4	130	0	2	2	10	NS		
		206-5	325	22	35	39	55	WDR		
		206-6	85	10	11	18	24	WDR		
		206-7	315	5	11	19	19	WDR		
		contralateral	sham	125-6	110	21	19	28	17	WDR
				125-7	280	2	3	6	7	LTM
125-8	270			20	15	63	69	LTM		
125-9	400			5	6	26	42	WDR		
125-10	330			7	6	9	16	WDR		
154-4	260			8	2	5	11	LTM		
154-5	150			3	2	15	17	NS		
154-6	150			21	19	63	122	WDR		
154-7	200			17	37	39	46	WDR		
186-6	260			5	2	9	48	WDR		
186-7	260			11	8	17	19	WDR		
186-8	340			7	5	4	7	LTM		
186-9	340			12	10	2	8	LTM		
186-10	190			0	0	44	64	LTM		
186-11	250			12	23	11	10	NS		
186-12	360			14	28	51	48	LTM		
189-7	320			5	3	4	12	WDR		
189-8	340			16	11	16	20	WDR		
189-10	300			1	6	14	18	LTM		
189-12	290			9	11	24	35	LTM		
190-7	160			53	26	57	24	NS		
190-9	260			13	53	67	108	WDR		
190-11	320			8	5	48	51	LTM		
190-12	350			4	18	20	40	WDR		
201-5	350			0	0	10	31	NS		
201-6	340			4	8	15	22	WDR		
204-6	220			2	8	25	22	NS		

side	group	ID	depth	1.4	4.0	10.0	26.0	phenotype
contralateral (cont.)	sham (cont.)	204-8	360	15	8	19	18	NS
		204-9	345	10	12	16	21	LTM
		204-10	310	0	0	8	8	LTM
		205-7	155	3	6	4	10	LTM
		205-9	350	18	44	84	56	WDR
		205-10	180	13	25	38	36	LTM
		205-11	235	2	5	10	33	WDR
	15 minute compression	122-4	140	5	11	15	21	WDR
		122-5	350	68	134	26	33	LTM
		122-6	340	9	24	21	31	LTM
		126-6	400	18	39	42	79	WDR
		126-7	200	8	23	13	54	WDR
		126-8	380	31	28	49	77	LTM
		127-6	320	0	28	32	65	LTM
		127-7	200	16	69	51	28	LTM
		127-8	280	14	26	49	81	LTM
		127-9	200	1	10	48	52	LTM
		127-10	110	5	0	12	25	WDR
		127-11	370	25	21	30	13	WDR
		153-5	250	0	8	23	53	WDR
		153-6	310	5	4	9	23	WDR
		188-7	270	13	35	55	72	NS
		188-8	90	0	0	53	61	LTM
		188-9	160	0	8	43	37	WDR
		188-10	260	0	2	4	12	WDR
		188-11	350	2	10	11	11	NS
		188-12	165	5	6	27	132	NS
		192-6	170	12	24	35	10	WDR
		192-7	260	7	16	73	24	NS
		192-8	60	11	13	15	14	WDR
		192-9	290	23	30	0	24	WDR
		192-10	290	10	17	34	71	WDR
		192-11	270	0	9	4	34	LTM
		192-12	170	2	7	69	52	LTM
		192-13	340	0	12	20	63	WDR
		203-6	290	5	16	21	56	WDR
		203-8	210	0	0	64	102	WDR
		206-8	365	0	7	7	8	WDR
		206-9	310	63	48	41	55	LTM
		206-10	295	53	59	122	125	WDR
206-11	320	29	30	35	30	LTM		
206-12	340	2	10	8	15	LTM		
206-13	310	3	4	4	4	LTM		

**Table E.2** Spinal neuron firing in the ipsilateral deep laminae at day 7.

<b>group</b>	<b>ID</b>	<b>depth</b>	<b>1.4g</b>	<b>4.0g</b>	<b>10.0g</b>	<b>26.0g</b>	<b>phenotype</b>
sham	7-1	750	4	10	10	13	WDR
	7-2	500	6	20	33	7	WDR
	7-3	450	0	0	10	5	LTM
	9-1	450	4	19	71	57	WDR
	9-2	600	1	2	8	12	WDR
	9-3	700	6	35	32	33	LTM
	9-4	545	1	3	19	20	WDR
	9-5	750	0	4	8	25	WDR
	9-6	1000	14	11	35	46	WDR
	9-9	500	10	0	17	41	LTM
	11-2	955	13	36	46	48	WDR
	11-3	645	5	14	16	13	WDR
	11-4	925	9	15	28	42	WDR
	11-5	555	0	6	10	21	WDR
	11-6	740	3	1	28	23	WDR
	11-7	450	0	0	4	7	WDR
	11-8	825	10	6	12	12	LTM
	11-9	575	6	8	8	6	LTM
	42-1	600	1	3	9	5	WDR
	42-2	800	3	27	9	10	LTM
	42-3	550	4	3	0	3	LTM
	42-4	525	4	4	4	4	LTM
	42-5	550	14	6	10	19	LTM
	42-6	525	38	98	115	117	WDR
	42-7	500	55	74	17	130	WDR
	42-8	600	4	23	90	151	WDR
	43-1	575	3	5	11	94	WDR
	43-2	600	2	9	13	23	WDR
	43-3	625	3	1	8	0	LTM
	43-4	600	6	10	11	4	LTM
	43-5	650	3	1	2	19	WDR
	43-6	725	0	13	21	46	WDR
	43-7	525	3	2	0	24	WDR
43-8	550	3	10	0	28	WDR	
3 minute compression	315-1	625	0	44	30	48	WDR
	315-2	525	6	5	3	8	LTM
	315-3	600	8	7	9	10	WDR
	315-4	550	11	43	65	50	WDR
	315-5	525	4	7	11	6	LTM
	315-6	650	11	25	41	52	WDR
	315-7	700	4	10	14	16	WDR
	316-1	550	4	4	8	6	LTM
	316-2	600	1	16	15	20	WDR

<b>group</b>	<b>ID</b>	<b>depth</b>	<b>1.4g</b>	<b>4.0g</b>	<b>10.0g</b>	<b>26.0g</b>	<b>phenotype</b>
15 minute compression	8-2	850	0	10	25	40	WDR
	10-3	450	1	17	14	36	WDR
	10-4	650	0	15	19	31	WDR
	10-6	750	19	78	156	130	WDR
	10-7	700	17	19	13	23	LTM
	10-8	800	6	18	63	55	WDR
	10-9	500	31	33	36	36	LTM
	10-7A	700	2	7	6	10	LTM
	30-1	550	3	7	17	20	WDR
	30-2	600	15	8	27	64	WDR
	30-3	600	3	3	6	15	WDR
	30-4	800	0	3	20	43	WDR
	30-6	550	1	6	25	33	WDR
	30-7	525	8	10	5	24	WDR
	30-8	575	5	16	18	36	WDR
	30-9	650	2	5	6	13	WDR
	34-1	600	2	4	5	6	LTM
	34-10	700	26	8	43	109	WDR
	34-11	625	34	17	28	34	WDR
	34-12	625	9	24	48	81	WDR
	34-2	800	8	2	5	36	WDR
	34-3	550	2	5	10	18	WDR
	34-4	640	5	38	35	51	WDR
	34-5	700	5	17	22	16	LTM
	34-7	600	4	8	12	22	WDR
	34-8	650	6	14	30	46	WDR
	34-9	800	21	77	70	81	WDR
	41-1	625	23	48	36	59	WDR
	41-2	550	3	9	5	7	LTM
	41-3	700	8	4	9	19	WDR
	41-4	650	0	4	8	4	WDR
	41-5	625	2	102	250	157	WDR
	41-6	575	1	3	21	36	WDR
	41-7	600	25	9	2	6	LTM
	41-8	550	3	38	81	53	WDR

**Table E.3** Spinal neuron firing after ceftriaxone treatment at day 7.

side	group	ID	depth	1.4	4.0	10.0	26.0	phenotype	
ipsilateral	sham+saline	301-1	470	1	10	1	9	WDR	
		301-2	780	3	0	6	13	WDR	
		301-3	840	4	5	15	26	WDR	
		301-4	740	1	4	0	25	LTM	
		301-5	550	15	11	79	183	WDR	
		302-1	570	2	1	2	11	LTM	
		302-2	890	2	2	2	5	LTM	
		302-3	700	2	12	12	12	LTM	
		302-4	580	3	12	23	16	WDR	
		302-5	810	3	13	33	67	WDR	
		303-1	420	0	2	10	21	WDR	
		303-2	870	0	6	5	0	WDR	
		303-3	470	1	2	15	5	WDR	
		303-5	770	4	10	13	12	LTM	
		304-11	430	2	20	8	10	LTM	
		304-12	550	0	12	19	18	WDR	
		304-14	770	5	10	12	15	LTM	
		306-1	420	4	4	16	11	WDR	
		306-2	670	10	23	16	20	LTM	
		306-3	560	1	1	8	2	LTM	
		306-4	560	5	16	7	0	LTM	
		306-5	840	3	11	35	62	LTM	
		313-1	420	6	6	4	4	WDR	
		313-2	630	8	11	22	14	WDR	
		313-4	870	0	11	52	79	WDR	
		314-1	430	9	6	61	101	WDR	
		314-2	820	6	7	6	5	LTM	
		314-3	820	3	10	8	20	WDR	
		314-4	490	0	2	16	36	WDR	
		314-5	910	0	0	19	35	WDR	
		injury+saline	287-1	420	18	22	26	38	WDR
			287-2	730	55	13	21	44	WDR
	287-3		530	4	12	9	43	WDR	
	288-1		790	9	0	13	71	WDR	
	288-2		530	2	3	3	24	WDR	
	288-3		670	12	44	68	118	WDR	
	297-1		420	7	12	17	13	WDR	
	297-2		540	2	8	14	16	WDR	
	298-1		610	26	63	190	243	WDR	
	298-2		810	8	25	45	39	WDR	
299-2	430		5	22	19	75	WDR		
299-3	710		24	75	127	85	WDR		
299-4	850		10	20	52	64	WDR		
299-5	560		32	18	45	37	WDR		

side	group	ID	depth	1.4	4.0	10.0	26.0	phenotype
ipsilateral (cont.)	injury+saline	299-6	700	4	17	50	34	WDR
		299-7	650	21	38	43	184	WDR
		300-1	680	0	10	19	36	WDR
		300-2	610	70	61	39	42	WDR
		300-3	790	31	55	64	86	WDR
		300-4	850	8	46	34	21	WDR
		300-5	640	21	39	13	166	WDR
		307-1	800	5	7	42	72	WDR
		307-2	530	10	6	47	116	WDR
		307-3	610	7	3	3	3	LTM
		307-4	630	0	20	155	428	WDR
		307-5	480	7	110	103	144	WDR
		307-6	720	8	11	12	19	LTM
		308-1	720	4	41	42	151	WDR
		308-2	860	45	56	76	90	WDR
		308-3	740	1	30	77	114	WDR
		308-4	770	13	12	16	20	LTM
		308-5	470	31	152	188	246	WDR
		308-6	420	32	23	20	98	WDR
		injury+10 $\mu$ g	285-1	420	6	14	28	27
	285-2		530	0	4	7	29	WDR
	285-3		590	3	17	14	16	LTM
	285-5		430	9	12	41	46	LTM
	286-1		600	0	4	8	4	WDR
	286-2		690	4	1	6	10	WDR
	286-3		800	1	3	15	35	WDR
	286-4		510	0	5	6	2	LTM
	290-1		620	13	48	54	81	LTM
	290-2		800	3	2	17	13	WDR
	290-3		520	4	2	13	33	WDR
	290-4		680	22	19	36	33	WDR
	290-5		850	0	23	24	77	WDR
	290-6		800	10	7	17	14	WDR
	293-1		480	4	5	13	9	LTM
	293-2		550	26	22	25	68	WDR
	293-3		500	0	11	69	143	WDR
	293-4		690	6	3	10	9	LTM
	293-5		650	19	27	26	27	LTM
	294-1		550	16	8	15	11	LTM
	294-2		730	6	6	19	32	WDR
	294-3		860	16	16	38	26	LTM
	294-4	540	6	20	32	75	WDR	
294-5	650	22	15	19	18	WDR		
296-1	480	8	15	32	25	LTM		
296-2	540	0	0	20	63	WDR		
296-3	550	6	3	3	14	WDR		
296-4	650	9	11	32	24	WDR		

side	group	ID	depth	1.4	4.0	10.0	26.0	phenotype
ipsilateral (cont.)	injury+10µg	296-5	800	15	19	19	27	LTM
		311-1	430	0	5	30	55	WDR
		311-2	600	2	8	10	24	WDR
		311-3	510	7	5	6	5	LTM
		311-4	740	8	20	78	120	WDR
		311-5	890	2	14	39	46	WDR
		312-1	660	1	15	54	61	WDR
		312-2	730	3	0	9	10	LTM
		312-3	820	5	26	41	79	WDR
		312-4	630	17	9	14	26	LTM
		312-5	560	1	0	6	11	WDR
	injury+150µg	283-1	560	4	7	10	6	WDR
		283-2	450	9	7	9	13	LTM
		283-3	610	5	3	14	11	WDR
		284-1	670	10	4	20	46	WDR
		284-2	730	14	11	17	9	LTM
		284-3	640	40	80	63	88	LTM
		284-4	590	0	2	5	7	LTM
		284-5	820	25	36	47	47	WDR
		289-1	510	3	2	4	2	WDR
		289-2	480	8	14	12	37	WDR
		289-3	550	1	3	9	15	WDR
		289-4	630	7	28	40	16	LTM
		291-1	430	9	5	24	27	WDR
		291-2	510	9	15	11	11	WDR
		291-3	650	0	6	92	159	WDR
		291-4	480	7	0	25	20	WDR
		291-5	560	1	7	9	36	WDR
		292-1	560	5	11	31	49	WDR
		292-2	450	3	4	114	240	WDR
		292-3	610	13	26	18	38	WDR
		292-4	860	15	14	22	54	LTM
		292-5	440	3	17	12	4	LTM
		292-6	730	5	7	13	97	LTM
295-1		480	13	35	45	51	WDR	
295-2		780	31	28	19	23	LTM	
295-3		780	10	11	15	14	WDR	
295-4		860	5	21	29	75	WDR	
295-5		490	3	6	10	33	WDR	
295-6		610	10	13	21	47	WDR	
309-1		720	1	3	1	1	LTM	
309-2		710	11	27	29	66	WDR	
309-3		570	6	15	19	22	LTM	
309-4		540	4	29	52	43	WDR	
309-5	450	11	16	23	38	LTM		
310-1	420	8	103	158	137	WDR		
310-2	760	3	18	37	70	WDR		

side	group	ID	depth	1.4	4.0	10.0	26.0	phenotype
ipsilateral (cont.)	injury+150µg	310-3	880	2	3	14	39	WDR
		310-4	520	3	6	4	3	LTM
		310-5	470	0	16	27	78	WDR
contralateral	sham+saline	301-10	590	13	14	59	56	WDR
		301-6	540	0	10	14	26	WDR
		301-7	900	7	22	14	9	LTM
		301-8	410	2	10	8	32	LTM
		301-9	680	1	29	78	121	WDR
		302-10	670	8	15	34	26	WDR
		302-6	540	2	11	19	23	WDR
		302-7	650	0	1	13	58	LTM
		302-8	720	1	2	2	5	WDR
		302-9	550	3	2	10	23	LTM
		303-10	850	1	3	5		LTM
		303-6	890	5	7	4	0	LTM
		303-7	670	1	36	32	76	WDR
		303-8	500	0	20	18	28	WDR
		303-9	580	4	1	27	17	WDR
		304-15	550	2	5	17	51	WDR
		304-16	500	9	10	37	34	WDR
		304-17	690	1	25	29	53	WDR
		304-18	850	1	2	84	105	WDR
		305-1	640	0	18	70	48	WDR
		305-2	900	6	40	26	24	LTM
		305-3	740	5	5	29	24	WDR
		305-4	870	4	12	7	23	WDR
		305-5	750	0	4	27	40	LTM
		306-6	820	4	22	18	22	LTM
		306-7	530	23	16	50	57	WDR
	306-8	620	15	14	16	19	LTM	
	313-5	670	8	10	6	3	LTM	
	313-6	740	0	6	6	5	LTM	
	313-7	820	7	10	9	27	WDR	
	313-8	610	8	4	9	6	LTM	
	314-6	720	0	1	3	9	WDR	
	314-7	740	6	8	5	5	WDR	
	314-8	850	0	3	6	13	WDR	
314-9	800	0	2	10	14	WDR		
injury+saline	287-4	570	6	19	40	68	WDR	
	288-5	740	17	53	86	88	WDR	
	288-6	600	1	3	5	37	WDR	
	288-7	430	7	8	4	10	LTM	
	288-8	630	22	14	22	7	WDR	
	288-9	540	13	10	21	15	LTM	
	298-3	440	6	12	31	94	WDR	
	298-4	750	5	15	9	59	WDR	
298-5	870	7	18	27	32	WDR		



side	group	ID	depth	1.4	4.0	10.0	26.0	phenotype
contralateral (cont.)	injury+saline	299-10	690	2	5	9	60	WDR
		299-8	940	2	30	144	243	WDR
		299-9	760	9	5	24	27	LTM
		300-6	730	10	7	8	9	WDR
		300-7	660	1	0	5	7	WDR
		300-8	570	0	7	21	20	WDR
		300-9	590	5	16	8	6	LTM
		307-10	850	12	21	27	48	WDR
		307-11	710	37	30	82	120	WDR
		307-7	490	0	75	180	266	WDR
		307-8	560	9	8	30	38	WDR
		307-9	620	7	3	16	18	WDR
		308-10	740	0	0	0	12	WDR
		308-7	690	0	8	68	19	LTM
		308-8	810	0	20	33	7	LTM
		308-9	660	13	15	20	24	LTM
		injury+10µg	285-6	760	19	21	22	26
	285-7		600	7	3	2	13	LTM
	285-8		440	1	11	23	9	WDR
	285-9		540	8	18	29	15	WDR
	286-10		470	15	8	45	39	WDR
	286-6		470	0	0	6	8	WDR
	286-7		510	4	8	17	37	WDR
	286-8		650	1	16	24	13	LTM
	286-9		830	12	78	166	219	WDR
	290-10		470	13	27	70	96	WDR
	290-7		630	2	5	14	19	WDR
	290-8		850	12	11	13	29	LTM
	290-9		650	0	0	17	45	WDR
	293-10		800	10	1	26	34	WDR
	293-11		680	15	4	29	25	LTM
	293-6		800	12	19	32	45	WDR
	293-7		450	0	18	123	118	WDR
	293-8		450	27	27	28	38	WDR
	293-9		750	7	4	43	81	WDR
	294-6		800	2	1	6	6	LTM
	294-7		800	11	24	26	26	WDR
	296-10		620	2	16	15	17	WDR
	296-6		720	12	30	93	106	WDR
	296-7		840	10	19	25	34	LTM
	296-8		800	0	5	6	10	LTM
	296-9		740	46	31	19	27	WDR
	311-6		720	3	3	4	2	LTM
	311-7		430	0	0	5	21	WDR
	311-8		620	1	2	11	23	WDR
311-9	780		6	6	35	32	WDR	
312-10	460		4	6	4	3	LTM	

side	group	ID	depth	1.4	4.0	10.0	26.0	phenotype
contralateral (cont.)	injury+10µg	312-11	600	4	8	6	12	WDR
		312-12	620	11	11	14	17	WDR
		312-6	560	0	6	14	6	WDR
		312-7	490	10	3	5	12	WDR
		312-8	730	8	11	8	12	LTM
		312-9	730	3	12	17	17	LTM
	injury+150µg	283-5	460	9	15		39	WDR
		283-6	700	4	1	10	14	WDR
		283-7	760	9	18	46	59	WDR
		283-8	690	13	14	10	15	LTM
		284-10	810	22	17	12	6	LTM
		284-11	470	20	27	35	32	LTM
		284-6	580	12	10	11	6	LTM
		284-7	750	1	5	16	16	WDR
		284-8	750	2	8	7	29	LTM
		284-9	660	68	17	28	27	WDR
		289-5	420	6	9	21	53	WDR
		289-6	730	0	3	1	18	WDR
		291-10	460	0	145	47	127	WDR
		291-6	460	12	37	10	14	WDR
		291-7	710	4	12	16	70	WDR
		291-8	500	6	2	10	12	WDR
		291-9	750	20	30	26	105	WDR
		292-10	500	12	16	53	58	WDR
		292-11	770	30	12	53	98	WDR
		292-7	620	2	5	12	15	LTM
		292-8	800	8	13	12	19	WDR
		292-9	660	17	17	25	27	LTM
		295-7	430	11	33	31	11	LTM
		295-8	800	16	17	31	26	LTM
		295-9	620	2	7	22	144	WDR
		309-10	880	2	5	7	12	LTM
		309-6	570	0	8	15	47	WDR
		309-7	490	10	41	80	52	WDR
		309-8	600	19	73		0	WDR
		309-9	910	40	8	57	49	WDR
		310-10	650	21	29	73	13	WDR
		310-6	510	0	1	10	26	WDR
		310-7	600	2	0	4	26	WDR
		310-8	730	3	9	11	25	LTM
		310-9	870	4	10	13	16	LTM

**Table E.4** Spinal neuron firing after Riluzole treatment at day 7.

side	group	ID	depth	1.4	4.0	10.0	26.0	Type
ipsilateral	sham+veh	259-1	440	14	4	9	56	LTM
		261-1	610	9	5	1	9	LTM
		261-2	560	2	13	0	7	LTM
		261-3	770	6	18	18	26	LTM
		261-4	660	2	6	29	35	WDR
		261-5	600	4	2	5	3	LTM
		261-6	640	4	4	0	26	LTM
		263-1	600	1	2	14	29	WDR
		263-2	570	5	11	5	8	LTM
		263-3	700	4	0	14	46	WDR
		263-4	450	0	7	7	14	LTM
		263-5	410	9	12	16	32	WDR
		263-6	620	8	13	15	30	WDR
		265-1	670	1	5	13	40	WDR
		265-2	700	0	11	4	29	LTM
		265-3	850	1	1	47	42	WDR
		265-4	440	2	9	15	15	WDR
		265-5	590	7	4	1	13	LTM
		265-6	660	9	18	60	88	WDR
		268-1	450	2	3	43	40	WDR
		268-2	440	0	11	16	57	WDR
		268-3	840	16	6	4	6	LTM
		268-4	620	5	2	11	38	WDR
		268-5	430	0	25	12	51	WDR
		269-1	430	12	37	14	14	LTM
		269-2	660	5	48	24	28	LTM
		269-3	610	14	9	5	13	LTM
		269-4	700	0	0	27	11	LTM
		269-5	750	3	8	23	79	WDR
		269-6	880	1	33	0	40	WDR
		271-1	710	3	0	16	51	WDR
		271-2	520	1	5	8	38	WDR
		271-3	610	2	3	5	83	WDR
		271-4	760	2	3	7	14	WDR
		271-5	550	1	12	153	17	WDR
		274-1	520	1	1	5	23	WDR
		274-2	560	43	44	166	261	WDR
		274-3	480	9	5	72	56	WDR
	injury+veh	244-2	670	4	10	13	59	WDR
		244-3	560	6	19	31	63	WDR
		244-4	475	2	41	75	71	WDR
		244-5	600	0	4	45	158	WDR
	246-1	760	1	1	13	65	WDR	

side	group	ID	depth	1.4	4.0	10.0	26.0	Type
ipsilateral (cont.)	injury+veh	246-2	720	16	44	33	84	WDR
		246-3	490	3	27	23	68	WDR
		246-4	670	13	17	34	110	WDR
		246-5	450	1	8	37	43	WDR
		249-1	430	13	34	75	95	WDR
		249-2	490	4	9	20	40	WDR
		249-3	545	13	34	93	135	WDR
		249-4	690	10	6	88	149	WDR
		244-1	440	16	17	26	22	LTM
		264-1	850	1	5	20	43	WDR
		264-2	720	1	10	21	50	WDR
		264-3	740	3	1	6	22	WDR
		264-4	720	7	8	20	35	WDR
		264-5	940	0	17	30	108	WDR
		264-6	420	6	5	37	46	WDR
		266-1	950	9	10	14	34	WDR
		266-2	550	5	5	9	33	LTM
		266-3	640	6	19	62	120	WDR
		266-4	870	6	14	11	17	WDR
		266-5	950	6	11	15	18	LTM
		266-6	780	14	14	71	186	WDR
		272-1	760	11	6	5	56	WDR
		272-2	820	13	6	34	52	LTM
		272-3	460	27	6	60	396	WDR
		272-4	630	19	44	69	123	WDR
		272-5	770	0	152	150	253	WDR
		273-1	530	0	1	5	5	LTM
		273-2	650	7	13	43	39	LTM
		273-3	480	2	3	28	42	WDR
		273-4	730	9	14	16	3	WDR
		273-5	240	9	40	109	195	WDR
		injury+Ril	243-1	650	9	15	38	185
	243-2		830	8	21	36	54	WDR
	243-3		580	8	32	40	44	WDR
	243-4		810	5	6	10	43	WDR
	243-5		710	1	8	39	77	WDR
	245-1		490	0	7	18	37	WDR
	248-3		530	0	3	4	41	WDR
	248-4		690	5	21	74	80	WDR
	248-5		840	5	13	17	56	WDR
	248-6a		730	4	11	9	40	LTM
	250-1		465	12	14	30	18	LTM
250-2	700		3	16	11	8	WDR	
248-2b	490		2	13	20	30	LTM	
248-1a	735		7	8	5	3	LTM	

side	group	ID	depth	1.4	4.0	10.0	26.0	Type		
ipsilateral (cont.)	injury+Ril	250-4	800	20	26	53	14	LTM		
		260-1	660	0	7	10	42	WDR		
		260-2	910	1	9	41	35	WDR		
		260-3	800	0	0	18	18	WDR		
		260-4	550	12	17	27	57	WDR		
		260-5	650	8	5	28	36	WDR		
		260-6	610	0	10	48	48	WDR		
		262-1	720	2	0	2	7	LTM		
		262-2	600	5	4	5	29	LTM		
		262-3	540	0	42	58	43	WDR		
		262-5	420	0	8	13	47	WDR		
		262-6	680	24	9	6	10	LTM		
		267-2	630	1	8	60	32	WDR		
		267-3	440	1	8	2	7	WDR		
		267-3a	440	0	8	1	7	LTM		
		267-4	510	3	7	8	12	LTM		
		270-1	420	5	27	30	29	LTM		
		270-2	600	7	17	16	16	LTM		
		270-3	720	4	5	65	207	WDR		
		270-4	630	1	3	6	17	WDR		
		270-5	800	18	21	14	10	LTM		
		270-6	560	4	11	14	23	LTM		
		contralateral	sham+veh	261-7	440	3	2	12	22	WDR
				261-8	820	4	13	42	143	LTM
261-9	430			16	14	29	38	LTM		
261-10	450			8	10	32	46	WDR		
261-11	470			0	5	29	86	WDR		
263-7	730			3	6	32	48	WDR		
263-8	790			3	35	35	37	LTM		
263-9	680			4	19	24	43	WDR		
263-10	780			27	60	50	86	WDR		
263-11	860			3	4	21	36	WDR		
263-12	840			27	14	7	6	LTM		
265-7	640			4	14	20	36	WDR		
265-8	590			9	4	9	9	LTM		
265-9	480			10	12	46	88	WDR		
265-10	560			0	12	22	84	WDR		
265-11	550			11	4	49	83	WDR		
265-12	630			2	0	3	57	WDR		
268-7	460			0	6	21	24	WDR		
268-8	760			6	17	25	31	LTM		
268-9	520			7	9	3	8	LTM		
268-10	610			1	23	32	48	WDR		
268-11	680			0	0	12	10	WDR		
268-12	810			12	16	47	120	WDR		

side	group	ID	depth	1.4	4.0	10.0	26.0	Type
contralateral (cont.)	sham+veh	269-7	550	1	5	5	16	LTM
		269-8	720	0	6	26	17	WDR
		269-9	810	0	18	22	16	LTM
		269-10	540	2	11	24	74	WDR
		271-6	660	11	8	8	12	LTM
		271-7	470	1	1	9	30	WDR
		271-8	490	6	6	33	29	WDR
		271-9	580	16	17	23	24	LTM
		271-10	760	2	3	7	19	WDR
		274-4	570	2	5	4	5	LTM
		274-6	580	6	2	27	21	WDR
		274-7	440	1	9	35	44	WDR
		274-8	560	0	7	26	32	WDR
		injury+veh	244-6	860	7	5	31	58
	244-7c		710	2	9	12	78	WDR
	244-8a		780	3	0	11	53	WDR
	244-9b		660	4	6	5	8	WDR
	246-8		550	3	32	41	37	WDR
	246-9		800	0	7	32	92	WDR
	246-10		705	13	21	26	40	WDR
	246-11		760	0	3	14	112	WDR
	249-5		480	2	25	37	51	WDR
	249-6		550	2	16	12	10	WDR
	249-7		650	3	0	77	5	WDR
	246-6		750	4	9	3	5	LTM
	246-7		805	7	28	33	53	LTM
	264-7		540	7	11	13	26	WDR
	264-8		770	4	19	72	56	WDR
	264-9		990	3	4	4	7	LTM
	264-10		670	3	6	22	34	WDR
	264-11		850	16	28	37	15	LTM
	264-12		650	10	8	43	242	WDR
	266-7		420	0	3	6	13	WDR
	266-8	630	2	2	15	24	WDR	
266-9	560	22	18	16	65	LTM		
266-10	730	43	17	31	70	WDR		
266-11	560	6	10	22	41	LTM		
266-12	890	2	27	57	70	WDR		
272-6	700	4	4	5	42	WDR		
272-7	840	4	15	21	85	WDR		
272-8	610	7	20	19	45	WDR		
272-9	590	0	5	49	30	WDR		
272-10	550	5	4	6	8	LTM		
272-11	610	7	17	17	57	WDR		
273-7	920	4	4	97	97	WDR		

side	group	ID	depth	1.4	4.0	10.0	26.0	Type
contralateral (cont.)	injury+veh	273-8	650	22	37	63	57	LTM
		273-9	650	19	45	107	97	WDR
		273-10	870	0	15	9	13	LTM
	injury+Ril	243-6	470	9	22	18	64	WDR
		243-7	670	0	2	28	116	WDR
		243-9	850	9	29	45	42	WDR
		245-2b	600	18	30	20	37	LTM
		248-8	610	4	12	36	35	WDR
		248-9	510	14	8	17	40	WDR
		248-10	770	11	21	43	55	WDR
		248-11	460	6	4	34	44	WDR
		250-5	740	11	9	40	55	WDR
		250-6	820	5	7	26	50	WDR
		250-7	525	5	7	52	42	WDR
		243-8	720	28	18	70	52	LTM
		248-7	645	3	7	15	25	LTM
		260-7	750	0	7	6	34	LTM
		260-8	560	0	2	7	11	LTM
		260-9	450	5	6	9	25	WDR
		262-7	830	2	2	40	32	WDR
		262-8	490	10	5	15	22	LTM
		262-9	420	22	31	54	76	WDR
		262-10	430	21	29	25	25	LTM
		262-11	820	9	7	7	22	LTM
		262-12	550	15	65	56	46	LTM
		267-5	800	2	7	5	21	WDR
		267-6	690	11	27	69	146	WDR
		267-7	560	0	1	5	21	WDR
		267-8	740	0	2	7	12	LTM
		267-9	760	7	9	11	13	LTM
		267-10	840	1	18	37	65	WDR
		270-7	620	13	34	39	98	WDR
		270-8	710	0	4	5	10	WDR
270-9	690	3	1	7	17	WDR		
270-10	550	10	4	4	68	WDR		
270-11	600	16	9	10	12	LTM		
270-12	570	1	2	20	27	WDR		

---

## APPENDIX F

### Matlab Code for Quantifying Immunohistochemistry of Spinal Cord Sections

---

The Matlab code that quantified the percent positive pixels in fluorescently labeled spinal cord sections throughout this thesis and summarized in Appendix D is provided in this Appendix. To run this script, the user must save the code and the images in the same file directory. Prior to running this script, the threshold (0-250) is defined and entered as `pos_thresh` in the code. Once the script is finished computing the percent positive pixels for all images, typing “D.name” into the command window will return a list of all the images that were processed. Entering “percpos” into the command window will return the percent positive pixels that were calculated for the corresponding images returned by the D.name command.



```

%% This script was written to calculate and visualize percent positive
%% pixels per image.
%% requires MATLAB 7.0 (or higher) and imaging toolbox.
%% Written by Kristen Nicholson (modified from L. Dong and K. Quinn)
%% December 2009

```

```

clear all;
close all;
clf;

```

```

D = dir('*.*tif'); %specify which images in the current directory to
                  %analyze (* = wildcard character)

```

```

for k=1:length(D);

```

```

    % Load the image
    file=D(k).name;
    imag_orig = imread(file);

```

```

    %for colabeled images only, select which label to use, otherwise use
    %the code to gray-scale the image
    %imag = imag_orig(:,:,1);%grab the red labeled image
    %imag = imag_orig(:,:,2);%grab the green labeled image
    imag = rgb2gray(imag_orig);%gray-scale the image
    invImag = 255-imag;%invert the image
    imag = invImag;

```

```

    %calc number of pixels
    [a b]=size(imag);
    tsize=a*b;
    low=double(min(imag(:)));
    high=double(max(imag(:)));
    whiteSpace = 0.85*high;
    pos_thresh = 200;%input based on normal run, higher value corresponds
                    %to a higher +ive threshold.

```

```

    backg=sum(sum(imag>whiteSpace));
    posp=sum(sum(imag<pos_thresh));
    %calc percent of positive pixels in tissue
    percpos(k)= posp/(tsize-backg);
    tpost(k) = posp;
    Iname(k) = {file};

```

```

    %map out pos and neg pixels

```

```

pmap=(imag<pos_thresh);
nmap=(imag>whiteSpace);

% make figure for each image, if you are processing a bunch of images, you
% may want to comment this part out

%make positive pixels more green, and background pixels less blue
imag1(:,,1)=double(imag)/255;
imag1(:,,2)=(1-pmap).*double(imag)/255+pmap;
imag1(:,,3)=double(imag)/255.*(1-nmap);

h = figure(1);
subplot(3,1,3);
subimage(imag);
axis image
axis off
subplot(3,1,2);
subimage(imag1);
axis image
axis off
colormap gray
subplot(3,1,1);
subimage(imag_orig)
axis image
axis off
drawnow

clear imag imag1
clf
end

```

---

## REFERENCES

---

Abbadie C, Brown JL, Mantyh PW, Basbaum AI (1996) Spinal cord substance P receptor immunoreactivity increases in both inflammatory and nerve injury models of persistent pain. *Neuroscience* 70:201–209

Abbed KM, Coumans J (2007) Cervical radiculopathy: pathology, presentation, and clinical evaluation. *Neurosurg* 60(1):28-34

Amin B, Hajhashemi V, Hosseinzadeh H, Abnous KH (2012) Antinociceptive evaluation of ceftriaxone and minocycline alone and in combination in a neuropathic pain model in rat. *Neuroscience* 224:15-25

Anderson CM, Swanson RA (2000) Astrocyte glutamate transport: reviews of properties, regulation, and physiological functions. *Glia* 32:1-14

Andreollo NA, dos Santos EF, Araujo MR, Lopes LR (2012) Rat's age versus human's age: what is the relationship? *Arq Bras Cir Dig* 25(1):49-51

Armstrong CM (2006) Na channel inactivation from open and closed states. *Proc Natl Acad Sci USA* 103(47):17991-17996

Aronica E, Catania MV, Geurts J, Yankaya B, Troost D (2001) Immunohistochemical localization of group I and II metabotropic glutamate receptors in control and amyotrophic lateral sclerosis human spinal cord: upregulation in reactive astrocytes. *Neuroscience* 105(2):509-520

Aronica E, Gorter JA, Ijlst-Keizers H, Rozemuller AJ, Yankata B, Leenstra S, Troost D (2003) Expression and functional role of mGluR3 and mGluR5 in human astrocytes and glioma cells: opposite regulation of glutamate transporter proteins. *Eur J Neurosci* 17:2106-2118

Asante, C.O., Wallace, V.C., and Dickenson, A.H. (2009) Formalin-induced behavioural hypersensitivity and neuronal hyperexcitability are mediated by rapid protein synthesis at the spinal level. *Mol Pain* 5:27

Baba H, Ji RR, Kohno T, Moore KA, Ataka T, Wakai A, Okamoto M, Woolf CJ (2003) Removal of GABAergic inhibition facilitates polysynaptic A fiber-mediated excitatory transmission to the superficial spinal dorsal horn. *Mol Cell Neurosci* 24:818-830

Bachetti T, Zanni ED, Balbi P, Bocca P, Prigione I, Deiana GA, Rezzani A, Ceccherinia I, Sechi G (2010) In vitro treatments with ceftriaxone promotes elimination of mutant glial fibrillary acidic protein and transcription down-regulation. *Exp Cell Res* 316:2152-2165

Backonja M, Stacey B (2004) Neuropathic pain symptoms relative to overall pain rating. *J Pain* 5(9):491-497

Basbaum AI, Bautista DM, Scherme G, Julius D (2009) Cellular and molecular mechanisms of pain. *Cell* 139:267-284

Beck KD, Nguyen HX, Galvan MD, Salazar DL, Woodruff TM, Anderson AJ (2010) Quantitative analysis of cellular inflammation after traumatic spinal cord injury:

evidence for a multiphasic inflammatory response in the acute to chronic environment. *Brain* 133(Pt 2):433-447

Bedford AM, Liechti KM (2000) *Mechanics of materials*. Prentice-Hall, Upper Saddle River, New Jersey

Beel JA, Groswald DE, Luttges MW (1984) Alterations in the mechanical properties of peripheral nerve following crush injury. *J Biomech* 17(3):185-193

Beel JA, Stodieck LS, Luttges MW (1986) Structural properties of spinal nerve roots: biomechanics. *Exp Neurol* 91(1):30-40.

Beller JA, Gurkoff GG, Berman RF, Lyeth BG (2011) Pharmacological enhancement of glutamate transport reduces excitotoxicity in vitro. *Rest Neurol Neurosci* 29:331-346.

Bellingham MC (2011) A review of the neural mechanisms of action and clinical efficiency of riluzole in treating amyotrophic lateral sclerosis: what have we learned in the last decade? *CNS Neuosci Ther* 17:4-31

Benarroch EE (2010) Glutamate transporters: diversity, function, and involvement in neurologic disease. *Neurology* 74:259-264

Benediktsson AM, Marrs GS, Tu JC, Worley PF, Rothstein JD, Bergles DE, Dailey ME (2012) Neuronal activity regulates glutamate transporter dynamics in developing astrocytes. *Glia* 60:175-188

Bennett AD, Chastain KM, Hulsebosch (2000) Alleviation of mechanical and thermal allodynia by CGRP<sub>8-37</sub> in a rodent model of chronic central pain. *Pain* 86:163-175

Bergfield T, Aulicio P (1988) Variation of the deep motor branch of the ulnar nerve at the wrist. *J Hand Surg Am* 13(3):368-369

Blackburn-Munro G, Ibsen N, Erichsen HK (2002) A comparison of the anti-nociceptive effects of voltage-activated Na<sup>+</sup> channel blockers in the formalin test. *Eur J Pharmacol* 445:231-238

Bleakman D, Alt A, Nisenbaum ES (2006) Glutamate receptors and pain. *Semin Cell Dev Biol* 17:592-604

Bose B, Wierzbowski LR, Sestokas AK (2002) Neurophysiologic monitoring of spinal nerve root function during instrumented posterior lumbar spine surgery. *Spine* 27(13):1444-1450

Bostrom O, Svensson M, Aldman B, Hansson H, Haland Y, Lovsund P, Seeman T, Suneson A, Saljo A, Ortengren T (1996) A new neck injury criterion candidate-based on injury findings in the cervical spinal ganglia after experimental neck extension trauma. *International IRCOBI Conference on the Biomechanics of Impact*: 123-136

Boulais N, Misery L (2008) The epidermis: a sensory tissue. *Eur J Dermatol* 18(2):119-127

Braz JM, Nasser MA, Wood JN, Basbaum AI (2005) Parallel "pain" pathways arise from subpopulations of primary afferent nociceptor. *Neuron* 47:787-793

Carette S, Fehlings M (2005) Cervical radiculopathy. *N Engl J Med* 353(4):392-399

Carlson GD, Gorden CD, Oliff HS, Pillai JJ, LaManna JC (2003) Sustained spinal cord compression. *J Bone Joint Surg* 85A(1):86-94

Carlstedt T, Anand P, Hallin R, Misra PV, Norén G, Seferlis T (2000) Spinal nerve root repair and reimplantation of avulsed roots into the spinal cord after brachial plexus injury. *J Neurosurg* 93:237-247

Carlton SA, Du, J, Tan HY, Nestic O, Hargett GL, Bopp AC, Yamani A, Lin Q, Willis WD, Hulsebosch CE (2009) Peripheral and central sensitization in remote spinal cord regions contribute to central neuropathic pain after spinal cord injury. *Pain* 147:265-276

Carter JW, Mirza SK, Tencer AF, Ching RP (2000) Canal geometry changes associated with axial compressive cervical spine fracture. *Spine* 25(1): 46-54

Cata JP, Weng HR, Chen JH, Dougherty PM (2006) Altered discharges of spinal wide dynamic range neurons and down-regulation of glutamate transporter expression in rats with paclitaxel-induced hyperalgesia. *Neuroscience* 138:329-338

Cavanaugh DJ, Lee H, Lo L, Shields SD, Zylka MJ, Basbaum AI, Anderson DJ (2009) Distinct subsets of unmyelinated primary sensory fibers mediate behavioral responses to noxious thermal and mechanical stimuli. *PNAS* 106(22):9075-9080

Chang YW, Winkelstein BA (2011) Schwann cell proliferation and macrophage infiltration are evident at day 14 after painful cervical nerve root compression in the rat. *J Neurotrauma* 12:2429-2438

Chao T, Pham K, Steward O, Gupta R (2008) Chronic nerve compression injury induces phenotypic switch of neurons within the dorsal root ganglia. *J Comp Neurol* 506:180-193

- Chaplan SR, Bach FW, Pogrel JW, Chung JM, Yaksh TL (1994) Quantitative assessment of tactile allodynia in the rat paw. *J Neurosci Methods* 53(1): 55-63
- Chen L, Seaber AV, Urbaniak JR (1993) The influence of magnitude and duration of crush load on functional recovery of the peripheral nerve. *J Reconstr Microsurg* 9(4):299-307
- Chen LE, Seaber AV, Glisson RR, Davies H, Murrell GA, Anthony DC, Urbaniak JR (1992) The functional recovery of peripheral nerves following defined acute crush injuries. *J Orthop Res* 10(5):657-664
- Christensen MD, Hulsebosch CD (1997) Spinal cord injury and anti-NGF treatment results in changes in CGRP density and distribution in the dorsal horn in the rat. *Exp Neurol* 147(2):463-475
- Cifra A, Mazzone GL, Nistri A (2012) Riluzole: what it does to spinal and brainstem neurons and how it does it. *Neuroscientist* 19(2):137-144
- Clancy WG, Brand RL, Bergfield JA (1977) Upper trunk brachial plexus injuries in contact sports. *Am J Sports Med* 5(5):209-216
- Clark WL, Trumble TE, Swiontkowski MF et al (1992) Nerve tension and blood flow in a rat model of immediate and delayed repairs. *J Hand Surg* 17A(4):677-687
- Coderre TJ, Kumar N, Lefebvre CD, Yu JSC (2007) A comparison of the glutamate release inhibition and anti-allodynic effects of gabapentin, lamotrigine, and riluzole in a model of neuropathic pain. *J Neurochem* 11:1289-1299



Colburn R, Rickman A, DeLeo J (1999) The effect of site and type of nerve injury on spinal glial activation and neuropathic pain behavior. *Exp Neurol* 157:289-304

Cornefjord M, Nyberg F, Rosengren L, Brisby H (2004) Cerebrospinal fluid biomarkers in experimental spinal nerve root injury. *Spine* 29: 1862–1868

Cornefjord M, Sato K, Olmarker K, Rydevik B, Nordborg C (1997) A model for chronic nerve root compression studies: presentation of a porcine model for controlled, slow-onset compression with analyses of anatomic aspects, compression onset rat, and morphologic and neurophysiologic effects. *Spine* 22(9):946-957

Costa HJZR, Da Silva CF, Costa MP, Lazarini PR (2007) Evaluation of the systemic use of riluzole in post-traumatic facial nerve regeneration: experimental study in rabbits. *Acta Otolaryngol* 127:1222-1225

Côté P, Cassidy JD, Carroll L (1998) The Saskatchewan health and back pain survey: the prevalence of neck pain and related disability in Saskatchewan adults. *Spine* 23(15): 1689-1698

Côté P, Cassidy JD, Carroll L (2000) The factors associated with neck pain and its related disability in the Saskatchewan population. *Spine* 25(9): 1109-1117

Côté P, Cassidy JD, Carroll L (2001) The treatment of low back pain: Who seeks care? Who goes where? *Med Care* 39(9)956-967.

Côté P, Cassidy JD, Carroll LJ, Kristman V (2004) The annual incidence and course of neck pain in the general population: a population-based cohort study. *Pain* 112:267-273.

Covey E, Kauer JA, Casseday JH (1996) Whole-cell patch-clamp recording reveals subthreshold sound-evoked postsynaptic currents in the inferior colliculus of awake bats. *J Neurosci* 16(9):3009-3018

Crosby ND, Weisshaar CL, Winkelstein BA (2013) Spinal neuronal plasticity is evident within 1 day after a painful cervical facet capsule injury. *Neurosci Lett* 542:102-106

Danbolt NC (2001) Glutamate uptake. *Prog Neurobiol* 65:1-105.

D'Antoni S, Berretta A, Bonaccorso CM, Bruno V, Aronica E, Nicoletti F, Catania MV (2008) Metabotropic glutamate receptors in glial cells. *Neurochem Res* 33(12):2436-2443

de Peretti F, Micallef JP, Bourgeon A, Argenson C, Rabischong P (1989) Biomechanics of the lumbar spinal nerve roots and the first sacral nerve root within the intervertebral foramina. *Surg Radiol Anat* 11(3):221-225

DeLaTorre S, Rojas-Piloni G, Martínez-Lorenzana G, Rodríguez-Jiménez J, Villanueva L, Condés-Lara M (2009) Paraventricular oxytocinergic hypothalamic prevention or interruption of long-term potentiation in dorsal horn nociceptive neurons: electrophysiological and behavioral evidence. *Pain* 144:320-328

DeLeo J, Tawfik V, LaCroix-Fralish M (2006) The tetrapartite synapse: path to CNS sensitization and chronic pain. *Pain* 122:17-21

DeLeo JA, Winkelstein BA (2002) Physiology of chronic spinal pain syndromes: from animal models to biomechanics. *Spine* 27(22):2526-2537.

Di Maio A, Skuba A, Himes BT, Bhagat SL, Hyun JK, Tessler A, Bishop D, Son YJ (2011) In vivo imaging of dorsal root regeneration: rapid immobilization and presynaptic differentiation at the CNS/PNS border. *J Neurosci* 31(12):4569-4852

Dirig DM, Salami A, Rathbun ML, Ozaki GT, Yaksh TL (1997) Characterization of variables defining hindpaw withdrawal latency evoked by radiant thermal stimuli. *J Neurosci Methods* 76:183-191

Doble A (1996) The pharmacology and mechanism of action of riluzole. *J Neurol* 47(4):233-241

Dogrul A, Ossipov MH, Lai J, Malan TP, Porreca F (2000) Peripheral and spinal antihyperalgesic activity of SIB-1757, a metabotropic glutamate receptor (mGluR5) antagonist, in experimental neuropathic pain in rats. *Neurosci Lett* 292:115-118

Dong L, Quindlen JC, Lipschutz DE, Winkelstein BA (2012) Whiplash-like facet joint loading initiates glutamatergic responses in the DRG and spinal cord associated with behavioral hypersensitivity. *Br Res* 1461:51-63

Dong L, Winkelstein BA (2010) Simulated whiplash modulates expression of the glutamatergic system in the spinal cord suggesting spinal plasticity is associated with painful dynamic cervical facet loading. *J Neurotrauma* 27(1):163-174

Duan S, Anderson CM, Stein BA, Swanson RA (1999) Glutamate induces rapid upregulation of astrocyte glutamate transport and cell-surface expression of GLAST. *J Neurosci* 19(23):10193-10200

Dunk NM, Nicholson KJ, Winkelstein BA (2011) Impaired performance on the angle board test is induced in a model of painful whiplash injury but is only transient in a model of cervical radiculopathy. *J Orthop Res* 29(4): 562-566

Dyck PJ, Lais AC, Giannini C, Engelstad JK (1990) Structural alterations of nerve during cuff compression. *Proc Natl Acad Sci* 87:9829-9832

Eichberger, A., Darok, M., Steffan, H., Leinzinger, P.E., and Bostrom, O., and Svensson, M.Y. (2000) Pressure measurements in the spinal canal of post-mortem human subjects during rear-end impact and correlation of results to the neck injury criterion. *Accid Anal Prev* 32(2): 251-260

Eljaja L, Bjerrum O, Honore PH, Abrahamsen (2011) Effects of the excitatory amino acid transporter subtype 2 (EAAT-2) inducer ceftriaxone on different pain modalities in rat. *Scan J Pain* 2:132-136

Featherston DE (2009) Intercellular glutamate signaling in the nervous system and beyond. *ACS Chem Neurosci* 1:4-12

Fehlings MG, Perrin RG (2006) The timing of surgical intervention in the treatment of spinal cord injury: a systemic review of recent clinical evidence. *Spine* 31(11):S28-S35

Fehlings MG, Wilson JR, Frankowski RF, Toups EG, Aarabi B, Harrop JS, Shaffrey CI, Harkema SJ, Guest JD, Tator CH, Burau KD, Johnson MW, Grossman RG (2012) Riluzole for the treatment of acute traumatic spinal cord injury: rationale and design of the NACTN Phase I clinical trial. *J Neurosurg* S17:151-156

Fumihiko H, Nobuo M, Nobuo H (1996) Changes in responses of wide dynamic range neurons in the spinal dorsal horn after dorsal root or dorsal root ganglion compression. *Spine* 21(12):1408-1414

Fung YC (1967) Elasticity of soft tissues in simple elongation. *Am J Phys* 213(6):1532-1544

Gabay E, Tal M (2004) Pain behavior and electrophysiology in the CCI model of neuropathic pain. *Pain* 110:354-360

Gagliese L, Melzack R (2000) Age differences in nociception and pain behaviors in the rat. *Neurosci Biobeh Rev* 24(8):843-854

Gallant PE (1992) The direct effects of graded axonal compression on axoplasm and fast axoplasmic transport. *J Neuropath Exp Neurol* 51(2):220-230

Gao YJ, Ji RR (2010) Targeting astrocyte signaling for chronic pain. *Neurother* 7:482-493

Garfin SR, Cohen MS, Massie JB, Abitbol JJ, Swenson MR, Myers RR, Rydevik BL (1990) Nerve-roots of the cauda equine: the effect of hypotension and acute graded compression on function. *J Bone Joint Surg A* 71-A(8):1185-1192

Geddes DM, Cargill RS, LaPlaca MC (2003) Mechanical stretch to neurons results in a strain rate and magnitude-dependent increase in plasma membrane permeability. *J Neurotrauma* 20(10):1039-1049

Gefen A, Margulies SS (2004) Are in vivo and in situ brain tissues mechanically similar? *J Biomech* 37(9):1339-1352

Gegelashvili G, Dehnes Y, Danbolt NC, Schousboe A (2000) The high-affinity glutamate transporters GLT1, GLAST, and EAAT4 are regulated via different signaling mechanisms. *Neurochemistry International* 37: 163-170

Ghosh M, Yang Y, Rothstein JD, Robinson MB (2011) Nuclear Factor- $\kappa$ B contributes to neuron-dependent induction of glutamate transporter-1 expression in astrocytes. *J Neurosci* 31(25):9159-9169

Gilad GM, Gilad VH, Wyatt RJ, Tizabi Y (1990) Region-selective stress-induced increase of glutamate uptake and release in the rat forebrain. *Br Res* 525:335-338.

González MI, Kazanietz MG, Robinson MB (2002) Regulation of the neuronal glutamate transporter excitatory amino acid carrier-1 (EAAC1) by different protein kinase C subtypes. *Mol Pharmacol* 62:901-910

Grace PM, Hutchinson MR, Manavis J, Somogyi AA, Rolan PE (2010) A novel animal model of graded neuropathic pain: utility to investigate mechanisms of population heterogeneity. *J Neurosci Methods* 193:47-53

Guertin AD, Zhang DP, Mak KS, Alberta JA, Kim HA (2005) Microanatomy of axon/glia signaling during Wallerian degeneration. *J Neuroscience* 25(13):3478-3487

Guillet BA, Velly LJ, Canolle B, Masméjean FM, Nieoullon AL, Pisano P (2005) Differential regulation by protein kinases of activity and cell surface expression of glutamate transporters in neuron-enriched cultures. *Neurochem Int* 46:337-346

Gwak YS, Hulsebosch CE (2005) Upregulation of group I metabotropic glutamate receptors in neurons and astrocytes in the dorsal horn following spinal cord injury. *Exp Neuro* 195:236-243

Haftck J (1970) Stretch injury of peripheral nerve: acute effects of stretching on rabbit nerve. *J Bone Joint Surg* 52B(2):354-365

Hains BC, Johnson KM, Eaton MJ, Willis WD, Hulsebosch CE (2003) Serotonergic neural precursor cell grafts attenuate bilateral hyperexcitability of dorsal horn neurons after spinal hemisection in rat. *Neuroscience* 116:1097-1110

Hajhashemi V, Hosseinzadeh H, Amin B (2012) Antiallodynia and antihyperalgesia effects of ceftriaxone in treatment of chronic neuropathic pain in rats. *Acta Neuropsych* doi: 10.1111/j.1601-5215.2012.00656.x

Haller FR, Haller AC, Low FN (1971) The fine structure of cellular layers and connective tissue space at spinal nerve root attachments in the rat. *Am J Anat* 133:109-124.

Hama A, Sagen J (2011) Antinociceptive effect of riluzole in rats with neuropathic spinal cord injury pain. *J Neurotrauma* 28:1-8.

Hammer NA, Lilleso J, Pederson JL, Kehlet H (1999) Effect of riluzole on acute pain and hyperalgesia in humans. *Br J Anaesth* 82(5):718-722.

Hanai F, Matsui N, Hongo N (1996) Changes in responses of wide dynamic range neurons in the spinal dorsal horn after dorsal root or dorsal root ganglion compression. *Spine* 21(12):1408-1414

Hao JX, Xu XJ, Yu YX, Seiger A, Wiesenfeld-Hallin Z (1992) Transient spinal cord ischemia induces temporary hypersensitivity of dorsal horn wide dynamic range neurons to myelinated, but not unmyelinated, fiber input. *J Neurophys* 68(2):384-391

Hargreaves K, Dubner R, Flores C, Joris J (1988) A new and sensitive method for measuring thermal nociception in cutaneous hyperalgesia. *Pain* 32:77-88

Hashizume H, DeLeo JA, Colburn RW et al (2000) Spinal glial activation and cytokine expression after lumbar root injury in the rat. *Spine* 25(10):1206-1217

Haugeto Ø, Ullensvang K, Levy LM, Chaudhry FA, Honoré T, Nielsen M, Lehre KP, Danbolt NC (1996) Brain glutamate transporter proteins form homomultimers. *J Biol Chem* 271(4):27715-27722

Hill J, Martyn L, Papageorgious AC, Dziedzic K, Croft P (2004) Predicting persistent neck pain. *Spine* 29(15):1648-1654

Hogg-Johnson S, van der Velde G, Carroll LJ, Holm LW, Cassidey JD, Guzman J, Côté P, Haldeman S, Ammendolia C, Carragee E, Hurwitz E, Nordin M, Peloso P (2008) The burden and determinants of neck pain the general population. *Spine* 33(45):S39-S51

Holmseth S, Dehnes Y, Huang YH, Follin-Arbelet VV, Grutle NJ, Mylonakou MN, Plachez C, Zhou Y, Furness DN, Bergles DE, Lehre KP, Danbolt NC (2012) The density of EAAC1 (EAAT3) glutamate transporters expressed by neurons in the mammalian CNS. *J Neurosci* 32(17):6000-6013

Hosmane S, Fournier A, Wright R, Rajbhandari L, Siddique R, Yang IH, Ramesh KT, Venkatesan A, Thakor N (2011) Valve-based microfluidic compression platform: single axon injury and regrowth. *Lab Chip* 11:3888-3895



Howe JF, Loeser JD, Calvin WH (1977) Mechanosensitivity of dorsal root ganglia and chronically injured axons: a physiological basis for the radicular pain of nerve root compression. *Pain* 3:25-41

Hoy DG, Protani M, De R, Buchbinder R (2010) The epidemiology of neck pain. *Best Pract Res Clin Rheumatol* 24:783-792.

Hu Y, Li W, Lu L, Cai J, Xian X, Zhang M, Li Q, Li L (2010) An anti-nociceptive role for ceftriaxone in chronic neuropathic pain in rats. *Pain* 148:284-301

Huang C, Zou W, Lee K, Wang E, Zhu X, Guo Q (2012) Different symptoms of neuropathic pain can be induced by different degrees of compressive force on the C7 dorsal root of rats. *Spine J* 12:1154-1160

Hubbard R, Chen Z, Winkelstein B (2008a) Transient cervical nerve root compression modulates pain: load thresholds for allodynia and sustained changes in spinal neuropeptide expression. *J Biomech* 41:677-685

Hubbard RD, Martínez JJ, Burdick JA, Winkelstein BA (2009) Controlled Release of GDNF Reduces Nerve Root-Mediated Behavioral Hypersensitivity. *J Orthop Res* 27(1):120-127

Hubbard RD, Quinn KP, Martínez JJ, Winkelstein BA (2008b) The role of graded nerve root compression on axonal damage, neuropeptides changes, and pain-related behaviors. *Stapp Car Crash J* 52:33-58

Hubbard RD, Rothman SM, Winkelstein BA (2004) Mechanisms of persistent neck pain following nerve root compression injury: understanding behavioral

hypersensitivity in the context of spinal cytokine responses and tissue biomechanics.  
North American Spine Society 19th Annual Meeting, #P49, Chicago, IL

Hubbard RD, Winkelstein BA (2005) Transient cervical nerve root compression in the rat induces bilateral forepaw allodynia and spinal glial activation: mechanical factors in painful neck injuries. *Spine* 30(17):1924-1932

Hubbard RD, Winkelstein BA (2008) Dorsal root compression produces myelinated axonal degeneration near the biomechanical thresholds for mechanical behavioral hypersensitivity. *Exp Neurol* 212:482-489

Hudson LJ, Bevan S, McNair K, Gentry C, Fox A, Kuhn R, Winter J (2002) Metabotropic glutamate receptor 5 upregulation in A-fibers after spinal nerve injury: 2-Methyl-6-(Phenylethynyl)-Pyridine (MPEP) reverses the induced thermal hyperalgesia. *J Neurosci* 22(7):2660-2668

Igarashi T, Yabuki S, Kikuchi S et al (2005) Effect of acute nerve root compression on endoneurial fluid pressure and blood flow in rat dorsal root ganglia. *J Orthop Res* 23(2):420-424

Inquimbert P, Bartels K, Babaniyi OB, Barrett LB, Tegeder I, Scholz J (2012) Peripheral nerve injury produces a sustained shift in the balance between glutamate release and uptake in the dorsal horn of the spinal cord. *Pain* 153:2422-2431

Jackson DL, Graff CB, Richardson JD, Hargreaves KM (1995) Glutamate participates in the peripheral modulation of thermal hyperalgesia of rats. *Eur J Pharma* 284:321-325.

Janahmadi M, Goudarzi I, Kaffashian MR, Behzadi G, Fathollahi Y, Hajizadeh S (2009) Co-treatment with riluzole, a neuroprotective drug, ameliorates the 3-acetylpyridine-induced neurotoxicity in cerebellar Purkinje neurones of rats: Behavioral and electrophysiological evidence. *Neurotoxicology* 30:393-402.

Jancalek R, Dubovy P (2007) An experimental animal model of spinal root compression syndrome: an analysis of morphological changes of myelinated axons during compression radiculopathy and after decompression. *Exp Brain Res* 179:111-119

Jehle T, Bauer J, Blauth E, Hummel A, Darstein M, Freiman TM, Feuerstein TJ (2000) Effects of riluzole on electrically evoked neurotransmitter release. *Br J Pharmacol* 130:1227-1234

Jenis L, An H (2000) Neck pain secondary to radiculopathy of the fourth cervical root: an analysis of 12 surgically treated patients. *J Spinal Disord* 13:345-349

Jensen TS, Gottrup H, Sindrup SH, Bach FW (2001) The clinical picture of neuropathic pain. *Eur J Pharmacol* 429:1-11

Jenson TS, Baron R (2003) Translation of symptoms and signs into mechanisms in neuropathic pain. *Pain* 102:1-8

Jia H, Rustioni A, Valtschanoff JG (1999) Metabotropic glutamate receptors in superficial laminae of the rat dorsal horn. *J Comp Neurol* 410(4):627-642

Jourdain P, Bergersen LH, Bhaukaurally K, Bezzi P, Santello M, Domercq M, Matute C, Tonello F, Gundersen V, Volterra A (2007) Glutamate exocytosis from astrocytes controls synaptic strength. *Nat Neuroscience* 10(3):331-339

Kelleher MO, Tan G, Sarjeant R, Fehlings MG (2008) Predictive value for intraoperative neurophysiological monitoring during cervical spine surgery: a prospective analysis of 1055 consecutive patients. *J Neurosurg Spine* 8:215-221

Keller AF, Beggs S, Salter MW, de Koninck Yves (2006) Transformation of the output of spinal lamina I neurons after nerve injury and microglia stimulation underlying neuropathic pain. *Mol Pain* 3:27

Kerr BJ, David S (2007) Pain behaviors after spinal cord contusion injury in two commonly used mouse strains. *Exp Neurol* 206:240-247

Khan GM, Chen SR, Pan HL (2002) Role of primary afferent nerves in allodynia caused by diabetic neuropathy in rats. *Neuroscience* 114(2):291-299

Kim Y, Park YK, Cho H, Kim J, Yoon YW (2011) Long-term changes in expressions of glutamate transporters after spinal cord injury. *Br Res* 1389:194-199

Knackstedt LA, Melendez RI, Kalivas PW (2010) Ceftriaxone restores glutamate homeostasis and prevents relapse to cocaine seeking. *Biol Psychiatry* 67:81– 84

Kobayashi S, Kokubo Y, Uchida K, Yayama T, Takeno K, Negoro K, Nakajima H, Baba H, Yoshizawa H (2005a) Effect of lumbar nerve root compression on primary sensory neurons and their central branches: changes in the nociceptive neuropeptides substance P and somatostatin. *Spine* 30(3):276-282

Kobayashi S, Meir A, Baba H et al (2005b) Imaging of intraneural edema by using gadolinium-enhanced MR imaging: experimental compression injury. *Am J Neuroradiol* 26:973-980

Kobayashi S, Uchida K, Kokubo Y, Takeno K, Yayama T, Miyazaki T, Nakajima H, Nomura E, Mwaka E, Baba H (2008) Synapse involvement of the dorsal horn in experimental lumbar nerve root compression. *Spine* 33(7):716-723

Kobayashi S, Yoshizawa H, Hachiya Y (1993) Vasogenic edema induced by compression injury to the spinal nerve root: distribution of intravenously injected protein tracers and gadolinium-enhanced magnetic-resonance-imaging. *Spine* 18(11):1410-1424

Kobayashi S, Yoshizawa H, Yamada S (2004) Pathology of lumbar nerve root compression Part 1: Intradicular inflammatory changes induced by mechanical compression. *J Orthop Res* 22:170-179.

Koeberle PD, Bahr M (2008) The upregulation of GLAST-1 is an indirect antiapoptotic mechanism of GDNF and neurturin in the adult CNS. *Cell Death Differ* 15:471-483

Kohno T, Moore KA, Baba H, Wollf CJ: Peripheral nerve injury alters excitatory synaptic transmission in lamina II of the rat dorsal horn. *J Physiol* 548(1):131-138, 2003

Kondo E, Iwata K, Ogawa A, Tashira A, Tsuboi Y, Fukuoka T, Yamanaka H, Dai Y, Morimoto T, Noguchi K (2002) Involvement of the glutamate receptors on hyperexcitability of wide dynamic range neurons in the gracile nucleus of the rats with experimental mononeuropathy. *Pain* 95:153-163

Krenz NR, Weaver LC (1998) Sprouting of primary afferent fibers after spinal cord transection in the rat. *Neuroscience* 85(2):443-458.

Krivickas LS, Wilbourn AJ (2000) Peripheral nerve injuries in athletes: a case series of over 200 injuries. *Semin Neurol* 20(2):225-232

Kuijper B, Tans JTJ, Schimscheimer RJ, van der Kallen BFW, Beelen A, Nollet F, de Visser M (2009) Degenerative cervical radiculopathy: diagnosis and conservative treatment. *Eur J Neurol* 16:15-20.

Kuijper B, Tans JTJ, Schimscheimer RJ, van der Kallen BFW, Nollet F, a Nijeholt GJL, de Visser M (2011) Root compression on MRI compared with clinical findings in patients with recent onset cervical radiculopathy. *J Neurol Neurosurg Psychiatry* 82:561-563

Kuner R (2010) Central mechanisms of pathological pain. *Nat Med* 16(11):1258-1266

Kuo JJ, Lee RH, Zhang L, Heckman CJ (2006) Essential role of the persistent sodium current in spike initiation during slowly rising inputs in mouse spinal neurons. *J Physiol* 574(3):819-834

Kwan, M., Wall, E., Massie, J., and Garfin, S. (1992) Strain, stress and stretch of peripheral nerve: rabbit experiments in vitro and in vivo. *Acta Orthop Scand* 63: 267-272

Kwon BK, Okon E, Hillyer J, Mann C, Baptiste D, Weaver LC, Fehlings MG, Tetzlaff W (2010) A systematic review of non-invasive pharmacologic neuroprotective treatments for acute spinal cord injury. *J Neurotrauma* 27:1-44

Laird JMA, Bennett GJ (1993) An electrophysiological study of dorsal horn neurons in the spinal cord of rats with an experimental peripheral neuropathy. *J Neurophysiol* 69(6):2072-2085

Lamanauskas N, Nistri A (2008) Riluzole blocks persistent Na<sup>+</sup> and Ca<sup>2+</sup> currents and modulates release of glutamate via presynaptic NMDA receptors on neonatal rat hypoglossal motoneurons in vitro. *Eur J Neurosci* 27:2501-2514

Lapirot O, Chebbi R, Monconduit L, Artola A, Dallel R, Laccarini P (2009) NK1 receptor-expressing spinoparabrachial neurons trigger diffuse noxious inhibitory controls through lateral parabrachial activation in the male rat. *Pain* 142:245-254

LaPlaca MC, Prado GR (2009) Membrane damage as a marker of neuronal injury. 31<sup>st</sup> Annual Conference of the IEEE EMBS 1113-1116

LaPlaca MC, Prado GR (2010) Neural mechanobiology and neuronal vulnerability to traumatic loading. *J Biomech* 43:71-78

LaPlaca MC, Thibault LE (1998) Dynamic mechanical deformation of neurons triggers acute calcium response and cell injury involving the N-methyl-D-aspartate glutamate receptor. *J Neurosci Res* 52(2):220-229

Lea PM 4th, Faden AI (2001) Traumatic brain injury: developmental differences in glutamate receptor response and the impact on treatment. *Ment Retard Dev Disabil Res Rev* 7(4):235-48

Lee RH, Heckman CJ (2000) Essential role of a fast persistent inward current in action potential initiation and control of rhythmic firing. *J Neurophysiol* 85(1):472-475

Lee SG, Su ZZ, Emdad L, Gupta P, Sarkar D, Borjabad A, Volsky DJ, Fisher PB: Mechanism of ceftriaxone induction of excitatory amino acid transporter-2 expression

and glutamate uptake in primary human astrocytes. *J Biol Chem* 283(19):13116-13123, 2008

Leinster VHL, Robson LG, Shortland PJ (2010) Differential effects of riluzole on subpopulations of adult rat dorsal root ganglion neurons in vitro. *J Neurosci* 166:942-951

Liaw WJ, Stephens RL Jr, Binns BC, Chu Y, Sepkuty JP, Johns RA, Rothstein JD, Tao YX (2005) Spinal glutamate uptake is critical for maintaining normal sensory transmission in rat spinal cord. *Pain* 115:60-70

Liboux AL, Cachia JP, Kirkesseli S, Gaultier JY, Guimart C, Montay G, Peeters PAM, Groen E, Jonkman JHG, Wemer J (1999) A comparison of the pharmacokinetics and tolerability of riluzole after repeated dose administration in healthy elderly and young volunteers. *J Clin Pharmacol* 39:480-486

Liebel JT, Swandulla D, Zeilhofer HU (1997) Modulation of excitatory synaptic transmission by nociception in superficial dorsal horn neurones of the neonatal rat spinal cord. *Br J Pharmacol* 121:425-432

Lim J, Lim G, Sung B, Wang S, Mao J (2006) Intrathecal midazolam regulates spinal AMPA receptor and function after nerve injury in rats. *Br Res* 1123:80-88

Lipski J, Wan CK, Bai JZ, Pi R, Li D, Donnelly D (2007) Neuroprotective potential of ceftriaxone in vitro models of stroke. *Neuroscience* 146:617-629, 2007

Liu FY, Qu XX, Wang FT, Xing GG, Wan Y (2011) Electrophysiological properties of spinal wide dynamic range neurons in neuropathic pain rats following spinal nerve ligation. *Neurosci Bull* 27(1):1-8



- Liu L, Rudin M, Kozlova EN (2000) Glial cell proliferation in the spinal cord after dorsal rhizotomy or sciatic nerve transection in the adult rat. *Exp Brain Res* 131(1):64-73
- Lotz JC, Chin JR (2000) Intervertebral disc cell death is dependent on the magnitude and duration of spinal loading. *Spine* 25(12):1477-1483
- Lloyd DR, Chen PB, Hargreaves KM (2012) Anti-hyperalgesic effects of anti-serotonergic compounds on serotonin- and capsaicin-evoked thermal hyperalgesia in the rat. *Neuroscience* 203:207-215
- Lutsar I, McCracken GH, Friedland IR (1988) Antibiotic pharmacodynamics in cerebrospinal fluid. *Clin Inf Dis* 27(5):1117-1127
- MacIver MB, Amagasa SM, Mikulec AA, Monroe FA (1996) Riluzole anesthesia: use-dependent block of presynaptic glutamate. *Anesthesiology* 85:626-634
- Maikos JT, Elias RAI, Shreiber DI (2008) Mechanical properties of dura mater from the rat brain and spinal cord. *J Neurotrauma* 25:38-51
- Mantz J, Chéramy A, Thierry AM, Glowinski J, Desmonts JM (1992) Anesthetic properties of riluzole (54274 RP), a new inhibitor of glutamate neurotransmission. *Anesthesiology* 76:844-848
- Mao J, Sung B, Ji RR, Lim G (2002) Chronic morphine induces downregulation of spinal glutamate transporters: implications in morphine tolerance and abnormal pain sensitivity. *J Neurosci* 22(18):8312-8323

Markowitz AJ, White MG, Kolson DL, Jordan-Sciutto KL (2007) Cellular interplay between neurons and glia: toward a comprehensive mechanism for excitotoxic neuronal loss in neurodegeneration. *J Cell Sci* 4:111–146

Martin BI, Deyo RA, Mirza SK, Turner JA, Comstock BA, Hollingworth W, Sullivan SD (2008) Expenditures and health status among adults with back and neck problems. *JAMA* 299(6):656-664

Martin RB, Burr DB, Sharkey NA (1998) *Skeletal Tissue Mechanics*. Springer, New York

Martindale J, Bland-Ward PA, Chessell IP (2001) Inhibition of C-fibre mediated sensory transmission in the rat following intraplantar formalin. *Neurosci Lett* 316(1):33-36

Martini FH, Timmons MJ, Tallitsch RB (2003) *Human Anatomy*. 4<sup>th</sup> Edition. Prentice Hall: Upper Saddle River, New Jersey

Mauderli AP, Acosta-Rua A, Vierck CJ (2000) An operant assay of thermal pain in conscious, unrestrained rats. *J Neurosci Methods* 97:19-29

Maves TJ, Pechman PS, Gebhart GF, Meller ST (1993) Possible chemical contribution from chronic gut sutures produces disorders of pain sensation like those seen in man. *Pain* 54:57–69

McMahon SB, Kett-White R (1991) Sprouting of peripherally regenerating primary sensory neurons in the adult central nervous system. *J Comp Neurol* 304:307-315.

McMahon SB, Malcangio M (2009) Current challenges in glia-pain biology. *Neuron* 64(1):46-54

Merksey H, Bogduk N (1994) *Classification of chronic pain*. IASP Press: Seattle

Milligan ED, Watkins LR (2009) Pathological and protective roles of glia in chronic pain. *Neurosci* 10:23-36

Mimura K, Tomimatsu T, Minato K, Jugder O, Kinugasa-Taniguchi Y, Kanagawa T, Nozaki M, Yanagihara I, Kimura T (2011) Ceftriaxone preconditioning confers neuroprotection in neonatal rats through glutamate transporter 1 upregulation. *Reprod Sci* 18(12):1193-1201

Mogil JS (2009) Animal models of pain: progress and challenges. *Nat Rev Neurosci* 10:283-294

Mogil JS, Davis KD, Derbyshire SW (2010) The necessity of animal models in pain research. *Pain* 151:12-17

Moloney N, Hall T, Doody C (2013) Sensory hyperalgesia is characteristic of nonspecific arm pain. *Clin J Pain* epub ahead of print

Morishita, Y., Hikda, S., Naito, M., Arimizu, J., Matsushima, U., and Nakamura, A. (2006) Measurement of the local pressure of the intervertebral foramen and electrophysiologic values of the spinal nerve roots in the vertebral foramen. *Spine* 31(26):3076-3080

Mosconi T, Kruger L (1996) Fixed-diameter polyethylene cuffs applied to the rat sciatic nerve induce a painful neuropathy: ultrastructural morphometric analysis of axonal alterations. *Pain* 64:37-57

Myers RR, Yamamoto T, Yaksh TL, Powell HC (1993) The role of focal nerve ischemia and Wallerian degeneration in peripheral nerve injury producing hyperesthesia. *Anesthesiology* 78:308-316

Nakatsuka T, Furue H, Yoshimura M, Gu JG (2002) Activation of central terminal vanilloid receptor-1 receptors and  $\alpha\beta$ -methylene-ATP-sensitive P2X receptors reveals a converged synaptic activity onto the deep dorsal horn neurons of the spinal cord. *J Neurosci* 22(4):1228-1237

Navajas D, Maksym GN, Bates JH (1995) Dynamic viscoelastic nonlinearity of lung parenchymal tissue. *J Appl Physiol* 79(1):348-356

Neugebauer V, Rumenapp P, Schaible HG (1996) Calcitonin gene-related peptide is involved in the spinal processing of mechanosensory input from the rat's knee joint and in the generation and maintenance of hyperexcitability of dorsal horn neurons during development of acute inflammation. *Neuroscience* 71(4): 1095-1109

Nguyen D, Deng P, Matthews EA, Kim DS, Feng G, Dickensen AH, Xu ZC, Luo ZD (2009) Enhanced pre-synaptic glutamate release in deep-dorsal horn contributes to calcium channel  $\alpha$ -2-delta-1 protein-mediated spinal sensitization and behavioral hypersensitivity. *Mol Pain* 5:6

Nicholson KJ, Gilliland TM, Winkelstein BA (2013a) Upregulation of GLT-1 by treatment with ceftriaxone alleviates radicular pain by reducing spinal astrocyte activation and neuronal hyperexcitability. *Eur J Pain*, submitted

Nicholson KJ, Guarino BB, Winkelstein BA (2012) Transient nerve root compression load and duration differentially mediate behavioral sensitivity and associated spinal astrocyte activation and mGluR5 expression. *Neuroscience* 209:187-195

Nicholson KJ, Quindlen JC, Winkelstein BA (2011) Development of a duration threshold for modulating evoked neuronal responses after nerve root compression injury. *Stapp Car Crash J* 55:1-24

Nicholson KJ, Zhang S, Winkelstein BA (2013b) Riluzole abolishes behavioral sensitivity and prevents the development of axonal damage and spinal modifications that are evident after painful nerve root compression. *J Neuropath Exp Neurol*, submitted

Nie H, Zhang H, Weng HR (2010) Minocycline prevents impaired glial glutamate uptake in the spinal sensory synapses of neuropathic rats. *Neuroscience* 170:901-912

Niederberger E, Schmidtko A, Coste O, Marian C, Ehnert C, Geisslinger (2006) The glutamate transporter GLAST is involved in spinal nociceptive processing. *Biochem Biophys Res Commun* 346:393-399

Nuckley DJ, Konodi MA, Raynak GC, Ching RP, Mirza SK (2002) Neural space integrity of the lower cervical spine. *Spine* 27(6):587-595

Okamoto M, Baba H, Goldstein PA, Higashi H, Shimoji K, Yoshimura M (2001) Functional organization of sensory pathways in the rat spinal dorsal horn following peripheral nerve injury. *J Physiol* 532(1):241-250

Olmarker K (1991) The spinal nerve roots. *Acta Orthop Scand* 62(S242):1-27

Olmarker K, Holm S, Rydevik B (1990) Importance of compression onset rate for the degree of impairment of impulse propagation in experimental compression injury of the porcine cauda equina. *Spine* 15(5):416-419

Olmarker K, Myers RR (1998) Pathogenesis of sciatic pain: role of herniated nucleus pulposus and deformation of spinal nerve root and dorsal root ganglion. *Pain* 78:99-105

Olmarker K, Rydevik B, Holm S (1989a) Edema formation in spinal nerve roots induced by experimental graded compression: an experimental study on the pig cauda equina with special reference to differences in effects between rapid and slow onset of compression. *Spine* 14(6):569-573

Olmarker K, Rydevik B, Holm S, Bagg U (1989b) Effects of experimental graded compression on blood flow in spinal nerve roots. A vital microscopic study of the porcine cauda equine. *J Orthop Res* 7:817-823

Ommaya AK (1968) Mechanical properties of tissues of the nervous system. *J Biomech* 1(2):127-138

Paixão S, Klein R (2010) Neuron-astrocyte communication and synaptic plasticity. *Curr Opin Neurobiol* 20:466-473.

Panjabi MM, Maak TG, Ivancic PC, Ito S (2006) Dynamic intervertebral foramen narrowing during simulated rear impact. *Spine* 31(5):128-134

Park E, Velumian AA, Fehlings MG (2004) The role of excitotoxicity in secondary mechanisms of spinal cord injury: a review with an emphasis on the implications for white matter degeneration. *J Neurotrauma* 21(6):754-774

Pedowitz RA, Garfin SR, Massie JB, Hargens AR, Swenson MR, Myers RR, Rydevik BL (1992) Effects of magnitude and duration of compression on spinal nerve root conduction. *Spine* 17(2):194-199.

Perea G, Navarrete M, Araque A (2009) Tripartite synapses: astrocytes process and control synaptic information. *Cell* 32(8):421-431.

Perego C, Vanoni C, Bossi M, Massari S, Basudev H, Longhi R, Pietrini G (2000) The GLT-1 and GLAST glutamate transporters are expressed on morphologically distinct astrocytes and regulated by neuronal activity in primary hippocampal cocultures. *J Neurochem* 75(3):1076-1084.

Petitjean H, Rodeau JL, Schlichter R (2012) Interactions between superficial and deep dorsal horn spinal cord neurons in the processing of nociceptive information. *Eur J Neurosci* 36:3500-3508

Pezet S, Marchand F, D'Mello R, Grist J, Clark AK, Malcangio M, Dickenson AH, Williams RJ, McMahon SB (2008) Phosphatidylinositol 3-Kinase is a key mediator of central sensitization in painful inflammatory conditions. *J Neurosci* 28(16):4261-4270

Pintér S, Gloviczki B, Szabó A, Márton G, Nógrádi A (2010) Increased survival and reinnervation of cervical motoneurons by riluzole after avulsion of the C7 ventral root. *J Neurotrauma* 27:2273-2282

Provenzano P, Lakes RS, Keenan T, Vanderby, R Jr (2001) Non-linear ligament viscoelasticity. *Ann Biomed Eng* 29:908-914

Queen SA, Kesslak P, Bridges RJ (2007) Regional distribution of sodium-dependent excitatory amino acid transporters in rat spinal cord. *J Spinal Cord Med* 30:263-271

Quinn KP, Dong L, Golder FJ, Winkelstein BA (2010) Neuronal hyperexcitability in the dorsal horn after painful facet joint injury. *Pain* 151:414-421

Radhakrishnan K, Litchy WJ, O'Fallon WM, Kurland LT (1994) Epidemiology of cervical radiculopathy: a population-based study from Rochester, Minnesota, 1976 through 1990. *Brain* 117(2):325-335

Raghavendra V, Tanga F, DeLeo JA (2003) Inhibition of microglial activation attenuates the development but not existing hypersensitivity in a rat model of neuropathy. *J Pharmacol* 306(2):624-630

Ramer MS, Priestley JV, McMahon SB (2000) Functional regeneration of sensory axons into the adult spinal cord. *Nature* 403:312-316

Ramos KM, Lewis MT, Morgan KN, Crysdale NY, Kroll JL, Taylor FR, Harrison JA, Sloane EM, Maier SF, Watkins LR (2010) Spinal upregulation of glutamate transporter GLT-1 by ceftriaxone: therapeutic efficacy in a range of experimental nervous system disorders. *Neuroscience* 169:1888-1900



Rasmussen BA, Baron DA, Kim JK, Unterwald EM, Rawls SM (2011)  $\beta$ -lactam antibiotic produces a sustained reduction in extracellular glutamate in the nucleus accumbens of rats. *Amino Acids* 40:761-764

Ren K, Dubner R (2008) Neuron-glia crosstalk gets serious: role in pain hypersensitivity. *Curr Opin Anaesthesiol* 21(5):570-579

Romero-Sandoval E, Chai N, Nutile-McMenemy N, DeLeo J (2008) A comparison of spinal Iba1 and GFAP expression in rodent models of acute and chronic pain. *Brain Res* 1219, 116–126

Ross JR, Porter BE, Buckley PT, Eberwine JH, Robinson MB (2011) mRNA for the EAAC1 subtype of glutamate transporter is present in neuronal dendrites in vitro and dramatically increases in vivo after a seizure. *Neurochem Int* 58:366–375

Rothman SM, Guarino BB, Winkelstein BA (2009a) Spinal microglial proliferation is evident in a rat model of painful disc herniation both in the presence of behavioral hypersensitivity and following minocycline treatment sufficient to attenuate allodynia. *J Neurosci Res* 87:2709-2717

Rothman SM, Huang Z, Lee KE, Weisshaar CL, Winkelstein BA (2009b) Cytokine mRNA expression in painful radiculopathy. *Journal of Pain* 10: 90-99

Rothman SM, Hubbard RD, Lee KE, Winkelstein BA (2007) Detection, Transmission, and Perception of Pain Interventions of the Spine: An Algorithmic Approach, Slipman C, Simeone F, Derby R, Eds. Elsevier, 29-37

Rothman SM, Kreider RA, Winkelstein BA (2005) Spinal neuropeptide responses in persistent and transient pain following cervical nerve root injury. *Spine* 30:2491–2496

Rothman SM, Nicholson KJ, Winkelstein BA (2010) Time-dependent mechanics and measures of glial activation and behavioral sensitivity in a rodent model of radiculopathy. *J Neurotrauma* 27:803-814

Rothman SM, Winkelstein BA (2007) Chemical and mechanical nerve root insults induce differential behavioral sensitivity and glial activation that are enhanced in combination. *Brain Res* 1181:30-43

Rothman SM, Winkelstein BA (2010) Cytokine antagonism reduces pain and modulates spinal astrocytic reactivity after cervical nerve root compression. *Ann Biomed Eng* 38(8): 2563–2576

Rothstein JD, Dykes-Hoberg M, Pardo CA, Bristol LA, Jin L, Kunczi RW, Kanai Y, Hediger MA, Wang Y, Schielke JP, Welty DF (1996) Knockout of glutamate transporters reveals a major role for astroglial transport in excitotoxicity and clearance of glutamate. *Neuron* 16:675-686

Rothstein JD, Patel S, Regan MR, Haenggeli C, Huang YH, Bergles DE, Jin L, Hoberg MD, Vidensky S, Chung DS, Toan SV, Bruijn LI, Su Z, Gupta P, Fisher PB (2005)  $\beta$ -Lactam antibiotics offer neuroprotection by increasing glutamate transporter expression. *Nature* 433:73-77

Rothstein JD, Van Kammen M, Levey AI, Martin LJ, Kuncl RW (1995) Selective loss of glial glutamate transporter GLT-1 in amyotrophic lateral sclerosis. *Ann of Neurol* 38: 73–84

Rydevik B, Brown MD, Lundborg G (1984) Pathoanatomy and pathophysiology of nerve root compression. *Spine* 9(1):7-15

Rydevik B, Kwan MK, Myers RR et al (1990) An in vitro mechanical and histological study of acute stretching on rabbit tibial nerve. *J Orthop Res* 8(5):694-701

Rydevik B, Lundborg G, Bagge U (1981) Effects of graded compression on intraneural blood flow. An in vivo study on rabbit tibial nerve. *J Hand Surg Am* 6(1):3-12

Rydevik BL, Pedowitz RA, Hargens AR, Swenson MR, Myers RR, Garfin SR (1991) Effects of acute, graded compression on spinal nerve root function and structure: an experimental study of the pig cauda equine. *Spine* 16(5):487-493

Sairyo K, Sakai T, Amari R, Yasui N (2010) Causes of radiculopathy in young athletes with spondylosis. *Am J Sports Med* 38:357-362

Saito K, Hitomi S, Suzuki I, Masuda Y, Kitagawa J, Tsuboi Y, Kondo M, Sessle BJ, Iwata K (2008) Modulation of trigeminal spinal subnucleus caudalis neuronal activity following regeneration of transected inferior alveolar nerve in rats. *J Neurophysiol* 99:2251-2263

Sandkuhler J (2009) Models and mechanisms of hyperalgesia and allodynia. *Physiol Rev* 89:707-758

Scherrer G, Imamachi N, Cao YQ, Contet C, Mennicken F, O'Donnell D, Kieffer BL, Basbaum AI (2009) Dissociation of the opioid receptor mechanisms that control mechanical and heat pain. *Cell* 137(6):1148-1159

Schumacher PA, Eubanks JH, Fehlings MG (1999) Increased calpain I-mediated proteolysis, and preferential loss of dephosphorylated NF200, following traumatic spinal cord injury. *Neuroscience* 91(2):733-744

Schwartz G, Fehlings MG (2001) Evaluation of the neuroprotective effects of sodium channel blockers after spinal cord injury: improved behavioral and neuroanatomical recovery with riluzole. *J Neurosurg* 94:245-256

Seagrove LC, Suzuki R, Dickenson AH (2004) Electrophysiological characterizations of rat lamina I dorsal horn neurones and the involvement of excitatory amino acid receptors. *Pain* 108:76-87

Sekiguchi M, Sekiguchi Y, Konno S, Kobayashi H, Homma Y, Kikuchi S (2009) Comparison of neuropathic pain and neuronal apoptosis following nerve root or spinal nerve compression. *Eur Spine J* (18)12:1978-1985

Sekiguchi Y, Kikuchi S, Myers RR, Campana WM (2003) ISSLS Prize Winner: Erythropoietin inhibits spinal neuronal apoptosis and pain following nerve root crush. *Spine* 28(23):2577-2484

Serbest G, Burkhardt MF, Siman R, Raghupathi R, Saatman KE (2007) Temporal profiles of cytoskeletal protein loss following traumatic axonal injury in mice. *Neurochem Res* 32:2006-2014

Shamji MF, Allen KD, So S, Jing L, Adams SB, Schuh R, Huebner J, Kraus VB, Friedman AH, Setton LA, Richardson WJ (2009) Gait abnormalities and inflammatory cytokines in an autologous nucleus pulposus model of radiculopathy. *Spine* 34(7):648-654

Sher PK, Hu S (1990) Increased glutamate uptake and glutamine synthetase activity in neuronal cell cultures surviving chronic hypoxia. *Glia* 3:350-357

Shi R (2004) The dynamics of axolemal disruption in guinea pig spinal cord following compression. *J Neurocytol* 33:203-211

Shi R, Whitebone J (2006) Conduction deficits and membrane disruption of spinal cord axons as a function of magnitude rate and strain. *J Neurophys* 95:3384-3390

Shim B, Kim DW, Kim BH, Nam TS, Leem JW, Chung JM (2005) Mechanical and heat sensitization of cutaneous nociceptors in rats with experimental peripheral neuropathy. *Neuroscience* 132:193-201.

Shortland PJ, Leinster VHL, White W, Robson LG (2006) Riluzole promotes cell survival and neurite outgrowth in rat sensory neurons in vitro. *Eur J Neurosci* 24:3343-3353

Simard JM, Tsymbalyuk O, Keledjian K, Ivanov A, Ivanova S, Gerzanich V (2012) Comparative effects of glibenclamide and riluzole in a rat model of severe cervical spinal cord injury. *Exp Neurol* 233:566-574.

Singh A, Kallakuri S, Chen C, Cavanaugh JM (2009) Structural and functional changes in nerve roots due to tension at various strains and strain rates: an in-vivo study. *J Neurotrauma* 26:627-640.

Singh, A, Lu, Y, Chen, C, Cavanaugh, JM (2006) Mechanical properties of spinal nerve roots subjected to tension at different strain rates. *J Biomech* 39: 1669-1676.

Siniscalchi A, Bonci A, Mercuri NB, Bernardi G (1997) Effects of riluzole on rate cortical neurons: an in vitro electrophysiological study. *Br J Pharmacol* 120:225-230.

Springer JE, Azbill RD, Mark RJ, Begley JG, Waeg G, Mattson MP (1997) 4-Hydroxynonenal, a lipid peroxidation product, rapidly accumulates following traumatic spinal cord injury and inhibits glutamate uptake. *J Neurochem* 68:2469-2476

Staal JA, Vickers JC (2011) Selective vulnerability of non-myelinated axons to stretch injury in an in vitro co-culture system. *J Neurotrauma* 28:841-847

Stafstrom CE (2007) Persistent sodium current and its role in epilepsy. *Epilepsy Curr* 7(1):15-22.

Stanfa LC, Sullivan AF, Dickenson AH (1992) Alterations in neuronal excitability and the potency of spinal mu, delta and kappa opioids after carrageenan-induced inflammation. *Pain* 50(3):345-354

Stodieck LS, Beel JA, Luttges MW (1986) Structural properties of spinal nerve roots: protein composition. *Exp Neurol* 91:41-51

Stoll G, Müller HW (1999) Nerve injury, axonal degeneration and neural regeneration: basic insights. *Brain Pathol* 9:313-325

Strain RE, Olson WH (1975) Selective damage of large diameter peripheral nerve fibers by compression: an application of Laplace's law. *Exp Neurol* 47:68-80

Stuber K (2005) Cervical collar and braces in athletic brachial plexus injury and excessive cervical motion prevention: a review of the literature. *J Can Chiropr Assoc* 49(3):216-222

Stutzmann JM, Pratt J, Boraud T, Gross C (1996) The effect of riluzole on post-traumatic spinal cord injury in the rat. *NeuroReport* 7:387-292

Sun RQ, Lawand NB, Lin Q, Willis WD (2004) Role of calcitonin gene-related peptide in the sensitization of dorsal horn neurons to mechanical stimulation after intradermal injection of capsaicin. *Journal of Neurophysiology* 92: 320-326

Sunderland S (1974) Mechanisms of cervical nerve root avulsion in injuries of the neck and shoulder. *J Neurosurg* 41:705-714

Sung B, Lim G, Mao J (2003) Altered expression and uptake activity of spinal glutamate transporters after nerve injury contribute to the pathogenesis of neuropathic pain in rats. *J Neurosci* 23(7):2899-2910

Suzuki R, Kontinen VK, Matthews E, Williams E, Dickenson AH (2000) Enlargement of the receptive field size to low intensity mechanical stimulation in the rat spinal nerve ligation model of neuropathy. *Exp Neurol* 163:408-413

Suzuki, R., Morcuende, S., Webber, M., Hunt, S.P., and Dickenson, A.H. (2002) Superficial HK1-expressing neurons control spinal excitability through activation of descending pathways. *Nat Neurosci* 5(12): 1319-1326

Svensson MY, Aldman B, Hansson HA, Lövsun P, Seeman T, Suneson A, Örtengren T (1993) Pressure effects in the spinal canal during whiplash extension motion: a possible cause of injury to the cervical spinal ganglia. *Proceedings of the IRCOBI Conference* 189-200

Swanik C, Henry T, Lephart S (1996) Chronic brachial plexopathies and upper extremity proprioception and strength. *J Athl Train* 31(2):119-124

Tabo E, Jinks SL, Eisele JH, Carstens E (1999) Behavioral manifestations of neuropathic pain and mechanical allodynia, and changes in spinal dorsal horn neurons, following L4-L6 dorsal root constriction in rats. *Pain* 80:503-520

Takahashi N, Yabuki S, Aoki Y, Kikuchi S (2003) Pathomechanisms of nerve root injury caused by disc herniation: an experimental study of mechanical compression and chemical irritation. *Spine* 28(5):435-441

Takahashi Y, Nakajima Y (1996) Dermatomes in the rat limbs as determined by antidromic stimulation of sensory C-fibers in spinal nerves. *Pain* 67:197-202

Takamori S, Rhee JS, Rosenmund C, Jahn R (2000) Identification of a vesicular glutamate transporter that defines glutamatergic phenotype in neurons. *Nature* 407:189-194

Takamori Y, Arimizu J, Izaki T, Naito M, Kobayashi T (2010) Combined measurement of nerve root blood flow and electrophysiological values. *Spine* 26(1):57-62

Takeda M, Takashashi M, Nasu M, Matsumoto S (2010) In vivo patch-clamp analysis of response properties of rat primary somatosensory cortical neurons responding to noxious stimulation of facial skin. *Mol Pain* 6:30

Tanaka N, Fujimoto Y, An HS, Ikuta Y, Yasuda M (2000) The anatomic relation among the nerve roots, intervertebral foramina, and intervertebral discs of the cervical spine. *Spine* 25(3):286-291

Tao Y, Gu J, Stephens RL (2005) Role of spinal cord glutamate transporter during normal sensory transmission and pathological pain states. *Mol Pain* 1:30



Terashima Y, Kawamata M, Takebayashi T, Tanaka S, Tanimoto K, Yahashia T (2011) Changes in synaptic transmission of substantia gelatinosa neurons in a rat model of lumbar radicular pain revealed by in vivo patch-clamp recording. *Pain* 152:1024-1032

Thoomes EJ, Scholten-Peeters GGM, de Boer AJ, Olsthoorn RA, Verkerk K, Lin C, Verhagen AP (2012) Lack of uniform diagnostic criteria for cervical radiculopathy in conservative intervention studies: a system review. *Eur Spine J* 21:1459-1470.

Thoomes EJ, Scholten-Peeters W, Koes B, Falla D, Verhagen AP (2013) The effectiveness of conservative treatment for patients with cervical radiculopathy. *Clin J Pain* epub ahead of print.

Tilleux S, Hermans E: Neuroinflammation and regulation of glial glutamate uptake in neurological disorders. *J Neurosci Res* 85:2059-2070, 2007

Todd AJ (2010) Neuronal circuitry for pain processing in the dorsal horn. *Nat Rev Neurosci* 11:823-836

Tominaga Y, Maak TG, Ivancic PC, Panjabi MM, Cunningham BW (2006) Head-turned rear impact causing dynamic cervical intervertebral foramen narrowing: implications for ganglion and nerve root injury. *J Neurosurg Spine* 4:380-387

Trantham-Davidson H, LaLumiere RT, Reissner KJ, Kalivas PW, Knackstedt LA (2012) Ceftriaxone normalizes nucleus accumbens synaptic transmission, glutamate transport, and export following cocaine self-administration and extinction training. *J Neurosci* 32(36):12406-12410

Urch CE, Dickenson AH (2003) In vivo single cell extracellular recordings from spinal cord neurones of rats. *Br Res* 12:26-34

Urch CE, Donovan-Rodriguez T, Dickenson AH (2003) Alterations of dorsal horn neurones in a rat model of cancer-induced bone pain. *Pain* 106:347-356

Vera-Porocarrero LP, Mills CD, Ye Z, Fullwood SD, McAdoo DJ, Hulscebosch CE, Westlund KN (2002) Rapid changes in expression of glutamate transporters after spinal cord injury. *Brain Res* 927:104-110

Verma R, Mishra V, Sasmal D, Raghubir R (2010) Pharmacological evaluation of glutamate transporter 1 (GLT-1) mediated neuroprotection following cerebral ischemia/reperfusion injury. *Eur J Pharmacol* 638:65-71

Vorwerk CK, Zurakowski D, McDermott LM, Mawrin C, Dreyer EB (2004) Effects of axonal injury on ganglion cell survival and glutamate homeostasis. *Brain Res Bull* 62:485-490

Wainner RS, Gill H (2000) Diagnosis and nonoperative management of cervical radiculopathy. *J Orthop Sports Phys Ther* 30(12):728-744.

Wall E, Kwan M, Rydevik B, Woo S, Garfin S (1991) Stress relaxation of a peripheral nerve. *J Hand Surg* 16:859-863

Wall EJ, Massie JB, Kwan MK et al (1992) Experimental stretch neuropathy. *J Bone Joint Surg* 74B:126-129

Wall P, Melzack R (1994) *Textbook of Pain*. 3<sup>rd</sup> edition. Churchill Livingstone: London

Wall PD, Fitzgerald M, Gibson SJ (1981) The response of rat spinal cord cells to unmyelinated afferents after peripheral nerve section and after changes in substance P levels. *Neuroscience* 6(11):2205-2215

Wang R, King T, Ossipov MH, Rossomando AJ, Vanderah TW, Harvey P, Cariani P, Frank E, Sah DW, Porreca F (2008a) Persistent restoration of sensory function by immediate or delayed systemic artemin after dorsal root injury. *Nat Neurosci* 11(4):488-496

Wang SJ, Wang KY, Wang WC (2004) Mechanisms underlying the riluzole inhibition of glutamate release from rat cerebral cortex nerve terminals synaptosomes. *Neuroscience* 125:191-201

Wang W, Wang W, Wang Y, Huang J, Wu S, Li YQ (2008b) Temporal changes of astrocyte activation and glutamate transporter-1 expression in the spinal cord after spinal nerve ligation-induced neuropathic pain. *Anatomical Record (Hoboken)* 291(5): 513-518

Wang ZB, Gan Q, Rupert RL, Zeng YM, Song XJ (2005) Thiamine, pyridoxine, cyanocobalamin and their combination inhibit thermal, but not mechanical hyperalgesia in rats with primary sensory neuron injury. *Pain* 114:266-277

Watkins LR, Maier SF (2003) Glia: a novel drug discovery target for clinical pain. *Nat Rev Drug Discov* 12:973-985

Weng HR, Chen JH, Cata JP (2006) Inhibition of glutamate uptake in the spinal cord induces hyperalgesia and increased responses of spinal dorsal horn neurons to peripheral afferent stimulation. *Neuroscience* 138:1351-1360

Wieseler-Frank J, Maier SF, Watkins LR (2004) Glial activation and pathological pain. *Neurochem Int* 45:389-395

Winkelstein BA, DeLeo JA (2002) Nerve root injury severity differentially modulates spinal glial activation in a rat lumbar radiculopathy model: considerations for persistent pain. *Brain Res* 956(2):294-301

Winkelstein BA, DeLeo JA (2004) Mechanical thresholds for initiation and persistence of pain following nerve root injury: mechanical and chemical contributions and injury. *J Biomech Eng* 126:258–263

Winkelstein BA, Weinstein JN, DeLeo JA (2002) The role of mechanical deformation in lumbar radiculopathy: an in vivo model. *Spine* 27(1):27-33

Woolf CJ, Fitzgerald M (1983) The properties of neurones recorded in the superficial dorsal horn of the rat spinal cord. *J Comp Neurol* 221:313-328

Woolf CJ, Mannion RJ (1999) Neuropathic pain: aetiology, symptoms, mechanisms, and management. *Pain* 353:1959-1964

Wu Y, Satkunendrarajah K, Teng Y, Chow DSL, Buttigieg J, Fehlings MG (2013) Delayed post-injury administration of riluzole is neuroprotective in a preclinical rodent model of cervical spinal cord injury. *J Neurotrauma* 30:1-12.

Xin W, Weng H, Dougherty PM (2009) Plasticity in expression of the glutamate transporter GLT-1 and GLAST in spinal dorsal horn glial cells following partial sciatic nerve ligation. *Mol Pain* 5:15

Yamada J, Jinno S (2011) Alterations in neuronal survival and glial reactions after axotomy by ceftriaxone and minocycline in the mouse hypoglossal nucleus. *Neurosci Lett* 504:295-300

Yang Y, Gozen O, Watkins A, Lorenzini I, Lepore A, Gao Y, Vidensky S, Brennan J, Poulsen D, Park JW, Jeon NL, Robinson MB, Rothstein JD (2009) Presynaptic regulation of astroglial excitatory neurotransmitter transporter GLT1. *Neuron* 61:880-894

Yoshizawa H, Kobayashi S, Kubota K (1989) Effects of Compression on Intraradicular Blood Flow in Dogs. *Spine* 15:1220-1225

Yu Y, Zhao F, Chen J (2009) Activation of ERK1/2 in the primary injury site is required to maintain melittin-enhanced wind-up of rat spinal wide-dynamic-range neurons. *Neurosci Lett* 459:137-141

Zhang S, Nicholson KJ, Smith JR, Syré PP, Gilliland TM, Winkelstein BA (2013) The roles of mechanical compression and chemical irritation in regulating spinal neuronal signaling in painful cervical nerve root injury. *Stapp Car Crash J*, submitted

Zou JY, Crews FT (2005) TNF $\alpha$  potentiates glutamate neurotoxicity by inhibiting glutamate uptake in organotypic brain slice cultures: neuroprotection by NF $\kappa$ B inhibition. *Br Res* 1034(1-2):11-24

Zimmermann, M (1983) Ethical guidelines for investigations of experimental pain in conscious animals. *Pain* 16:109–110